ERRATA and ADDENDUM

p 4 para 1, third line: “orbitals increases” to “orbitals decreases”
p 6 para 2, second sentence: “Schnockel” to “Schnöckel”
p 7 para 1, last sentence: “group, and is in most cases negligible.” to “group.”
p 8 para 2, first sentence: “carbene analogous” to “carbene analogues”
p 8 para 2, fourth sentence: “the carbene at the…” to “the carbene. At the…”
p 10 para 2, second sentence: space between “GaI” and “(Scheme 2)”
p 10 para 2, third sentence: “memebered” to “membered”
p 10 para 2, third sentence: delete period after “analogues”
p 14 para 1, third sentence: delete comma after “as”
p 14 para 2, fourth sentence: “very low yielding” to “obtained in low yield”
p 15 para 1, second line: “began” to “begun”
p 23 para 3, second sentence: “$LiNTMS_2$” to “ $LiN(TMS)_2$”
p 24 and throughout thesis: delete space between metal and oxidation state
p 34 para 1, third sentence: “deprotanated” to “deprotonated”
p 38 table 4, “substituion” to substitution”
p 38 para 1, second sentence: LDA = lithium diisopropylamide
p 59 para 1, third sentence: “were successful in affording” to “successfully afforded”
p 60 para 1, second sentence: “afforded” to “obtained”
p 61 para 2, fifth sentence: “reacted” to “allowed to react”
p 71 para 1, second sentence: “in-situ” to “in situ”
p 72 para 1, third sentence and throughout thesis: “**56**” to “(**56**)” when complex is first assigned a number
p 73 para 1, third sentence: “crystalographically” to crystallographically”
p 79 para 1, fourth sentence: “which is…” to “which reacted with excess tmeda is…”
p 86 para 1, first sentence: “allow the isolation” to “allow for the isolation”
p 88 para 1, ninth line: “crystalographically” to “crystallographically”
p 95 para 2, fifth sentence: “Ottago” to “Otago”
p 96 para 2, first sentence: weight of $[CaI_2(OEt_2)_n]$ is 0.15g.
p 98 para 2, tenth line and throughout thesis: insert space between “300” and “K” and “70” and “eV”
p 100 para 2, third line: “C6D6” to “C_6D_6”
p 102 ref 12: “A. Stasch” to “Stasch, A.;”
p 106 para 2, fourth sentence: “$[\{(MeCN)_3YbFe(CO)_4\}_2.MeCN]_\infty$” to “$[\{(MeCN)_3YbFe(CO)_4\}_2\cdot MeCN]_\infty$”

p 108 para 1, sixth line: “allowing coordination” to “favors coordination”
p 109 para 2, second sentence: fc = $[Fe(C_4H_4)_2]$ should be in abbreviation list
p 110 para 2, first sentence: “group13-lanthanide” to “group 13-lanthanide”
p 112 para 1, first sentence: “preprared” to “prepared”
p 113 para 1, second sentence: “realized through” to “obtained by”
p 116 para 1, first sentence: “reports” to “reported”
p 122 para 1, second sentence: delete “afforded”
p 122 para 1, fourth sentence: “was not possible to synthesize...” to “could not be synthesized…”
p 122 para 1, fifth sentence: delete commas after “complexes” and “)”
p 123 para 1, second sentence: “(COD=cyclo-octadiene)” to “(COD = 1,5-Cyclooctadiene)”
p 123 para 1, fifth sentence: “crystals which…” to “crystals. This compound has been structurally…”
p 127 para 2, third sentence: “prepared” to “obtained”
p 139 para 2, seventh line: “Yield: 23 %.” to “Yield: 0.07g (23%)”
p 141 ref 1: “*Dalton Transactions*.” to “*Dalton Trans.*”
p 141 ref 4: delete semicolon after “Shore, S.G.;”
p 141 ref 6 and 7: delete comma after “*Chem.,*”
p 143 ref 32 and p 144 ref 43: insert period at end of reference
p 148 para 2, fifth sentence: “rather than pyramidal.” to “rather than pyramidal as well as extensive delocalization of the spin density onto the phenyl group.”
p 149 para 3, second sentence: “comopounds” to “compounds”
p 154 scheme 5: “$Li(THF)_4$” to “$Li(THF)_4^+$”
p 157: For final results and discussions see: Woodul, W.D.; Carter, E.; Müller, R.; Richards, A.F.; Stasch, A.; Kaupp, M.; Murphy, D.M.; Driess, M.; Jones, C.; *J. Am. Chem. Soc.*, **2011**, *133*, 10074.
p 181 para 2, first and fifth sentence: delete “very”
p 181 para 2, second sentence: “*ν*/cm-1” to “ν/cm^{-1}”
p 184: “hydrogen atoms are omitted…” to “hydrogen atoms and methyl and mes groups are omitted…”
p 185 para 1, third sentence and throughout thesis: “OTF” to “OTf”
p 188 second line: space between “1” and “M”
p 188 para 2, first sentence: space between “1.6” and “M”
p 193 para 1, fourth sentence: “diflurobenzene” to “1,2-Difluorobenzene”
p 212 para 1, second line: “isostrucutral” to “isostructural”
p 212 para 1, third line: delete “chemically”
p 215/217 Figure captions: isopropyl groups are not omitted
p 220 and throughout thesis: “cm^3” to “mL”

Studies of Low Oxidation State Group 13 and 14 Metallacycles

by

William D. Woodul

Thesis presented to the School of Chemistry, Monash University, for the degree of

Doctor of Philosophy, February 2011

Summary

This thesis is mainly concerned with investigations into the reactivity of the gallium(I) *N*-heterocyclic carbene (NHC) analogue, [K(tmeda)][**:**Ga{[N(Dip)C(H)]$_2$}] (Dip = $C_6H_3Pr^i_2$-2,6). The preparation of the first monomeric Ge(I) radical was also investigated. Work carried out in these areas is divided into five chapters. Chapter 1 provides a general introduction to sub-valent group 13 and 14 chemistry, with an emphasis on the preparation of group 13 metal(I) and group 14 metal(II) *N*-heterocyclic carbene analogues. Chapter 2 summarizes investigations into the reactivity of [K(tmeda)] [**:**Ga{[N(Dip)C(H)]$_2$}] towards groups 2 and 12 metal precursors. Reactions of magnesium, calcium, strontium, barium, zinc, and cadmium halides with [K(tmeda)][**:**Ga{[N(Dip)C(H)]$_2$}] are discussed, and the first structurally characterized cadmium-gallium bonded molecular complex is reported. Chapter 3 summarizes investigations into the reactivity of [K(tmeda)] [**:**Ga{[N(Dip)C(H)]$_2$}] towards selected lanthanide metal precursors. Reactions of samarium(II), europium(II), ytterbium(II), thulium(II), and cerium(III) iodides with [K(tmeda)][**:**Ga{[N(Dip)C(H)]$_2$}] have given rise to a number of novel lanthanide-gallyl species, including the first structurally characterized GaTm or GaSm bonded complexes. Chapter 4 details the preparation of the first monomeric Ge(I) radical *via* the reduction of a bulky β-diketiminato germanium(II) precursor. The verification of the +1 oxidation state in this species was achieved using a combination of crystallographic, EPR and ENDOR spectroscopic, and theoretical analyses. Chapter 5 describes several miscellaneous results, largely derived from attempts to prepare bulky guanidinato complexes of *p*-block elements in low oxidation states.

Acknowledgements

First and foremost I'd like to thank my parents and family, for without their support, none of this would have been possible. I would also like to thank my parents for the many overseas trips they took during my candidature. I would especially like to thank my Dad for the Fox and Friends Skyping.

Secondly, I would like to thank Cameron for providing me with this wonderful opportunity, the continued support and guidance and for the fun times all over the world. I would also like to tell Anne how much I have appreciated her friendship over the last several years, and for making me aware of this opportunity.

Finally, I would like to thank everyone who I have worked with in either Australia or Germany. Thanks to Andreas for being so very helpful in and out of the lab and for his wine knowledge. A special thanks to Shaun, Andreas, Simon, Sam, Deepak, Lea, Owen, Alex, Tash, Eric, Brant, DTM, Christian, and Jay for keeping the lab time enjoyable and for putting up with Texas Country Fridays. Also, thanks to you all and Susie for all of the group outings, wine tastings, TGI's and Friday Night Poker.

This Thesis is Dedicated to the Memory of: ChuChu and Pampaw

Table of Contents

Chapter 2

Groups 2 and 12 Metal Gallyl Complexes Containing Unsupported Ga-M Covalent Bonds (M = Mg, Ca, Sr, Ba, Zn, or Cd)

Chapter 3

Complexes of an Anionic Gallium(I) *N*-heterocyclic Carbene Analogue with Selected Lanthanide Metals.

Chapter 4

Synthesis of the First Monomeric Germanium(I) Radical

Chapter 5

Miscellaneous *p*-Block Element Guanidinate Chemistry

Glossary

Å	Angstrom, 1 x 10^{-10} m
a_o	Hyperfine coupling value
ab initio	A quantum chemistry method
Ar, Ar', Ar''	A general aryl substituent
br.	Broad
Bu^t	Tertiary butyl
Bu^n	Primary butyl
ca.	*Circa*
cm^{-1}	Wavenumber, unit of frequency (ν/c)
Cp	Cyclopentadienyl
Cp'	A general cyclopentadienyl
Cp*	Pentamethylcyclopentadienyl
Cy	Cyclohexyl
δ	Chemical shift in NMR spectroscopy (ppm)
DAB	Diazabutadiene
d	Doublet
dec.	Decomposition
DFT	Density Functional Theory
Dip-DAB	*N*,*N'*-bis(diisopropylphenyl)diazabutadiene
DME	1,2-Dimethoxyethane
E	A general element
EPR	Electron Paramagnetic Resonance

Et_2O	Diethyl ether
FT-IR	Fourier transform infrared spectroscopy
η	Hapta
g_{iso}	Isotropic g value
G	Gauss
$Giso^-$	*N*,*N*′-Bis(2,6-diisopropylphenyl)dicyclohexylguanidinate
θ	Fold angle
HOMO	Highest Occupied Molecular Orbital
Hz	Hertz, s^{-1}
ipso	*Ipso*-substituent
IR	Infrared
$^nJ_{xy}$	Coupling constant between nuclei X and Y, over n bonds, in Hz
K	Kelvin
k	A rate constant
kcal	Kilocalorie (1 kcal = 4.184 J)
kJ	Kilojoule
L	A general ligand
LUMO	Lowest Unoccupied Molecular Orpital
μ	Bridging
μB	Bohr Magneton, JT^{-1}
μ_{eff}	Effective magnetic susceptibility
m	*Meta*-substituent

m	Multiplet, medium
M	A general metal or molar ($moldm^{-3}$)
M^+	A molecular ion
Me	Methyl
Mes	Mesityl (2,4,6-trimethylphenyl)
Mes*	Supermesityl (2,4,6-tritertiarybutylphenyl)
mol	Mole
Mp	Melting point
MS(APCI)	Atmospheric Pressure Chemical Ionisation Mass Spectrometry
MS(EI)	Electron Ionisation Mass Spectrometry
m/*z*	Mass/charge ratio
NBO	Natural Bond Orbital
NHC	*N*-heterocyclic carbene
NMR	Nuclear Magnetic Resonance
o	*Ortho*-substituent
p	*Para*-substituent
Ph	Phenyl
$Piso^-$	*N*,*N'*-Bis(2,6-diisopropylphenyl)tertiarybutylamidinate
Pr^i	Isopropyl
$Priso^-$	*N*,*N'*-Bis(2,6-diisopropylphenyl)diisopropylguanidinate
ppm	Parts per million
pw	Peak width

q	Quartet
R	General organic substituent
s	Singlet or strong
sept	Septet
t	Triplet
THF	Tetrahydrofuran
tmeda	*N*,*N*,*N'*,*N'*-Tetramethylethylene-1,2-diamine
TMS	Trimethylsilyl or tetramethylsilane
UV	Ultraviolet
X	A general halide

STATEMENT

To the best of the author's knowledge and belief, this thesis contains no material which has been accepted for the award of any other degree or diploma in any university and contains no material previously published or written by another person except where due reference is made.

William Woodul

School of Chemistry

Monash University

Chapter 1

A General Introduction

1.1 The Physical and Chemical Properties of the Group 13 and 14 Elements

Looking at the periodic table, the group 13 elements are comprised of boron, aluminum, gallium, indium and thallium, whereas, the group 14 elements are composed of carbon, silicon, germanium, tin, and lead in that descending order. This thesis will mostly encompass work from the group 13 and 14 elements, and as such, their physical and chemical properties will be briefly discussed here.

The ground state valence electron configuration of the group 13 elements is ns^2np^1, with the core electronic configurations varying on descent of the group.[1] They are commonly known as "electron-deficient" due to the fact that all of the elements have fewer valence electrons than valence orbitals which results in their neutral compounds exhibiting Lewis acidic characteristics.[2] Boron does not display chemical or physical properties that are closely related to its group 13 members. It has more in common with carbon and silicon, and due to this fact, boron is usually discussed separately.[3]

The remaining four elements from group 13 are all soft metals with low melting points, which display high electrical conductivity. A summary of a few of the physical and electronic properties of the group 13 elements can be found in Table 1. Gallium is especially important in this work. It is an extremely interesting element, due to the facts that it is a rare example of a low-melting solid (29.8ºC) that expands upon freezing, has the longest liquid range of any element and is surprisingly non-toxic.

Property	B	Al	Ga	In	Tl
Atomic Number	5	13	31	49	81
Covalent Radius (Å)	0.81	1.25	1.25	1.50	1.55
Ionisation Energy (kJ mol^{-1}) (1st 3 electrons)	6887	5044	5521	5084	5439
Electronegativity (Pauling)	2.04	1.61	1.81	1.78	2.04
Electronegativity (Allred and Rochow)	2.01	1.47	1.82	1.49	1.44
Melting Point (ºC)	2300	660.1	29.8	156.2	302.4

Table 1. Selected physical and chemical properties of the group 13 elements.

The group 14 elements are arguably the most important of all with carbon providing the basis for life on Earth and silicon being vital for the physical structure of the natural environment in the form of crustal rocks.[2] The ground state valence electron configuration of the group 14 elements is ns^2np^2. Carbon and silicon, which are the lightest members of the group, are nonmetals, germanium is a metalloid, and the heaviest, tin and lead are metals. The increase in ionic radius and the associated decrease in ionization energy upon descent of the group is the reason for carbon being a nonmetal whereas lead is a metal. Furthermore, the low ionization energies of the heavier elements lead them to form cations more readily down the group. A summary of a few of the physical and electronic properties of the group 14 elements can be found in Table 2.[2]

Property	C	Si	Ge	Sn	Pb
Atomic Number	6	14	32	50	82
Atomic radius/pm	77	117	122	162	175
First ionisation Energy (kJ mol^{-1})	1090	786	762	707	716
Electronegativity (Pauling)	2.5	1.8	2.0	2.0	2.3
Melting point (ºC)	3730	1410	937	232	327

Table 2. Selected physical and chemical properties of the group 14 elements[2]

The chemistry of groups 13 and 14 is dominated by the fact that upon descent of the groups, the oxidation state predicted by the periodic table is not always exhibited. With their valence electron configurations being ns^2np^1 and ns^2np^2, one would expect that the elements would adopt, in their compounds, the +3 and +4 oxidation states respectively. However, this is indeed not the case, and upon descent of the groups, a lower oxidation state is sometimes favored. For example, the most common oxidation state of thallium is +1 and lead is +2. This phenomenon is due to the inert pair effect, and it is a recurring theme within the *p* block.[2]

The reasons for the inert pair effect are not simple, but can generally be summed up in the following ways. The first reason arises from relativistic effects. As the size of the atom increases, the velocities of the 1*s* electrons increase, causing them to contract closer towards the nucleus. This leads to a contraction of the 2*s*-6*s* orbitals, but at the same time leaving the 2*p*-6*p* orbitals less contracted. This in turn leaves a larger energy gap between

$6s^2$ and $6p^1$ orbitals, therefore, leaving the 6*s* electrons less available for bonding. Secondly, going down a *p*-block group, the difference in energy between valence *s* and *p* orbitals increases. Therefore, the s→p promotion energy increases, making the *s* electrons more reluctant to bonding. Finally, the main factor why heavier atoms in group 13 and 14 prefer the +1 or +2 oxidation states in their compounds is given by the fact that if the energy required to promote the valence *s*-orbital electrons is higher than the energy gained when forming E-X bonds, the *s*-orbital electrons will remain paired. For example, when comparing $AlCl_3$ to $TlCl_3$, the bonds in $AlCl_3$ are much stronger and require much less promotional energy to form than $TlCl_3$. The more diffuse orbitals in $TlCl_3$ are weaker, as are the E-X bond enthalpies for all the heavier *p*-block elements (Table 3).[2]

E\X	**H**	**F**	**Cl**	**Br**	**I**
B	334	757	536	423	220
Al	284	664	511	444	370
Ga	274	577	481	444	339
In	243	506	439	414	331
Tl	188	445	372	334	272

Table 3. Group 13 element hydride and halide mean bond enthalpies (kJ mol^{-1})[2] (EX_3).

1.2 Subvalent Group 13 Chemistry

The accessibility of the lower oxidation states of aluminum and gallium have been a main area of interest, and have become increasingly popular over the last twenty years. During this time, two general synthetic routes have been implemented as standards for accessing subvalent states. First is the substitution of the halide in subhalides, EX (E = Al, Ga, X = Cl, Br, I), with alkyl or aryl groups using RM (M = Li, Na, K), where R = alkyl or aryl, and second being the dehalogenation of $[R_2EX]$ or $[REX_2]$ through reduction with an alkali metal (Scheme 1). The latter method is mostly seen in the syntheses of aluminum and gallium diyls, **:**E—R. In order to avoid thermodynamically favorable disproportionation processes, it has been shown that incorporating sterically demanding R substituents is generally required to kinetically stabilize and protect the group 13 element in low oxidation state group 13 compounds.

$$EX + RM \longrightarrow :ER + MX \quad (E = Al, Ga;\ X = Cl, Br, I;\ M = Li, Na, K)$$

$$2\,[R_2EX] + 2\,M \longrightarrow 2\,MX + [R_2E{-}ER_2]$$

$$n\,[REX_2] + 2n\,M \longrightarrow 2n\,MX + [(ER)_n] \quad (n = 1 - 4)$$

Scheme 1. General syntheses of subvalent aluminum and gallium compounds.

Compounds containing aluminum and gallium in low oxidation states are accessible from their halides, as will be briefly discussed here. In 1996 Schnöckel and co-workers, with the use of a very specialized apparatus, were able to make gallium(I) and aluminum(I) "metastable" halide solutions by introducing $HX_{(g)}$ into a vacuum chamber containing liquid aluminum or gallium at high temperatures. The resulting $MX_{(g)}$ vapor was then

condensed on the walls of the liquid nitrogen cooled vessel.[4] While this source for aluminum(I) and gallium(I) halides has led to the synthesis of extremely interesting compounds such as :AlCp*[5] and :GaCp*[6], it is clearly not a very practical one.

In 1990, Green and co-workers' publication of a much simpler route to a gallium(I) halide, has led to an increased interest in low oxidation state gallium chemistry.[7] "GaI" is made under an inert atmosphere through ultrasonication of gallium metal and half an equivalent of iodine in toluene or other non-coordinating solvents. After three hours of sonication, a bright green flocculent solid is formed which is represented as "GaI". The actual structure of "GaI" is not known, but Coban and co-workers have found through Raman studies that it is a mixture of subhalides, with the ionic species $[Ga]^{+}_{2}[Ga_2I_6]^{2-}$, predominating.[8] The reagent is an extremely useful source of gallium(I), and has subsequently been reviewed.[9]

The halides of intermediate valency are known for aluminum, gallium and indium. Schnockel and co-workers introduced a novel method of synthesizing metastable Al(I) halide structures by reacting HX and molten aluminum metal (*ca*. 800-1000°C) together. Condensation of the Al(I)X (X=Cl, Br, I) gases by cooling to *ca*. 70K generates metastable AlX solutions. It was later seen that these solutions could form aluminum dihalide complexes through donor stabilization.[4] A few examples for gallium are the dianions, $[Ga_2X_6]^{2-}$ (X = Cl, Br, I),[10] and the donor-solvent stabilized compounds, $[Ga_2X_4L_2]$ (X = Cl, Br, I; L = dioxane, pyridine, phosphine).[11] Indium has also been shown to form dihalide complexes, which can been seen in $[In_2I_4(PPr^{n})_2]$.[12]

As previously noted, aluminum and gallium diyls **:**E**—**R, are most often made through the dehalogenation of $[R_2EX]$ or $[REX_2]$ through reduction with an alkali metal

(Scheme 1). Their increasing popularity is relevant to this thesis and they will be briefly discussed.[15a-b,16] The metal diyls can be seen as having a singlet lone pair of electrons in a valence *sp*-hybridized orbital in their monomeric state, with two vacant *p*-orbitals orthogonal to the E-C bond (Figure 1). As they are isolobal with carbon monoxide, they are able to donate their lone pair of electrons to other metals to form a σ-bond. However, the use of their empty *p*-orbitals for π backbonding in transition metal complexes has been placed under much scrutiny. While there is still some debate surrounding the issue, it can be said that the degree of π backbonding relies heavily upon the R group, and is in most cases negligible.[17]

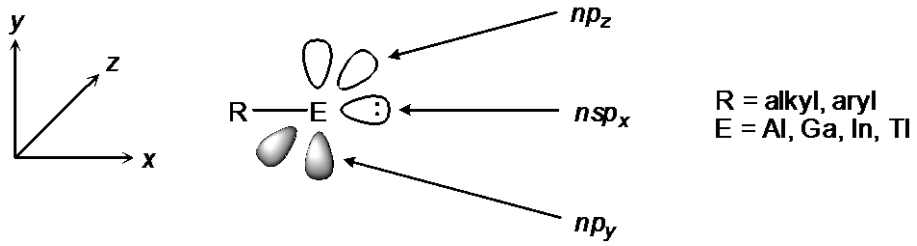

Figure 1. A representation of the valence orbitals in group 13 metal diyls.

1.3 *N*-Heterocyclic Carbenes

N-Heterocyclic carbenes, (NHCs), play an extremely important role in many areas of chemistry. This thesis incorporates the use of NHC analogues, and as such, their properties and importance will be discussed. NHCs are a special class of carbenes. A carbene in its simplest form is defined as a neutral complex possessing an electron deficient divalent carbon atom.[17] The central carbon atom in a carbene has six valence electrons, with two not involved in bonding. These two electrons can either be in a singlet or triplet

state (Figure 2). The singlet state requires the two electrons not involved in bonding to be spin-paired and to reside in the σ orbital. The triplet state has the electrons unpaired with one electron in the σ-orbital and one in the p_π-orbital. In NHCs, both states are possible, but a large $\sigma \rightarrow p_\pi$ energy gap (> 2 eV) favors the singlet ground state, which is generally more stable.[17] Triplet ground state carbenes are generally short-lived and difficult to stabilize. The preferred singlet state leaves an empty p_π-orbital on the carbene, which will be shown to dramatically affect their chemistry.

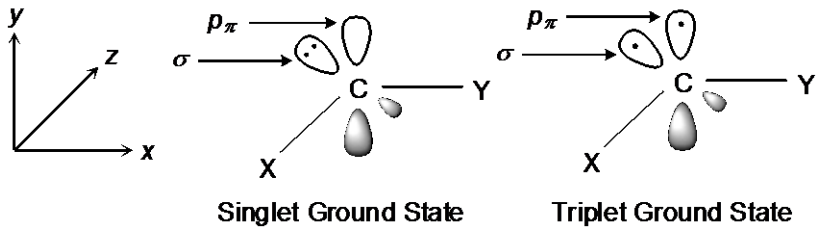

Figure 2. Singlet and triplet ground states for carbenes.

Diaminocarbenes, which have amino groups on either side of the central carbon, are closely related to the group 13 carbene analogous used in this study. As was previously mentioned, most NHCs, which are in the singlet state, possess an empty p_π-orbital. The nitrogen atoms in the diaminocarbenes can donate their p-orbital lone pair electrons into the empty carbene p_π-orbital, thereby stabilizing the carbene at the same time σ-electron density is transferred to the N-centers, due to the greater electronegativity of that element. This stabilization process is known as a push, push mesomeric – pull, pull inductive substitution pattern. This is represented in Figure 3 and results in the triplet state in NHCs being less energetically accessible. In addition, it leads to little π- back bonding in metal complexes formed with NHCs.

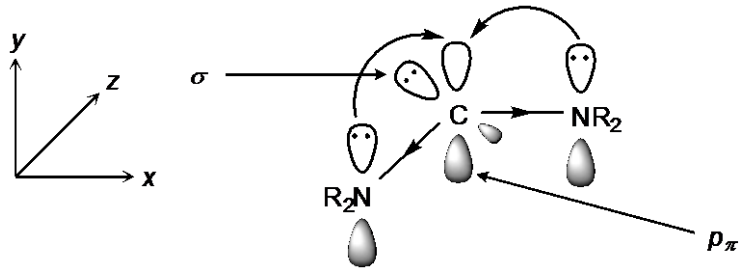

Figure 3. The inductive and mesomeric stabilization of diaminocarbenes

1.4 Group 13 Metal(I) *N*-Heterocyclic Carbene Analogues

This thesis relies heavily upon the use of NHCs and their analogues to study the group 13 elements in the +1 oxidation state. This section will cover chemistry of the four, five, and six membered NHC analogues with a group 13 element(I) with the general form of **A-C**, (Figure 4). While only heterocycles of the type B are true valence isoelectronic analogues of the classical "Arduengo" N-heterocyclic carbenes, heterocycle types **A** and **C**, with their singlet lone pairs, can be thought of as isolobal with four- and six- membered N-heterocyclic carbenes.[18]

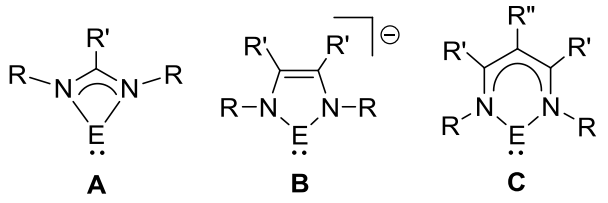

Figure 4. General structures of group 13 metal(I) N-heterocycles

In 2004, Grubbs and Despagnet-Ayoub reported the first four-membered NHC, :C{(DipN)$_2$PNPr$^i_2$} (Dip = 2,6-diisopropylphenyl).[19] To date, a related stable four membered boron(I) heterocycle remains elusive, but Cowley and co-workers have carried

out DFT and MP2 calculations on the model boron(I) guanidinate complex, [:B{$(PhN)_2CNMe_2$}]. Their findings showed that the calculated singlet-triplet energy gaps, 6.0 and 10.1 kcal mol^{-1} respectively, should be suitable for the formation of singlet boron(I) guanidinate complexes, given the right steric protection of the boron(I) center.[20] They were also able to deduce that the lone pair, associated with the singlet state, would be found in the HOMO, giving rise to considerable nucleophlicity of such heterocycles.

To date, four-membered N-heterocyclic aluminum(I) compounds remain elusive. Jones and co-workers, however, have carried out theoretical calculations on the aluminum(I) complex, [:Al{$N(Ph)\}_2CNMe_2$].[21] With the HOMO-LUMO gap calculated to be 61.8 kcal/mol, it would seem that the realization of a complex of this type is achievable. As is the case with most group 13 N-heterocyclic carbene analogues, it was suggested that this type of complex should also exhibit strong σ-donor characteristics, yet be relatively reluctant to act as a π- acceptor.

The only known example of a four-membered gallium(I) heterocycle is the bulky guanidinate complex, **1**. It is formed via the salt elimination reaction of the lithium salt, [Li(Giso)] (Giso = $[(DipN)_2CNCy_2]^-$, Cy = cyclohexyl)[22] with "GaI"(Scheme 2).[7,9] Theoretical studies carried out on the model, [:Ga{$N(Ph)\}_2CNMe_2$], showed that four-memebered gallium(I) heterocycles should have a higher HOMO-LUMO gap than their aluminum analogues, (67.4 kcal/mol).[21] The study also found that such species should behave as σ-donor ligands, while at the same time being weak π-acceptor ligands, due to the high energy of the LUMO. This, however, has not always been the experimentally observed case. Complex **1** has been shown to be less nucleophilic than gallium diyls, and in the case of late transition metal complexes, some π-backbonding may occur.[23] While

complex **1** may be less nucleophilic than gallium diyls, a small number of its coordination complexes have been reported.[23,24,25]

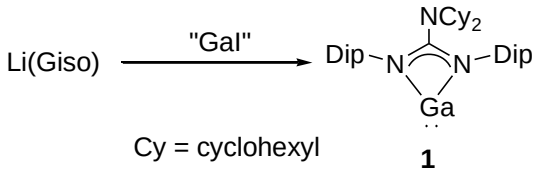

Scheme 2. Synthesis of **1**.

The chemistry of four-membered indium(I) heterocycles has been found to rely heavily on the steric bulk of the backbone carbon substituent. The larger or sterically bulkier the backbone substituent is, the greater the chance of forming the four-memebered indium(I) analogue. For example, with its very bulky guanidinate ligand, [:In(Giso)] **2** (Figure 5), is formed in high yield through a salt elimination reaction.[21,26] With a slightly less bulky substituent, **3** is formed, but not as cleanly as **2**. A by-product in the formation of complex **3** is an indium(II) disproportionation product. When incorporating guanidinate ligands of less bulk, only indium(II) products could be isolated.[26] In a reaction involving an amidinate ligand, the "five-membered" N-,Dip-chelated complex, **4** was obtained (Figure 5). It is thought that in such systems, bulkier substituents are needed in order to prevent disproportionation, by increasing the chelating effect of the nitrogens towards the indium center.

Theoretical studies carried out on the model, [:In{N(Ph)}$_2$CNMe$_2$], show it to be electronically similar to aluminum and gallium analogues with a HOMO-LUMO energy gap of 63.5 kcal/mol.[21] The studies have also shown that while the singlet lone pair resides in the HOMO, its σ-donor properties will not be as pronounced as those in the gallium and aluminum heterocycles due to the larger size of indium. For example, in relation to the theoretical studies, complexes formed with **2** have proven it to be a weaker nucleophile

than the gallium analogue, **1**. In addition, complex **2** has been shown to be a stronger electrophile than **1**, most likely due to the greater Lewis acidity of In relative to Ga.[18]

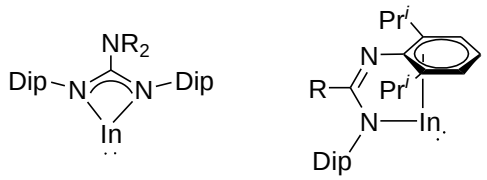

NR_2 = NCy_2 **2**
or $NC_5H_8Me_2$-2,6 **3**

R = Bu^t **4**

Figure 5. Indium(I) heterocycles incorporating bulky guanidinate, or amidinate ligands.

Four-membered thallium(I) heterocycles are not known to date. Attempts to form four-membered thallium(I) heterocycles, have so far only yielded N,Dip-chelated "five-membered" isomers e.g. [Tl(N,Ar-Piso)].[21,26,27] Computational studies have yet to be performed on models of four-membered thallium(I) heterocycles.

Five-membered boron(I) heterocycles have recently become known. Prior to this, Weber and co-workers, while trying to synthesize five-membered boryl anions, made instead the boron(III) and boron(II) products, e.g. [HB{N(Bu^t)C(H)}$_2$] or [{B[N(Bu^t)C(H)]$_2$}$_2$].[28,29] It was proposed that the desired boron(I) product was an intermediate, however, spectroscopic evidence was lacking. It wasn't until 2006 when Segawa and co-workers prepared the first dimeric lithium boryl complex, **5**.[30] They achieved this via the reduction of [BrB{N(Dip)C(H)}$_2$] **6**, with lithium metal in DME, in the presence of a catalytic amount of naphthalene. This was a significant achievement as the complex could be seen as an example of a boryl anion. Upon publication of this work, several articles were reported which highlighted this advance in boron chemistry.[31,32]

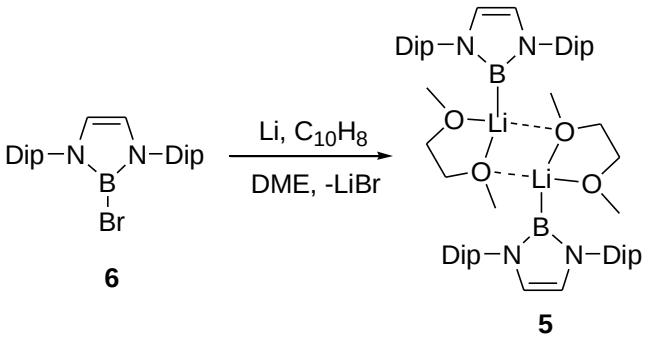

6 **5**

Scheme 3. Synthesis of **5**.

Leading up to the isolation of **5**, theoretical studies had been carried out which examined the geometry and electronic structure of a model N-heterocyclic boryl anion, $[:B\{N(H)C(H)\}_2]^-$. The studies showed that while the singlet-triplet energy gap was quite small (20.2-23.1 kcal/mol), the formation of N-heterocyclic boryl anions was theoretically possible.[33] *Ab initio*[33,34] calculations, and a NBO analysis further suggested that the five-membered boron(I) heterocycle should be very nucleophilic. As is seen in NHCs, it was also shown through theoretical calculations, and by comparisons to its group 13-16 heterocycle analogues, that the boron(I) anion should exhibit weak π- back bonding capabilities in its transition metal complexes.[35] The same study reinstated the finding that cyclic boryl anions should exhibit strong nucleophilic character. The increase of the steric bulk of the heterocycle substituents leading to an increase in kinetic stability has been a major factor in the success of this field as shown by Lai and co-workers.[36] While in many aspects boryl anions are very similar to NHCs, theoretical studies show them to have less aromatic stabilization.[18] The calculated intra-ring geometry of the parent boryl anion $[:B\{N(H)C(H)\}_2]^-$, for example, bears this out and is very close to what Segawa and co-workers observed in **5**.

Five-membered anionic aluminum heterocycles still remain elusive. This is very surprising because the extensive theoretical studies that have been carried out on models show that a complex of this type should be achievable.[18] This is mainly due to the fact that, based on models such as, $[:Al\{N(H)C(H)\}_2]^-$, the singlet-triplet energy gap has been calculated to be 41.3-45.3 kcal/mol,[33,34,35] which is substantially larger than for the boron analogue. It is not to say that preparation of five-membered anionic aluminum heterocycles has not been attempted. Jones and co-workers attempted the reduction of a paramagnetic aluminum(III) precursor, $[I_2Al\{[N(Ar)C(H)]_2\cdot\}]$, with potassium metal, but this led to over reduction and the deposition of aluminum metal.[37] It is conceivable that with time, a synthetic route to an anionic five-membered aluminum(I) species will be discovered.

Of most relevance to this thesis is the study of five-membered anionic gallium(I) heterocycles. Several examples have been reported, **7**-**14**, and are represented in Figure 6. Complexes **7**[38] and **9**[39] were made via the potassium reduction of $[\{Ga(Bu^t\text{-DAB})\}_2]$ (Bu^t-DAB = $\{N(Bu^t)C(H)\}_2$), in the presence of 18-crown-6 or tmeda respectively. Complex **9** was initially very low yielding, however, in 2002, Jones and co-workers, using similar reaction conditions as Schmidbaur, developed a much higher yielding synthesis utilizing the paramagnetic gallium(II) dimer $[\{GaI(Bu^t\text{-DAB}\cdot)\}_2]$[37] as a precursor. Similar reductions of the paramagnetic gallium(III) compounds, $[GaI_2(Ar\text{-DAB}\cdot)]$[40] or $[GaI_2(Ar\text{-}^{Me}DAB\cdot)]$[41] (Ar-DAB = $\{N(Dip)C(H)\}_2$, Ar-^{Me}DAB = $\{N(Dip)C(Me)\}_2$) gave **8** and **10**-**12**,[37,41] whilst the lithium or sodium cleavage of the Ga-Ga bond of $[\{Ga(Ar\text{-BIAN})\}_2]$ (Ar-BIAN = $(DipNC)_2C_{10}H_6$) afforded the alkali metal gallyl complexes, **13** and **14**.[42]

Theoretical studies on models of these group 13 metal(I) NHC analogues show them to be similar to the five-membered anionic aluminum(I) heterocycles.[33,35,38] For

example, they exhibit relatively similar singlet-triplet energy gaps. The value reported for the model, $[:Ga\{N(H)C(H)\}_2]^-$, was 52.0 kcal/mol.[33] In addition, the gallium heterocycle exhibits the same strong polarity between the metal and nitrogen centers that is seen in the aluminum analogue. They are also shown to have, at their gallium centers, an sp-hybridized singlet lone pair of electrons.[18]

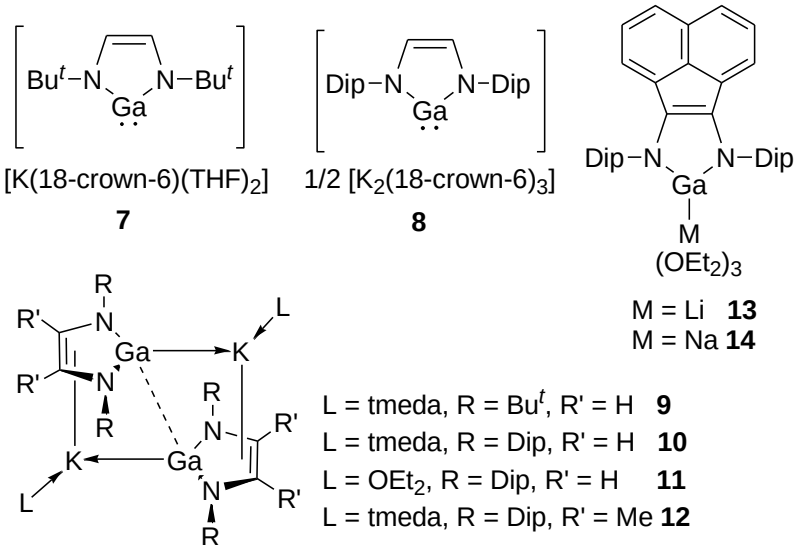

Figure 6. Complexes **7-14**, alkali metal salts and complexes of anionic gallium(I) heterocycles.

Anionic five-membered indium(I) heterocycles are not known as of yet. There have, however, been theoretical studies carried out on the model $[:In\{N(H)C(H)\}_2]^-$.[33,35] The model possesses similar electronic characteristics to the aluminum and gallium analogues, but with a slightly smaller singlet-triplet energy gap of 38.8 kcal/mol. Due to indium's greater size, as was found to be the case in four-membered indium(I) heterocycles, the lone pair on the metal center was calculated to be more diffuse, but should still exhibit nucleophilic characteristics.[35] In hopes of preparing an anionic five-membered

indium(I) heterocycle, the Jones group has carried out reductions of the paramagnetic indium(II) dimer, [{InCl(Ar-DAB·)}$_2$], but these have so far proved unsuccessful.[43]

To date, no work, synthetic or computational, on anionic five-membered thallium(I) heterocycles has been reported.

Six-membered N-heterocyclic boron(I) systems are unknown to date. While examples are known for all of the heavier group 13 elements, it is thought that the singlet-triplet energy gap of the boron(I) systems would be too small for their existence. This was suggested to be the case, with a calculated energy gap of <3.5 kcal/mol found for the heterocycles [:B{[(N(R)C(R')]$_2$CH}] (R = H, Me or Ph; R' = H or Me).[44,45]

The chemistry of neutral six-membered aluminum(I) heterocycles has been an area of much interest lately. In 2000, Roesky and co-workers reported the first example of aluminum(I) heterocycles incorporating β-diketiminate (Nacnac) ligands, **15**, followed by Cui and co-workers in 2007 with the synthesis of **16** (Figure 7).[46,47] This was achieved via the potassium metal reduction of the corresponding aluminum(III) iodide complexes, [I$_2$Al(^{Dip}Nacnac)] or [I$_2$Al($^{t Bu}$Nacnac)] ([{N(Dip)C(R)}$_2$CH]$^-$ R = Me (^{Dip}Nacnac), R = Bu^t ($^{t Bu}$Nacnac). The theoretical calculations conducted on models showed that as in the five-membered anionic aluminum(I) heterocycle model, the six-membered heterocycles should also exhibit a substantial positive charge on the Al center with their Al-N bonds being strongly polarized. They were also shown to have similar singlet-triplet energy gap values, 34.3-45.7 kcal/mol. The calculations also predicted, as was later proven, that the six-membered species would act as both a nucleophile, through the singlet lone pair on the aluminum, and as an electrophile with a relatively empty Al p-orbital due to little donation from the flanking nitrogen centers.[46] To date, the coordination chemistry[48,49], redox

chemistry[50], and cycloadditions towards unsaturated substrates[51,52], of **15** and **16** have began to be examined.

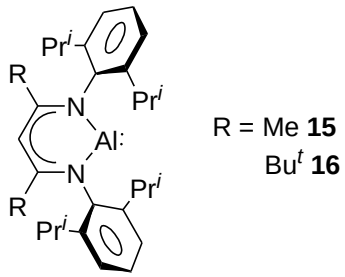

Figure 7. Six-membered aluminum(I) hetereocycles, **15** and **16**.

There is one six-membered gallium(I) heterocycle known to date. [:Ga(^{Dip}Nacnac)], **17**, was made via the lithiation of [H(^{Dip}Nacnac)], followed by the addition of "GaI", and finally reduction over potassium metal (Scheme 4).[53] Theoretical studies conducted on models of type, [:Ga{[(N(R)C(R')]$_2$CH}] (R = H, Me, Ph or Dip; R' = H or Me), show the gallium species to have a slightly higher singlet-triplet energy gap (51.7-55.5 kcal/mol) than their aluminum analogues, but electronically similar none the less.[44,45,54,55] The lone pair on the gallium is of lower energy than in the aluminum counterparts due to the greater singlet-triplet energy gap. It has also been shown that the gallium center acts as a nucleophile, while at the same time having some electrophilic characteristics. The chemistry of the six-membered gallium(I) heterocycle **17** has been studied extensively, as is shown by more than thirty complexes being formed with it. The general reaction types that **17** has been utilized for are (i) coordination to unsaturated fragments[56]; (ii) displacement of labile ligands from transition metal complexes[57]; (iii) insertion of its Ga^I center into E-X bonds (E = hydrogen or a p- or d-block element; X = halide, alkyl,

hydrogen etc.)[58]; (iv) reduction of main group halides or pseudo-halides[59]; (v) formation of gallium imides and amides from organo-azides[60] and (vi) oxidation of its Ga^{I} center.[61]

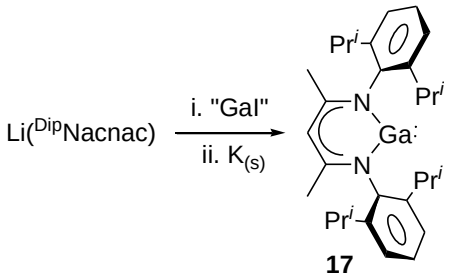

17

Scheme 4. Synthesis of **17**.

A number of neutral six-membered indium(I) heterocycles have been prepared to date, **18 - 22** (Figure 8).[55,62,63,64] Complexes **18**, **19**, and **20** crystallize in the monomeric state, whereas **21** and **22** are dimers. This is most likely due to the greater ligand steric bulk of **18**, **19**, and **20** compared to that of dimeric **21** and **22**. While **21** and **22** crystallize in the dimeric state, they have been shown to be monomers in non-coordinating solvent solutions.[64] Theory on models of these complexes, [:In{[(N(R)C(R')]$_2$CH}] (R = H, Me, Ph or Dip; R' = H, Me or CF_3), has given much insight into their bonding.[44,45,54,55] As in the previously discussed indium(I) heterocycles, the six-membered species exhibit similar electronic characteristics to their aluminum and gallium counterparts, but have higher singlet-triplet energy gaps of 55.1-67.1 kcal/mol.[44,45] In addition, the lone pair on the indium center was found to reside in the HOMO. It was also found that should the backbone substituents be replaced by electron withdrawing groups, the HOMO energy would be reduced, thereby reducing the nucleophilic character of the heterocycle.[18]

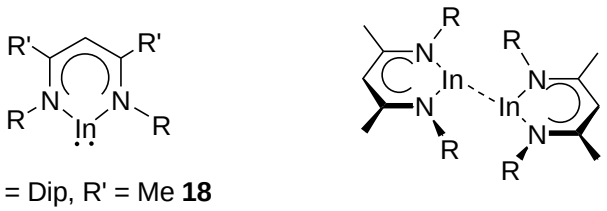

R = Dip, R' = Me **18**
R = Dip, R' = CF_3 **19**
R = Dip/C_6H_4OMe-2, R' = Me **20**

R = $C_6H_2Me_3$-2,4,6 **21**
R = $C_6H_3Me_2$-2,6 **22**

Figure 8. Neutral six-membered indium(I) heterocycles.

Six-membered thallium(I) heterocycles have been synthesized as well as theoretically studied. To date, complexes **23-27** (Figure 9) have been prepared via salt elimination reactions using the β-diketiminate class of ligand.[55, 65-67] Complexes **23-26** are found in the monomeric state, while **27**, with less ligand steric bulk, crystallizes in the dimeric state. Theoretical calculations on the models, [:Tl{[(N(R)C(R')]$_2$CH}] (R = Ph or Dip; R' = Me), suggest that the six-membered thallium(I) heterocycles are quite different from their aluminum and gallium counterparts. For example, their HOMOs are ligand based with the metal lone pair now residing in the HOMO-2. The LUMO is comprised of the empty p-orbital at thallium and the HOMO-2-LUMO gap is *ca.* 115 kcal/mol. This great disparity between the lighter and heavier congeners can be attributed to the "inert pair" effect.[45,55]

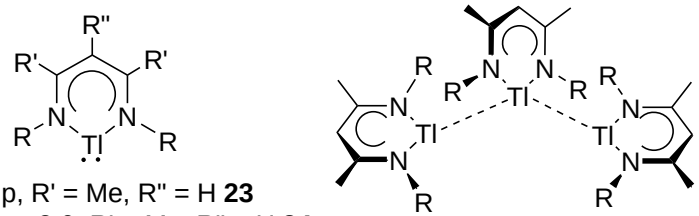

R = Dip, R' = Me, R'' = H **23**
R = $C_6H_3Me_2$-2,6, R' = Me, R'' = H **24**
R = $SiMe_3$, R' = Ph, R'' = H **25**
R = Dip, R' = H, R'' = Ph **26**

R = $C_6H_3Me_2$-3,5 **27**

Figure 9. β-Diketiminato thallium(I) complexes.

1.5 Subvalent Group 14 Chemistry

The accessibility of the lower oxidation states of the group 14 elements has been a main area of interest, and has become increasingly popular over the last several years. The strive for lower oxidation states of the group 14 elements is mostly aimed at silicon, germanium and tin, as lead almost exclusively prefers the divalent state. Lead's preference of the +2 oxidation state is most likely due to the inert pair effect as was discussed in a previous section. In reference to the group 14 elements, the term "lower valence" indicates the use of fewer than four electrons in bonding.[68] The divalent state of the group 14 elements is of great interest to the field, due to silicon, germanium and tin species of this type being considered carbene analogues. They are considered carbene analogues because of their bent structure with a lone pair, and because they undergo the general type of carbene reactions to give new bonds to the element as seen in Figure 10.[68] The greatest advancement of stabilization of low oxidation state group 14 elements has come from the use of bulky ligands and these will be subsequently addressed in section 1.6. This section will serve only as a general introduction to the field.

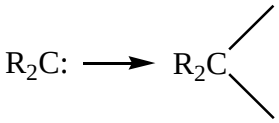

Figure 10. General carbene reaction.

The initial investigations into low oxidation state silicon chemistry began with attempts to prepare the silicon dihalides. Divalent silicon species are thermodynamically unstable under normal conditions; however, it was found that by carrying out a comproportionation reaction at high temperature and then trapping the desired product through rapid chilling using liquid nitrogen, divalent SiF_2 could be obtained (Scheme

5).[68,69] SiF_2 is a reddish-brown solid with a bond angle of 101°C that is only stable for a few minutes under reduced pressure. The related $SiCl_2$ species was prepared via a similar synthetic route, as well as by other means. For example, the reaction of Si_2Cl_6 with KSi at highly elevated temperatures afforded the divalent silicon chloride species $SiCl_2$ (Scheme 5).[68,70] At about the same time, divalent silicon iodide species were also prepared. While they are not monomeric SiI_2 species, treatment of $(SiPh_2)_n$ with HI and $AlCl_3$ affords polymeric divalent compounds such as Si_4I_8, Si_5I_{10}, and Si_6I_{12}.[68,71]

$$SiF_4 + Si \xrightleftharpoons{1150^\circ C} 2SiF_2$$

$$Si_2Cl_6 \xrightarrow[1450^\circ C]{KSi} 3SiCl_2$$

Scheme 5. Divalent silicon halide examples.

Subvalent germanium halide compounds have also been accessed. For example, GeF_2 is formed when anhydrous HF is placed in a bomb at 200°C with Ge. The resulting GeF_2 is a white crystalline solid that is very stable, with a melting point slightly exceeding 110°C. GeF_2 may also be prepared via the reaction of Ge and GeF_4 at elevated temperatures.[68,72] In addition, while much less stable than their fluoride analogue, all of the other germanium dihalides may be prepared as shown in scheme 6.

$$Ge + GeX_4 \longrightarrow 2GeX_2$$

X= Cl, Br, I

Scheme 6. General synthesis of germanium dihalides.

Tin(II) species are much more prevalent than their lighter congeners due to the increase in stability of the lower oxidation states as the group descends. Because of this fact, several tin(II) compounds are known and have been known for quite some time. For

example, the fluoride, chloride and bromide divalent species are known. $SnCl_2$ and SnF_2 are prepared by the reaction of Sn metal in the presence of gaseous HCl or HF respectively. The analogous bromide is made by dissolving tin metal in aqueous HBr and then later purifying by distillation.[68] Although they are hydrolyzed by water over time, these complexes are relatively stable as demonstrated by SnF_2 being used in toothpaste for the purpose of hardening tooth enamel.[68] In addition, there are several examples of Sn^{2+} ions occurring in solutions. These solutions are extremely air and moisture sensitive, usually leading to the formation of tin(IV) species. In 1980 it was shown that under anhydrous conditions, a tin(II) hydroxide could be formed.[73] Furthermore, there are several known carboxylates and carboxylato anion complexes that present tin in the +2 oxidation state. These include but are not limited to the $Sn(O_2CCF_3)_2$ and $[Sn(O_2CMe)_3]^-$ complexes.[68]

The most preferred and observed oxidation state for lead is +2. This is due by in large to the inert pair effect which has been previously discussed. This being the case, divalent lead chemistry is extremely well known. For example, all of the lead(II) halides are known and easily accessible. In contrast to the tin analogues, the lead(II) halides are all very stable and anhydrous as would be expected upon descent of the group.[68] In addition, there are several other crystalline lead(II) salts that are known, such as $PbSO_4$ and $PbCrO_4$. Most of these are insoluble.[68] Furthermore, lead(II) oxide is known and has two forms: litharge, red with a layer structure and massicott, yellow with a chain structure.[68]

1.6 Group 14 Metal(II) *N*-Heterocyclic Carbene Analogues

Aspects of this thesis deal with the increasingly popular area of low oxidation state group 14 metal(II) NHC analogues. As such, this realm of chemistry and their complexes prepared to date, shall be introduced and summarized.[18] It will focus on the four, five, and six-membered silicon, germanium, tin, and lead analogues. Carbon will not be discussed as carbene chemistry is well known, and several reviews have been published.[15a,74] Amidinate, guanidinate, diazobutadiene (DAB), and β-diketiminate (Nacnac) ligands with varying steric bulk have been used throughout the field in order to stabilize group 14 metal(II) heterocycles.

The four-membered group 14 metal(II) NHC analogues have the general form of **D**, **E**, and **E'** (Figure 11). The amidinate and guanidinate species[75], **D**, will include species in the form of **E**, as they are still clearly in the +2 oxidation state.[18]

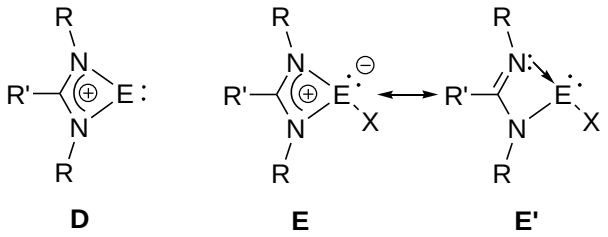

R, R', R" = H, alkyl, aryl etc.
X = Cl, Br, I
E = Group 14 element

Figure 11. General forms of four-membered group 14 metal(II) NHC analogues.

Four-membered silicon(II) NHC analogues of type **D**, have yet to be prepared. Roesky and co-workers have carried out reduction reactions leading to the synthesis of the imine stabilized amino chloro silylene, **28**, with the form of **E'**.[76] Complex **28** was also prepared, and in a much higher yield, by the addition of $LiNTMS_2$ to precursor **29b** as seen in Scheme **7**.[77] In addition, complexes **30a-d** are formed via the substitution of one chlorine

from **29a** with a variety of R groups, followed by reduction with potassium.[78] Finally, Roesky and co-workers, have prepared complex **31**, and although it has two silicon(I) centers, it is mentioned here due to it being stabilized by an amidinate and its influence on the understanding of low oxidation state silicon chemistry.

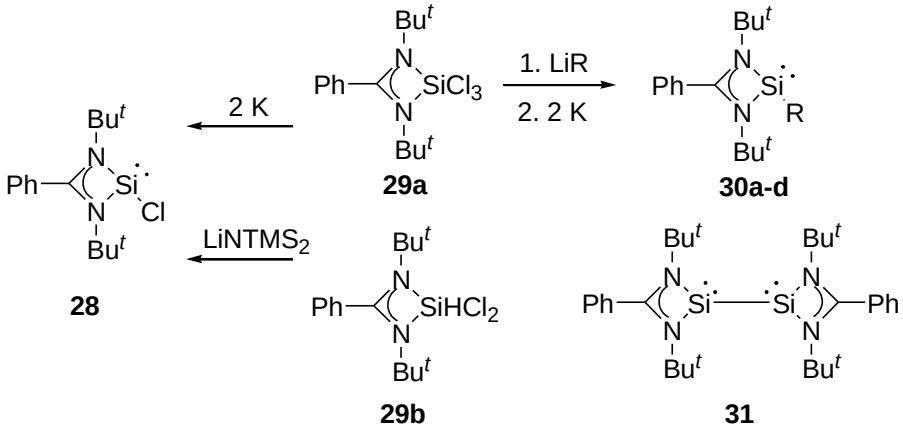

For **30**, R = (**a**) NMe_2, (**b**) OBu^t, (**c**) OPr^i, and (**d**) $P(Pr^i)_2$

Scheme 7. Further chemistry of **29**.

Four-membered germanium(II) NHC analogues of type **D** are unknown. The bulk of known four-membered germanium(II) heterocycles are synthesized via the lithiation of an amidinate or guanidinate followed by the addition to $GeCl_2$·dioxane (Scheme 8). Complexes **32a-c** are tri-coordinate germanium(II) species which have the form of **E**. In addition, it was found that by reducing the steric bulk of the ligand, the tetra-coordinate germanium (II) species, **33a-b**, are formed.[79,80] Furthermore, the addition of diaminogermanium(II) **34** to diisopropyl carbodiimide, also yields a tricoordinate germanium(II) species, guanidinato(amino)germanium (II) **35** (Scheme 9).[81] Although not germanium(II) species, it is worth mentioning that complexes **32a-c**, can be reduced to form the corresponding germanium(I) dimers.[82,83]

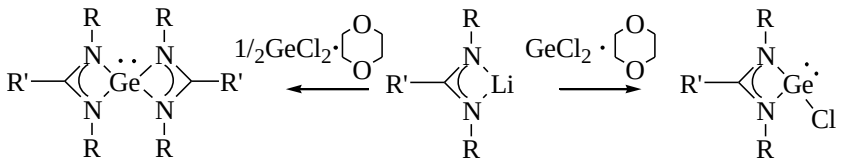

33a: R = Dip R' = H
33b: R = Pr^i R' = TMS

32a: R = Dip R' = Bu^t
32b: R = Dip R' = N(Pr^i)$_2$
32c: R = Bu^t R' = Ph
32c: R = Dip R' = N(Cy)$_2$
32c: R = Dip R' = *cis*-2,6-Me$_2$C$_5$H$_8$N

Scheme 8. Synthesis of **32** and **33**.

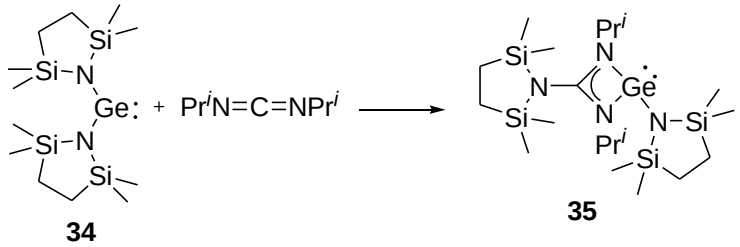

34 **35**

Scheme 9. Synthesis of **35**.

Four-membered tin(II) heterocycles of type **D** have not been reported and there are very few examples of type **E**. One example of a chloride complex of type **E** is formed by the addition of $SnCl_2$ to tris(trimethylsilyl)phenylamidine with elimination of trimethylsilylchloride.[84] Another two examples are complexes **36** and **37a**, which are prepared by reacting the lithium amidinate with $SnCl_2$ (Figure 12).[85,86] Complexes analogous to **37a** have been prepared via the substitution of the chloride using a variety of lithium bases LiR (R = OPr^i, NMe$_2$, and N(TMS)$_2$) to give **37b-d**.[86] Several other analogues, but with differing backbones and R groups, can be obtained by sequential addition of the lithium amidinate and lithium amide to give complexes **37e-k**.[87,88,89,90] Furthermore, it was shown that upon reduction of ligand steric bulk, that the tetracoordinate tin(II) complex, **38a**[86] was prepared. Several analogues of **38a**, (**38a-i**) have been prepared via the same method, all with slight changes to their corresponding R groups and

backbones.[91-94] One of particular interest is complex **38b** which is the bicyclic analogue of **36**, which was prepared via the addition of two equivalents of the lithium amidinate to $SnCl_2$.[85]

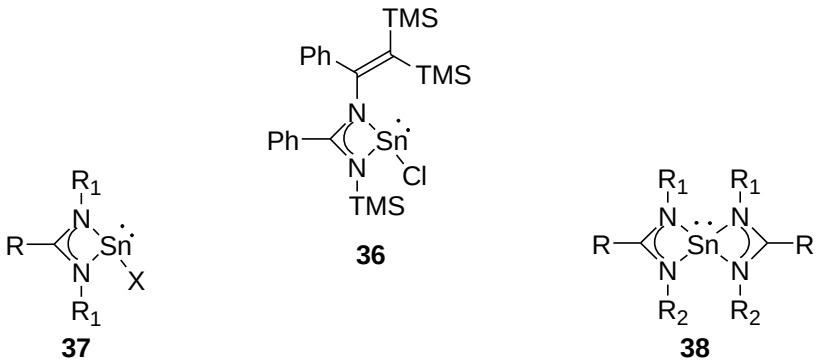

36 **37** **38**

37a: R = Bu^t R_1 = Dip X = Cl
37b: R = Bu^t R_1 = Dip X = OPr^i
37c: R = Bu^t R_1 = Dip X = $N(Me)_2$
37d: R = Bu^t R_1 = Dip X = $N(TMS)_2$
37e: R = Me R_1 = Cy X = $N(TMS)_2$
37f: R = Bu^t R_1 = Cy X = $N(TMS)_2$
37g: R = Bu^t R_1 = TMS X = $N(TMS)_2$
37h: R = Ph R_1 = TMS X = $N(TMS)_2$
37i: R = Ph R_1 = $Si(Me)_2Ph$ X = $N(TMS)_2$
37j: R = Ph R_1 = TMS X = $OC(Ph)_3$
37k: R = Ph R_1 = $Si(Me)_2Ph$ X = $OC(Ph)_3$

38a: R = Me R_1 = R_2 = Dip
38b: R = Ph R_1 = C(Ph)=$C(TMS)_2$ R_2 = TMS
38c: R = Ph R_1 = R_2 = TMS
38d: R = 4-Ph-C_6H_4 R_1 = R_2 = TMS
38e: R = Me R_1 = R_2 = Cy
38f: R = Bu^t R_1 = R_2 = Cy
38g: R = Me R_1 = R_2 = TMS
38h: R = Ph R_1 = R_2 = $Si(Me)_2Ph$
38i: R = Ph R_1 = Bu^t R_2 = TMS

Figure 12. Mono- and bicyclic tin(II) compounds.

There are only a handful of four-membered lead(II) heterocycles known to date. Complexes **39a-c** (Figure 13) are of form **E**, and are prepared via the reaction of one equivalent of either the amidinate or guanidinate lithium precursor with $PbCl_2$ to give the expected lead(II) chlorides. Another example is the tetra-coordinate lead(II) complex, **40** (Figure 13), which is formed via the reaction of two equivalents of a lithium amidinate with $PbCl_2$.

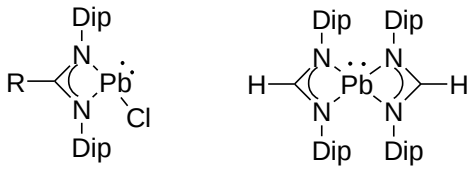

39 **40**

39a: R = Bu^t
39b: R = N(Cy)$_2$
39c: R = NH(Dip)

Figure 13. Lead(II) four-membered ring systems.

This section will serve as an overview of the five-membered group 14 element(II) analogues that have been prepared to date. These have the general form of **F** (Figure 14).[18]

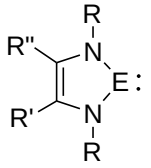

F

R, R', R'' = H, alkyl, aryl etc.
E = Group 14 element

Figure 14. General form of five-membered group 14 element(II) NHC analogues.

Five-membered silicon(II) heterocycles are well known, and have been studied for many years. The initial discovery of a NHC silicon(II) analogue was by West and coworkers in 1994, and this has become an ever increasing area of chemistry since. The popularity of N-heterocyclic silylenes has arisen due to the fact that they are the largest group of silylenes and provide the largest diversity in structure and reactivity of such systems. This area of chemistry has been reviewed.[95]

Since West and coworkers discovery in 1994, a number of other isolable silylenes have been reported and these can be classified into three groups. The first group is comprised of unsaturated silylenes represented by **41**. Complex **41a** is the first five-membered silicon(II) heterocycle, to be reported by West and coworkers (Figure 15).[96] In

addition, in 2009, Cui and coworkers added to this chemistry by synthesizing **41b-c**[97], which are aryl substituted versions of **41a**. Complex **41c** was synthesized via the hexachlorodisilyldiamine precursor, [{Si_2Cl_6(Ar-DAB)$_2$}] (Ar-DAB = {N(Dip)C(H)}$_2$), by reduction with six equivalents of potassium graphite.[97] The synthesis of **41a-b** involves the reduction of the dihalosilane precursor in a polar solvent with potassium, followed by the dehydrochlorination of the corresponding chlorosilanes with a bulky NHC.[98]

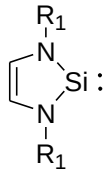

41

41a: R_1 = Bu^t
41b: R_1 = Mes
41c: R_1 = Dip

Figure 15. Unsaturated five-membered silicon(II) heterocycles.

The second group of known isolable silylenes are the saturated examples represented by **42** (Figure 16). The first of these, **42a**, was also reported by West and coworkers.[99] Since West's publication, the analogous compounds, **42b-e**, were prepared.[100,101] All of the analogues can be synthesized via the reduction of a dihalosilane precursor in a polar solvent with either potassium metal, a sodium-potassium alloy or potassium graphite.

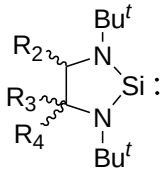

42

42a: $R_2 = R_3 = R_4 = H$
42b: $R_2 = R_3 = Me$, $R_4 = H$
42c: $R_2 = R_3 = H$, $R_4 = Me$
42d: $R_2 = R_3 = H$, $R_4 = Bu^t$
42e: $R_2 = H$, $R_3 = R_4 = Me$

Figure 16. Saturated five-membered silicon(II) heterocycles.

The third group of five-membered silicon(II) heterocycles are known as benzo-fused and are represented by **43** (Figure 17). Four examples of benzo-fused five-membered silicon(II) heterocycles have been prepared, **43a-d**, including the only example of a bis-silylene **43d**.[102-104] These were prepared via the same general route as the saturated examples. The dihalosilane precursor was reduced in a polar solvent with either potassium, sodium-potassium alloy, or potassium graphite.

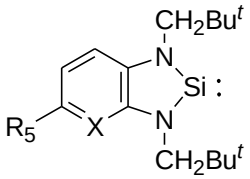

43

43a: $R_5 = H$, X = CH
43b: $R_5 = Me$, X = CH
43c: $R_5 = H$, X = N
43d: R_5 = **43a**, X = CH

Figure 17. Benzo-fused five-membered silicon(II) heterocycles.

Five-membered germanium(II) heterocycles are common, and have been known even before the corresponding carbenes. There is a large array of five-membered N-heterocyclic germylenes incorporating many backbones and substituents. The most related to the general form of **F** are complexes **44** and **45**. Complexes **44a-d** are unsaturated

analogues with differing substituents, whereas complexes **45a-d** are saturated examples with differing backbones (Figure 18).[41,105,106,107] In addition, and also of similar form to **F**, complexes **46a-f** have been prepared, and are known as benzannulated species.[103,108,109] Complexes **46a-c** were the first examples of five-membered germanium(II) heterocycles. Other examples but with a much larger backbone, are the acenaphthene substituted species, **47a-c**.[110] These are prepared via the addition of the dimagnesium precursor to $GeCl_2$·dioxane, which directly gives the desired product.[110] In addition, similar to **46** in that there is a benzene ring fused to the backbone, the bis(germylene) complexes **48a-e**, are connected via a variety of linkers (Figure 19).[111,112,113] The only known example of a macrocyclic five-membered germanium(II) heterocycle is **49**.[114] Complexes **48g-i** and **49** are prepared by the one step addition of two equivalents of $Ge[N(TMS)_2]_2$ to a tetra-amino precursor.[112,113,114] The remaining examples of five-membered germanium(II) heterocycles are cationic species. Reactions of **50**, which can be seen as a donor stabilized chlorogermylene[115], with either AgOTf or two equivalents of $ZrCpCl_3$ lead to the abstraction of the chloride resulting in the cationic species.

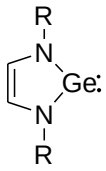

44

44a: R = Bu^t
44b: R = Np
44c: R = Dip
44d: R = Mes

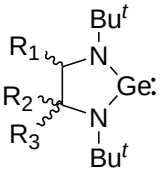

45

45a: $R_1 = R_2 = R_3 = H$
45b: $R_1 = R_2 = Me$, $R_3 = H$
45c: $R_1 = R_2 = H$, $R_3 = Me$
45d: $R_1 = R_2 = H$, $R_3 = Bu^t$

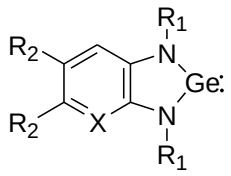

46

46a: $R_1 = H$, $R_2 = H$, X = CH
46b: $R_1 = Me$, $R_2 = H$, X = CH
46c: $R_1 = TMS$, $R_2 = H$, X = CH
46d: $R_1 = Np$, $R_2 = -(CH)_4-$, X = CH
46e: $R_1 = Np$, $R_2 = H$, X = CH
46f: $R_1 = Np$, $R_2 = H$, X = N

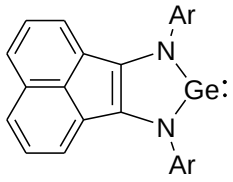

47

47a: Ar = Dip
47b: Ar = Dtb
47c: Ar = Dph

Figure 18. N-Heterocyclic germylenes (Dtb = 2,5-ditert-butylphenyl, Dph = 2-Ph-phenyl).

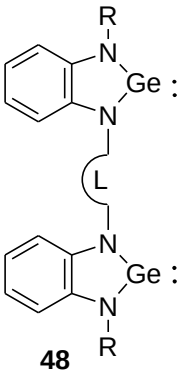

48

48a: R = Np, L = 1,3-Ph
48b: R = Np, L = 2,6-Py
48c: R = Np, L = $C(Me)_2$
48d: R = Np, L = $-(CH_2)_2-$
48e: R = Np, L = $-(CH_2)_3-$
48f: R = Np, L = 1,2-Ph
48g: R = Et, L = $-(CH_2)_2-$
48h: R = Et, L = $-(CH_2)_3-$
48i: R = Et, L = 1,3-Ph

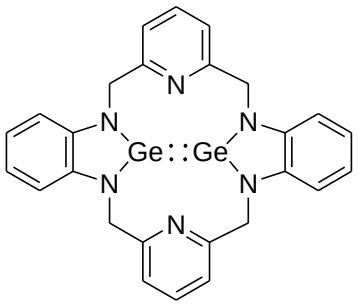

49

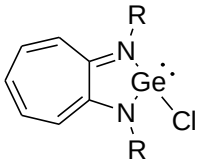

50

50a: R = Me
50b: R = Pr^i
50c: R = Pr^n

Figure 19. Bis(germylenes) and donor stabilized chloro germylene **50**.

Five membered tin NHC analogues have been synthesized and are well represented in the literature. Most reported synthetic routes involve the deprotonation of a diamine followed by addition of $SnCl_2$ or the direct addition of $Sn[N(TMS)_2]$ to a diamine. The

five-membered tin NHC analogues can generally be grouped into three main categories of saturated (**51**),[116] unsaturated (**52**),[117,118] and benzo-fused (**53**) (Figure 20).[103,109,119,120,121,122] Also among the large variety of five-membered tin NHC analogues are the bis(stannylenes) **54** with different linkers.[123,124,125,126]

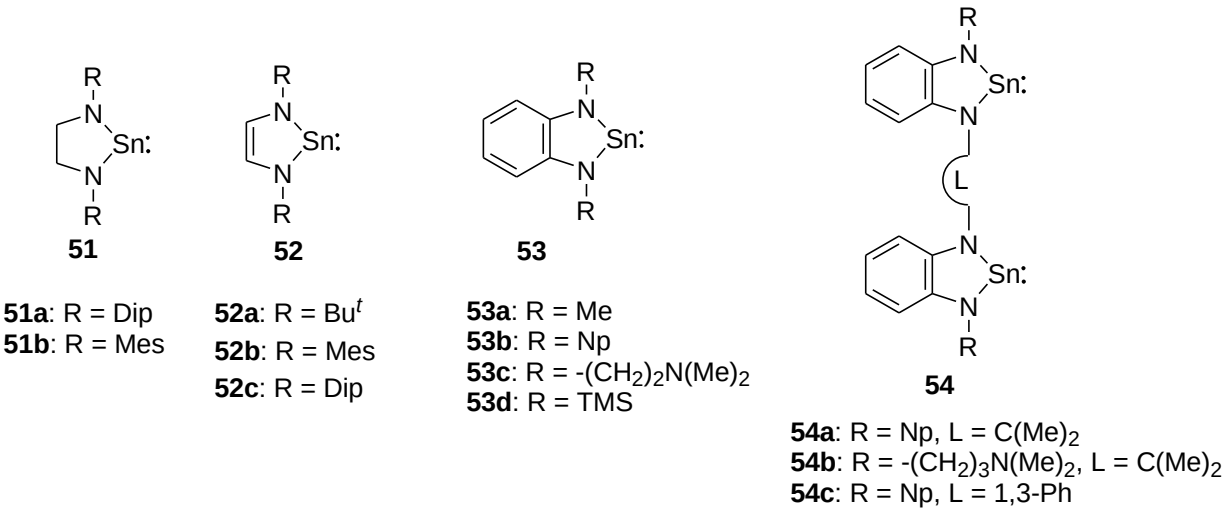

Figure 20. Examples of five-membered N-heterocyclic stannylenes.

As is the theme throughout this area of chemistry, the bulkier substituent groups on **51a**, prevent the species from dimerizing. This, however, is not the case with the sterically less hindered **51b**, which has been shown to dimerize in the solid state to give a donor-acceptor dimer involving bonds between the low valent tin centers and the lone pair of one nitrogen of each heterocycle to give a four-membered Sn_2N_2 ring. The ^{119}Sn NMR spectrum indicates that this dimeric structure does not exist in solution.[116]

Five-membered lead NHC analogues have also been prepared. Unlike their tin counterparts, only the benzo-fused **55** and saturated backbone **56** species have been synthesized to date (Figure 21). Although not fully characterized, Lappert and co-workers were the first to report such a species, **55a**.[127] Since this time, a series of five-membered benzo-fused lead heterocycles (**55a-d**) have been prepared and characterized via the

addition of $Pb[N(TMS)_2]_2$ to the corresponding 1,2-diaminobenzene.[128] The crystal structures of both **55a** and **55d** were obtained and it was found that they exist as dimers in the solid state with the low coordinate lead center stabilized by interaction with the aromatic ring of the second plumbylene.

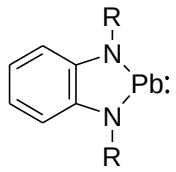

55

55a: R = Np
55b: R = Me
55c: R = Et
55d: R = Bu^i

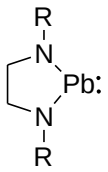

56

56a: R = Dip
56b: R = Mes

Figure 21. N-heterocyclic plumbylenes.

The two examples of saturated five-membered plumbylenes **56a** and **56b** (Figure 21), were prepared either from the appropriate diamine and $Pb[N(TMS)_2]_2$ or by addition of $PbCl_2$ to the dilithium salt. It is not surprising that **56b** gives way to a weak dimeric species in the solid state because of its smaller substituent group on the nitrogen atoms.[129]

This section will serve as an overview of the six-membered group 14 metal(II) NHC analogues that have been prepared to date. The overview will look at nacnac complexes in the general form of **G** as well as **H** because they are clearly still in the +2 oxidation state as can be seen in Figure 22.[18] The vast array of chemistry that has been carried out after the preparation of the initial six-membered group 14 metal(II) NHC analogues will not be covered.

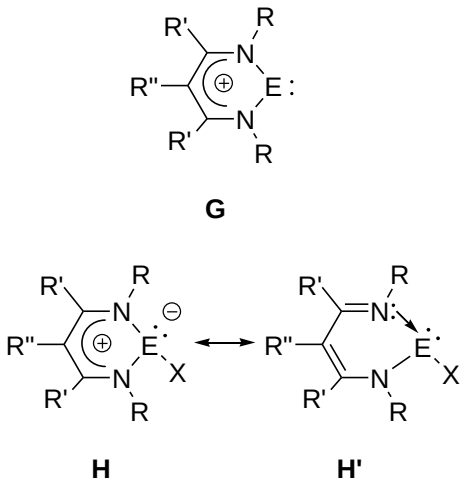

Figure 22. General structure of six-membered group 14 metal(II) heterocycles

In 2006, Driess and coworkers prepared the first six-membered silicon(II) heterocycle, **57**.[130] This is the only known species that is stable and has been isolated to date. It is shown in Scheme 10 that upon addition of the lithiated nacnac ligand to $SiBr_4$/TMEDA (TMEDA = tetramethylethylenediamine), the methyl backbone of the nacnac ligand is deprotanated. After reduction with potassium graphite, the resulting species is the neutral six-membered silicon(II) heterocycle which has two distinct resonance structures. Complex **57** will be discussed in greater detail in the later chapters. Theoretical calculations of complex **57** have recently been carried out in order to compare it against its carbon and germanium analogues.[131]

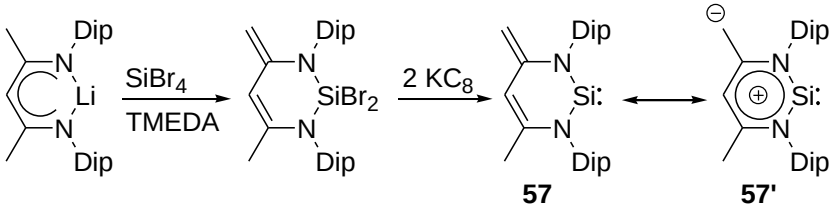

Scheme 10. Synthesis of **57**.

These two distinct resonance structures (**57** and **57′**) allow for two nucleophilic sites and therefore dominate the species' chemistry. Complex **58**, a cationic silylene, is prepared by the addition of $[H(OEt_2)_2]^+[B(C_6F_5)_4]^-$ to **57** (Figure 23).[132] Furthermore, via the negatively charged methyl backbone in **57**, complex **59** is prepared by the addition of $B(C_6F_5)_3$, giving rise to a zwiterionic borate/ silyl cation species (Figure 23).[133]

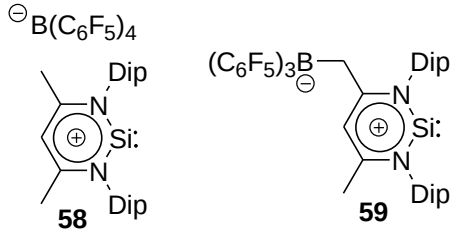

Figure 23. Complexes **58** and **59**.

Six-membered germanium(II) heterocycles are well known and there are several different groups of them. The first are the cationic species, **60a-b**, which have the structure of **G**. The second are the donor stabilized nacnac complexes, **61a-g**, all with different combinations of N-substituents and halides. In addition, the benzo-fused species, **62a-b**, have been described. Finally, the analogue of **57**, the neutral germylene **63**, has now been reported (see below).

The cationic six-membered germanium(II) heterocycles, **60a-b**, are prepared by chloride abstraction from a donor stabilized chlorogermylene (Figure 24).[134-135] In the case of **60a**, the synthesis involved the reaction of one equivalent of $B(C_6F_5)_3$ with the chlorogermylene precursor in the presence of water.[134] The other cationic example described to date, **60b**, is prepared via the straight forward salt metathesis using $NaBPh_4$.[135] The compound has yet to be crystallographically characterized.

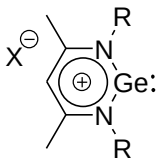

60a: R = Dip
X = $HO[B(C_6F_5)_3]_2$
60b: R = Ph
X = BPh_4

Figure 24. Cationic six-membered germanium(II) heterocycles

The second and most prominent group of six-membered germanium(II) heterocycles are the β-diketiminate or nacnac donor stabilized chlorogermylenes **61a-g** (Figure 25). This group comprises examples with a wide variety of N-substituent groups. Complexes **61a-f** are all easily prepared via the deprotonation of the nacnac ligand followed by addition of $GeCl_2$·dioxane.[135,136,137,138,139] Complex **61g**, is prepared in the same manner as above except GeI_2 is used as the germanium(II) source.[135] Another group of donor stabilized six-membered germanium(II) heterocycles are the nacnac benzo-fused species **62a-b** (Figure 25).[140]

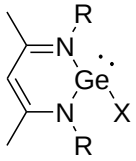

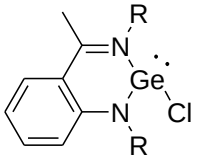

61a: R = Dip, X = Cl
61b: R = 2,6-Me_2Ph, X = Cl
61c: R = Mes, X = Cl
61d: R = Pr^i, X = Cl
61e: R = Ph, X = Cl
61f: R = C_6F_5, X = Cl
61g: R = Ph, X = I

62a: R = Dip
62b: R = Mes

Figure 25. Complexes **61** and **62**

Analogous to complexes **61a-g** are a wide range of substituted products, where the halide has been replaced by another group, as seen in Scheme 11. The newly formed complexes remain in the +2 oxidation state and a list of them can be found in Table 4.

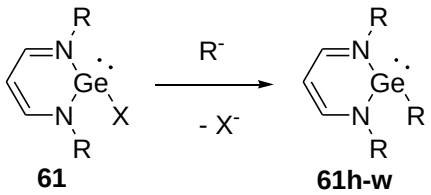

61 **61h-w**

Scheme 11. See Table 4.

Germanium (II) Precursor	Reagent(s)	Product (61, R=…)	ref.
61c	NaN_3	**61h**, N_3	137
61a, 61b	Me_3SnF	**61i**, **61j**, F	136b
61a, 61e	MeLi	**61k**, **61l**, Me	141,142
61a	^{n}BuLi	**61m**, Bu^{n}	142
61a	$LiNMe_2$	**61n**, NMe_2	143
61e	$LiN(TMS)_2$	**61o**, $N(TMS)_2$	135
61e, 62	LiOMe	**61p**, **62c**, OMe	140,141
61a	$LiPH_2$	**61q**, PH_2	144
61a	$LiP(TMS)_2$	**61r**, $P(TMS)_2$	144
61e	AgOTf	**61s**, OTf	135
61a	$NaBH_4/PMe_3$ or $AlH_3{\cdot}NMe_3$ or $K[HB(iBu)_3]$	**61t**, H	136b,145,146
61a, 61b	H_2O/NHC	**61u**, **61v**, OH	147
61a	$K[FeCp(CO)_2]$	**61w**, $FeCp(CO)_2$	148

Table 4[18]**.** Nucleophilic substituion reactions of nacnac germanium(II) chloride complexes (see Scheme 11)

Another example of a six-membered germanium(II) N-heterocycle is the neutral germylene, **63**, shown in Figure 26. In 2006, Driess and coworkers prepared **63** initially from the reaction of **60a** with amide bases LDA or $LiN(TMS)_2$, but soon found that reaction of **61a** with one equivalent of $LiN(TMS)_2$ yielded the same product.[149] In addition, very similar to the silicon analogue, **57**, complex **63** can be a precursor to other six-

membered germanium(II) N-heterocycles. Roesky and co-workers found that the borate complex **64** is prepared by the attack on the backbone methylene group after the addition of $B(C_6F_5)_3$.[150] Treating complex **64** with an NHC forms the anionic six-membered germanium(II) N-heterocycle **65** by deprotonating the unsubstituted methyl backbone (Figure 26). Reaction of **63** with either 1,2-dibromoethane or Br_2 yields **66**, a dimeric germanium(II) bromide N-heterocycle.[149]

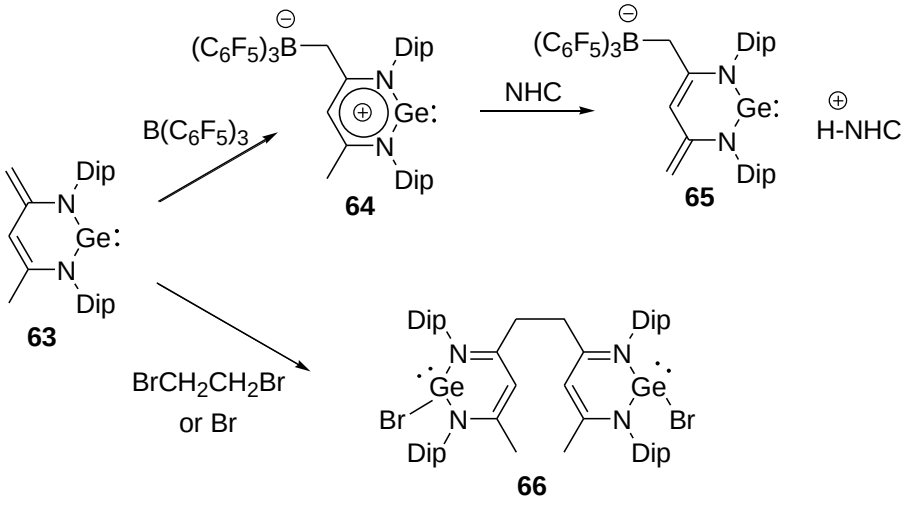

Figure 26. Neutral germylene **63** and its selected reactivity.

Six-membered tin(II) N-heterocycles are well known. For example, as is the case with germanium, there are several examples (**67a-j**) of donor stabilized complexes of form **H** (Figure 27). Complexes (**67a-j**) are all made via the deprotonation of a β-diketiminate ligand and subsequent addition of SnX_2 (X = Cl or I).[151] Complexes **67a-i**, while having the same backbone, vary greatly in their N-substituents, with them ranging from the smaller phenyl to the larger diisopropylphenyl groups. Instead of methyl groups on the backbone, complex **67j** has larger tert-butyl groups.[151] In addition, complexes **68a-b**, and **69** have been synthesized. They incorporate an anilido-imine system and a phenyl group at the γ-position respectively.[140,152] Furthermore, the dipyrromethene complex **70**, which has not

been seen in lighter group 14 element(II) N-heterocycles, has been prepared.[153] The tin analogue of **57** and **63** has not been synthesized. There are, however, two other examples of neutral six-membered N-heterocyclic stannylenes. The first is a 1,8-diaminonaphthalene derivative which is prepared either by the addition of $Sn[N(TMS)_2]_2$ to a 1,8-diamine or the addition of $SnCl_2$ to the corresponding dilithium salt.[154,155] The second is a saturated unsubstituted system with di-isopropylphenyl groups attached to the nitrogen atoms, easily prepared by the addition of $SnCl_2$ to the dilithium salt.[117] There is one example of a cationic species with the form of **H**, but it has yet to be crystallographically characterized.[156]

67a: R_1 = Ph, X = Cl
67b: R_1 = Ph, X = I
67c: R_1 = Mes, X = Cl
67d: R_1 = Dip, X = Cl
67e: R_1 = Dip, X = I
67f: R_1 = 2,6-$(C_6H_3)(C_2H_6)_2$, X = Cl
67g: R_1 = 2,6-$C_6H_3Cl_2$, X = Cl
67h: R_1 = 2,4,6-$C_6H_3Cl_3$, X = Cl
67i: R_1 = 2,4,6-$C_6H_3Br_3$, X = Cl
67j: R_1 = Dip, R_2 = Bu^t,X = Cl

R_2 = Me

68a: R = Dip
68b: R = Mes

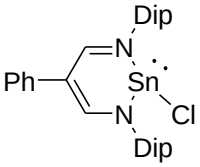

69

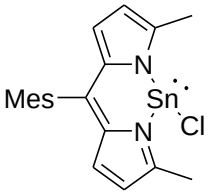

70

Figure 27. Tin(II) halide six-membered ring systems.

Several six-membered lead(II) N-heterocyclic analogues are known. In 2005, Lappert and co-workers synthesized the tetra-coordinate bis(nacnac) lead(II) complex, **71** (Figure 28).[156] This was achieved via the addition of two equivalents of the nacnac potassium salt to $PbCl_2$. Later the same group increased the steric bulk of the nacnac N-substituents to access mono nacnac lead(II) halide complexes. By the reaction of PbX_2 (X

= Cl, Br, or I) with nacnac anions, Lappert and co-workers were successful and complexes **72a-c** (Figure 28), were reported.[157] The neutral plumbylene analogue of **57** and **63** has yet to be prepared, however, complex **73**, which is a stable plumbylene, has been reported by Wass and coworkers (Figure 28).[129] They found that in the solid state, **73** is weakly dimeric, with interactions from the lead centers to neighboring aryl groups.[18]

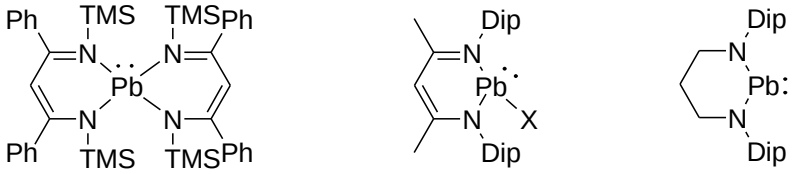

71 **72** **73**

72a: X = Cl
72b: X = Br
72c: X = I

Figure 28. Lead(II) six-membered N-heterocyclic ring systems.

1.7 References

1. Greenwood, N.N.; Earnshaw, A.; *The Chemistry of the Elements*, 2nd Edition, Oxford, Butterworth-Heinemann, **1997**.
2. Shriver, D.F.; Atkins, P.W.; Overton, T.L.; Rourke, J.P.; Weller, M.T.; Armstrong, F.A. *Inorganic Chemistry*, 4th Edition, Oxford, **2006**.
3. Ed. A.J. Downs, *Chemistry of Aluminium, Gallium, Indium and Thallium*, Glasgow, Blackie Academic and Professional, **1993**.
4. Dohmeier, C.; Loos, D.; Schnöckel, H. *Angew. Chem. Int. Ed. Engl.*, **1996**, *35*, 129, and references therein.
7. Green, L.; Mountford, P.; Smout, G.J.; Speel, S.R. *Polyhedron*, **1990**, *9*, 2763.
8. Coban, S. Diplomarbeit, Universität Karlsruhe, **1999**.
9. Baker, R.J.; Jones, C. *Dalton Trans*., **2005**, 1341.
10. (a) Hönle, W.; Miller, G.; Simon, A. *J. Solid State Chem.*, **1988**, *75*, 147; (b) Hönle, W.; Simon, A. *Z. Naturforsch.*, **1986**, *41b*, 1391.
11. (a) Beamish, J.C.; Small, R.W.H.; Worral, I.J. *Inorg. Chem.*, **1979**, *18*, 220; (b) Wei, P.; Li, X. –W.; Robinson, G.H. *Chem. Commun*., **1999**, 1287; (c) Brown, K.L.; Hall, D. *Dalton Trans*., **1973**, 1843; (d) Gerlach, G.; Hönle, W.; Simon, A. *Z. Anorg. Allg. Chem*., **1982**, *486*, 7.
12. Godfrey, S.M.; Kelly, K.J.; Kramkowski, P.; McAuliffe, C.A.; Pritchard, R.G. *Chem. Commun*., **1997**, 1001.
5. Dohmeier, C.; Robl, C.; Tacke, M.; Schnöckel, H. *Angew. Chem. Int. Ed. Engl.*, **1991**, *30*, 564.
6. Loos, D.; Schnöckel, H. *J. Organomet. Chem*., **1993**, *463*, 37.

15. (a) Schnöckel, H.; Schnepf, A. *Adv. Organomet. Chem*., **2001**, *47*, 235; (b) Linti, G.; Schnöckel, H. *Coord. Chem. Rev*., **2000**, *206-207*, 285, and references therein.

16. (a) Gemel, C.; Steinke, T.; Cokoja, M.; Kempter, A.; Fischer, R.A. *Eur. J. Inorg. Chem*., **2004**, 4161; (b) Fischer, R.A.; Weiss, J. *Angew. Chem. Int. Ed*., **1999**, *38*, 2830; (c) Uhl, W. *Coord. Chem. Rev*., **1997**, *163*, 1, and references therein.

17. (a) Bourissou, D.; Guerret, O.; Gabbai, F.P.; Bertrand, G. *Chem. Rev*., **2000**, *100*, 39; (b) Kirmse, W. *Eur. J. Org. Chem*., **2005**, 237; (c) Herrmann, W.A. *Angew. Chem. Int. Ed*., **2002**, *41*, 1290; (d) Crudden, C.M.; Allen, D.P. *Coord. Chem. Rev*., **2004**, *248*, 2247; (e) Kuhn, N.; Al-Sheikh, A. *Coord. Chem. Rev*., **2005**, *249*, 829; (f) Carmalt, C.J.; Cowley, A.H. *Adv. Inorg. Chem*., **2000**, *50*, 1, and references therein.

18. Assay, M.; Jones, C.; Driess, M. *Chem. Rev.,* advanced article published online.

19. Despagnet-Ayoub, E.; Grubbs, R.H. *J. Am. Chem. Soc.,* **2004**, *126*, 10198.

20. Findlater, M.; Hill, N.J.; Cowley, A.H. *Dalton Trans.,* **2008**, 4419.

21. Jones, C.; Junk, P.C.; Platts, J.A.; Stasch, A. *J. Am. Chem. Soc.,* **2006**, *128*, 2206.

22. Jin, G.; Jones, C.; Junk, P.C.; Lippert, K.-A.; Rose, R.P.; Stasch, A. *New J. Chem.,* **2009**, *33*, 64.

23. Green, S.P.; Jones, C.; Stasch, A. *Inorg. Chem.,* **2007**, *46*, 11.

24. Moxey, G.J.; Jones, C.; Stasch, A.; Junk, P.C.; Deacon, G.B.; Woodul, W.D.; Drago, P.R. *Dalton Trans.,* **2009**, 2630.

25. Jones, C.; Stasch, A.; Moxey, G.J.; Junk, P.C.; Deacon, G.B. *Eur. J. Inorg. Chem.,* **2009**, 3593.

26. Jones, C.; Junk, P.C.; Stasch, A.; Woodul, W.D. *New J. Chem.*, **2008**, *32*, 835.

27. Jones, C.; Junk, P.C.; Platts, J.A.; Rathmann, D.; Stasch, A. *Dalton Trans.,* **2005**, 2497.

28. Weber, L. *Coord. Chem. Revs.*, **2008**, *252*, 1.

29. Weber, L.; Schneider, M.; Lönnecke, P. *J. Chem. Soc., Dalton Trans.*, **2001**, 3459.

30. Segawa, Y.; Yamashita, M.; Nozaki, K. *Science,* **2006**, *314*, 113.

31. Marder, T. *Science*, **2006**, *314*, 69.

32. Braunschweig, H. *Angew. Chem. Int. Ed.,* **2007**, *46*, 1946.

33. Sundermann, A.; Reiher, M.; Schoeller, W.W. *Eur. J. Inorg. Chem.,* **1998**, 305.

34. Metzler-Nolte, N. *New J. Chem.,* **1998**, 793.

35. Tuononen, H.M.; Roesler, R.; Dutton, J.L.; Ragogna, P.J. *Inorg. Chem.*, **2007**, *46*, 10693.

36. Lai, C.-H.; Chou, P.-T. *Open Chem. Phys. J.,* **2008**, *1*, 51.

37. Baker, R.J.; Farley, R.D.; Jones, C.; Kloth, M.; Murphy, D.M. *J. Chem. Soc.; Dalton Trans.,* **2002**, 3844.

38. Schmidt, E.S.; Jockisch, A.; Schmidbaur, H. *J. Am. Chem. Soc.*, **1999**, *121*, 9758.

39. Schmidt, E.S.; Schier, A.; Schmidbaur, H. *J. Chem. Soc., Dalton Trans.,* **2001**, 505.

40. Pott, T.; Jutzi, P.; Kaim, W.; Schoeller, W.W.; Neumann, B.; Stammler, A.; Stammler, H.G., Wanner, M. *Organometallics,* **2002**, *21*, 3169.

41. Baker, R.J.; Jones, C.; Mills, D.P.; Pierce, G.A.; Waugh, M. *Inorg. Chim. Acta*, **2008**, *361*, 427.

42. Fedushkin, I.; Lukoyanov, A.N.; Fukin, G.K.; Ketkov, S.Y.; Hummert, M.; Schumann, H. *Chem. Eur. J.*, **2008**, *14*, 8465.

43. Baker, R.J.; Farley, R.D.; Jones, C.; Kloth, M.; Murphy, D.M. *Chem. Commun.*, **2002**, 1196.

44. Reiher, M.; Sundermann, A. *Eur. J. Inorg. Chem.*, **2002**, 1854.

45. Chen, C.-H.; Tsai, M.-L.; Su, M.-D. *Organometallics*, **2006**, *25*, 2766.

46. Cui, C.; Roesky, H.W.; Schmidt, H.-G.; Noltemeyer, M.; Hao, H.; Cimpoesu, F. *Angew.Chem. Int. Ed.*, **2000**, *39*, 4274.

47. Li, X.; Cheng, X.; Song, H.; Cui, C. *Organometallics*, **2007**, *26*, 1039.

48. Kempter, A.; Gemel, C.; Fischer, R.A. *Chem. Commun.*, **2006**, 1551.

49. Kempter, A.; Gemel, C.; Fischer, R.A. *Chem. Eur. J.*, **2007**, *13*, 2990.

50. See for example: Zhu, H.; Chai, Y.; Jancik, V.; Roesky, H.W.; Merrill, W.A.; Power, P.P. *J. Am. Chem. Soc.*, **2005**, *127*, 10170.

51. Cui, C.; Köpke, S.; Herbst-Irmer, R.; Roesky, H.W.; Noltemeyer, M.; Schmidt, H.-G.; Wrackmeyer, B. *J. Am. Chem. Soc.*, **2001**, *123*, 9091.

52. Hardman, N.J.; Cui, C.; Roesky, H.W.; Fink, W.H.; Power, P.P. *Angew. Chem. Int. Ed.*, **2001**, *40*, 2172.

53. Hardman, N.J.; Eichler, B.E.; Power, P.P. *Chem. Commun.*, **2000**, 1991.

54. Hardman, N.J.; Power, P.P. *ACS Symp. Ser.*, **2002**, *822*, 2.

55. Hill, M.S.; Hitchcock, P.B.; Pontavornpinyo, R. *Dalton Trans.*, **2005**, 273.

56. Hardman, N.J.; Power, P.P.; Gorden, J.D.; Macdonald, C.L.B.; Cowley, A.H. *Chem. Commun.*, **2001**, 1866.

57. Kempter, A.; Gemel, C.; Cadenbach, T.; Fischer, R.A. *Organometallics*, **2007**, *26*, 4257.

58. Kempter, A.; Gemel, C.; Hardman, N.J.; Fischer, R.A. *Inorg. Chem.,* **2006**, *45*, 3133.

59. Prabusankar, G.; Kempter, A.; Gemel, C.; Schröter, M.-K.; Fischer, R.A. *Angew. Chem. Int. Ed.,* **2008**, *47*, 7234.

60. Hardman, N.J.; Power, P.P. *Chem. Commun.,* **2001**, 1184.

61. Hardman, N.J. Power, P.P. *Inorg. Chem.,* **2001**, *40*, 2474.

62. Hill, M.S.; Hitchcock, P.B. *Chem. Commun.,* **2004**, 1818.

63. Hill, M.S.; Hitchcock, P.B.; Pontavornpinyo, R. *Angew. Chem. Int. Ed.,* **2005**, *44*, 4231.

64. Hill, M.S.; Hitchcock, P.B.; Pontavornpinyo, R. *Dalton Trans.,* **2007**, 731.

65. Dai. X.; Warren, T.H. *Chem. Commun.,* **2001**, 1998.

66. Cheng, Y.; Hitchcock, P.B.; Lappert, M.F.; Zhou, M. *Chem. Commun.,* **2005**, 752.

67. Hill, M.S.; Pontavornpinyo, R.; Hitchcock, P.B. *Chem. Commun.,* **2006**, 3720.

68. F. A. Cotton and G. Wilkinson, *Advanced Inorganic Chemistry,* 5th Edition, John Wiley & Sons, Inc., **1988**.

69. Gusel'nikov, L. E.; Nametkin, N. S.; *Chem. Rev.*, **1979**, *79*, 529.

70. see for example: Hargittai, I. *J. Am. Chem. Soc*., **1983**, *105*, 2895.

71. Hengge, E.; Kovar, D. *Angew. Chem. Int. Ed. Engl.*, **1981**, *20*, 678.

72. S. M. van der Kirk *Polyhedron*, **1983**, *2*, 509.

73. Neudart, B.; du Mont, W-W. *Angew. Chem. Int. Ed. Engl*., **1980**, *19*, 553.

74. For carbene reviews see: (a) Hahn, F. E.; Jahnke, M. C. Angew. *Chem., Int. Ed.,* **2008**, *47*, 3122.

75. For reviews on amidinate and guanidinate complexes see: (a) Edelmann, F.T. *Adv. Organomet. Chem*., **2008**, *57*, 183. (b) Kissounko, D.A.; Zabalov, M.V.; Brusova, G.P.; Lemenovskii, D.A. *Russ. Chem. Rev.*, **2006**, *75*, 351.

76. (a) So, C. –W.; Roesky, H.W.: Magull, J.; Oswald, R.B. *Angew. Chem. Int. Ed.*, **2006**, *45*, 3948. (b) Weidenbruch, M. *Angew. Chem. Int. Ed.*, **2006**, *45*, 4241.

77. Sen, S.S.; Roesky, H.W.; Stern, D.; Henn, J.; Stalke, D. *J. Am. Chem. Soc.,* **2010**, *132*, 1123.

78. So, C. –W.; Roesky, H.W.; Gurubasavaraj, P.M.; Oswald, R.O.; Gamer, M.T.; Jones, P.G.; Blaurock, S. *J. Am. Chem. Soc.*, **2007**, *129*, 12049.

79. Jones, C.; Rose, R.P.; Stasch, A. *Dalton Trans.*, **2008**, 2871.

80. Karsch, H.H.; Schlueter, P.A.; Reisky, M. *Eur. J. Inorg. Chem.*, **1998**, 433.

81. Chen, T.; Hunks, W.; Chen, P.S.; Stauf, G.T.; Cameron, T.M.; Xu, C.; DiPasquale, A.G.; Rheingold, A.L. *Eur. J. Inorg. Chem.*, **2009**, 2047.

82. Green, S.P.; Jones, C.; Junk, P.C.; Lippert, K.–A.; Stasch, A. *Chem. Commun.*, **2006**, 3978.

83. Nagendran, S.; Sen, S.S.; Roesky, H.W.; Koley, D.; Grubmueller, H.; Pal, A.; Herbst-Irmer, R. *Organometallics*, **2008**, *27*, 5459.

84. Dehnicke, K.; Ergezinger, C.; Hartmann, E.; Zinn, A. *J. Organomet. Chem.*, **1988**, *352*, C1.

85. Hitchcock, P.B.; Lappert, M.F.; Layh, M. *J. Chem. Soc., Dalton Trans.*, **1998**, 3113.

86. Nimitsiriwat, N.; Gibson, V.C.; Marshall, E.L.; White, A.J.P.; Dale, S.H.; Elsegood, M.R.J. *Dalton Trans.*, **2007**, 4464.

87. Foley, S.R.; Yap, G.P.A.; Richeson D.S. *J. Chem. Soc., Dalton Trans.*, **2000**, 1663.

88. Foley, S.R.; Zhou, Y.; Yap, G.P.A.; Richeson, D.S. *Inorg. Chem.*, **2000**, *39*, 924.

89. Aubrecht, K.B.; Hillmyer, M.A.; Tolman, W.B. *Macromolecules*, **2002**, *35*, 644.

90. Foley, S.R.; Yap, G.P.A.; Richeson, D.S. *Organometallics*, **1999**, *18*, 4700.

91. Roesky, H.W.; Meller, B.; Noltemeyer, M.; Schmidt, H.-G.; Scholz, U.; Sheldrick, G.M. *Chem. Ber.*, **1988**, *121*, 1403.

92. Kilimann, U.; Noltemeyer, M.; Edelmann, F.T. *J. Organomet. Chem.*, **1993**, *443*, 35.

93. Zhou, Y.; Richeson, D.S. *J. Am. Chem. Soc.*, **1996**, *118*, 10850.

94. Antolini, F.; Hitchcock, P.B.; Khvostov, A.V.; Lappert, M.F. *Can. J. Chem.*, **2006**, *84*, 269.

95. See: (a) Kira, M.; Iwamoto, T.; Ishida, S. *Bull. Chem. Soc. Jpn.*, **2007**, *80*, 258. (b) Takeda, N.; Tokitoh, N. *Synlett*, **2007**, *16*, 2483. (c) Ottosson, H.; Steel, P.G. *Eur. J. Inorg. Chem.*, **2006**, *12*, 1577. (d) Hill, N.J.; West. R. *J. Organomet. Chem.*, **2004**, *689*, 4165. (e) Kira, M. *J. Organomet. Chem.*, **2004**, *689*, 4475. (f) Okazaki, M.; Tobita, H.; Ogino, H. *Dalton Trans.*, **2003**, 493. (g) Gehrhus, B.; Lappert, M.F. *J. Organomet. Chem.*, **2001**, *617*, 209. (h) Haaf, M.; Schmedake, T.A.; West, R. *Acc. Chem. Res.*, **2000**, *33*, 704.

96. Denk, M.; Lennon, R.; Hayashi, R.; West, R.; Belyakov, A.V.; Verne, H.P.; Haaland, A.; Wagner, M.; Metzler, N. *J. Am. Chem. Soc.*, **1994**, *116*, 2691.

97. Kong, L.; Zhang, J.; Song, H.; Cui, C. *Dalton Trans.*, **2009**, 5444.

98. (a) Cui, H.; Shao, Y.; Li, X.; Kong, L.; Cui, C. *Organometallics*, **2009**, *28*, 5191, (b) Ghadwal, R.S.; Roesky, H.W.; Merkel, S.; Henn, J.; Stalke, D. *Angew. Chem. Int. Ed.*, **2009**, *48*, 5683.

99. West, R.; Denk, M. *Pure Appl. Chem.,* **1996**, *68*, 785.

100. Li, W.; Hill, N.J.; Tomasik, A.C.; Bikzhanova, G.; West, R. *Organometallics,* **2006**, *25*, 3802.

101. Tomasik, A.C.; Mitra, A.; West, R. *Organometallics,* **2009**, *28*, 378.

102. Gehrhus, B.; Lappert, M.F.; Heinicke, J.; Boese, R.; Blaeser, D. *J. Chem. Soc., Chem. Commun.,* **1995**, 1931.

103. Heinicke, J.; Oprea, A.; Kindermann, M.K.; Karpati, T.; Nyulaszi, L.; Veszpremi, T. *Chem.Eur. J.,* **1998**, *4*, 541.

104. Gehrhus, B.; Hitchcock, P.B.; Lappert, M.F. *Z. Anorg. Allg. Chem.,* **2005**, *631*, 1383.

105. Herrmann, W. A.; Denk, M.; Behm, J.; Scherer, W.; Klingan, F.–R.; Bock, H.; Solouki, B.; Wagner, M. *Angew. Chem. Int. Ed. Engl.,* **1992**, *31*, 1485.

106. Kuehl, O.; Loennecke, P.; Heinicke, J. *Polyhedron,* **2001**, *20*, 2215.

107. Tomasik, A.C.; Hill, N. J.; West, R. *J. Organomet. Chem.,* **2009**, *694*, 2122.

108. (a) Pfeiffer, J.; Noltemeyer, M.; Meller, A. *Z. Anorg. Allg. Chem.,* **1989**, 145. (b) Pfeiffer, J.; Noltemeyer, M.; Meller, A. *Chem. Ber.,* **1989**, 245.

109. Heinicke, J.; Operea, A. *Heteroatom Chem.,* **1998**, *9*, 439.

110. Fedushkin, I.L.; Skatova, A.A.; Chudakova, V.A.; Khvoinova, N.M.; Baurin, A.Y.; Dechert, S.; Hummert, M.; Schumann, H. *Organometallics,* **2004**, *23*, 3714.

111. Hahn, F.E.; Zabula, A.V.; Pape, T.; Hepp, A. *Eur. J. Inorg. Chem.,* **2007**, 2405.

112. Zabula, A.V.; Hahn, F.E.; Pape, T.; Hepp, A. *Organometallics,* **2007**, *26*, 1972.

113. Hahn, F.E.; Zabula, A.V.; Pape, T.; Hepp, A. *Z. Anorg. Allg. Chem.,* **2008**, *634*, 2397.

114. Hahn, F.E.; Zabula, A.V.; Pape, T.; Hupka, F. *Z. Anorg. Allg. Chem.,* **2009**, *635*, 1341.

115. Dias, H.V.R.; Wang, Z. *J. Am. Chem. Soc.,* **1997**, *119*, 4650.

116. Mansell, S.M.; Russell, C.A.; Wass, D. F. *Inorg. Chem.,* **2008**, *47*, 11367.

117. Gans-Eichler, T.; Gudat, D.; Nieger, M. *Angew. Chem. Int. Ed.,* **2002**, *41*, 1888.

118. Gans-Eichler, T.; Gudat, D.; Naettinen, K.; Nieger, M. *Chem. Eur. J.,* **2006**, *12*, 1162.

119. Braunschweig, H.; Gehrhus, B.; Hitchcock, P.B.; Lappert, M.F. *Z. Anorg. Allg. Chem.,* **1995**, *621*, 1922.

120. Hahn, F.E.; Wittenbecher, L.; Huehn, M.; Luegger, T.; Froehlick, F. *J. Organomet. Chem.,* **2001**, *617*, 629.

121. Hahn, F.E.; Wittenbecher, L.; Van, D.L.; Zabula, A.V. *Inorg. Chem.,* **2007**, *46*, 7662.

122. Ullah, F.; Kuehl, O.; Rehman, W.; Jones, P.G.; Heinicke, J. *Polyhedron,* **2010**, *29*, 1041.

123. Zabula, A.V.; Pape, T.; Hepp, A.; Hahn, F.E. *Dalton Trans.,* **2008**, 5886.

124. Zabula, A.V.; Pape, T.; Hepp, A.; Schappacher, F.M.; Rodewald, U.C.; Poettgen, R.; Hahn, F.E. *J. Am. Chem. Soc.,* **2008**, *130*, 5648.

125. Zabula, A.V.; Pape, T.; Hepp, A.; Hahn, F.E. *Organometallics,* **2008**, *27*, 2756.

126. Hahn, F.E.; Zabula, A.V.; Pape, T.; Hepp, A.; Tonner, R.; Haunschild, R.; Frenking, G. *Chem. Eur. J.,* **2008**, *14*, 10716.

127. Gerhrus, B.; Hitchcock, P.B.; Lappert, M.F. *J. Chem. Soc., Dalton Trans.,* **2000**, 3094.

128. Hahn, F.E.; Heitmann, D.; Pape, T. *Eur. J. Inorg. Chem.,* **2008**, 1039.

129. Charmant, J.P. H.; Haddow, M.F.; Hahn, F.E.; Deitmann, D.; Froehlick, R.; Mansell, S.M.; Russell, C.A.; Wass, D. F. *Dalton Trans.,* **2008**, 6055.

130. Driess, M.; Yao, S.; Brym, M.; van Wuellen, C.; Lentz, D. *J. Am. Chem. Soc*., **2006**, *128*, 9628.

131. Nyiri, K.; Veszpremi, T. *Organometallics,* **2009**, *28*, 5909.

132. Driess, M.; Yao, S.; Brym, M. van Wuellen, C. *Angew. Chem. Int. Ed.,* **2006**, *45*, 6730.

133. Wang, R. –H.; Su, M. –D. *J. Phys. Chem. A,* **2008**, *112*, 7689.

134. Stender, M.; Phillips, A.D.; Power, P.P. *Inorg. Chem.,* **2001**, *40*, 5314.

135. Akkari, A.; Byrne, J.J.; Saur, I.; Rima, G.; Gornitzka, H.; Barrau, J. *J. Organomet. Chem.,* **2001**, *622*, 190.

136. (a) Ding, Y.; Roesky, H.W.; Noltemeyer, M.; Schmidt, H.–G. *Organometallics,* **2001**, *20*, 1190. (b) Ding, Y.; Hao, H.; Roesky, H.W.; Noltemeyer, M.; Schmidt, H.–G. *Organometallics,* **2001**, *20*, 4806.

137. Ayers, A.E.; Klapoetke, T.M.; Dias, H.V.R. *Inorg. Chem.,* **2001**, *40*, 1000.

138. Arii, H.; Nakadate, F.; Mochida, K. *Organometallics,* **2009**, *28*, 4909.

139. Yang, Z.; Ma, X.; Roesky, H.W.; Yang, Y.; Zhu, H.; Magull, J.; Ringe, A. *Z. Anorg. Allg. Chem.,* **2008**, *634*, 1490.

140. Mcheik, A.; Katir, N.; Castel, A.; Gornitzka, H.; Massou, S.; Riviere, P.; Hamieh, T. *Eur. J. Inorg. Chem.,* **2008**, 5397.

141. Saur, I.; Miqueu, K.; Rima, G.; Barrau, J.; Lemierre, V.; Chrostowska, A.; Sotiropoulos, J.–M.; Pfister-Guillouzo, G. *Organometallics,* **2003**, *22*, 3143.

142. Ding, Y.; Ma, Q.; Roesky, H.W.; Herbst-Irmer, R.; Uson, I.; Noltemeyer, M.; Schmidt, H.–G. *Organometallics,* **2002**, *21*, 5216.

143. Jana, A.; Roesky, H.W.; Schulzke, C.; Samuel, P.P.; Doering, A. *Inorg. Chem.* **2010**, *49*.

144. Yao, S.; Brym, M.; Merz, K.; Driess, M. *Organometallics,* **2008**, *27*, 3601.

145. Pineda, L.W.; Jancik, V.; Starke, K.; Oswald, R.B.; Roesky, H.W. *Angew. Chem. Int. Ed.,* **2006**, *45*, 2602.

146. Jana, A.; Ghoshal, D.; Roesky, H.W.; Objartel, I.; Schwab, G.; Stalke, D. *J. Am. Chem. Soc.*, **2009**, *131*, 1288.

147. Pineda, L.W.; Jancik, V.; Roesky, H.W.; Neculai, D. Neculai, A. M. *Angew. Chem. Int. Ed.,* **2004**, *43*, 1419.

148. Inoue, S.; Driess, M. *Organometallics,* **2009**, *28*, 5032.

149. Driess, M.; Yao, S.; Brym, M.; van Wuellen, C. *Angew. Chem. Int. Ed.,* **2006**, *45*, 4349.

150. Jana, A.; Objartel, I.; Roesky, H.W.; Stalke, D. *Inorg. Chem.,* **2009**, *48*, 7645.

151. Dove, A.P.; Gibson, V.C.; Marshall, E.L.; Rzepa, H.S.; White, A.J.P.; Williams, D.J. *J. Am. Chem. Soc.,* **2006**, *128*, 9834.

152. Doyle, D.J.; Hitchcock, P.B.; Lappert, M.F.; Li, G. *J. Organomet. Chem.,* **2009**, *694*, 2611.

153. Kobayashi, J.; Kushida, T.; Kawashima, T. *J. Am. Chem. Soc.,* **2009**, *131*, 10836.

154. Bazinet, P.; Yap, G.P.A.; DiLabio, G.A.; Richeson, D.S. *Inorg. Chem.,* **2005**, *44*, 4616.

155. (a) Schaeffer, C.D.; Zuckerman, J.J. *J. Am. Chem. Soc.*, **1974**, *96*, 7160. (b) Drost, C.; Hitchcock, P.B.; Lappert, M.F. *Angew. Chem. Int. Ed.*, **1999**, *38*, 1113. (c) Avent, A.G.; Drost, C.; Gehrhus, B.; Hitchcock, P.B.; Lappert, M.F. *Z. Anorg. Allg. Chem.*, **2004**, *630*, 2090. (d) Jimenez-Perez, V.M.; Munoz-Flores, B.M.; Roesky, H.W.; Schulz, R.; Pal, A.; Beck, T.; Yang, Z.; Stalke, D.; Santillan, R.; Witt, M. *Eur. J. Inorg. Chem.*, **2008**, 2238.

156. Hitchcock, P.B.; Lappert, M.F.; Protchenko, A. V. *Chem. Commun.*, **2005**, 951.

157. Chen, M.; Fulton, J.R.; Hitchcock, P.B.; Johnstone, N.C.; Lappert, M.F.; Protchenko, A.V. *Dalton Trans.*, **2007**, 2770.

Chapter 2

Groups 2 and 12 Metal Gallyl Complexes Containing Unsupported Ga-M Covalent Bonds (M = Mg, Ca, Sr, Ba, Zn, or Cd)

2.1 Introduction

This area of study began in 1999 with the report of the first anionic group 13 five-membered *N*-heterocyclic carbene, NHC, analogue, [**:**Ga{[N(Bu^t)C(H)]$_2$}]$^-$ **1**.[1] Schmidbaur and co-workers synthesized **1** via a multi-step route using $GaCl_3$ as the precursor. While the initial yield was low (4%), it was shown that upon addition of the bidentate amine tmeda (*N*,*N*,*N'*,*N'*-tetramethylethylenediamine) to the final reduction step, the yield could be improved to 18%.[2] This synthetic approach, albeit with a higher yield of the final product, still required several steps and a total of fourteen days to be complete (Scheme 1).[2] In search of a higher yielding synthetic route to the desired gallium(I) species, Schmidbaur and co-workers prepared a (chloro)galla-imidazole with a moderate yield (80%) via the treatment of [{LiN(Bu^t)C(H)}$_2$] (Li_2Bu^t-DAB) with $GaCl_3$.[2,3] They then reduced the gallium(III) species with two equivalents of potassium in THF which after ten days afforded a gallium(II) dimer. Further reduction and the addition of tmeda produced the desired gallium(I) species after four days. The [K(tmeda)]$^+$ salt of **1** was found to be a dimer in the solid state with Ga·····K contacts of 3.438 Å and 3.4681 Å. While the desired gallium(I) species was synthesized by both methods, no further coordination chemistry would be carried out due to the long reduction times and low yields.

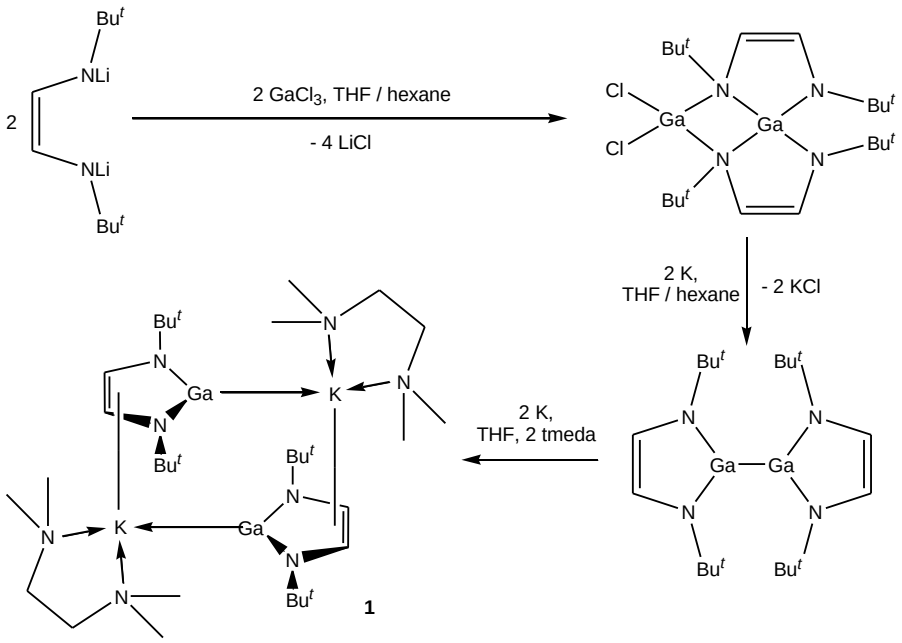

Scheme 1. The synthesis of a potassium salt of **1**.

It was not until 2002 that a high-yielding synthetic route to an anionic five-membered gallium(I) NHC analogue was reported. Jones and co-workers prepared a gallium(I) NHC analogue, [**:**Ga{[N(Dip)C(H)]$_2$}]$^-$ **2** (Dip = $C_6H_3Pr^i_2$-2,6), by using the novel reagent "GaI" as a gallium(I) source (Scheme 2).[3] The one-electron reduction of Dip-DAB ({N(Dip)C(H)}$_2$) with "GaI" in the non-coordinating solvent toluene gave, with the loss of one equivalent of gallium metal, a high yield (> 90 %) of the paramagnetic gallium(III) compound, [I_2Ga{[N(Dip)C(H)]$_2^{\cdot}$}], which was independently synthesized by another group.[4] The brownish-red solid, [I_2Ga{[N(Dip)C(H)]$_2^{\cdot}$}] was then stirred over a potassium mirror and periodically sonicated in THF for forty-eight hours. After the reduction, the product was treated with a tmeda/Et_2O mixture, and upon work up and crystallization from diethyl ether, the salt [K(tmeda)][**2**] was afforded in good yield, presumably via the known gallium(II) dimer, [Ga{[N(Dip)C(H)]$_2$}]$_2$.[5] [K(tmeda)][**2**] is extremely interesting in that the Ga·····Ga distance is only 2.88 Å, which is only 13 %

longer than a typical Ga—Ga single bond. This is in stark contrast to the complex reported by Schmidbaur, [K(tmeda)][**1**], where the Ga·····Ga distance is 4.21 Å.[2] This short Ga·····Ga distance in [K(tmeda)][**2**] is thought to be mostly due to the partial donation of electron density from the gallium centers into the empty gallium *p*-orbital of an adjacent heterocycle. With a short and high-yielding synthesis of a gallium(I) NHC analogue, came investigations into its coordination chemistry. This has become a rapidly growing field, which has been reviewed.[6]

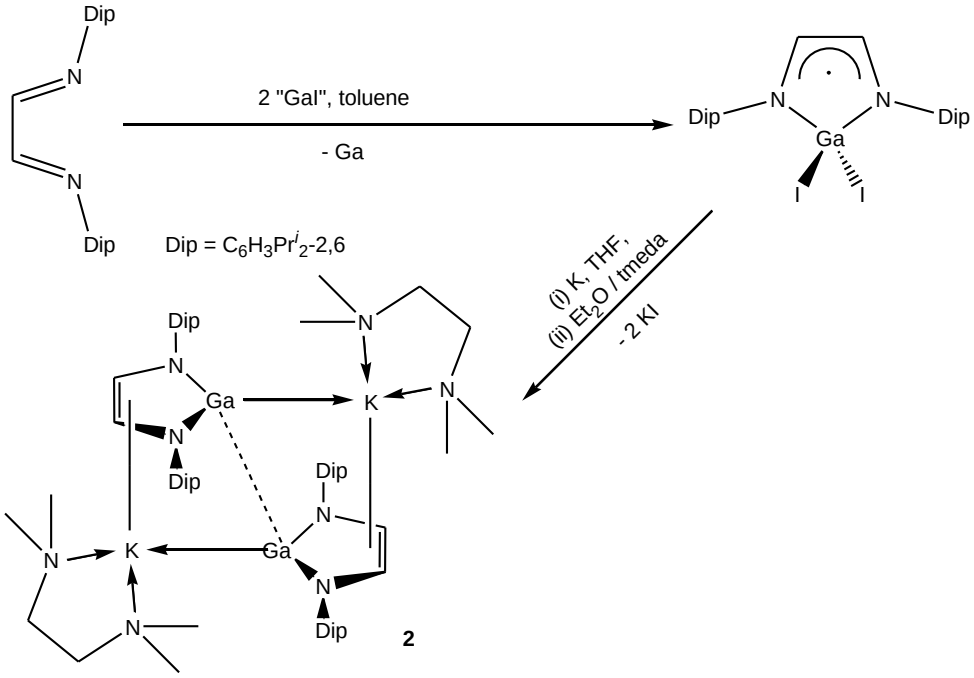

Scheme 2. Synthesis of [K(tmeda)][**2**].

Since the report of **2**, the curiosity into the coordination chemistry of such a complex has grown and has led to many new complexes being formed with metals from throughout the periodic table. For example, a great deal of work has gone into investigating the coordination chemistry of **2** with group 13 precursors. In the 2:1 reaction, carried out in diethyl ether, of [K(tmeda)][**2**] with the group 13 hydrides, [$InH_3(NMe_3)$] and [GaH_3(quinuclidine)], the trimetallic hydrides, **3** and **4**, were afforded in high yields

(Scheme 3).[7] Complex **3** is the first structurally characterized Ga-In bonded compound. It is thought that KH is eliminated, leaving the neutral monosubstituted intermediates to be subsequently attacked by a second equivalent of [K(tmeda)][**2**] leaving the desired products, **3** and **4**. Attempts to further the chemistry with aluminium hydride analogues were futile. In addition, reactions of group 13 cyclopentadienyl complexes with [K(tmeda)][**2**] have been investigated. InCp and TlCp were shown to cause the oxidative coupling of **2** with the group 13 metal being deposited and KCp being generated to give the π-cyclopentadienyl-bridged digallane(4), **5**.[8] Complex **5** exhibits the first structurally characterized example of a π-interaction with a gallium(II) center. It was found that **5** can be directly prepared via the reaction of KCp, tmeda, and the digallane $[Ga\{[N(Dip)C(H)]_2\}]_2$.

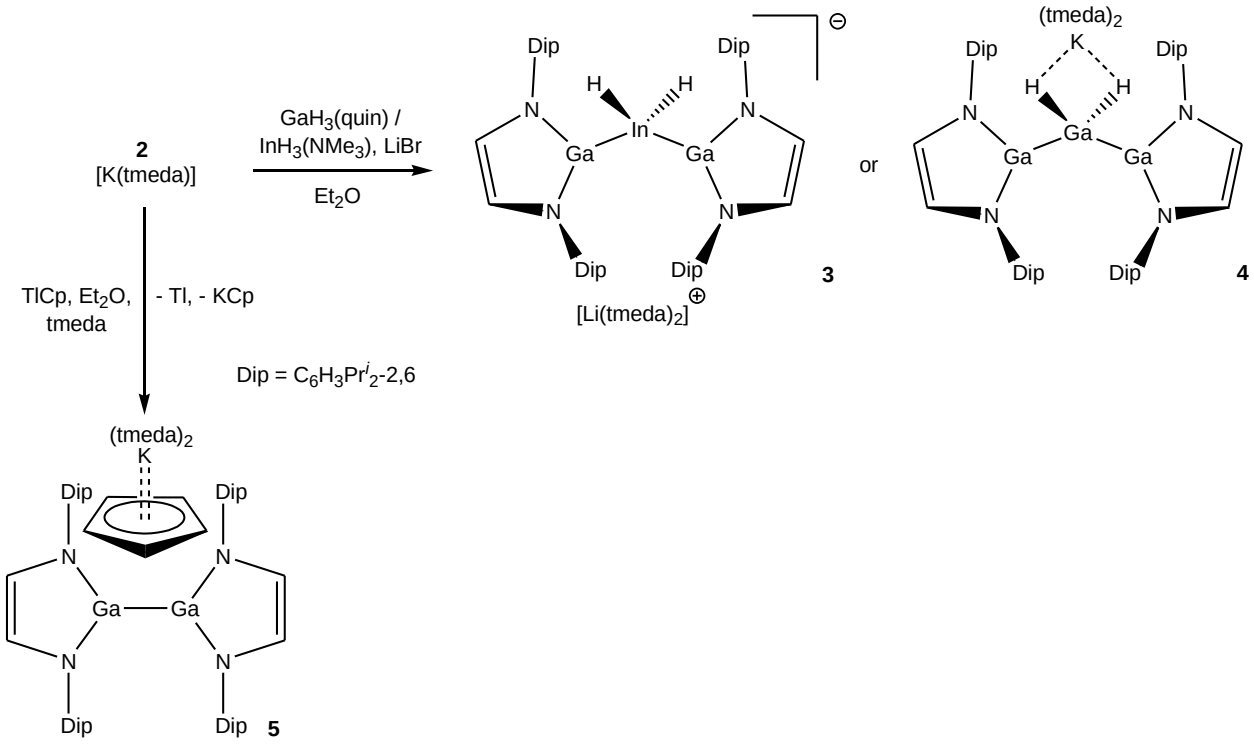

Scheme 3. Reactions of [K(tmeda)][**2**] with group 13 complexes.

Investigations into the coordination chemistry of [K(tmeda)][**2**] with group 14 elements have also been described. The first result from the reaction of a group 14 precursor with [K(tmeda)][**2**], was the oxidative insertion of its gallium center into the C—H bond of the imidazolium salt, IMes.HCl, affording the NHC-gallium hydride complex, **6** (Scheme 4).[9] It was also found that the hydroxide-bridged gallium hydride salt, **7**, was afforded if the previous reaction mixture was exposed to a trace amount of water.

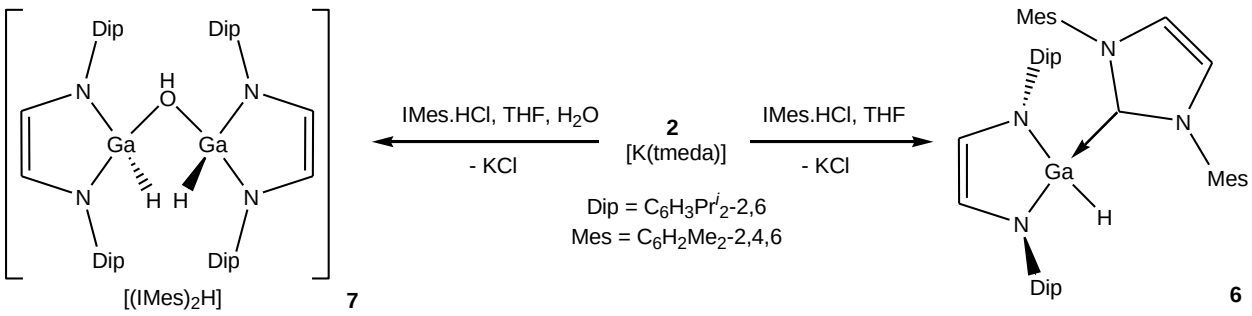

Scheme 4. Reactions of [K(tmeda)][**2**] with group 14 complexes.

More recently several other complexes derived from reactions of [K(tmeda)][**2**] with group 14 precursors have been prepared. In the hope of proving the expected ability of [K(tmeda)][**2**] to act as an NHC analogue, [K(tmeda)][**2**] was reacted with heavier group 14 alkene analogues, $R_2E=ER_2$, E = Ge, Sn or Pb, just as Weidenbruch and co-workers had previously done with known NHCs.[10,11] When E = Ge or Sn, the reactions were successful in affording the anionic complexes **8** and **9** (Scheme 5).[12] A slight variation of **8** was achieved by Baines and co-workers upon substitution of its $CH(SiMe_3)_2$ groups for mesityl substituents, as in **10**.[13] Reaction of **9** with another equivalent of [K(tmeda)][**2**] afforded the digallyl stannate complex, **11** (Scheme 5).[12] It was thought by the Jones group that the formation of **11** occured via a dianionic intermediate, **12**.

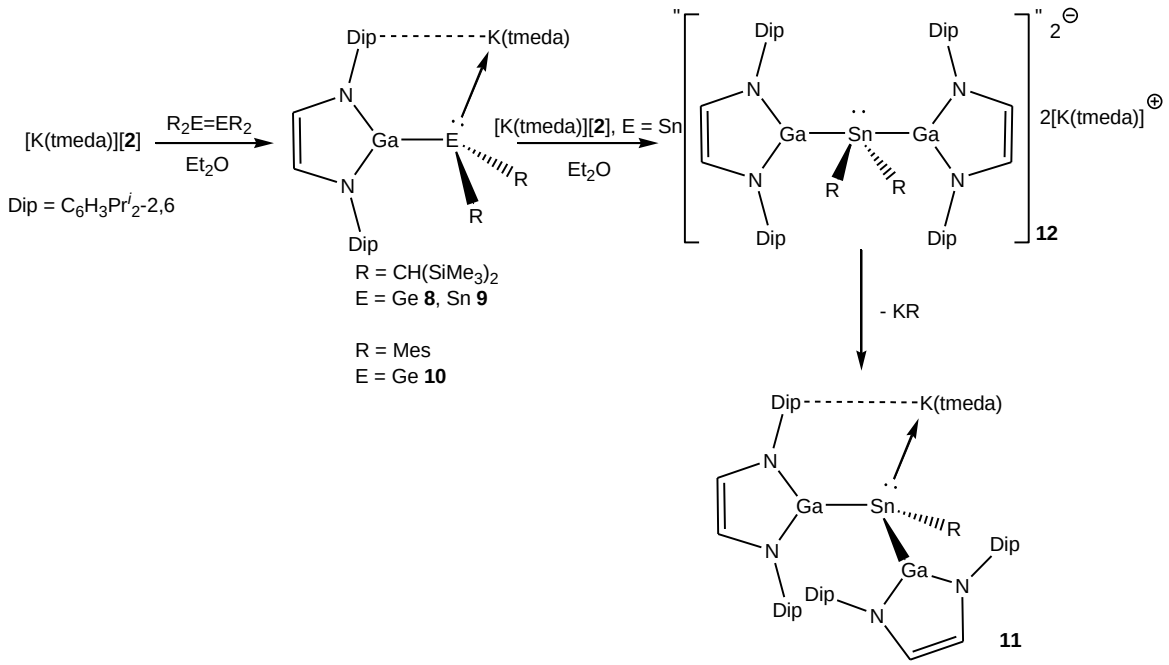

Scheme 5. The synthesis of **8 – 11**.

Further reactivity studies of [K(tmeda)][**2**] with differently substituted group 14 alkene analogues were carried out. When [K(tmeda)][**2**] was reacted with $Ar'_2E{=}EAr'_2$ (Ar' = $C_6H_2Pr^i_3$-2,4,6) (E = Ge, Sn, Pb), the anionic tin complex **13** was afforded. In the case of E=Pb, it was found that elemental lead was deposited and the galladiazole, **14**, was isolated (Scheme 6).[12]

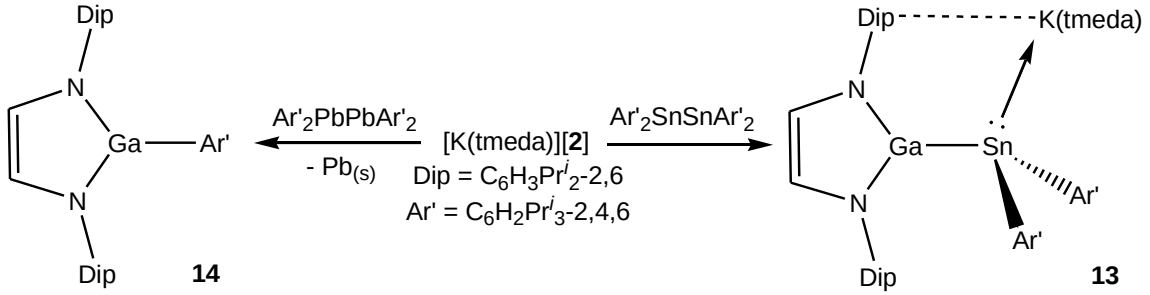

Scheme 6. The synthesis of **13** and **14**.

The coordination chemistry of [K(tmeda)][**2**] towards group 14 precursors incorporating very bulky amidinate and guanidinate ligands, e.g. (Piso$^-$ = [{N(Dip)}$_2$CBu^t]$^-$) and (Priso$^-$ = [{N(Dip)]$_2$}CNPr$^i_2$]$^-$) has been reported. The 1 : 1 reactions of [K(tmeda)][**2**] with [(Piso)GeCl] and [(Priso)ECl], E = Ge or Sn, in toluene led to good yields of the monomeric germanium or tin-gallyl complexes, **15 – 17** (Scheme 7).[12]

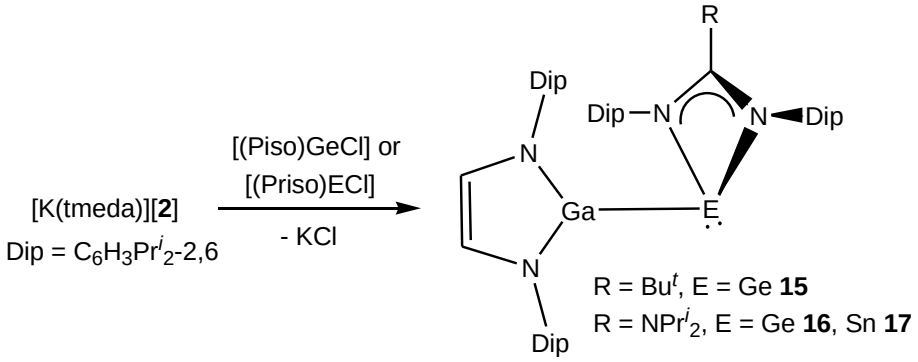

Scheme 7. The synthesis of **15 – 17**.

The reactivity of [K(tmeda)][**2**] towards group 15 species has also been investigated. For example, when the five-membered anionic gallium(I) complex, [K(tmeda)][**2**], reacts with the triphosphabenzene, 1,3,5-P$_3$C$_3$Bu$^t_3$, the known diphospholyl anion, [1,3-P$_2$C$_3$Bu$^t_3$]$^-$, is produced, most likely via phosphorus abstraction from the heterobenzene (Scheme 8).[14] A similar result occurs from the reaction of the triphosphabenzene, 1,3,5-P$_3$C$_3$Bu$^t_3$, with elemental potassium, thus highlighting the strong reducing potential of [K(tmeda)][**2**].[15] [K(tmeda)][**2**] has also been shown to oxidatively insert into a P—P bond of *cyclo*-(PPh)$_5$ to give the spirocyclic complex, **18**, (Scheme 8).[16] In addition to phosphorus, a nitrogen precursor, PhN=NPh, was reacted with [K(tmeda)][**2**] affording the novel ionic spirocyclic species, **19**, (Scheme 8).[16]

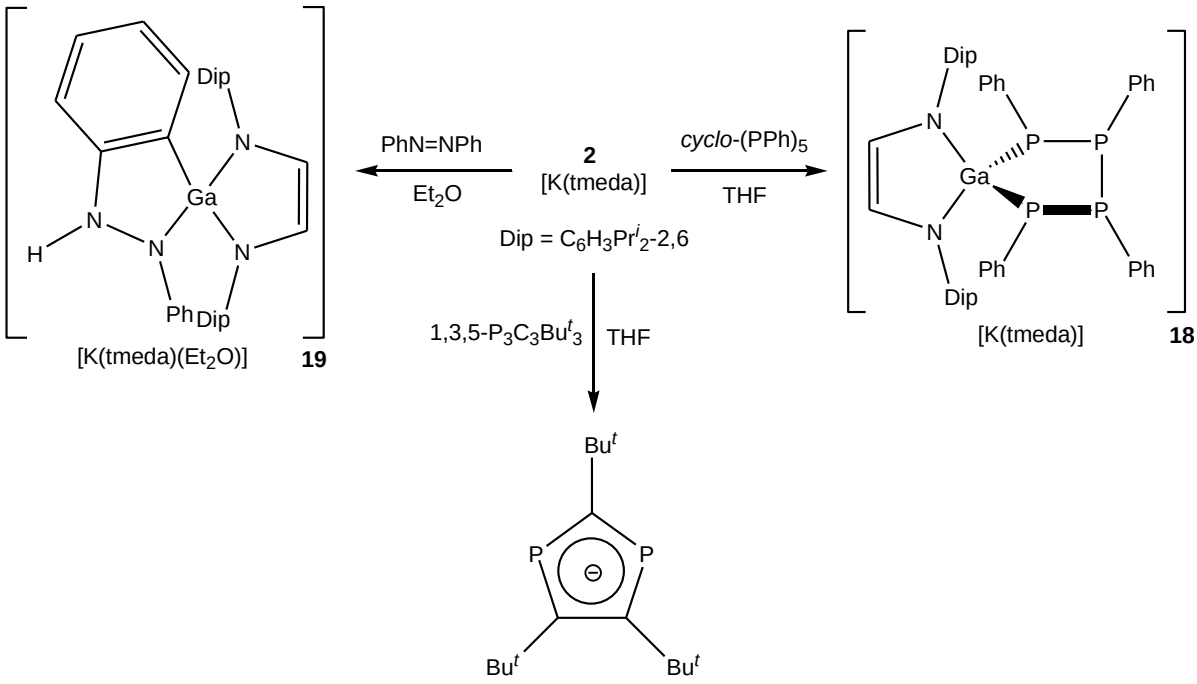

Scheme 8. Reactions of [K(tmeda)][**2**] with group 15 compounds.

Reactions of [K(tmeda)][**2**] with group 16 precursors have also been carried out. For example, when exposed to a stoichiometric amount of $N_2O_{(g)}$, [K(tmeda)][**2**] is oxidized to give the dimeric dianionic complex, **20** (Scheme 9).[17] Complex **20** is analogous to the dimeric species **21**, which is formed by the reaction of (Te)PEt_3 with [K(tmeda)][**2**]. [K(tmeda)][**2**] has also been shown to form complexes with selenium and tellurium compounds. The reaction of the anionic gallium(I) heterocycle with the dichalcogenides, PhEEPh (E = Se, Te), resulted in the insertion of the gallium(I) heterocycle into the E—E bond of the dichalcogenides affording complexes **22** and **23**.[17]

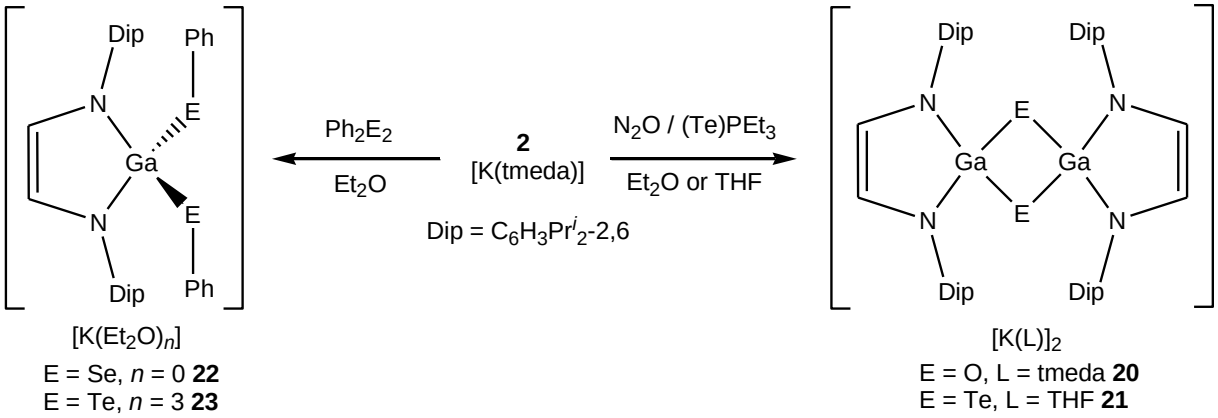

Scheme 9. Reactions of [K(tmeda)][**2**] with group 16 precursors.

The reactivity of [K(tmeda)][**2**] towards a vast array of transition metal precursors has been extensively studied. It was originally thought by the Jones group to prepare gallyl transition metal complexes by the treatment of nickelocene or cobaltocene with [K(tmeda)][**2**]. These reactions afforded the bis(gallyl) metal(II) salts, **24** and **25** (Scheme 10).[6,18] It was realized by the Jones group that [K(tmeda)][**2**], in the formation of **24** and **25**, had acted very much like the NHC, [**:**C{[N(Me)C(Me)]$_2$}], **26**, in the formation of [CpNi{C{[N(Me)C(Me)]$_2$}}$_2$][Cp].[19] Although attempts to study the comparative σ-donor abilities of [K(tmeda)][**2**] and **26** were unsuccessful, the reaction between **24** and **26** yielded the neutral complex **27**.[18] A cobalt analogue of **27** was not obtained. While the method of using metallocenes to form gallyl transition metal complexes worked for cobalt and nickel, this was not the case for sandwich complexes of vanadium, chromium, manganese and iron.[20]

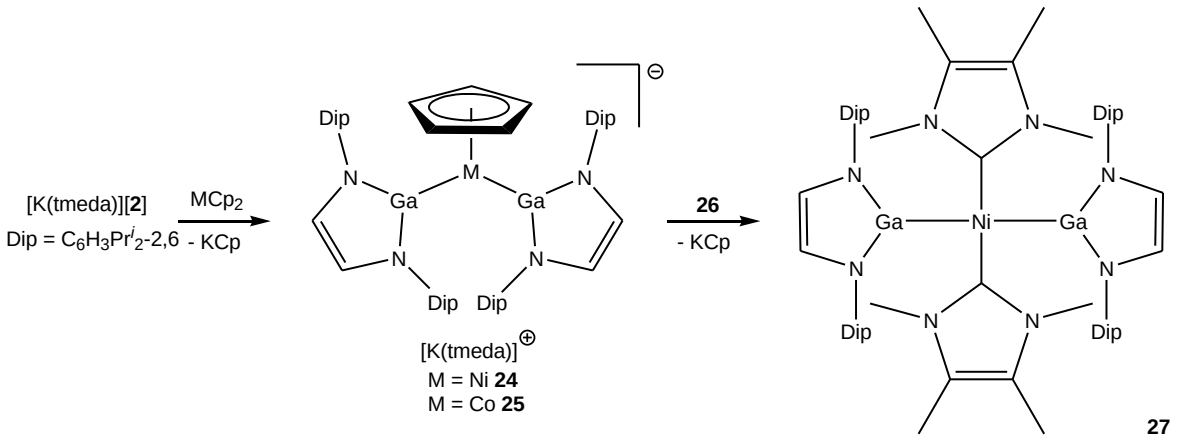

Scheme 10. The synthesis of **24**, **25** and **27**.

In an attempt to further prepare gallium—transition metal bonded complexes using metallocene precursors, it was thought that the reaction of the digallane(4), $[Ga\{[N(Dip)C(H)]_2\}]_2$ (Dip = $C_6H_3Pr^i$-2,6), with a metallocene would lead to the metallocene oxidatively inserting into the Ga—Ga bond of $[Ga\{[N(Dip)C(H)]_2\}]_2$. This sort of behavior had previously been seen in the case of the insertion of "WCp_2" into the B—B bond of the diborane, $B_2Cat'_2$ (Cat' = 4-$Bu^tC_6H_3O_2$-1,2 or 3,5-$Bu^t_2C_6H_2O_2$-1,2).[21] This proposal was subsequently proved when, after reacting "$ZrCp_2$" with $[Ga\{[N(Dip)C(H)]_2\}]_2$ and an excess of Bu^nLi, the unusual Zr^{III} salt, **28**, resulted (Scheme 11).[22] It was noted that while the target Zr^{IV} complex, $[Cp_2Zr\{Ga\{[N(Dip)C(H)]_2\}\}_2]$, was not prepared, it was believed to be an intermediate in the process, which was subsequently reduced by the alkyllithium reagent. Further attempts at oxidatively inserting metallocenes into the Ga—Ga bond of $[Ga\{[N(Dip)C(H)]_2\}]_2$ were carried out. The metallocenes, $M(C_5H_4Me)_2$ (M = V, Cr), were reacted with $[Ga\{[N(Dip)C(H)]_2\}]_2$ to give the neutral mono-gallyl complexes, **29** and **30** (Scheme 12).[6,20] Complex **31** is thought to be a bis-gallyl M^{IV} intermediate in the reaction, which later comproportionates with $M(C_5H_4Me)_2$ to

afford **29** and **30**. Unlike what was seen for complex **27**, there was no reaction between **29** or **30** with the NHC **26**. Complex **29** did however react with [K(tmeda)][**2**] to afford the bis-gallyl salt, **32**. This was thought to occur due to its more sterically accessible vanadium center.

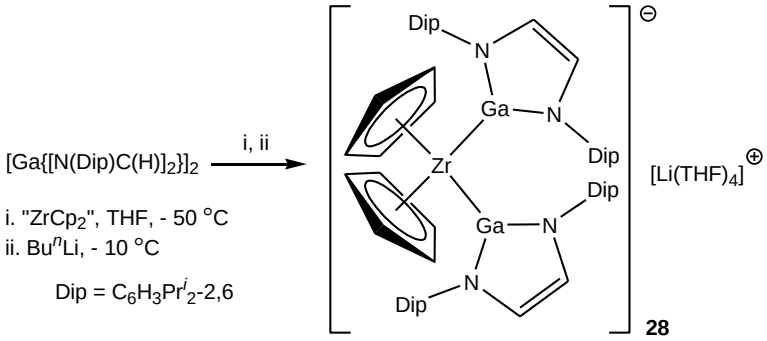

Scheme 11. The synthesis of **28**.

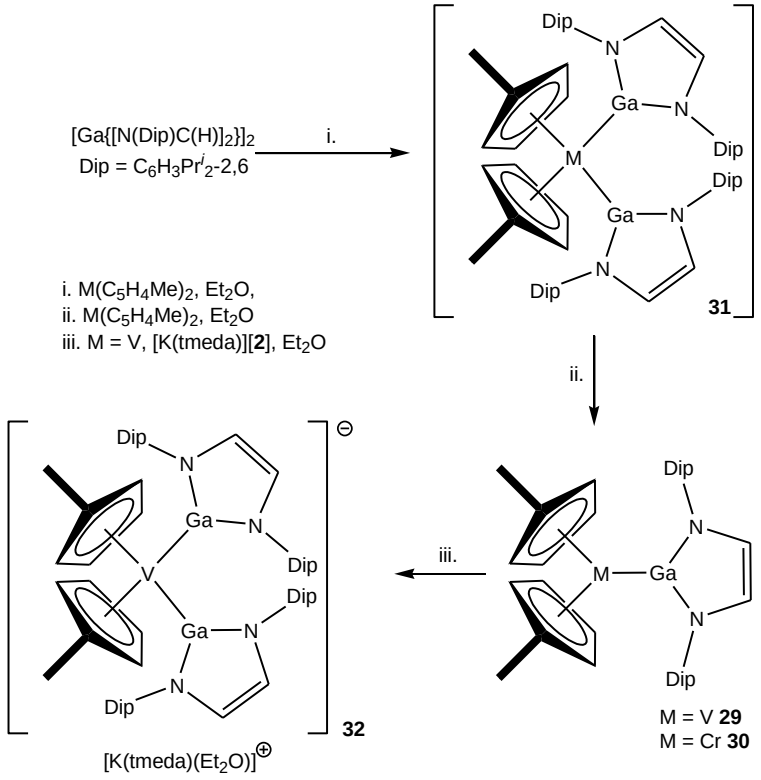

Scheme 12. The synthesis of **29** – **32**.

The success of preparing several gallyl transition metal complexes led to continued investigations into the d-block chemistry of [K(tmeda)][**2**]. Using the cyclopentadienyl-metal carbonyl complexes, [Cp'M(CO)$_n$] (M = V, Cp' = Cp, n = 4; M = Mn, Cp' = MeCp, n = 3; M = Co, Cp' = Cp, n = 2), as precursors, and reacting them with [K(tmeda)][**2**], resulted in the loss of only one carbonyl group and the preparation of the half-sandwich anionic complexes of [K(tmeda)][**2**], **33-35** (Scheme 13).[6,20] This proved to be very interesting as several analogous NHC complexes had been previously prepared, which are important in catalysis.[23]

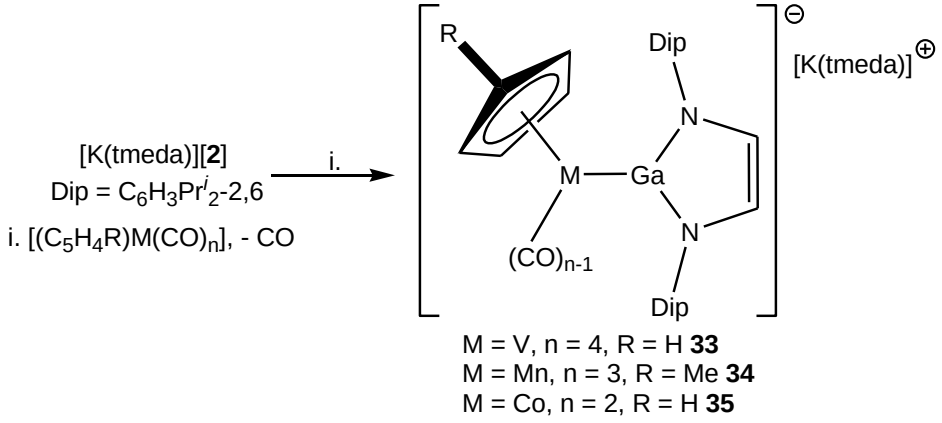

Scheme 13. The synthesis of **33 – 35**.

In other reactions of [K(tmeda)][**2**] with transition metal precursors, an iron complex **36** and a manganese complex **37** were prepared. For example, due to the anionic gallium(I) heterocycle's strong σ-donor capability, [K(tmeda)][**2**] was able to displace CO from iron pentacarbonyl (Scheme 14).[24] In addition, the manganese(II) precursor, [Mn{CH(SiMe$_3$)$_2$}$_2$], was reacted with [K(tmeda)][**2**] affording **37**. The Ga—Mn bond in **37** is comparatively weak, being much longer (> 0.3 Å) than that in the half-sandwich manganese complex, **34**.

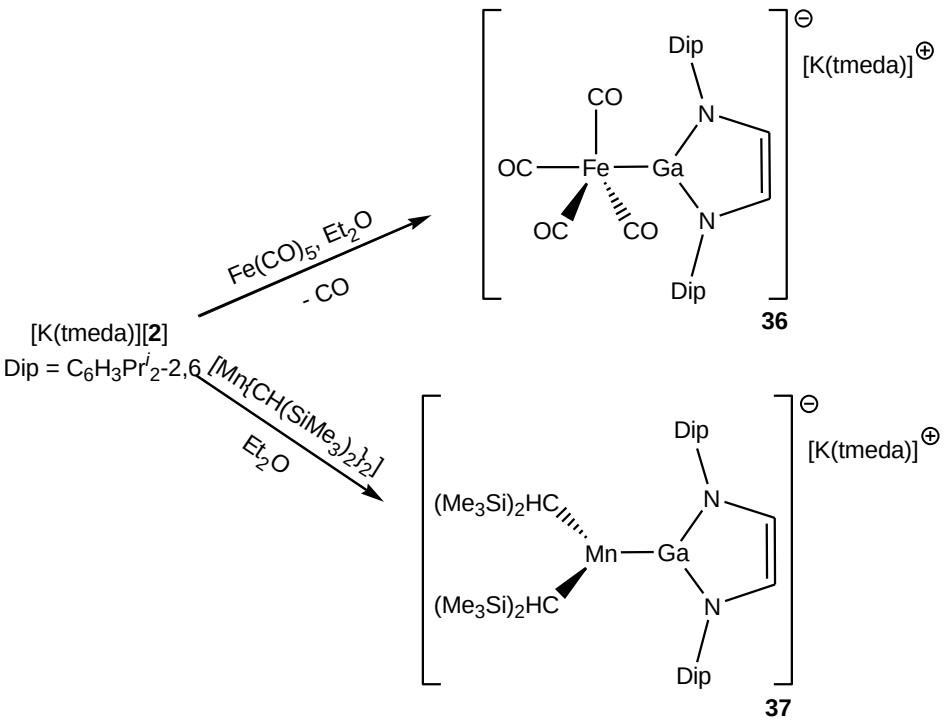

Scheme 14. The synthesis of **36** and **37**.

Bulky aminidinate and guanidinate complexes of transition metal halides have been successfully reacted with [K(tmeda)][**2**]. This same technique was used to access the group 14 analogues which have been previously mentioned in this chapter. For example, the reaction of [(Priso)ZnCl] (Priso$^-$ = [{N(Dip)}$_2$CNPr$^i_2$]$^-$) with [K(tmeda)][**2**] afforded the neutral zinc-gallyl complex, **38** (Scheme 15).[25] In addition, another zinc-gallyl complex, **39**, was prepared when [K(tmeda)][**2**] was reacted with [(tmeda)ZnCl$_2$] in a 2 : 1 fashion. Complexes **38** and **39** contained the first structurally characterized examples of gallium-zinc bonds. Extremely relevant to this study is the fact that the strong reducing potential of [K(tmeda)][**2**] seemed to prevent the formation of the cadmium analogue of **39** as cadmium metal deposited in the reaction of [K(tmeda)][**2**] with [(tmeda)CdCl$_2$].

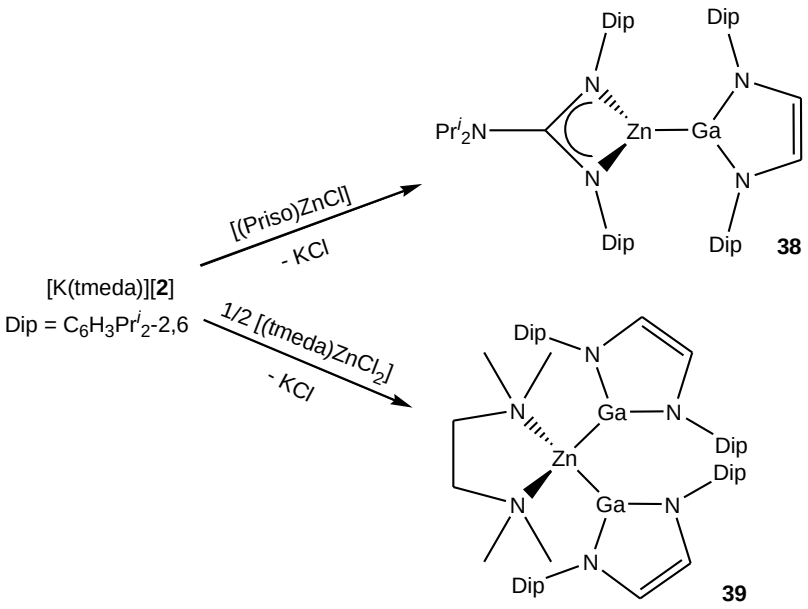

Scheme 15. The synthesis of **38** and **39**.

The ability to prepare gallyl-transition metal complexes from tmeda containing transition metal precursors, as seen for complex **39**, inspired the Jones group to look into the possibility of synthesizing other d-block analogues of this complex. The preparation of such complexes were shown to be possible via the 2 : 1 reactions of [K(tmeda)][**2**] and the metal(II) complexes, [(tmeda)$_n$MX$_2$] (M = Mn, Fe, Co, Ni; X = Cl, Br; n = 1 or 2), which afforded complexes **40** – **43** (Scheme 16).[26] The copper analogue was not prepared via this method, instead the reaction resulted in the deposition of copper metal.

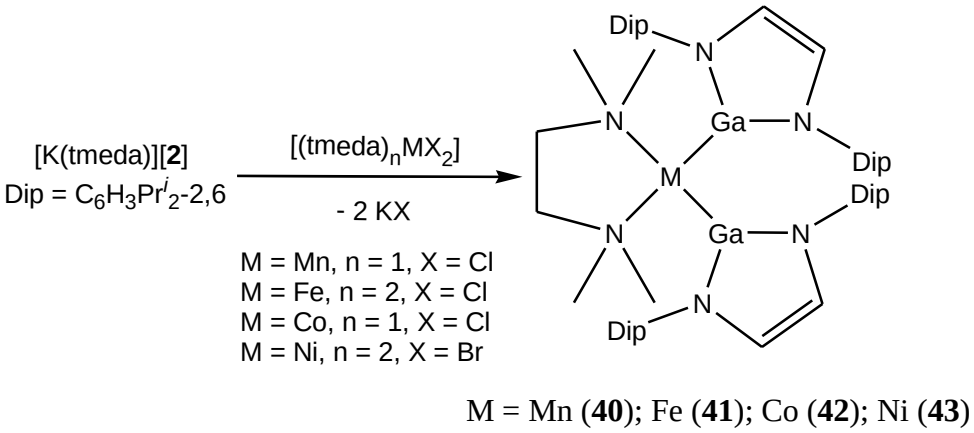

Scheme 16. The synthesis of **40 – 43**.

An interesting gallyl-chromium complex, **44**, that is related to the previously discussed species **24** and **25**, was prepared via the salt metathesis reaction of [K(tmeda)][**2**] with the chromium(II) complex, [(η^5-Cp)Cr(IMes)Cl][27] (Scheme 17).[26] This result led to other salt metathesis reactions to be investigated, using IMes coordinated metal halide precursors. The reactions of [(η^4-COD)M(IMes)Cl] (M = Ir, Rh) with one equivalent of [K(tmeda)][**2**] yielded complexes **45** and **46**, (Scheme 18).[28]

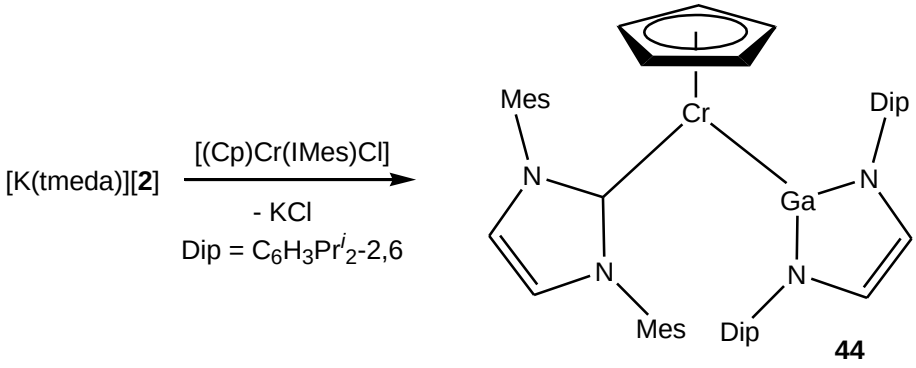

Scheme 17. The synthesis of **44**.

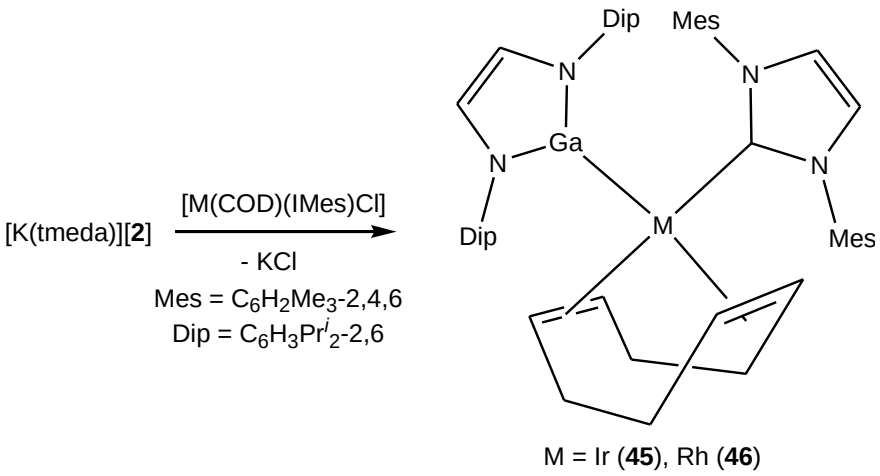

Scheme 18. The synthesis of **45** and **46**.

The success of the previous salt metathesis reactions led to investigations into the formation of group 11 gallyl complexes. For example, [K(tmeda)][**2**] was reacted with a variety of NHC stabilized group 11 metal(I) halides in a 1 : 1 fashion. The reactions of [K(tmeda)][**2**] with [(NHC)MCl] (M = Cu, Ag or Au; NHC = IMes or IPr) led to the desired products, **47** – **52** (Scheme 19).[28] Interestingly, the yields of the complexes incorporating the NHC IMes were found to be lower, which was attributed to IMes being a less bulky NHC than IPr. In addition, two other reactions with group 11 precursors have been carried out. The first was the 1 : 2 reaction of the copper(I) dimer, $[(dppe)CuI]_2$, with [K(tmeda)][**2**] which afforded the copper-gallyl complex, **53** (Scheme 19).[26] Complex **53** exhibited the first structurally characterized example of a Ga—Cu bond. The second was the reaction of [K(tmeda)][**2**] with $[(ICy_{Me})CuCl]$ (ICy_{Me} = [**:**C{$[N(C_6H_{11})C(Me)]_2$}]) affording the expected complex **54**.[28] It was proposed that even though ICy_{Me} is smaller than IMes, the greater donor strength of ICy_{Me} allowed **54** to be a viable product.

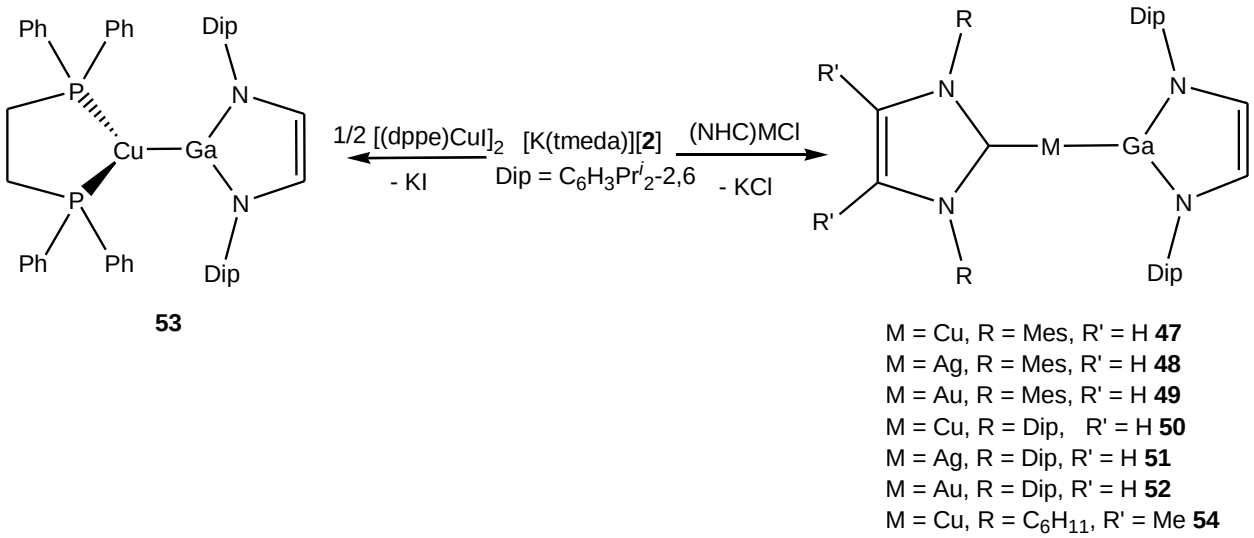

Scheme 19. The synthesis of **47 – 54**.

More recently, in collaboration with the Liddle group at the University of Nottingham, the Jones group prepared the first example of an unsupported gallium-yttrium bonded complex. The addition of one equivalent of [K(tmeda)][**2**] to an in-situ prepared solution of [Y(BIPM)(I)(THF)$_2$] (BIPM = {C(PPh$_2$NSiMe$_3$)$_2$}$^{2-}$) yielded the novel complex [Y{Ga(NArCH)$_2$}(BIPM)(THF)$_2$], **55**, as yellow crystals in a moderate yield, (Scheme 20).[29] Its Ga—Y bond length is 3.1757(4) Å, which is only slightly longer than the sum of the covalent radii of gallium and yttrium (3.12 Å).

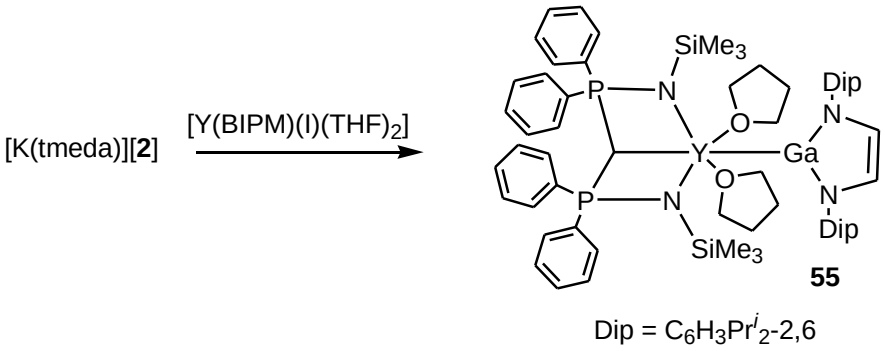

Scheme 20. Synthesis of **55**.

Of most relevance to this chapter is the previous work carried out with gallyl complexes of the group 2 elements. In a similar fashion to the preparation of [K(tmeda)][**2**], the gallium(III) heterocycle $[I_2Ga\{[N(Dip)C(H)]_2^{\cdot}\}]$[4] was reduced by either Mg or Ca in the presence of mercury in THF. This lead to the formation of the novel bis(gallyl) magnesium, $[Mg(THF)_3\{Ga\{[N(Dip)C(H)]_2\}\}_2]$ **56**, and calcium, $[Ca(THF)_4\{Ga\{[N(Dip)C(H)]_2\}\}_2]$ **57**, complexes (Scheme 21).[30] It was thought that the reduction occurred via several steps. The first was the formation of the paramagnetic gallium(II) dimer $[IGa\{[N(Dip)C(H)]_2^{\cdot}\}]_2$, followed by the diamagnetic digallane(4), $[Ga\{[N(Dip)C(H)]_2\}]_2$, and finishing with the group 2 metal oxidatively inserting into the Ga—Ga bond of $[Ga\{[N(Dip)C(H)]_2\}]_2$. Complexes **56** and **57** are extremely interesting due to the fact that they are the first structurally characterized examples of Ga-Mg and Ga-Ca bonded complexes. The Ga—Mg bond of 2.7222 Å (mean) and the Ga—Ca bond of 3.1587 Å (mean) are both outside the sum of the covalent radii of these element pairs (Ga—Mg 2.61 Å; Ga—Ca 2.91 Å).[32] Attempts to synthesize the strontium and barium analogues via the same method were unsuccessful.

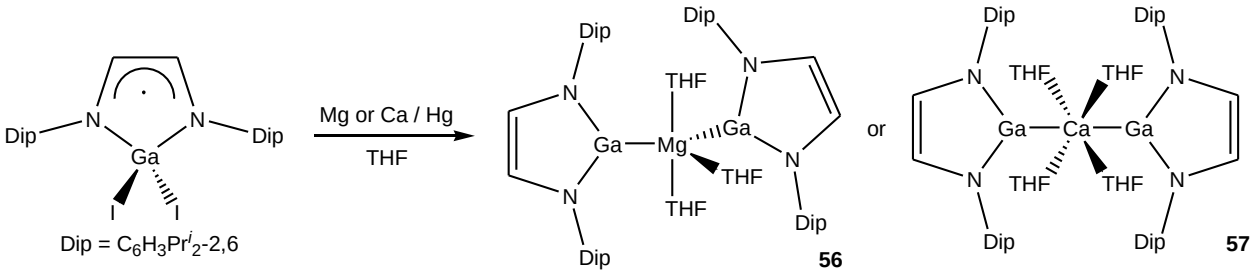

Scheme 21. The synthesis of **56** and **57**.

Very recently, Fedushkin and co-workers prepared a series of gallyl-group 2 complexes analogous to **56** and **57**. The complexes [{(Dip-bian)Ga}$_2$M(thf)$_n$] (M=Mg (**58**), n=3; M=Ca (**59**), Sr (**60**), n=4; M=Ba (**61**), n=5), were prepared via the reduction of a digallane precursor, [(Dip-bian)Ga-Ga(Dip-bian)] (Dip-bian = 1,2-bis[(2,6-diisopropylphenyl)imino]acenaphthene) with the corresponding group 2 metal in THF (Scheme 22).[31] All were isolated as dark brown crystals but only **61** was crystalographically characterized, revealing gallium-barium bond lengths of 3.6433(5) and 3.5964(7) Å.

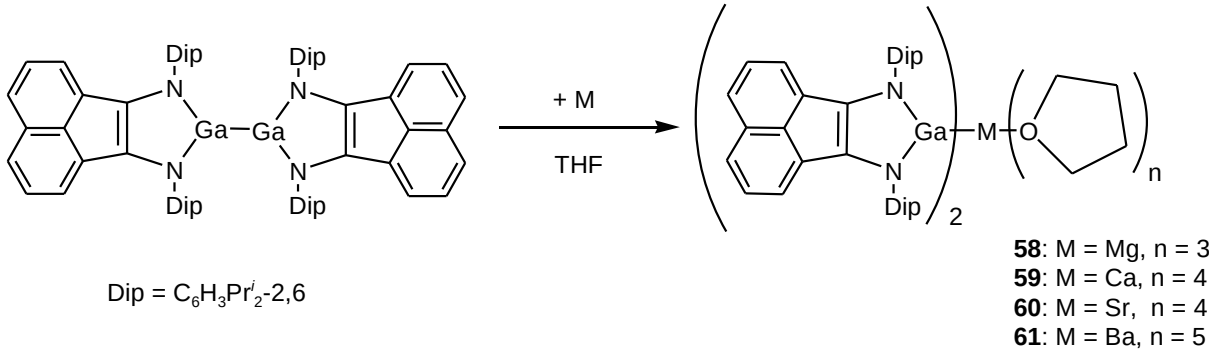

Scheme 22. Synthesis of **58** – **61**.

2.2 Research Proposal

Complexes of group 2 and 12 elements with the five-membered anionic gallium(I) heterocycle, [K(tmeda)][**2**], are known.[25,30] For example, the novel bis(gallyl) magnesium, [Mg(THF)$_3${Ga{[N(Dip)C(H)]$_2$}}$_2$] **56**, and calcium, [Ca(THF)$_4${Ga{[N(Dip)C(H)]$_2$}}$_2$] **57**, complexes have been prepared, but attempts at preparing the analogous strontium and

barium systems were unsuccessful. In addition, [K(tmeda)][**2**] has been shown to react with the group 12 precursors, [(Priso)ZnCl] and [(tmeda)$ZnCl_2$], giving rise to novel gallyl-zinc species, **38** and **39** (Scheme 15). The attempted formation of analogous cadmium complexes was unsuccessful. The aim of this study was to investigate the possibility of extending the coordination chemistry of [K(tmeda)][**2**] towards heavier group 2 and 12 precursors using different synthetic methodologies.

2.3 Results and Discussion

2.3.1 Preparation of Group 2 Gallyl Complexes

In an attempt at preparing mono gallyl-group 2 complexes, [K(tmeda)][**2**] was reacted in a 1 : 1 ratio with the β-diketiminate calcium complex, [(Nacnac)CaI(OEt_2)]. It was thought that should the reaction be successful, this method would be suitable for the heavier group 2 analogues. The reaction of [K(tmeda)][**2**] and [(Nacnac)CaI(OEt_2)] in a 1:1 ratio in toluene, instead afforded, in low yield, the bis(gallyl) calcium complex, **62**, encompassing two coordinating tmeda ligands. This was likely a result of redistribution in solution of [(Nacnac)CaI(OEt_2)] to CaI_2 and [$(Nacnac)_2Ca$], which then allowed [K(tmeda)][**2**] to react with the free CaI_2 and tmeda. Interestingly, it was previously seen that treatment of [K(tmeda)][**2**] with MI_2 (M = Mg or Ca) in THF did not yield the metal gallyls, **56** and **57**.[25] Accordingly, it was thought that treatment of [K(tmeda)][**2**] with CaI_2 in toluene in the presence of excess tmeda would lead to the formation of complex **62**. This was in fact the case. Given this success, it was decided to revisit the aforementioned

unsuccessful reactions between group 2 metal iodides and [K(tmeda)][**2**], but by carrying out the reactions in toluene and including tmeda as a co-reactant.

Treatment of toluene suspensions of MI_2 (M = Ca, Sr or Ba) with two equivalents of [K(tmeda)][**2**] in the presence of an excess of tmeda afforded low to good yields of the bis(gallyl) metal complexes, **62**, **63**, and **64** (Scheme 23), after recrystallization of the crude products from diethyl ether. The isolated yield decreases with the molecular weight of the group 2 metal involved. This is possibly due to the expected increasing weakness of the M-Ga bond as the group is descended. In addition, it appears that for the barium gallyl, **64**, the chelating tmeda ligand is more labile than in **62** and **63**. This is evidenced by the fact that when **64** was recrystallized from diethyl ether, low yields of the bis(etherate) complex, *trans*-[Ba{Ga(Dip-DAB)}$_2$(tmeda)(OEt$_2$)$_2$], **65**, consistently co-crystallized with **64**. Addition of a few drops of tmeda to the diethyl ether solutions of **64** used for recrystallization, prevented the formation of *trans*-[Ba{Ga(Dip-DAB)}$_2$(tmeda)(OEt$_2$)$_2$]. Attempts to prepare the mono(gallyl) complexes, *trans*-[MI{Ga(Dip-DAB)}(tmeda)$_2$], using 1:1 reaction stoichiometries yielded approximately 50:50 mixtures of **62**-**64** and unreacted MI_2. This suggests that *trans*-[MI{Ga(Dip-DAB)}(tmeda)$_2$] are unstable with respect to redistribution reactions, as is common for other heteroleptic heavier group 2 halide complexes, RMX, (R = alkyl, amide etc.; X = halide).[33]

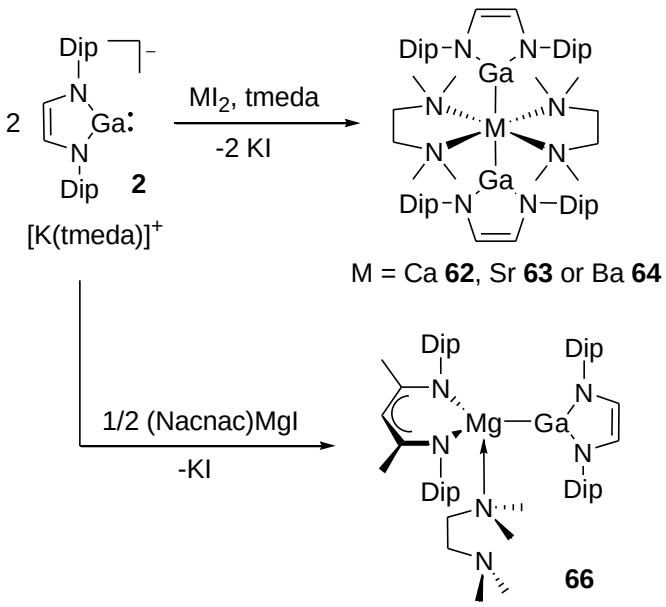

Scheme 23. Synthesis of **62-64, 66**

The 2:1 reactions of [K(tmeda)][**2**] with MgI_2 in THF were also carried out, though no products analogous to **62-64** were obtained. This is not surprising given the preference for lower coordination numbers for the smaller metal, as already exhibited by **56** (Scheme 21). In order to obtain a mono(gallyl) magnesium complex, in a reaction similar to the formation of complex **62**, the β-diketiminate magnesium complex, [(Nacnac)MgI(OEt_2)], was treated with one equivalent of [K(tmeda)][**2**]. Interestingly, this gave a low yield (16%) of **66** (Scheme 23), the tmeda ligand of which is derived from the gallium(I) starting material. Repeating the reaction, but with excess tmeda added to the mixture, did not lead to an increased yield of **66**.

The ^{1}H NMR spectra of complexes **62-64** each displays a major set of resonances which is consistent with its solid state structure (*vide infra*). The spectra also exhibit more complex, minor sets of resonances which possibly correspond to the *cis*-isomers of the compounds (major isomer:minor isomer ratio is *ca.* 80:20 for all compounds). The most

persuasive evidence for this proposal is that in each spectrum there are signals corresponding to two chemically inequivalent sets of backbone protons for the gallyl ligands (which resonate as an AB spin system). The fact that these protons are inequivalent suggests that the bulky heterocyclic ligands of the "*cis*-complex" are interlocked and cannot rotate freely with respect to each other. Very similar spectra have been observed for square planar transition metal complexes, e.g. *cis*-[Pd{Ga(DAB)}$_2$(tmeda)].[34] That the two isomers of **62-64** exist in dynamic equilibrium in solution is borne out by the fact that dissolving crystallographically authenticated samples of the *trans*-isomer of each compound in C_6D_6 led to spectra corresponding to isomeric mixtures. Moreover, because only the *trans*-isomer of each complex can be crystallized from solutions of the isomeric mixtures, it seems that this is the thermodynamically favored form of the compounds. The low solubility of **62-64** in aromatic solvents at low temperature precluded variable temperature NMR studies of the equilibrium between the isomers.

Compound **66** also exhibits fluxional behavior in solution, but its enhanced solubility relative to **62-64** allowed this to be studied by variable temperature ^{1}H NMR spectroscopy. At 30 ^{o}C the spectrum of the compound exhibits two broad isopropyl methine resonances, and singlet resonances for the backbone protons of the DAB and Nacnac ligands (Figure 1). Upon cooling the solution to -50 ^{o}C, the methine resonances resolve into six broad septet resonances, the individual integration of four of which is slightly greater than that of the other two. The nacnac backbone resonance splits into two singlets, while the DAB backbone signal separates into a singlet resonance and a broad AB pattern. The relative integrations of the two sets of both nacnac and DAB backbone resonances is *ca.* 70:30. A corresponding increase in the number of methyl and aromatic

signals is seen upon sample cooling, though the complexity of overlapping signals in these regions make meaningful interpretation difficult. Cooling the sample below -50 ^{o}C led to broadening of all observed resonances without further resolution, which is probably a result of a significant increase in the viscosity of the solution and/or partial precipitation of **66** from the solution. It is thought that the shoulder on the signal at *ca.* δ 4.8 ppm in each spectrum is due to a low level impurity of unknown composition.

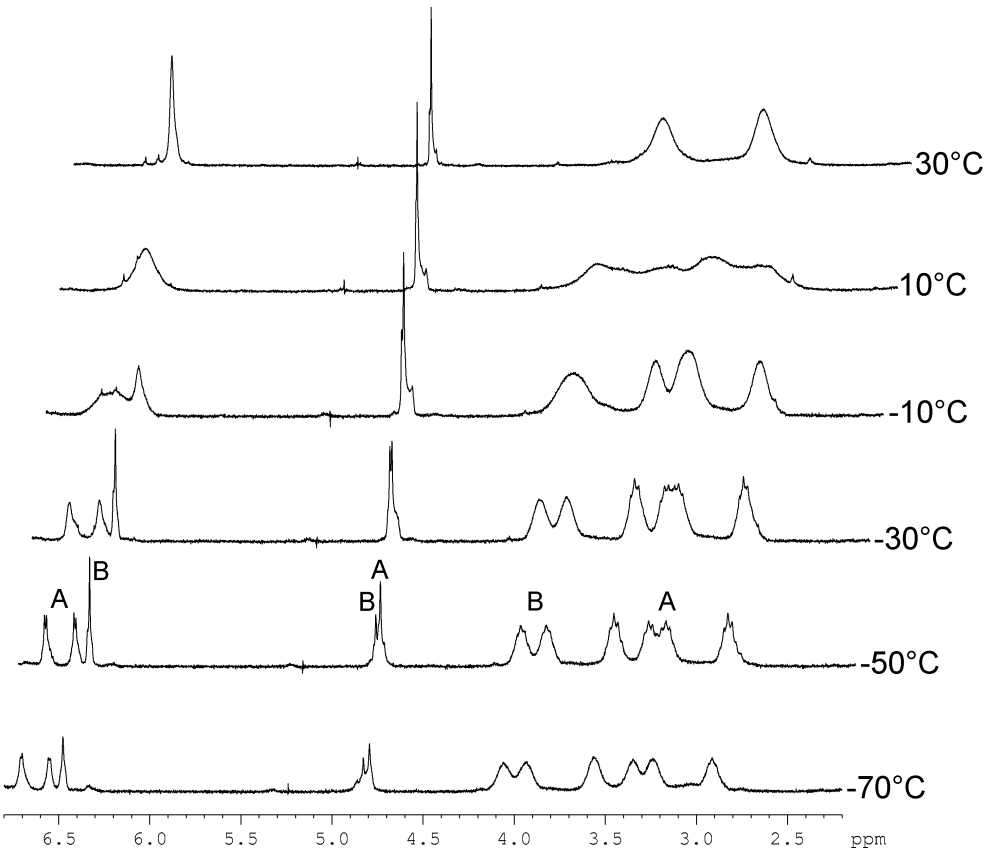

Figure 1. Variable temperature ^{1}H NMR spectra of [(Nacnac)(κ^{1}-tmeda)Mg{Ga(Dip-DAB)}] **66** recorded in d_8-toluene. Resonances associated with two possible isomers are labeled A and B.

The spectral pattern displayed by the predominant set of resonances marked A in Figure 1 is consistent with the solid state structure of **66**. It cannot be sure what gives rise to the set of signals marked B in Figure 1, but one possibility is a more symmetrical isomer of **66**, which is in equilibrium with the predominant isomer. This isomer could be a polymer or oligomer/cyclic oligomer of **66** *viz.* [{(DAB)GaMg(Nacnac)(μ-tmeda)}$_n$], the trigonal bipyramidal Mg centers of which are coordinated at their axial sites by two N-atoms of bridging tmeda ligands. Another possibility is that the B resonances are associated with the three-coordinate complex, [(Nacnac)Mg{(Dip-DAB)Ga}], which is in equilibrium with **66** and free tmeda. However, this is less likely as no signals for uncoordinated tmeda were observed at any temperature. The possibility that the minor set of resonances corresponds to a five-coordinate, tmeda chelated complex, [(Nacnac)Mg{(Dip-DAB)Ga}(κ^2-tmeda)], was also considered. This seems unlikely, as the square based pyramidal and trigonal bipyramidal forms of this species (with the gallyl ligand in apical and equatorial sites respectively) should theoretically exhibit four and eight methine resonances respectively.

In the solid state, compounds **62-64** are isostructural (though not isomorphous). The molecular structures and selected geometrical parameters of **62-64** are depicted in Figures 2-4. Compounds **62-64** are closely related to **57**. Their metal centers have distorted octahedral geometries with the gallyl ligands *trans*- to each other, while the M-Ga and M-N distances in the compounds increase with the molecular weight of the group 2 metal. Interestingly, the Ga—Ca bond length of 3.2276 Å (mean) in complex **62**, is slightly longer than the Ga—Ca bond of 3.1587 Å (mean) in **57**. This is most certainly due to the larger tmeda ligand coordinated to the metal center of **62**.

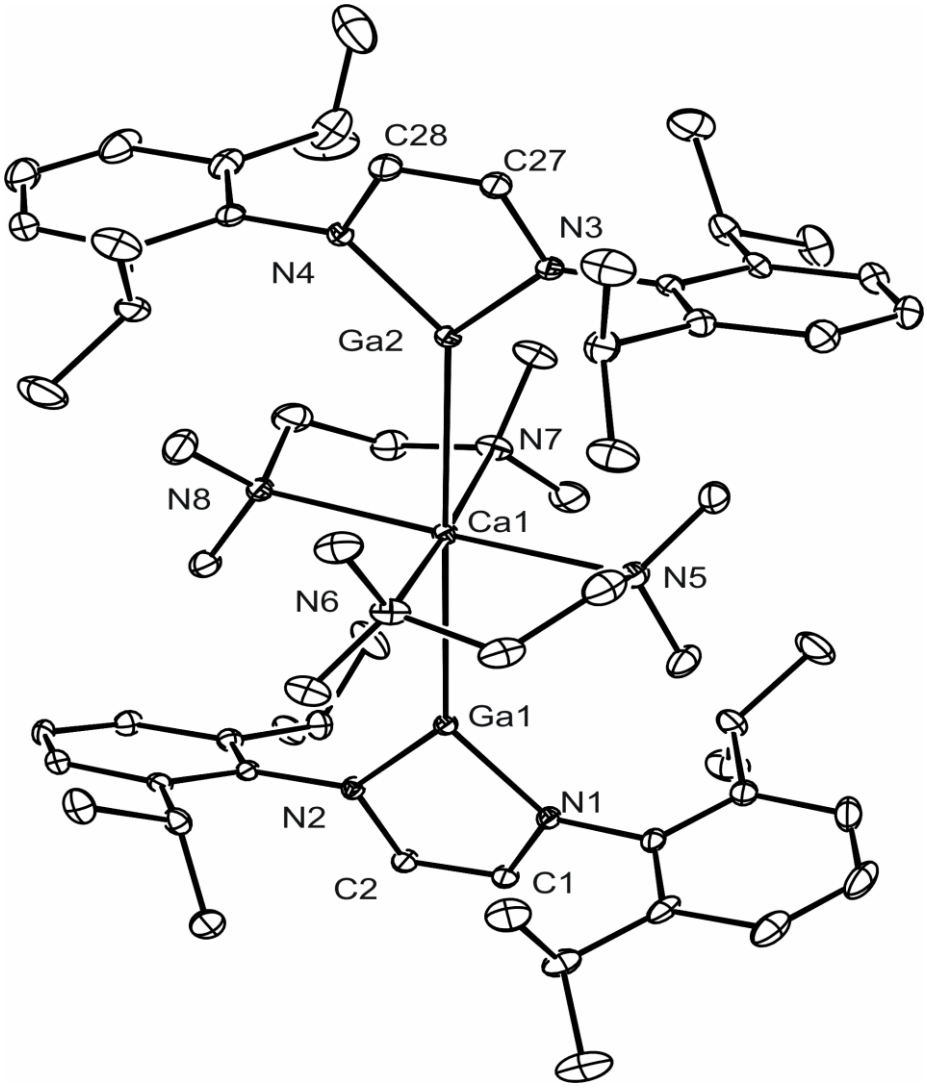

Figure 2. Thermal ellipsoid plot (25% probability surface) of the molecular structure of *trans*-[Ca{Ga(Dip-DAB)}$_2$(tmeda)$_2$] (**62**); hydrogen atoms are omitted for clarity. Selected bond lengths (Å) and angles (°): Ga(1)-N(1) 1.935(2), Ga(1)-N(2) 1.942(3), Ga(1)-Ca(1) 3.2568(8), Ga(2)-Ca(1) 3.1983(8), Ga(2)-N(3) 1.934(3), Ga(2)-N(4) 1.936(2), Ca(1)-N(5) 2.552(3), Ca(1)-N(8) 2.562(3), Ca(1)-N(7) 2.582(3), Ca(1)-N(6) 2.601(3), Ga(1)-Ca(1)-Ga(2) 179.24(2), N(1)-Ga(1)-N(2) 83.44(10), N(3)-Ga(2)-N(4) 83.58(10), N(5)-Ca(1)-N(6) 74.34(10), N(7)-Ca(1)-N(8) 74.84(10).

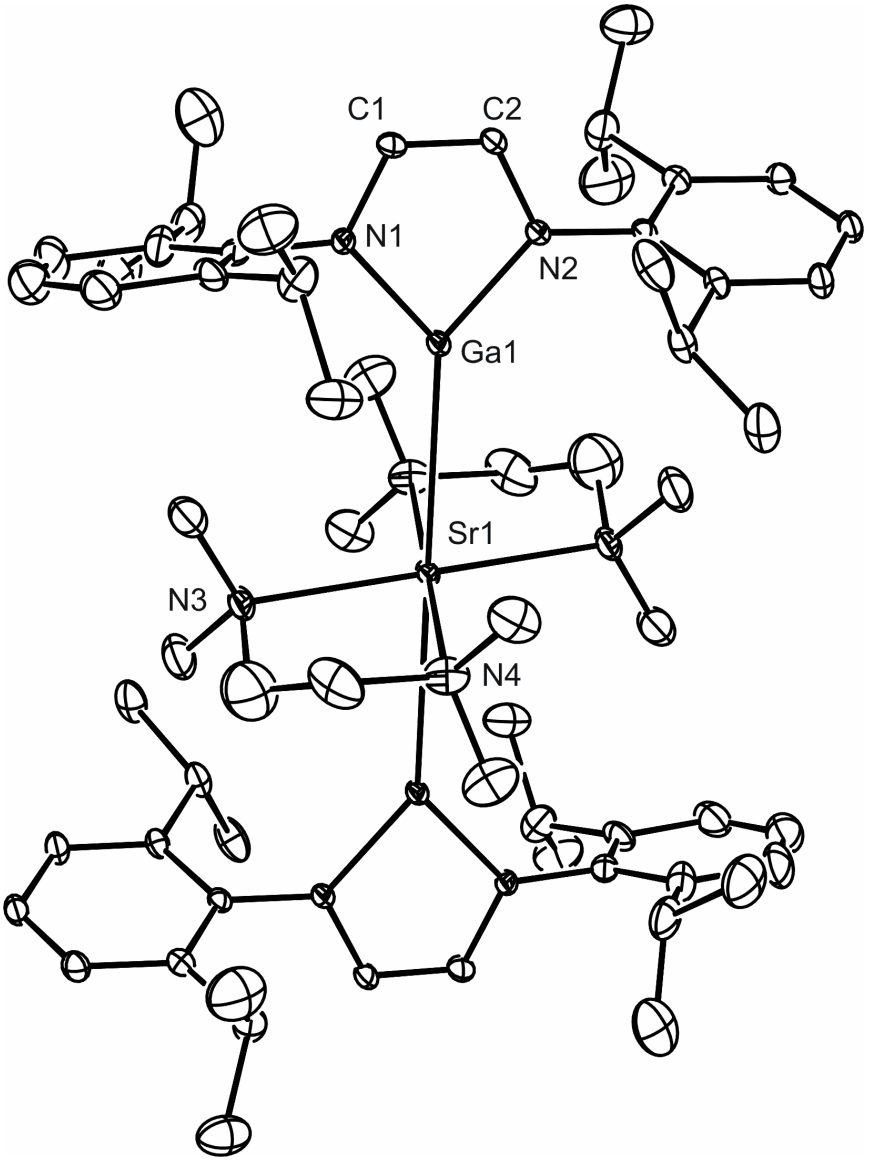

Figure 3. Thermal ellipsoid plot (25% probability surface) of the molecular structure of *trans*-[Sr{Ga(Dip-DAB)}$_2$(tmeda)$_2$] (**63**); hydrogen atoms are omitted for clarity. Selected bond lengths (Å) and angles (°): Ga(1)-N(1) 1.925(5), Ga(1)-N(2) 1.938(4), Ga(1)-Sr(1) 3.3241(11), Sr(1)-N(3) 2.656(6), Sr(1)-N(4) 2.704(7), Ga(1)-Sr(1)-Ga(1) 180.00(2), N(1)-Ga(1)-N(2) 83.69(19), N(3)-Sr(1)-N(4) 72.4(2).

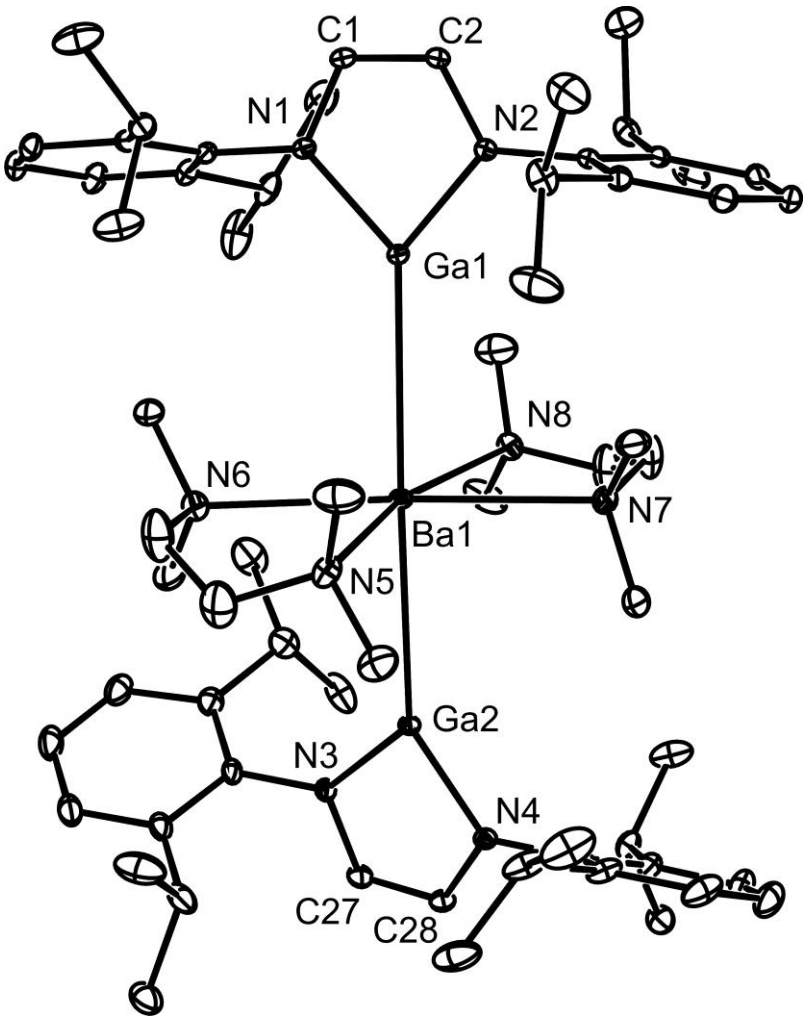

Figure 4. Thermal ellipsoid plot (25% probability surface) of the molecular structure of *trans*-[Ba{Ga(Dip-DAB)}$_2$(tmeda)$_2$] (**64**); hydrogen atoms are omitted for clarity. Ga(1)-N(1) 1.940(3), Ga(1)-N(2) 1.937(3), Ga(1)-Ba(1) 3.4625(6), Ga(2)-Ba(1) 3.4658(6), Ga(2)-N(3) 1.940(3), Ga(2)-N(4) 1.947(3), Ba(1)-N(5) 2.873(3), Ba(1)-N(6) 2.855(3), Ba(1)-N(7) 2.839(3), Ba(1)-N(8) 2.906(3), Ga(1)-Ba(1)-Ga(2) 173.620(11), N(1)-Ga(1)-N(2) 83.53(11), N(3)-Ga(2)-N(4) 83.65(12), N(5)-Ba(1)-N(6) 63.73(10), N(7)-Ba(1)-N(8) 64.48(9).

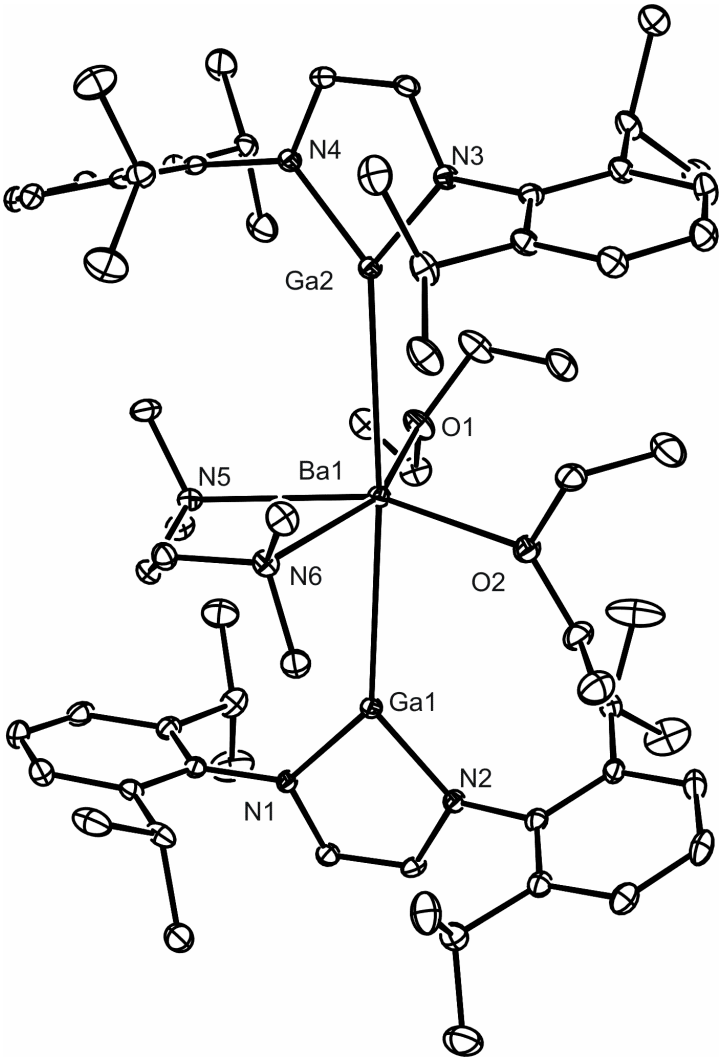

Figure 5. Thermal ellipsoid plot (25% probability surface) of the molecular structure of t*rans*-[Ba{Ga(Dip-DAB)}$_2$(tmeda)(OEt$_2$)$_2$], (**65**); hydrogen atoms are omitted for clarity. Selected bond lengths (Å) and angles (°): Ga(1)-N(1) 1.941(2), Ga(1)-N(2) 1.932(2), Ga(1)-Ba(1) 3.4832(5), Ga(2)-Ba(1) 3.4757(5), Ga(2)-N(3) 1.941(2), Ga(2)-N(4) 1.935(2), Ba(1)-N(5) 2.822(2), Ba(1)-N(6) 2.839(2), Ba(1)-O(1) 2.710(2), Ba(1)-O(2) 2.7217(19), Ga(1)-Ba(1)-Ga(2) 173.221(9), N(1)-Ga(1)-N(2) 83.29(8), N(3)-Ga(2)-N(4) 83.25(9), N(5)-Ba(1)-N(6) 65.32(7), O(1)-Ba(1)-O(2) 117.00(6).

Compound **66** was also crystallographically characterized and its molecular structure and selected geometrical parameters are depicted in Figure 6. This shows its magnesium center to have a distorted tetrahedral coordination geometry, which includes ligation by the tmeda molecule through only one of its N-centers.[35] Although the Mg-N(5) bond is significantly longer than either of the Mg-N_{Nacnac} separations, it is at the short end of the reported range for Mg-N_{tmeda} interactions (2.10-2.52 Å),[36] and should, therefore, be considered relatively strong. The Ga-Mg distance is slightly longer than those in the only other compound exhibiting such bonds, *viz.* **56** (2.722 Å mean[31]), despite the higher Mg coordination number in the latter.

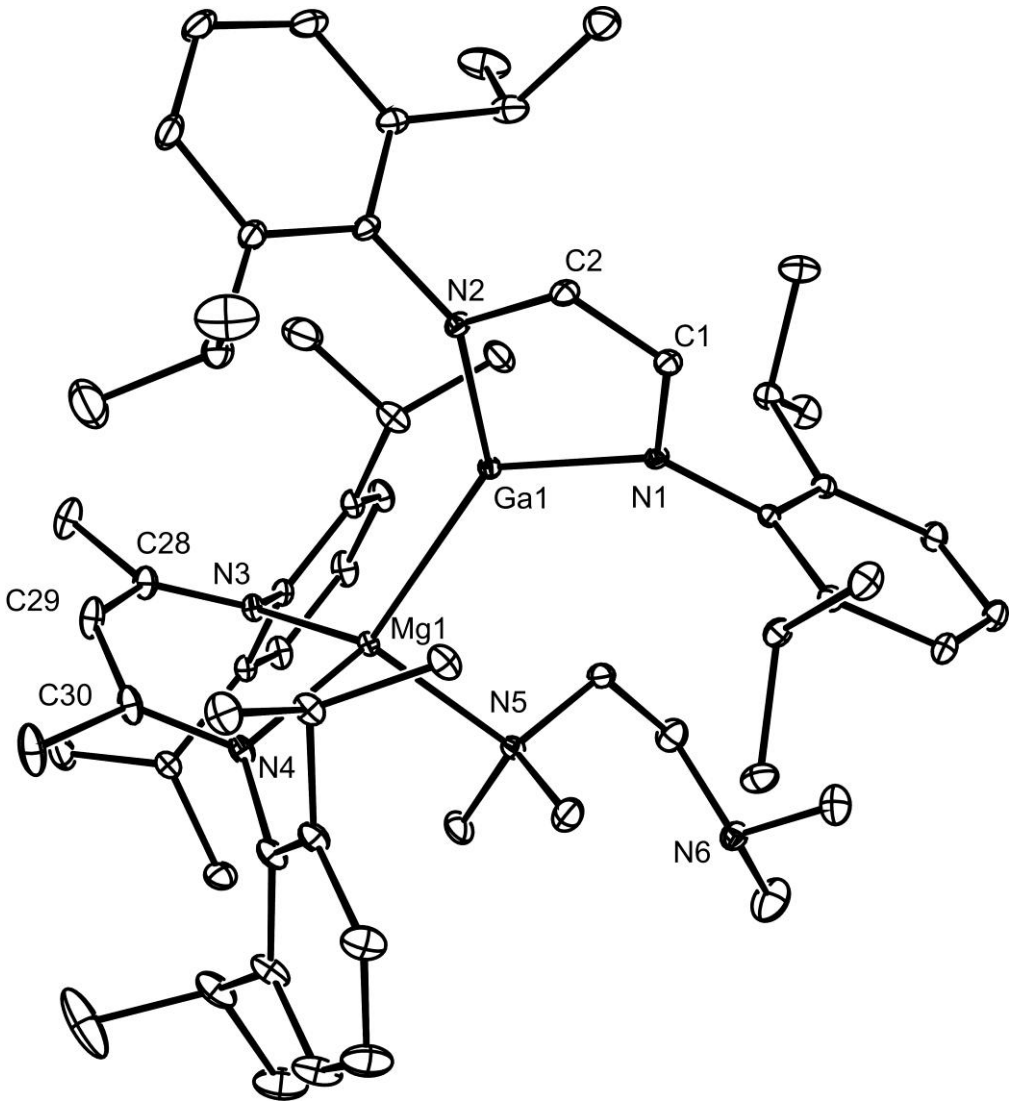

Figure 6. Thermal ellipsoid plot (25% probability surface) of the molecular structure of [(Nacnac)(κ^1-tmeda)Mg{Ga(Dip-DAB)}] (**66**); hydrogen atoms are omitted for clarity. Selected bond lengths (Å) and angles (°): Ga(1)-N(2) 1.9238(13), Ga(1)-N(1) 1.9360(14), Ga(1)-Mg(1) 2.7470(7), Mg(1)-N(3) 2.0678(15), Mg(1)-N(4) 2.0822(14), Mg(1)-N(5) 2.1733(16), N(2)-Ga(1)-N(1) 85.55(6), N(2)-Ga(1)-Mg(1) 139.87(4), N(1)-Ga(1)-Mg(1) 132.15(4), N(3)-Mg(1)-N(4) 91.50(6), N(3)-Mg(1)-N(5) 110.80(6), N(4)-Mg(1)-N(5) 111.52(6), N(3)-Mg(1)-Ga(1) 123.35(5), N(4)-Mg(1)-Ga(1) 118.72(4), N(5)-Mg(1)-Ga(1) 101.20(4).

2.3.2 Group 12 Gallyl Complexes

Although the preparation of heteroleptic gallyl group 2 metal iodide complexes was not successful, it was thought that the expected greater covalency of Ga-group 12 metal bonds might allow the isolation of related heteroleptic group 12 metal gallyl complexes incorporating the [Ga(Dip-DAB)] ligand. Such complexes were seen as potentially useful precursors to access metal(I) dimers of the type, [{(Dip-DAB)Ga}MM{Ga(Dip-DAB)}], *via* reduction methodologies. In this respect [K(tmeda)][**2**] can be regarded as being related to the bulky monodentate terphenyl ligand, $C_6H_3(Dip)_2$-2,6 (Ar'), which has been utilized by Power and coworkers for the stabilization of the homologous series of complexes, [Ar'MMAr'] (M = Zn, Cd or Hg).[37]

Whereas the 1:1 reaction of [K(tmeda)][**2**] with [$ZnCl_2$(tmeda)] previously led to intractable product mixtures,[25] repeating the reaction with [$ZnBr_2$(tmeda)] afforded a good isolated yield of the heteroleptic complex **67** after recrystallization from hexane (Scheme 24). A moderate isolated yield of the cadmium analogue of this compound, *viz.* **68**, was obtained using a similar synthetic methodology. In contrast, the 2:1 reaction of [K(tmeda)][**2**] with [CdI_2(tmeda)] led to decomposition with associated deposition of cadmium metal and the formation of the gallium(II) dimer, [{Ga(Dip-DAB)}$_2$].[27] This outcome attests to the reducing ability of [K(tmeda)][**2**], as does the fact that the 1:1 reaction of [K(tmeda)][**2**] with [HgI_2(tmeda)] resulted in the deposition of elemental mercury at *ca.* -30 °C. A number of attempts were made to reduce **67** and **68** to metal-metal bonded dimers, [{(Dip-DAB)Ga}MM{Ga(Dip-DAB)}], using various reagents, e.g. potassium metal, KC_8, KH and LiH. In all cases deposition of the group 12 metal occurred at room temperature. On only one occasion was a soluble product identified in these

reactions. This came from the reduction of **67** with LiH in THF, and was identified by NMR spectroscopy and X-ray crystallography to be the contact ion pair, $[Li(THF)_2\{H_2Ga(Dip\text{-}DAB)\}]$, **69**. One explanation for the formation of this compound involves the generation of a zinc hydride intermediate, e.g. [{(Dip-DAB)Ga}ZnH(tmeda)] (*cf.* $[\{Ar'Zn(\mu\text{-}H)\}_2]$[37]), which decomposes to Zn metal and [HGa(Dip-DAB)] *via* a hydrogen transfer process. The neutral gallium hydride species could then react with excess LiH to give the observed product. No further attempts were made to reduce **67** or **68**.

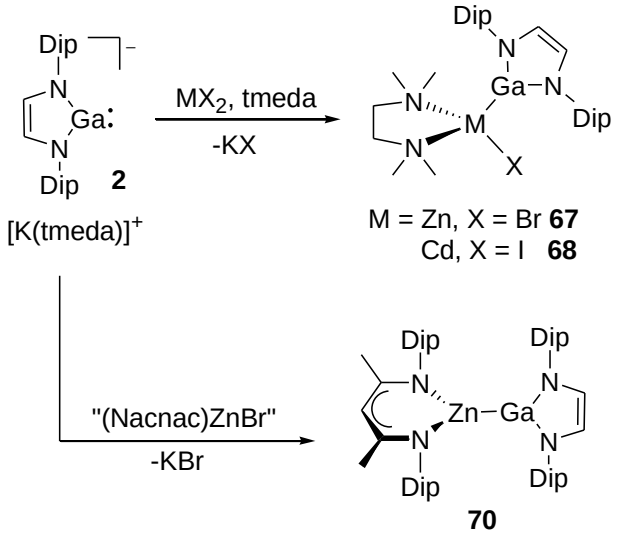

Scheme 24. Synthesis of **67, 68, 70**

Attention then turned to the preparation of group 12 analogues of **66**, which are also notionally related to the previously reported complex, **38**. Treatment of $[(Nacnac)Zn(\mu\text{-}Br)_2Li(OEt_2)_2]$ with one equivalent of [K(tmeda)][**2**] in diethyl ether afforded a good yield of the zinc gallyl complex, **70**, as an orange crystalline solid (Scheme 24). Complex **70** can be seen as an analogue of recently prepared zinc boryl complexes, e.g. $[Zn\{B(Dip\text{-}DAB)\}_2]$.[38] In contrast, the only product isolated from the equivalent reaction of

[K(tmeda)][**2**] with [(Nacnac)Cd(μ-I)$_2$Li(OEt$_2$)$_2$] was the cadmium gallyl, **68**, which was obtained in a 23% yield. One explanation for the formation of this compound is that the starting material, [(Nacnac)Cd(μ-I)$_2$Li(OEt$_2$)$_2$], is involved in a "Schlenk equilibrium" with [Cd(Nacnac)$_2$], CdI$_2$ and LiI. If so, the preferential reaction of [K(tmeda)][**2**] with CdI$_2$, relative to its reaction with bulkier [(Nacnac)Cd(μ-I)$_2$Li(OEt$_2$)$_2$], could shift the equilibrium in favor of CdI$_2$, which in turn would lead to the formation of more **68**. Interestingly, a small amount of the unusual dicadmium complex, [(Nacnac)CdI(μ-I)CdI(μ-I)Li(OEt$_2$)$_3$], **71**, was isolated from one preparation of [(Nacnac)Cd(μ-I)$_2$Li(OEt$_2$)$_2$] using the literature procedure.[39] Complex **71** was crystalographically characterized as can be seen in Figure 11. No further data was obtained on **71** due to its low yield. No further attempts were made to prepare a cadmium analogue of **70**. It is of note, however, that although **70** is related to the magnesium gallyl, **66**, it does not incorporate a tmeda ligand, even when an excess of tmeda was added to the reaction mixture that generated it. This is most likely because of the lower Lewis acidity of Zn^{2+} relative to Mg^{2+}.

Complexes **67**, **68**, and **70** are thermally stable at room temperature, though the cadmium gallyl, **68**, slowly decomposes above 50 ^{o}C with the deposition of cadmium metal. The NMR spectroscopic data for **67**, **68**, and **70** are fully consistent with their solid state structures (*vide infra*) and do not show any indication of the isomerism and/or fluxional behavior exhibited by the group 2 gallyl complexes, **62**-**64**, and **66**.

In the solid state, the monomeric compounds **67** and **68** are isostructural. The molecular structures and selected geometrical parameters, of **67** and **68** are depicted in Figures 7 and 8. Interestingly, as can be seen in Figure 8, compound **68** can also crystallize as an unsymmetrically iodide bridged dimer. The fact that this compound can crystallize as

either a monomer or a dimer suggests that its energy of dimerization is low, i.e. of a similar order as crystal packing forces. The zinc gallyl complex, **70**, along with selected geometrical parameters is depicted in Figure 10. The Zn and Cd centers of monomeric **67** and **68** have distorted tetrahedral coordination geometries, whereas the Cd centers of dimeric **68** are distorted trigonal bipyramidal with N(3) and I(1)' taking up the axial sites. In contrast, the Zn atom of **70** has a trigonal planar coordination environment, while the dihedral angle between its two heterocycles is 55.6^{o}. The gallium atoms in all the complexes in this study have trigonal planar geometries. However, the N-Ga-N angles exhibited by the group 12 complexes are significantly more obtuse than those of the group 2 complexes. This observation is in line with the expected greater covalent nature of the group 12 metal-Ga bonds. The Ga-Zn distances in **67** and **70** are close to those reported for **38**, but slightly shorter than those of the more sterically crowded species, **39** (2.440 Å mean[36]). Compound **68** possess the first structurally authenticated Ga-Cd bonds in a molecular compound, the lengths of which in each of its structural modifications are well within the sum of the covalent radii (2.66 Å) for the two elements.[40] Both the Zn-Br separation in **67** and the Cd-I distances in **68** are in the normal ranges for such interactions.[36]

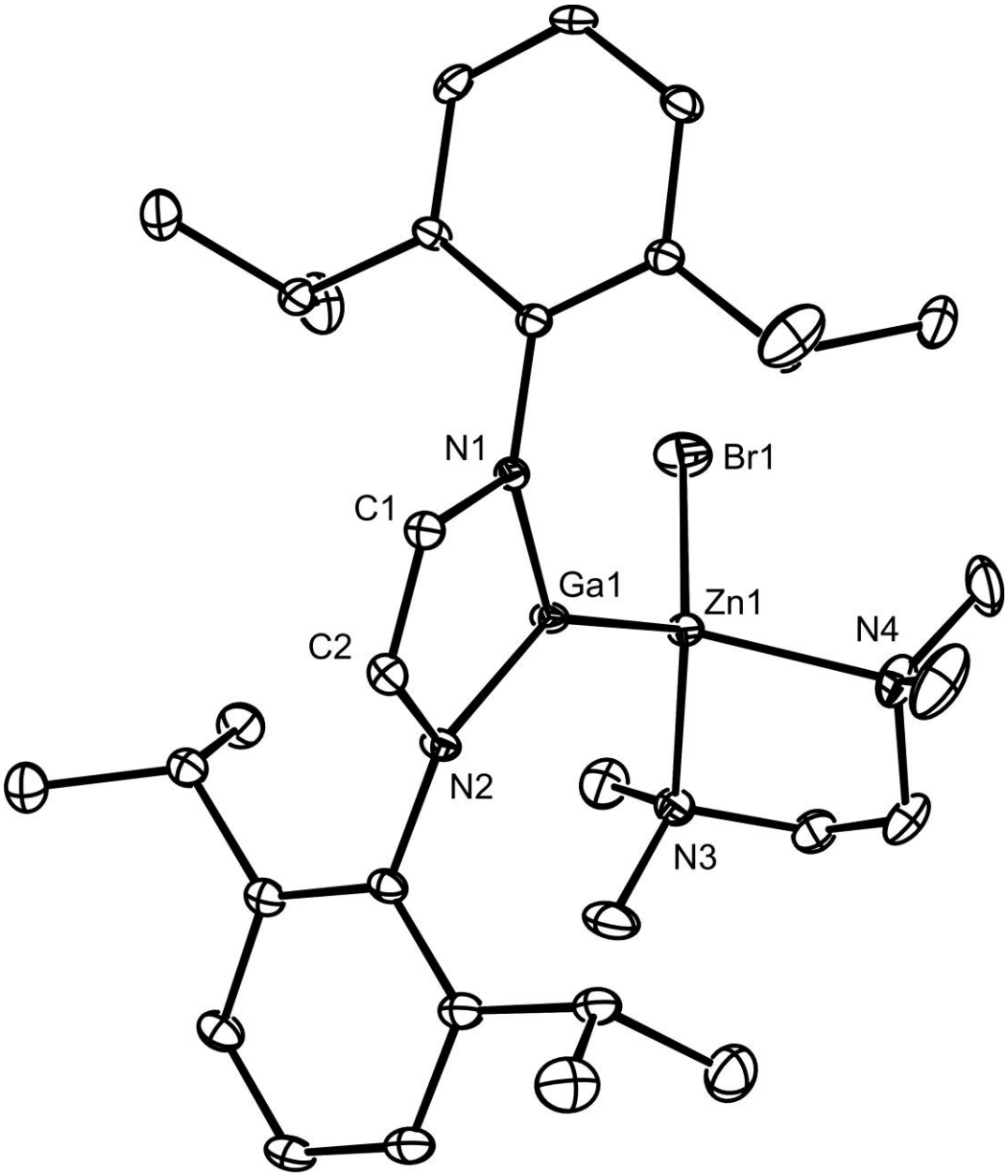

Figure 7. Thermal ellipsoid plot (25% probability surface) of the molecular structure of [(tmeda)ZnBr{Ga(Dip-DAB)}] (**67**); hydrogen atoms are omitted for clarity. Selected bond lengths (Å) and angles (°): Ga(1)-N(1) 1.879(2), Ga(1)-N(2) 1.874(2), Ga(1)-Zn(1) 2.3829(8), Zn(1)-N(3) 2.144(3), Zn(1)-N(4) 2.142(3), Zn(1)-Br(1) 2.3598(7), N(1)-Ga(1)-N(2) 86.85(11), N(3)-Zn(1)-N(4) 85.74(12), Ga(1)-Zn(1)-Br(1) 121.01(2).

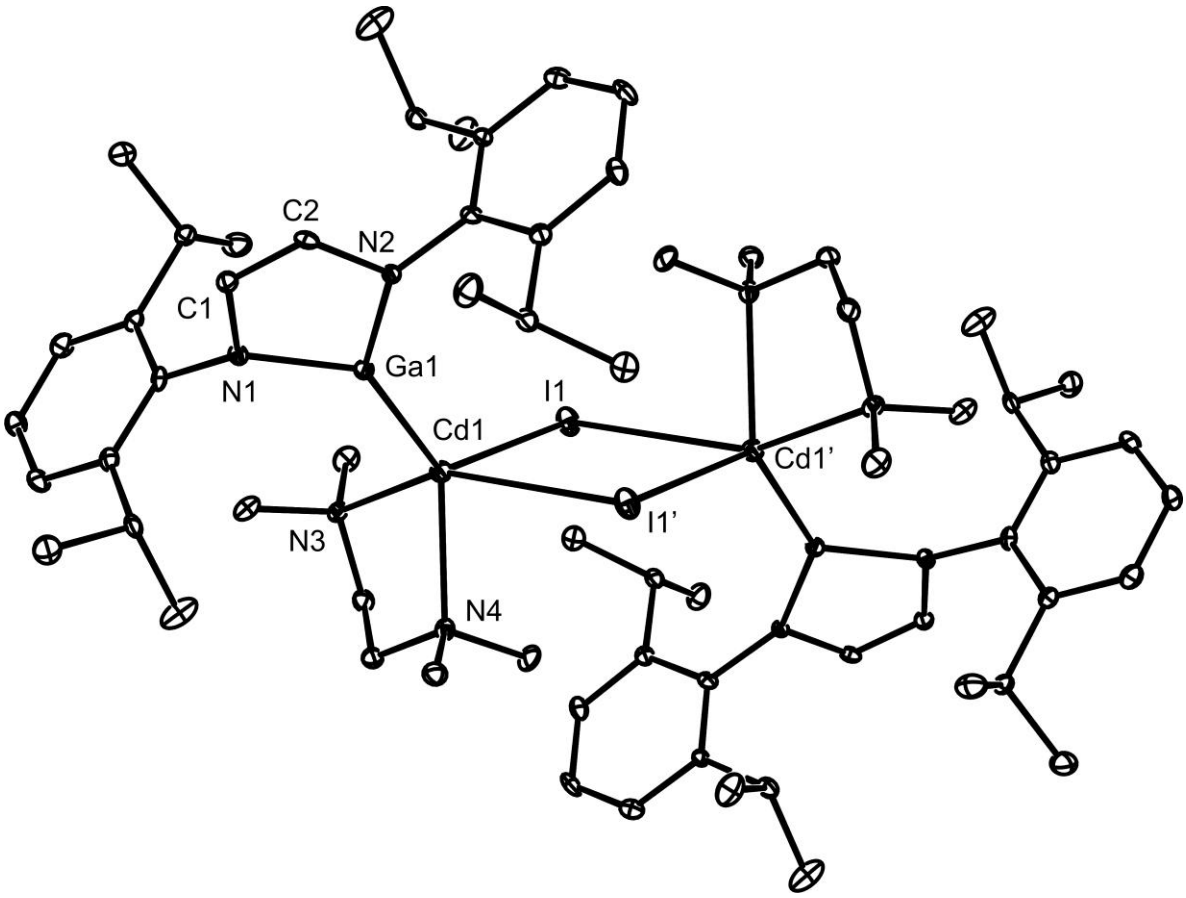

Figure 8. Thermal ellipsoid plot (25% probability surface) of the molecular structure of the dimeric structural modification of [(tmeda)CdI{Ga(Dip-DAB)}] (**68**); hydrogen atoms are omitted for clarity. Selected bond lengths (Å) and angles (°): Ga(1)-N(1) 1.885(4), Ga(1)-N(2) 1.899(4), Ga(1)-Cd(1) 2.5479(9), Cd(1)-N(3) 2.500(4), Cd(1)-N(4) 2.384(4), Cd(1)-I(1) 2.7970(8), N(1)-Ga(1)-N(2) 86.90(18), N(3)-Cd(1)-N(4) 76.03(14), Ga(1)-Cd(1)-I(1) 126.28(3).

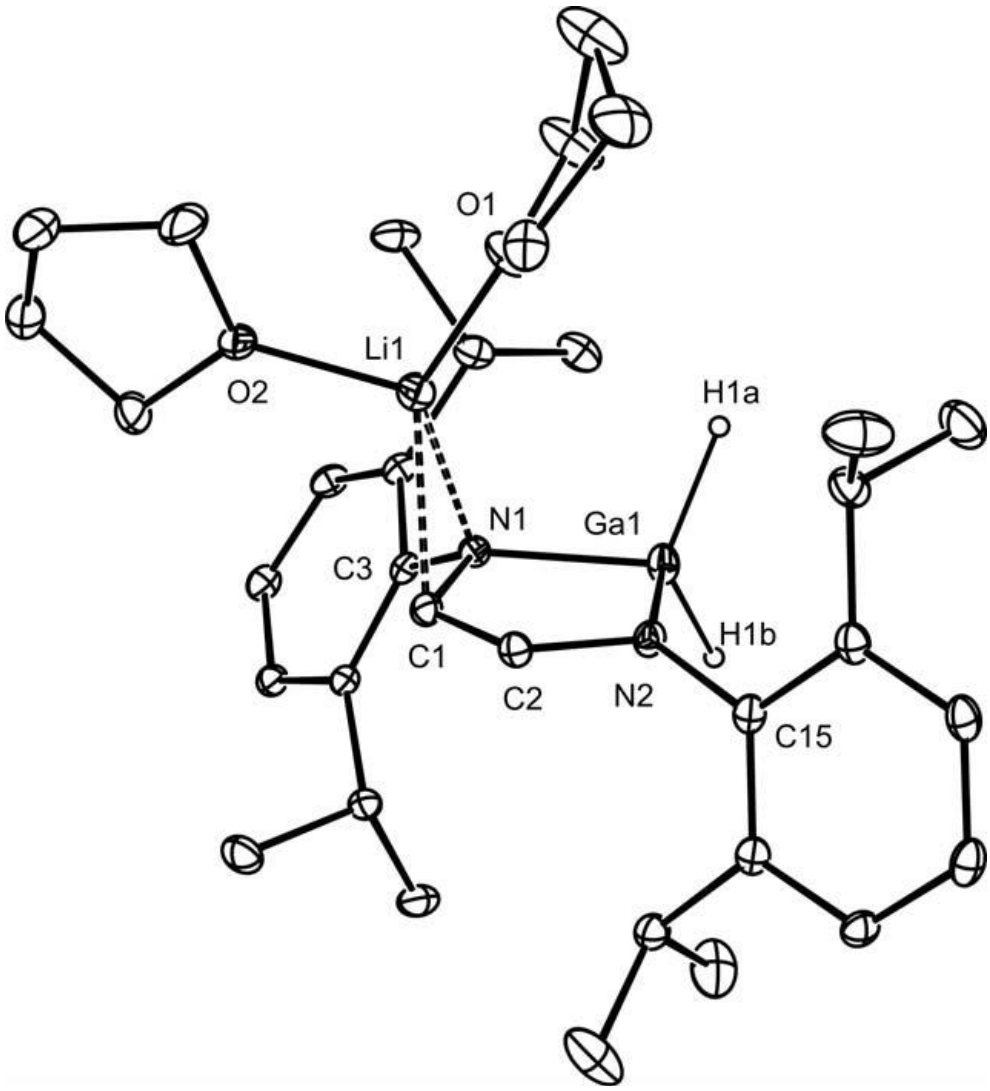

Figure 9. Thermal ellipsoid plot (25% probability surface) of the molecular structure of [Li(THF)$_2${H_2Ga(Dip-DAB)}] (**69**); hydrogen atoms (except hydrides) are omitted for clarity. Selected bond lengths (Å) and angles (°): Ga(1)-N(2) 1.937(2), Ga(1)-N(1) 1.980(3), Ga(1)-Li(1) 3.269(6), Ga(1)-H(1A) 1.55(4), Ga(1)-H(1B) 1.54(5), O(1)-Li(1) 1.874(6), N(1)-Li(1) 2.024(6), C(1)-Li(1) 2.233(6), N(1)-C(1) 1.443(4), N(2)-C(2) 1.387(4), C(1)-C(2) 1.331(4), N(2)-Ga(1)-N(1) 86.76(10), H(1A)-Ga(1)-H(1B) 118(2).

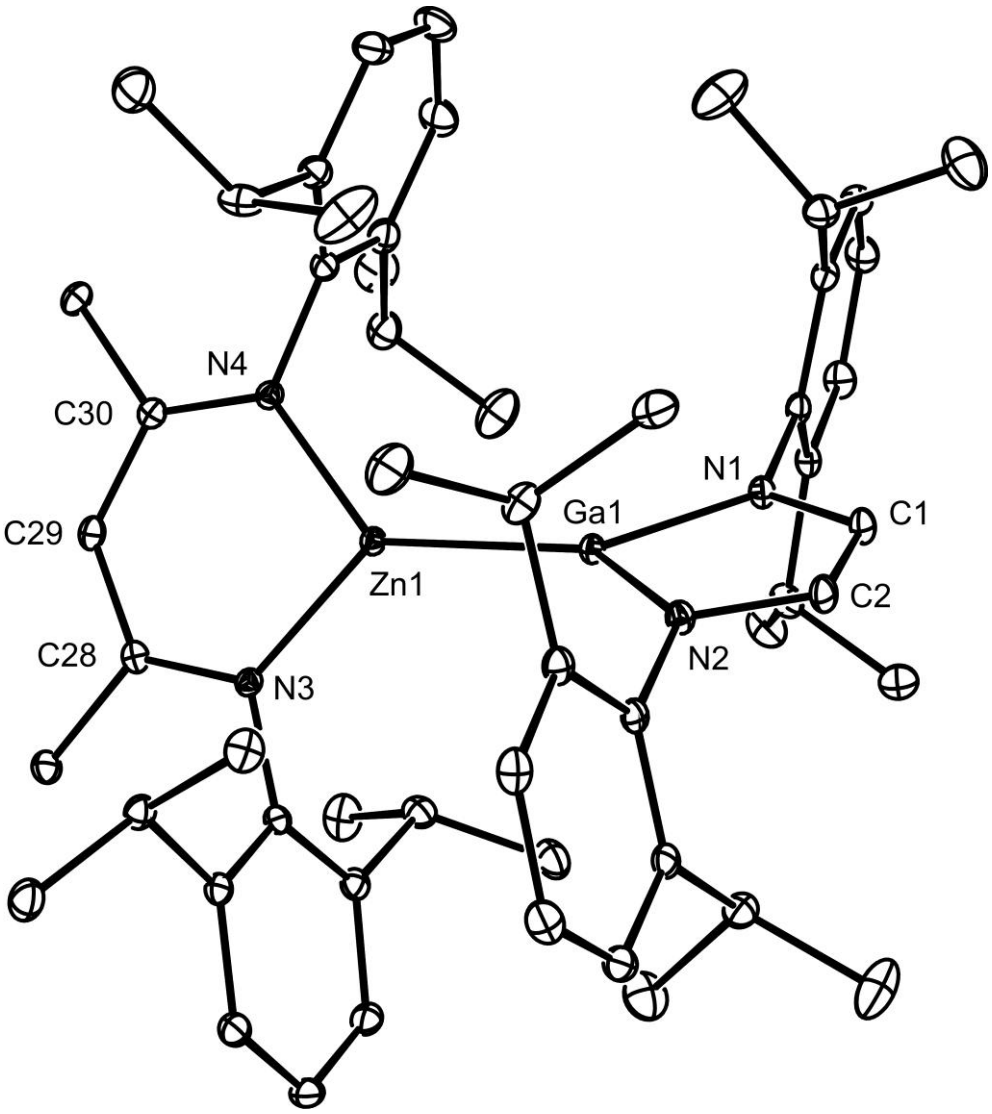

Figure 10. Thermal ellipsoid plot (25% probability surface) of the molecular structure of [(Nacnac)Zn{Ga(Dip-DAB)}] (**70**); hydrogen atoms are omitted for clarity. Selected bond lengths (Å) and angles (°): Ga(1)-N(1) 1.885(2), Ga(1)-N(2) 1.885(2), Ga(1)-Zn(1) 2.3841(6), Zn(1)-N(3) 1.958(2), Zn(1)-N(4) 1.958(2), N(1)-Ga(1)-N(2) 87.13(7), N(3)-Zn(1)-N(4) 98.17(6).

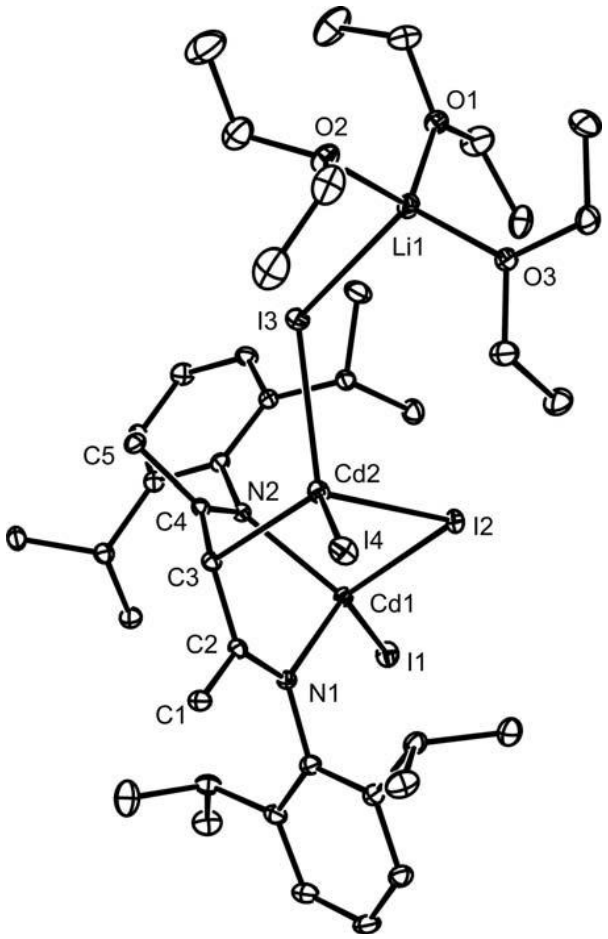

Figure 11. Thermal ellipsoid plot (25% probability surface) of the molecular structure of [(Nacnac)CdI(μ-I)CdI(μ-I)Li(OEt_2)$_3$] (**71**); hydrogen atoms are omitted for clarity. Selected bond lengths (Å) and angles (°): I(1)-Cd(1) 2.6650(9), Cd(1)-N(2) 2.221(3), Cd(1)-N(1) 2.231(3), Cd(1)-I(2) 2.8513(6), O(1)-Li(1) 1.957(7), Li(1)-O(3) 1.936(7), Li(1)-O(2) 1.940(7), Li(1)-I(3) 2.867(7), I(2)-Cd(2) 2.8681(11), Cd(2)-C(3) 2.368(3), Cd(2)-I(4) 2.7391(8), Cd(2)-I(3) 2.7634(7), N(1)-C(2) 1.291(4), N(2)-C(4) 1.304(4), C(2)-C(3) 1.468(5), C(3)-C(4) 1.453(4), N(2)-Cd(1)-N(1) 91.04(10), I(1)-Cd(1)-I(2) 122.972(13), Cd(1)-I(2)-Cd(2) 88.515(16), C(3)-Cd(2)-I(4) 114.22(8), C(3)-Cd(2)-I(3) 111.16(8), I(4)-Cd(2)-I(3) 111.814(19), C(3)-Cd(2)-I(2) 100.51(8), I(4)-Cd(2)-I(2) 114.61(3), I(3)-Cd(2)-I(2) 103.56(2).

2.4 Conclusion

In summary, the ability of [K(tmeda)][**2**] to participate in salt metathesis reactions with a range of group 2 and 12 metal halide complexes has been demonstrated. These reactions have given rise to a variety of metal gallyl compounds possessing polar covalent M-Ga (M = Mg, Ca, Sr, Ba, Zn or Cd) bonds, including the first example of a cadmium-gallium bonded molecular species, [(tmeda)CdI{Ga(Dip-DAB)}]. Crystallographic data on the compounds have provided evidence that the Ga-M interactions are more polar for the group 2 metals than the group 12 metals.

2.5 Experimental

General methods. All manipulations were carried out using standard Schlenk and glove box techniques under an atmosphere of high purity dinitrogen. Toluene, THF and hexane were distilled over potassium whilst diethyl ether was distilled over Na/K alloy. ^{1}H and ^{13}C{^{1}H} NMR spectra were recorded on either Bruker DXP300 or DRX400 spectrometers and were referenced to the resonances of the solvent used. Mass spectra were obtained from the EPSRC National Mass Spectrometric Service at Swansea University. IR spectra were recorded using a Nicolet 510 FT-IR spectrometer as Nujol mulls between NaCl plates. Microanalyses were carried out by Campbell Microanalytical, Ottago. Reproducible microanalyses could not be obtained for the group 2 gallyl complexes due to their extreme air and moisture sensitivity. Melting points were determined in sealed glass capillaries under dinitrogen and are uncorrected. The compounds [K(tmeda)][**2**],[3] [(Nacnac)MgI(OEt_2)],[41] [$ZnBr_2$(tmeda)],[42] [CdI_2(tmeda)][42] and [(Nacnac)Zn(μ-

$Br)_2Li(OEt_2)_2]$[39] were synthesized by variations of literature procedures. $[CaI_2(OEt_2)_n]$ and $[MI_2(THF)_n]$ (M = Sr or Ba) were prepared by reacting the freshly filed metal with one equivalent of diiodine in either diethyl ether or THF for 5 days. All other reagents were used as received.

Preparation of *trans*-[Ca{Ga(Dip-DAB)}$_2$(tmeda)$_2$] (62): A solution of [K(tmeda)][**2**] (0.30 g, 0.50 mmols) in toluene (15 mL) was added over 5 min to a suspension of $[CaI_2(OEt_2)_n]$ (0.25 mmols) in toluene (45 mL) and tmeda (1.0 ml, 6.67 mmols) at –80 °C. The mixture was slowly warmed to room temperature and stirred for 15 h. All volatiles were then removed *in vacuo,* the residue was extracted into diethyl ether (25 mL) and filtered. The filtrate was stored at –30 °C overnight yielding orange crystals of **62** (0.21 g, 75 %). M.p. 163-165 °C (decomp); ^{1}H NMR (300 MHz, C_6D_6, 298 K): major isomer δ 1.26 (d, 24 H, $^3J_{HH}$ = 6.8 Hz, CH(C*H*$_3$)$_2$), 1.45 (d, 24 H, $^3J_{HH}$ = 6.8 Hz, CH(C*H*$_3$)$_2$), 1.89 (br., 32 H, tmeda), 3.95 (sept., 8 H, $^3J_{HH}$ = 6.8 Hz, C*H*(CH$_3$)$_2$), 6.55 (s, 4H, NC*H*), 7.02-7.34 (m, 12 H, Ar-*H*); ^{13}C{^{1}H} NMR (100.6 MHz, C_6D_6, 300K): δ 23.7 (CH(*C*H$_3$)$_2$), 24.1 (CH(*C*H$_3$)$_2$), 28.3 (*C*H(CH$_3$)$_2$), 47.1 (N(*C*H$_3$)$_2$), 56.1 (N*C*H$_2$), 117.2 (N*C*H), 122.6, 125.0, 145.7, 151.2 (Ar-*C*); IR ν/cm^{-1} (Nujol): 1587w, 1378s, 1356s, 1319m, 1256m, 1103m, 754m; MS (EI 70eV), *m*/*z* (%): 445.2 (Ga(DAB)$^+$, 30), 378.1 (DABH$^+$, 35), 333.3 (DAB-Pr^{i+}, 100).

Preparation of *trans*-[Sr{Ga(Dip-DAB)}$_2$(tmeda)$_2$] (63): A solution of [K(tmeda)][**2**] (0.30 g, 0.50 mmols) in toluene (15 mL) was added over 5 min to a suspension of $[SrI_2(THF)_n]$ (0.25 mmols) in toluene (30 mL) and tmeda (1.0 ml, 6.67 mmols) at –80 °C. The mixture was slowly warmed to room temperature and stirred for 15 h. All volatiles were then removed *in vacuo,* the residue was extracted into diethyl ether (20 mL) and

filtered. The filtrate was stored at –30 °C overnight yielding orange crystals of **63** (0.14 g, 47 %). M.p. 175-180 °C (decomp); ^{1}H NMR (300 MHz, C_6D_6, 298 K): major isomer δ1.25 (d, 24 H, $^{3}J_{HH}$ = 6.8 Hz, CH(C*H*$_3$)$_2$), 1.46 (d, 24 H, $^{3}J_{HH}$ = 6.8 Hz, CH(C*H*$_3$)$_2$), 1.90 (br., 32 H, tmeda), 3.55 (sept., 8 H, $^{3}J_{HH}$ = 6.8 Hz, C*H*(CH$_3$)$_2$), 6.57 (s, 4H, NC*H*), 7.00-7.34 (m, 12 H, Ar-*H*); ^{13}C{^{1}H} NMR (100.6 MHz, C_6D_6, 300K): δ 23.9 (CH(*C*H$_3$)$_2$), 24.4 (CH(*C*H$_3$)$_2$), 28.1 (*C*H(CH$_3$)$_2$), 45.7 (N(*C*H$_3$)$_2$), 65.7 (N*C*H$_2$), 117.1 (N*C*H), 122.5, 124.9, 142.6, 145.0 (Ar-*C*); IR ν/cm^{-1} (Nujol): 1587w, 1378s, 1356s, 1320m, 1258m, 1103m, 754m; MS (EI 70eV), *m*/*z* (%): 445.2 (Ga(DAB)$^{+}$, 27), 378.1 (DABH^{+}, 12), 333.3 (DAB-Pr^{i+}, 100).

Preparation of *trans*-[Ba{Ga(Dip-DAB)}$_2$(tmeda)$_2$] (64): A solution of [K(tmeda)][**2**] (0.30 g, 0.50 mmols) in toluene (20 mL) was added over 5 min to a suspension of [BaI$_2$(THF)$_n$] (0.25 mmols) in toluene (25 mL) and tmeda (1.5 ml, 10.0 mmols) at –80 °C. The mixture was slowly warmed to room temperature and stirred for 15 h. All volatiles were then removed *in vacuo*, the residue extracted into diethyl ether (30 mL) and filtered. A few drops of tmeda were added to the filtrate, which was then stored at –30 °C overnight yielding red-orange crystals of **64** (0.045 g, 14 %). M.p. 178-182 °C (decomp); ^{1}H NMR (300 MHz, C_6D_6, 298 K): major isomer δ 1.33 (d, 24 H, $^{3}J_{HH}$ = 6.8 Hz, CH(C*H*$_3$)$_2$), 1.47 (d, 24 H, $^{3}J_{HH}$ = 6.8 Hz, CH(C*H*$_3$)$_2$), 2.15 (v. br., 32 H, tmeda), 3.52 (sept., 8 H, $^{3}J_{HH}$ = 6.8 Hz, C*H*(CH$_3$)$_2$), 6.61 (s, 4H, NC*H*), 7.02-7.34 (m, 12 H, Ar-*H*); ^{13}C{^{1}H} NMR (100.6 MHz, C_6D_6, 300K): δ 24.2 (CH(*C*H$_3$)$_2$), 26.3 (CH(*C*H$_3$)$_2$), 28.4 (*C*H(CH$_3$)$_2$), 46.0 (v. br., N(*C*H$_3$)$_2$), 67.0 (v. br.; N*C*H$_2$), 117.3 (N*C*H), 122.7, 125.0, 142.9(Ar-*C*), *ipso* Ar-*C* not observed; IR ν/cm^{-1} (Nujol): 1586w, 1377s, 1356s, 1319m, 1261m, 1101m, 754m; MS (EI 70eV), *m*/*z* (%): 445.2 (Ga(DAB)$^{+}$, 100), 378.1 (DABH^{+}, 15), 333.3 (DAB-Pr^{i+}, 90).

N.B. If tmeda is not added to the filtered diethyl ether extract of **64** prior to cooling to –30 °C, *trans*-[Ba{Ga(Dip-DAB)}$_2$(tmeda)(OEt$_2$)$_2$], **65**, reproducibly co-crystallizes with **64** in low yield. No spectroscopic data have been obtained for this compound.

Preparation of [(Nacnac)(κ^1-tmeda)Mg{Ga(Dip-DAB)}] (66): A solution of [K(tmeda)][**2**] (0.37 g, 0.61 mmols) in toluene (20 mL) was added over 5 min to a solution of [(Nacnac)MgI(OEt$_2$)] (0.40 g, 0.62 mmols) in toluene (45 mL) at –80 °C. The mixture was slowly warmed to room temperature and stirred for 15 h. All volatiles were then removed *in vacuo*, the residue extracted into hexane (20 mL) and filtered. The filtrate was then stored at –30 °C overnight yielding orange crystals of **66** (0.10 g, 16 %). M.p. 300-305 °C (decomp); ^{1}H NMR (300 MHz, C_6D_6, 298 K): δ1.09 (br., 36 H, CH(C*H*$_3$)$_2$), 1.35 (br., 12 H, CH(C*H*$_3$)$_2$), 1.85 (br., 6 H, NCC*H*$_3$), 1.90 (br., 16 H, tmeda), 3.02 (br., 4 H, Nacnac C*H*(CH$_3$)$_2$), 3.56 (br., 4 H, DAB C*H*(CH$_3$)$_2$), 4.84 (br. s, 2 H, NCC*H*), 6.26 (br. s, 2 H, NC*H*), 7.00-7.15 (m, 12 H, Ar-*H*); ^{13}C{^{1}H} NMR (100.6 MHz, C_6D_6, 300K): δ 23.3, 24.2, 24.6, 25.0, 25.8 (5 x br., 4 × CH(*C*H$_3$)$_2$, 1 × C*C*H$_3$), 28.3, 28.5 (2 x br., 2 x *C*H(CH$_3$)$_2$), 44.8 (v br., N(*C*H$_3$)$_2$), 54.1 (v br., N*C*H$_2$), 95.4 (br., *C*H), 117.1 (N*C*H), 122.8, 123.4, 124.0, 124.4, 126.2, 141.9, 145.3, 148.3 (8 x br., Ar-*C*), 171.2 (*C*CH$_3$); IR ν/cm^{-1} (Nujol): 1520w, 1377s, 1364m, 1316m, 125m, 1102m, 796m, 756m; MS (EI 70eV), *m*/*z* (%): 888.2 (M$^+$-tmeda, 21), 445.2 (Ga(DAB)$^+$, 100), 418.4 (NacnacH$^+$, 22), 403.3 (NacnacH$^+$-CH$_3$, 45), 333.3 (DAB-Pr^{i+}, 90).

Preparation of [(tmeda)ZnBr{Ga(Dip-DAB)}] (67): To a solution of [ZnBr$_2$(tmeda)] (0.17 g, 0.50 mmol) in THF (20 mL) at -80 °C was added [K(tmeda)][**2**] (0.30 g, 0.50 mmol) in THF (20 mL). The reaction mixture was warmed to ambient temperature over 4 h, whereupon volatiles were removed *in vacuo*. The yellow residue was extracted into

hexane (50 mL), the extract filtered and the filtrate stored at -30 °C overnight to yield yellow crystals of **67** (0.21 g, 60 %). M.p. 124-126 °C (decomp.); ^{1}H NMR (300 MHz, C_6D_6, 300K): δ 1.45 (d, $^{3}J_{HH}$ = 6.9 Hz, 12 H, CH(C*H*$_3$)$_2$), 1.49 (d, $^{3}J_{HH}$ = 6.9 Hz, 12 H, CH(C*H*$_3$)$_2$), 1.65 (s, 12 H, N(C*H*$_3$)$_2$), 1.97 (s, 4 H, NC*H*$_2$), 3.94 (sept., $^{3}J_{HH}$ = 6.9 Hz, 4 H, C*H*(CH$_3$)$_2$), 6.61 (s, 2 H, NC*H*), 7.22-7.35 (m, 6 H, Ar-*H*); ^{13}C{^{1}H} NMR (100.6 MHz, C_6D_6, 300K): δ 25.2 (CH(*C*H$_3$)$_2$), 25.4 (CH(*C*H$_3$)$_2$), 28.2 (*C*H(CH$_3$)$_2$), 47.6 (N(*C*H$_3$)$_2$), 56.2 (N*C*H$_2$), 122.6 (N*C*H), 123.0, 124.9, 145.6, 146.9 (Ar-*C*); IR $\tilde{\nu}$/cm^{-1} (Nujol): 1657w, 1557w, 1377m, 1359m, 1287w, 1260m, 1101m, 1023m, 797m, 760m; MS (EI/70eV), *m*/*z* (%): 706.1, (M^{+}, 4), 445.2 (Ga(DAB)$^{+}$, 15), 378.1 (DABH^{+}, 48), 333.3 (DAB-Pr^{i+}, 100); anal. calc. for $C_{32}H_{52}BrGaN_4Zn$: C 54.30 %, H 7.41 %, N 7.92 %; found: C 53.92 %, H 7.27 %, N 7.77 %.

Preparation of [(tmeda)CdI{Ga(Dip-DAB)}] (68): To a solution of [CdI_2(tmeda)] (0.24 g, 0.50 mmol) in THF (20 mL) at -80 °C was added [K(tmeda)][**2**] (0.30 g, 0.50 mmol) in THF (20 mL). The reaction mixture was warmed to ambient temperature over 4 h, whereupon volatiles were removed *in vacuo*. The orange residue was extracted into hexane (30 mL), the extract filtered and the filtrate stored at -30 °C overnight to yield orange crystals of **68** (0.15 g, 38 %). M.p. 130-135 °C (decomp.); ^{1}H NMR (300 MHz, C_6D_6, 300K): δ 1.43 (d, $^{3}J_{HH}$ = 6.9 Hz, 12 H, CH(C*H*$_3$)$_2$), 1.48 (d, $^{3}J_{HH}$ = 6.9 Hz, 12 H, CH(C*H*$_3$)$_2$), 1.65 (s, 12 H, N(C*H*$_3$)$_2$), 1.94 (s, 4 H, NC*H*$_2$), 3.86 (sept., $^{3}J_{HH}$ = 6.9 Hz, 4 H, C*H*(CH$_3$)$_2$), 6.62 (s, 2 H, NC*H*), 7.22-7.33 (m, 6 H, Ar-*H*); ^{13}C{^{1}H} NMR (100.6 MHz, C_6D_6, 300K): δ 25.0 (CH(*C*H$_3$)$_2$), 25.6 (CH(*C*H$_3$)$_2$), 28.3 (*C*H(CH$_3$)$_2$), 48.0 (N(*C*H$_3$)$_2$), 56.6 (N*C*H$_2$), 122.9 (N*C*H), 123.0, 125.3, 145.6, 147.0 (Ar-*C*); IR $\tilde{\nu}$/cm^{-1} (Nujol): 1660w, 1558w, 1378m, 1355m, 1285w, 1255m, 1101m, 1026m, 793m, 758m; MS (EI/70eV), *m*/*z*

(%): 445.2 ($Ga(DAB)^+$, 100), 378.1 ($DABH^+$, 15), 333.3 ($DAB\text{-}Pr^{i+}$, 53); anal. calc. for $C_{32}H_{52}IGaN_4Cd$: C 47.93 %, H 6.54 %, N 6.99 %; found: C 47.57 %, H 6.48 %, N 6.83 %.

Preparation of [Li(THF)$_2${H$_2$Ga(Dip-DAB)}] (69): Spectroscopic data for a low yield (ca. 5%) of this compound crystallized from the reaction of **67** with an excess of LiH in THF. M.p. 78-80°C (decomp.); ^{1}H NMR (300 MHz, C6D6, 300 K) δ 1.19 (d, $^3J_{HH}$ = 6.9 Hz, 12 H, $CH(CH_3)_2$), 1.20 (d, $^3J_{HH}$ = 6.9 Hz, 12 H, $CH(CH_3)_2$), 1.27 (br. m, 8 H, OCH_2CH_2), 3.41 (br. m, 8 H, OCH_2), 3.83 (sept., $^3J_{HH}$ = 6.9 Hz, 4 H, $CH(CH_3)_2$), 5.79 (br. s, 2H, GaH), 6.60 (s, 2 H, NCH), 6.85-7.33 (m, 6 H, Ar-H); IR ν/cm^{-1} (Nujol): 1768m (Ga-H str.), 1654w, 1378m, 1361m, 1219m, 754m; MS (EI/70eV), m/z (%): 445.2 ($Ga(DAB)^+$, 70), 378.1 ($DABH^+$, 15).

Preparation of [(Nacnac)Zn{Ga(Dip-DAB)}] (70): A solution of [K(tmeda)][**2**] (0.22 g, 0.36 mmols) in diethyl ether (20 mL) was added over 5 min to a solution of [(Nacnac)Zn(μ-Br)$_2$Li(OEt$_2$)$_2$] (0.29 g, 0.36 mmols) in diethyl ether (20 mL) at –80 °C. The mixture was slowly warmed to room temperature, whereupon volatiles were removed *in vacuo* leaving an orange residue. This was extracted into hexane (35 mL) and filtered. The filtrate was stored at –30 °C overnight yielding orange crystals of **70** (0.17 g, 51 %). M.p. 140-142 °C; ^{1}H NMR (300 MHz, C_6D_6, 300 K): δ 1.04 (d, $^3J_{HH}$ = 6.9 Hz, 12 H, $CH(CH_3)_2$), 1.11 (d, $^3J_{HH}$ = 6.9 Hz, 12 H, $CH(CH_3)_2$), 1.15 (d, $^3J_{HH}$ = 6.9 Hz, 12 H, $CH(CH_3)_2$), 1.33 (d, $^3J_{HH}$ = 6.9 Hz, 12 H, $CH(CH_3)_2$), 1.51 (s, 6 H, $NCCH_3$), 3.04 (sept., $^3J_{HH}$ = 6.9 Hz, 4 H, $CH(CH_3)_2$), 3.47 (sept., $^3J_{HH}$ = 6.9 Hz, 4 H, $CH(CH_3)_2$), 5.02 (s, 1 H, NCCH), 6.28 (s, 2 H, NCH), 7.05-7.30 (m, 12 H, Ar-H); ^{13}C NMR (100.6 MHz, C_6D_6, 300 K): δ 23.2, 23.8, 24.3, 24.8, 25.4 (4 × $CH(CH_3)_2$, 1 × CCH_3), 28.7, 28.8 (2 x $CH(CH_3)_2$), 97.9 (NCCH), 123.2 (NCH), 124.0, 124.2, 125.2, 125.8, 126.9, 141.8, 145.4, 148.5 (8 x br.,

Ar-*C*), 169.1 (*C*CH_3); IR ν/cm^{-1} (Nujol): 1656w, 1519m, 1380m, 1317m, 1261m, 1179m, 1159m, 1099m, 1022m, 796m, 758m; MS (EI/70eV), *m*/*z* (%): 928.5 (M^+, 100), 481.3 ((Nacnac)Zn^+, 49), 445.2 (Ga(DAB)$^+$, 12), 403.3 (NacnacH^+-CH_3, 9), 333.3 (DAB-Pr^{i+}, 15); acc. mass EI: calc. for $C_{55}H_{77}N_4GaZn$ 926.4690; found 926.4688; anal. calc. for $C_{55}H_{77}N_4GaZn$: C 71.08 %, H 8.35 %, N 6.03 %; found: C 70.71 %, H 8.16 %, N 5.93 %.

2.6 References

1. Schmidt, E.S.; Jockisch, A.; Schmidbaur, H. *J. Am. Chem. Soc.*, **1999**, *121*, 9758.
2. Schmidt, E.S.; Schier, A.; Schmidbaur, H. *Dalton Trans.*, **2001**, 505.
3. Baker, R.J.; Farley, R.D.; Jones, C.; Kloth, M.; Murphy, D.M. *Dalton Trans.*, **2002**, 3844.
4. Pott, T.; Jutzi, P.; Kaim, W.; Schoeller, W.W.; Neumann, B.; Stammler, A.; Stammler, H.-G.; Wanner, M. *Organometallics*, **2002**, *21*, 2169.
5. Pott, T.; Jutzi, P.; Schoeller, W.W.; Stammler, A.; Stammler, H.-G. *Organometallics*, **2001**, *20*, 5492.
6. Baker, R.J.; Jones, C. *Coord. Chem. Rev.*, **2005**, *249*, 1857.
7. Baker, R.J.; Jones, C.; Kloth, M.; Platts, J.A. *Angew. Chem. Int. Ed.*, **2003**, *42*, 2660.
8. Baker, R.J.; Jones, C.; Kloth, M.; Platts, J.A. *Organometallics*, **2004**, *23*, 4811.
9. Jones, C.; Mills, D.P.; Rose, R.P. *J. Organomet. Chem.*, **2006**, *691*, 3060.
10. Schäfer, A.; Weidenbruch, M.; Saak, W.; Pohl, S. *Chem. Commun.* **1995**, 1157.
11. Stabenow, F.; Saak, W.; Weidenbruch, M. *Chem. Commun.*, **1999**, 1131.
12. Green, S.P.; Lippert, K.-A.; Jones, C.; Mills, D.P. A. Stasch, *Inorg. Chem.*, **2006**, *45*, 7242.
13. Rupar, P.A.; Jennings, M.C.; Baines, K.M. *Can. J. Chem.*, **2007**, *85*, 141.
14. Jones, C.; Waugh, M. *Dalton Trans.*, **2004**, 1971.
15. Cloke, F.G.N.; Hitchcock, P.B.; Nixon, J.F.; Wilson, D.J. *Organometallics*, **2000**, *19*, 219.

16. Baker, R.J.; Jones, C.; Mills, D.P.; Murphy, D.M.; Hey-Hawkins, E.; Wolf, R. *Dalton Trans*., **2006**, 64.

17. Baker, R.J.; Jones, C.; Kloth, M. *Dalton Trans*., **2005**, 2106.

18. Baker, R.J.; Jones, C.; Platts, J.A. *J. Am. Chem. Soc*., **2003**, *125*, 10534.

19. (a) Abernethy, C.D.; Cowley, A.H.; Jones, R.A.; McDonald, C.L.B.; Shulka, P.; Thompson, L.K. *Organometallics*, **2001**, *20*, 3629; (b) Abernethy, C.D.; Clyburne, J.A.C.; Cowley, A.H.; Jones, R.A. *J. Am. Chem. Soc*., **1999**, *121*, 2329.

20. Aldridge, S.; Baker, R.J.; Coombs, N.D.; Jones, C.; Rose, R.P.; Rossin, A.; Willock, D.J. *Dalton Trans*., **2006**, 3313.

21. Hartwig, J.F.; He, X. *Organometallics*, **1996**, *15*, 5350.

22. Baker, R.J.; Jones, C.; Murphy, D.M. *Chem. Commun*., **2005**, 1339.

23. For examples, see: (a) Fooladi, E.; Dalhus, B.; Tilset, M. *Dalton Trans*., **2004**, 3909; (b) Buchgraber, P.; Toupet, L.; Guerchais, V. *Organometallics*, **2003**, *22*, 5144; (c) Dioumaev, V.K.; Szalda, D.J.; Hanson, J.; Franz, J.A.; Bullock, R.M. *Chem. Commun*., **2003**, 1670; (d) Simms, R.W.; Drewitt, M.J.; Baird, M.C. *Organometallics*, **2002**, *21*, 2958.

24. Baker, R.J.; Jones, C.; Platts, J.A. *Dalton Trans*., **2003**, 3673.

25. Jones, C.; Rose, R.P.; Stasch, A. *Dalton Trans*., **2007**, 2997.

26. Jones, C.; Mills, D.P.; Rose, R.P.; Stasch, A.; Woodul, W.D. *J. Organomet. Chem.* **2010**, *695*, 2410.

27. Voges, M.H.; Rømming, C.; Tilset, M. *Organometallics*, **1999**, *18*, 529.

28. Green, S.P.; Jones, C.; Mills, D.P.; Stasch, A. *Organometallics*, **2007**, *26*, 3424.

29. Liddle, S.T.; Mills, D.P.; Gardner, B.M.; McMaster, J.; Jones, C.; Woodul, W.D. *Inorg. Chem.*, **2009**, *48*, 3520.

30. Jones, C.; Mills, D.P.; Platts, J.A.; Rose, R.P. *Inorg. Chem*., **2006**, *45*, 3146.

31. Fedushkin, I.L.; Lukoyanov, A.N.; Tishkina, A.N.; Fukin, G.K.; Lyssenko, K.A.; Hummert, M. *Chem. Eur. J.* **2010**, *16*, 7563.

32. Emsley, J. *The Elements*, 3rd Edition, New York, Oxford University Press, **1998**.

33. Westerhausen, M. *Coord. Chem. Revs*., **2008**, *252*, 1516.

34. Jones, C.; Mills, D.P.; Rose, R.P.; Stasch. A. *Dalton Trans.*, **2008**, 4395.

35. Several complexes incorporating κ^1-tmeda ligands have been previously reported. See for example Iravani, E.; Neumuller, B. *Organometallics*, **2003**, *22*, 4129.

36. As determined from a survey of the Cambridge Crystallographic Database (February, 2010).

37. Zhu, Z.; Brynda, M.; Wright, R.J.; Fischer, R.C.; Merrill, W.A.; Rivard, E.; Wolf, R.; Fettinger, J.C.; Olmstead, M.M.; Power, P.P. *J. Am. Chem. Soc.*, **2007**, *129*, 10847.

38. Kajiwara, T.; Terabayashi, T.; Yamashita, M.; Nozaki, K. *Angew. Chem. Int. Ed.*, **2008**, *47*, 6606.

39. Prust, J.; Most, K.; Muller, I.; Stasch, A.; Roesky, H.W.; Unson, I. *Eur. J. Inorg. Chem.*, **2001**, 1613.

40. Cordero, B.; Gomez, V.; Platero-Prats, A.E.; Reves, M.; Echeverria, J.; Cremades, E.; Barragan, F.; Alvarez, S. *Dalton Trans.*, **2008**, 2832.

41. (a) Bonyhady, S.J.; Jones, C.; Nembenna, S.; Stasch, A.; Edwards, A.J.; McIntyre, G.J. *Chem. Eur. J.*, **2010**, *16*, 938; (b) Prust, J.; Most, K.; Müller, I.; Alexopoulos, E.; Stasch, A.; Uson, I.; Roesky, H.W. *Z. Anorg. Allg. Chem.*, **2001**, *627*, 2032.

42. Abraham, M.H.; Parret, F.W. *Can. J. Chem.*, **1970**, *48*, 181.

Chapter 3

Complexes of an Anionic Gallium(I) *N*-heterocyclic Carbene Analogue with Selected Lanthanide Metals.

3.1 Introduction

The chemistry of complexes containing f-block elements bonded to main group elements is relatively new and largely unknown. Recently, Liddle and Mills reviewed this exciting area of chemistry.[1] The f-block encompasses the lanthanide and actinide elements. This section will serve as an introduction into the chemistry of complexes containing bonds between f-block-metals and transition metals, aluminum, silicon, germanium, tin, antimony and bismuth. More specifically, works carried out with the five-membered anionic gallium(I) heterocycle, [:Ga{[N(Dip)C(H)]$_2$}[K(tmeda)] (Dip = $C_6H_3Pr^i_2$-2,6; tmeda=tetramethylethylenediamine) **1** will be summarized.[2]

To date, only a handful of examples of structurally authenticated f-block-transition metal bonded complexes have been reported.[1] In the early 1990's, Shore and Deng reported a series of ytterbium-iron complexes.[3,4] Three equivalents of ytterbium metal in liquid ammonia reduced $Fe_2(CO)_{12}$, affording the novel compound [$(NH_3)_x$YbFe$(CO)_4$], **2**, as a yellow solid which has a polymeric ladder structure. Leaving **2** in cold acetonitrile afforded orange crystals of [{$(MeCN)_3$YbFe$(CO)_4$}$_2$.MeCN]$_\infty$, **3** having a polymeric sheet structure. Finally, in 1996, a solvent-free form of **3** was prepared, i.e. [$(MeCN)_3$YbFe$(CO)_4$]$_\infty$, **4**. The Yb-Fe interactions of **2** and **3** are detailed in Figure 1.

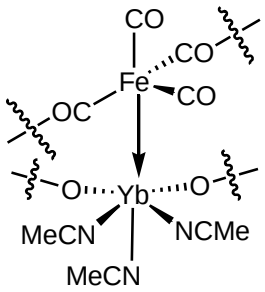

Yb-Fe interaction in **2** and **3**

Figure 1. The Yb-Fe interactions of complexes **2** and **3**.

With interest spurred in the field of metal-f-block bonded complexes, Beletskaya and Voskoboynikov set out to prepare lutetium-ruthenium and lutetium-iron bonded complexes. The reaction of $[(\eta^5\text{-}C_5H_5)_2LuCl(THF)]$ and $Na[Ru(\eta^5\text{-}C_5H_5)(CO)_2]$ in THF afforded colorless crystals of the desired complex, $[(\eta^5\text{-}C_5H_5)_2Lu(THF)\text{-}Ru(\eta^5\text{-}C_5H_5)(CO)_2]$ **5**, which was structurally authenticated (Scheme 1).[5] The analogous lutetium-iron complex was prepared, but was only characterized by infrared spectroscopy due to its decomposition within one hour of preparation.[1]

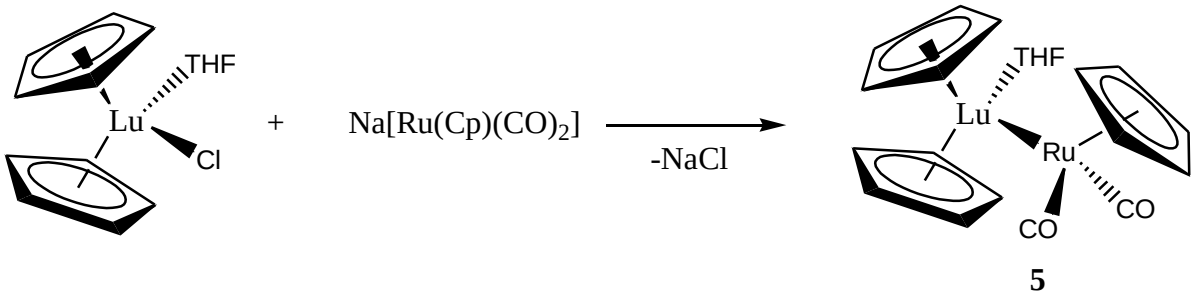

5

Scheme 1. Synthesis of **5**.

In 1998, Kempe and co-workers successfully synthesized two neodymium-transition metal bonded complexes.[6] Using the bis-aminopyridinato ligands, Kempe was able to prepare a novel neodymium-rhodium bonded complex as well as a neodymium-

palladium bonded complex. The neodymium-rhodium complex, [{O(SiMe$_2$N-2-C$_5$H$_3$N-4-Me)$_2$}$_2$NdRh(η^2-C$_2$H$_4$)], **6**, is yellow with a Nd—Rh bond length of 2.974(2) Å (Figure 2). The neodymium-palladium bonded complex, [{O(SiMe$_2$N-2-C$_5$H$_3$N-4-Me)$_2$}$_2$Nd(THF)Pd(Me)], **7**, is also yellow, with a Nd—Pd bond length of 3.035(2) Å (Figure 2).[6] In both complexes, it can be seen that the bis-aminopyridinato ligands saturate the coordination sphere of neodymium leaving excess donor sites open which allows coordination to the transition metal fragment.[1]

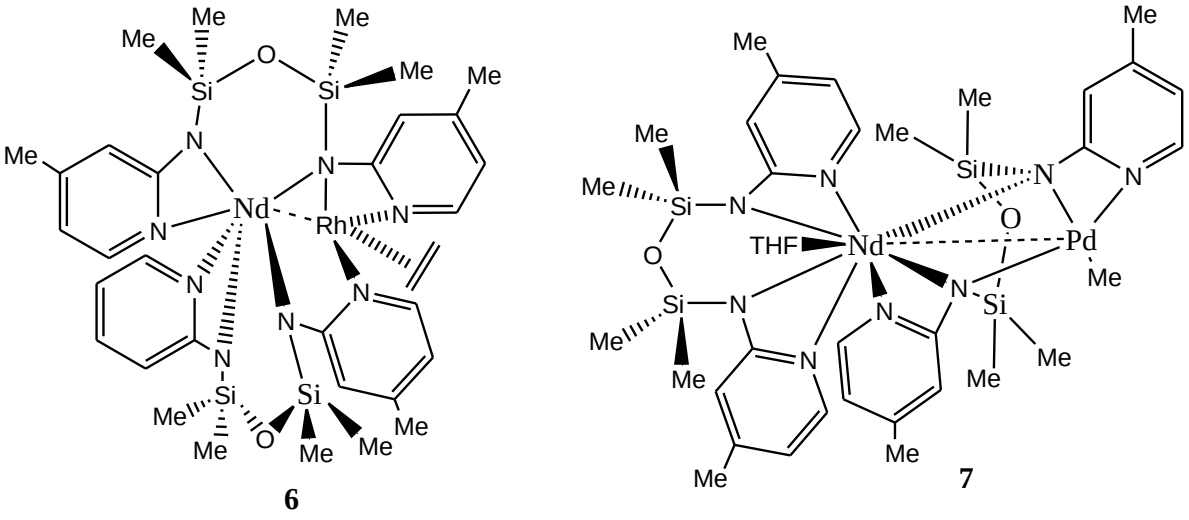

Figure 2. Complexes **6** and **7**.

More recently Kempe and co-workers have prepared an example of a polarized covalent yttrium-rhenium bonded complex as well as a ytterbium-rhenium bonded complex (Scheme 2).[7] The Y-Re complex, [(η^5-C$_5$H$_5$)$_2$Y-Re(η^5-C$_5$H$_5$)$_2$], **8**, formed as an orange solid and exhibited a Y-Re bond length of 2.962(2) Å. The polarized nature of the Y-Re bond in complex **8** was realized through density functional theory calculations, which revealed the bond to have 84% rhenium and 14% yttrium character.[1] The Yb-Re complex,

[(η^5-C_5H_5)$_2$Yb-Re(η^5-C_5H_5)$_2$], **9**, was prepared, like complex **8**, via alkane elimination. Complex **9** is green with a Yb-Re bond length of 2.897(2) Å.

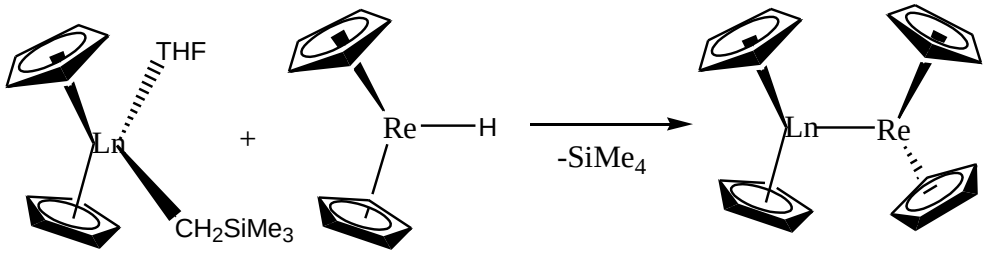

Ln = Y (**8**); Yb (**9**)

Scheme 2. Synthesis of complexes **8** and **9**.

Two complexes with examples of weak dative Fe → Sc interactions have been prepared by Diaconescu and co-workers using a ferrocene diamide ligand.[8] The first, [Sc{fc(NSiMe$_2$Bu^t)$_2$}(CH$_2$C$_6$H$_3$-3,5-Me$_2$)(THF)] (**10**, fc = [Fe(C$_4$H$_4$)$_2$]) exhibits an iron-scandium bond distance of 3.167(2) Å (Figure 3). The second, [Sc{fc(NSiMe$_2$Bu^t)$_2$}(Me)(THF)$_2$] (**11**), incorporates a second THF molecule as well as a higher coordination number for scandium. The scandium-iron distance in complex **11** is 3.258(1) Å slightly longer than in complex **10**, which was said to be reasonable due to the increase in coordination number.

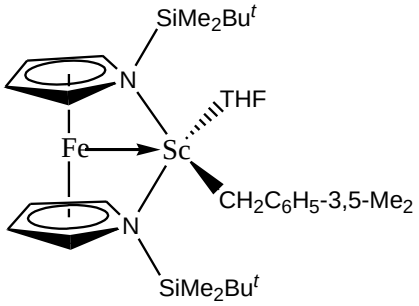

10

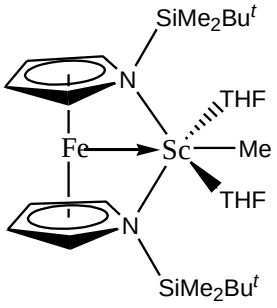

11

Figure 3. Complexes **10** and **11**.

Another example of a lanthanide bonded to a transition metal is found in the neodymium iron complex, [Nd(L′)(N″){Fe(η^5-C_5H_5)$(CO)_2$}], **12**, prepared by Arnold and co-workers.[9] The reported yellow complex was prepared via the salt-methasis reaction of a half an equivalent of the neodymium amido-tethered NHC precursor [{Nd(L′)(N″)(μ−I)}$_2$] [L′=Bu^{t}NCH$_2$CH$_2${C(NCSiMe$_3$CHNBu^t)}; N″=N(SiMe$_3$)$_2$] with K[Fe(η^5-C_5H_5)$(CO)_2$], (Scheme 3). It was found through a DFT study that the Nd-Fe bond is highly polarized and could be considered electrostatic in nature. The DFT study also shed some light on the relatively short Nd-Fe bond length of 2.994(1) Å, suggesting that the length is mostly due to the low coordination number of neodymium, since covalency was thought to be negligible.

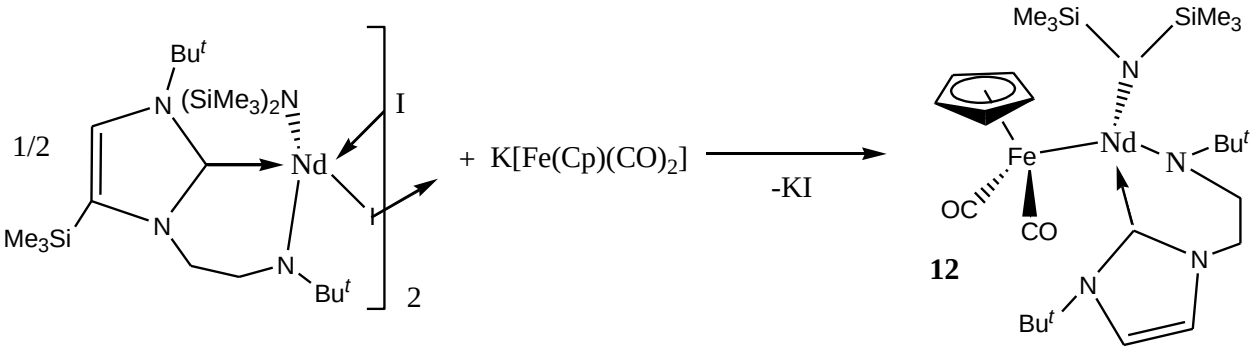

Scheme 3. Synthesis of complex **12**.

Lanthanide-Group 13 Metal Bonded Complexes

The first report of a group13-lanthanide interaction was by Roesky and co-workers in 2006, with the first dative aluminum-europium and aluminum-ytterbium bonds.[10] This was achieved by the solvent free reaction of a quarter molar equivalent of [{Al(η^5-C_5Me_5)}$_4$] with one molar equivalent of [Ln(η^5-C_5Me_5)$_2$] (Ln=Eu; Yb) at 120°C in an

evacuated ampoule. This resulted in red and green crystals of $[(\eta^5\text{-}C_5Me_5)_2Ln\text{-}Al(\eta^5\text{-}C_5Me_5)]$ (Ln=Eu: **13**; Yb: **14**) respectively (Scheme 4). The measured bond lengths of 3.365(2) and 3.198(2) Å for complexes **13** and **14** respectively are quite long, which gives rise to them dissociating in solution.

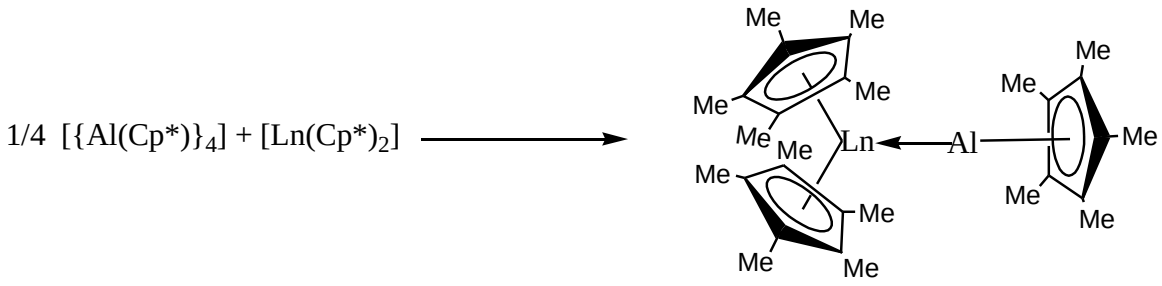

Scheme 4. Synthesis of **13** and **14**.

In 2007, Jones and Arnold prepared the first polar covalent lanthanide-group 13 bonded complex.[11] The reaction of **1** with half an equivalent of $[\{Nd(L')(N'')(\mu\text{–}I)\}_2]$ afforded in high yield, red crystals of [Nd(L′)(N″){Ga(Dip-DAB)}(THF)], **15** (Scheme 5). The Nd-Ga bond length was measured to be 3.220(2) Å. A DFT study showed the Nd-Ga bond to have 87% gallium character. This novel complex is very interesting not only because it is the first of its kind, but because it is prepared in high yield via traditional techniques. This discovery would later lead the Jones group to investigate the reactivity of **1** towards an array of lanthanide precursors.

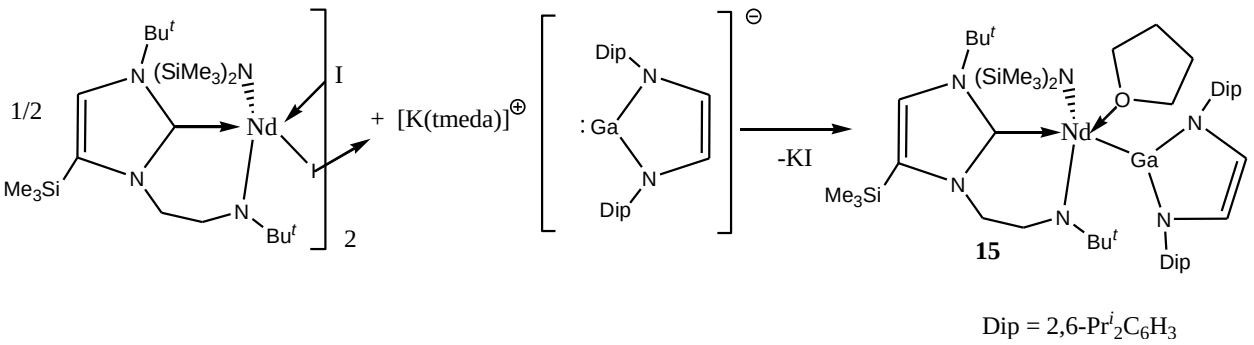

Scheme 5. Synthesis of **15**.

Similar to complexes **13** and **14**, Roesky and co-workers later preprared gallium analogues. However, unlike **13** and **14**, the gallium analgoues were prepared via traditional methods as was the case with **15**. The purple-red europium complex [(η^5-C_5Me_5)$_2$Eu{Ga(η^5-C_5Me_5)}$_2$], **16** and the red ytterbium complex [(η^5-C_5Me_5)$_2$YbGa(η^5-C_5Me_5)(THF)], **17**, were prepared in non-coordinating solvents (Scheme 6).[12] It is interesting that due to the larger size of europium, two gallium heterocycles coordinate to the metal center whereas only one is able to coordinate to the smaller ytterbium center. The Ga-Eu bond lengths were found to be 3.250(2)/3.391(2) Å and the Ga-Yb bond length was measured at 3.287(2) Å.

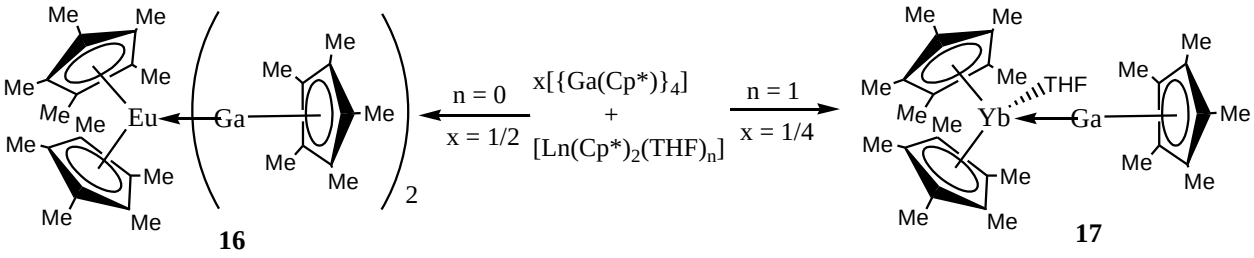

Scheme 6. Synthesis of **16** and **17**.

Lanthanide-Group 14 Element Bonded Complexes

In the late '80's and early '90's, Schumann and co-workers prepared the first examples of lanthanide-silicon bonded complexes, $[(\eta^5\text{-}C_5H_5)_2Ln(SiMe_3)_2][Li(DME)_3]$ (Ln=Sm: **18**; Lu: **19**) (Figure 4).[13,14] These novel species were realized through the reaction of $[(\eta^5\text{-}C_5H_5)_2LnCl{\cdot}NaCl{\cdot}2DME]$ (Ln=Sm, Lu; DME=1,2-dimethoxyethane) with two equivalents of $[Li(SiMe_3)]$. Complexes **18** and **19** were found to be 'ate' complexes and were isolated as yellow crystals. The Sm-Si bond length was measured to be 2.880(2) Å, and the Lu-Si was found to be 2.888(2) Å.

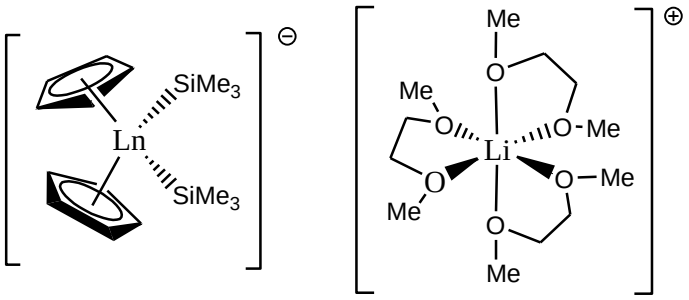

Ln = Sm (**18**); Lu (**19**)

Figure 4. Complexes **18** and **19**.

In 1991 Cloke and Lawless reported the first complex containing a lanthanide-tin bond.[15] The ytterbium-tin complex, $[Yb\{Sn(CH_2Bu^t)_3\}_2(THF)_2]$, **20**, was prepared via the reaction of ytterbium(II) di-iodide and an *in situ* prepared $[K\{Sn(CH_2Bu^t)_3\}]$ in THF (Scheme 7). The orange crystals of complex **20**, were analyzed by X-ray diffraction and were shown to have a Yb-Sn bond length of 3.216(1) Å. Very soon after Cloke and Lawless' discovery, Bochkarev and co-workers reported two more complexes containing Yb-Sn bonds (Figure 5).[16,17] Two products were found to be produced from the reaction of ytterbium naphthalenide with tetraphenyltin and/or hexaphenyldistannane. The yellow

[Yb(SnPh$_3$)$_2$(THF)$_4$], **21**, and the dark ruby [(Ph$_3$Sn)(THF)$_2$Yb(μ−Ph)$_3$Yb(THF)$_3$], **22**, were separated by fractional crystalization and independently characterized. Complexes **21** and **22** were shown to have Yb-Sn bond lengths of 3.305(1) and 3.379(1) Å respectively.

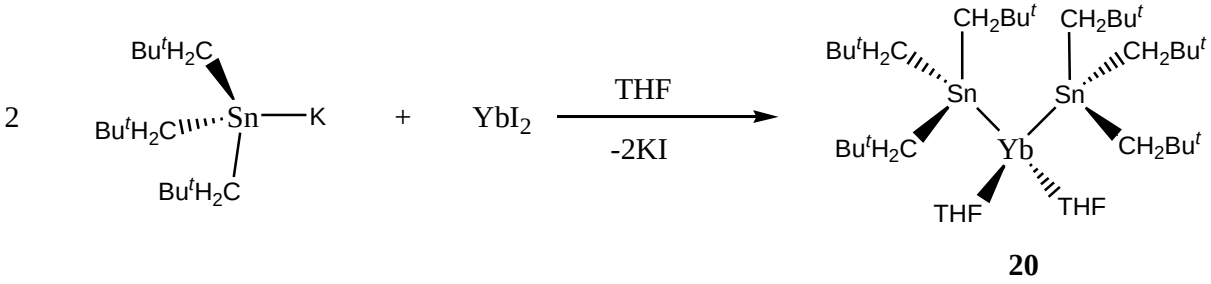

20

Scheme 7. Synthesis of **20**.

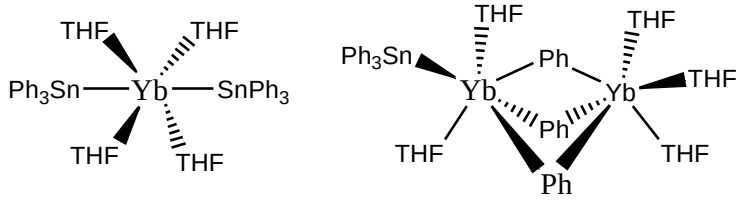

21 **22**

Figure 5. Complexes **21** and **22**.

In the mid '90's, the samarium-silicon complex, [Sm(η^5-C$_5$Me$_5$)$_2${SiH(SiMe$_3$)$_2$}], **23**, was prepared by Tilley and co-workers.[18,19] The reaction of [Sm(η^5-C$_5$Me$_5$)$_2${CH(SiMe$_3$)$_2$}] with five equivalents of SiH$_2$(SiMe$_3$)$_2$ led to red crystals of **23** (Figure 6). In the solid state, complex **23** is a dimer. The Sm-Si bond length was measured to be 3.052(8) Å. A lutetium analogue of **23** has been described, but this has not been crystalographically characterized to date. Tilley and co-workers reported a scandium-silicon complex, [Sc(η^5-C$_5$H$_5$)$_2$(THF){Si(SiMe$_3$)$_3$}], **24**, which is similar to **23** (Figure 6).[21] The yellow crystalline solid was prepared from the reaction of [{Sc(η^5-C$_5$H$_5$)$_2$(μ-Cl)}$_2$]

with two equivalents of [Li{Si(SiMe$_3$)$_3$}]. The resulting scandium-silicon complex exhibited a Sc-Si bond length of 2.862(2) Å. Reaction of **23** with phenylsilane led to three samarium(III) clusters incorporating Sm-Si bonds (Scheme 8).[20] Complexes **25-27** were obtained as red crystals.

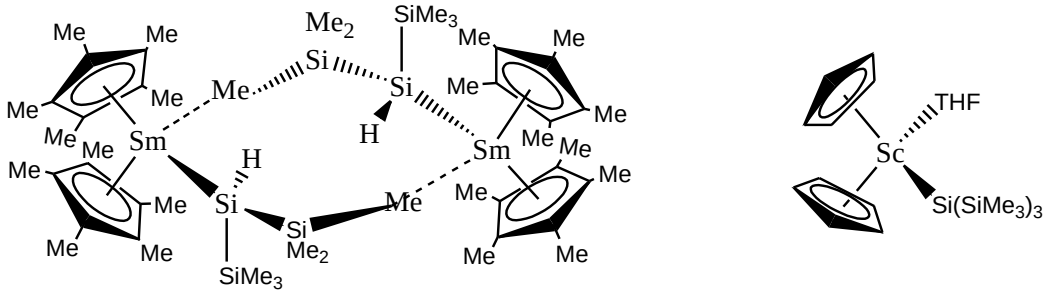

23 **24**

Figure 6. Complexes **23** and **24**.

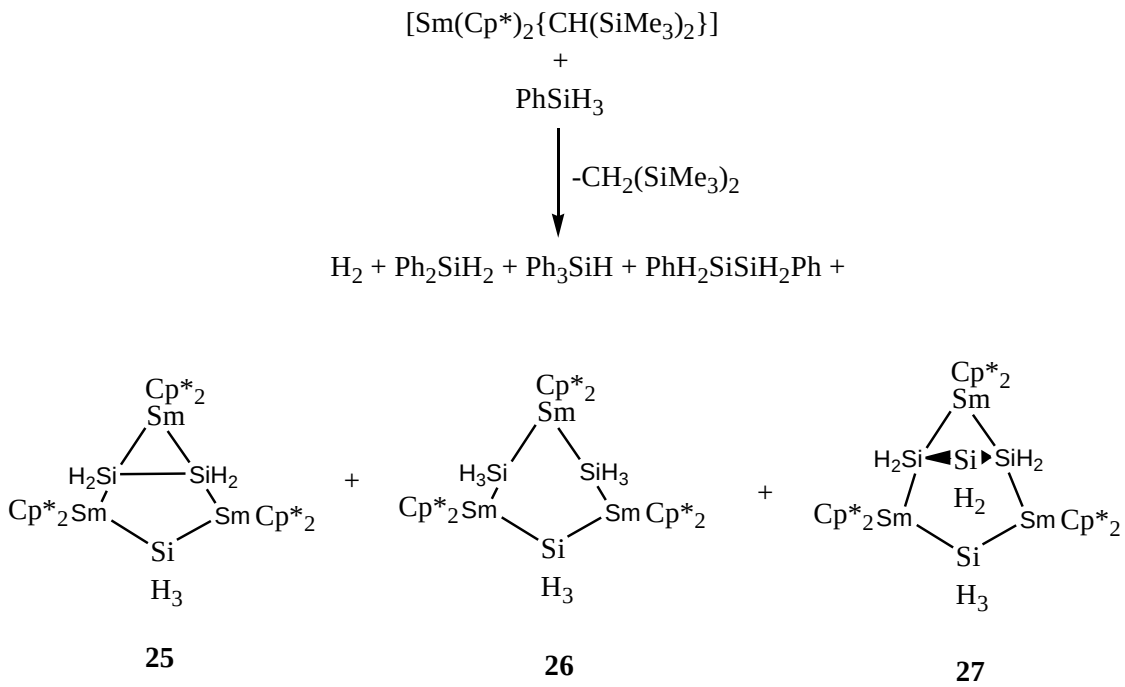

25 **26** **27**

Scheme 8. Synthesis of complexes **25-27**.

Not long after Bochkarev and co-workers' first reports on group 14-lanthanide complexes, several more interesting examples were prepared by the same group.[22-25] For example, $[Ln\{Sn(SnMe_3)_3\}_2(THF)_4]$ (Ln = Sm: **28**, Yb: **29**) and $[Yb(EPh_3)_2(THF)_4]$ (E = Si: **30**, Ge: **31**) were prepared by the reaction of samarium or ytterbium metal with corresponding alkyl/aryl group 14 halides (Figure 7). Complexes **28** and **29** were isolated as dark green and yellow crystals with lanthanide-tin bond lengths of 3.394(4) Å (av.) and 3.294(4) Å (av.) respectively. Complexes **30** and **31** crystallized as yellow and yellow-brown solids with group 14-ytterbium bonds lengths of 3.158(2) Å and 3.156(2) Å (av.) respectively. In addition, the europium complex $[Eu(GePh_3)_2(DME)_3]$, **32**, was prepared via the reaction between europium naphthalenide and Ph_3GeH in DME (Figure 7). The yellow crystals were studied by X-ray diffraction and the Eu-Ge bond was measured at 3.348(1) Å. Another ytterbium-germanium complex, $[Yb\{(GePh_2)_4\}(THF)_4]$, **33** was prepared, but this time via the reaction between ytterbium metal and Ph_2GeCl_2 (Figure 7). Complex **33** crystallized as a light brown solid with Yb-Ge bond lengths of 3.104(2) Å which is notably shorter than for **31**.

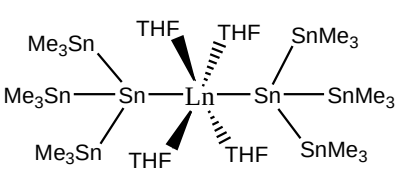

Ln = Sm (**28**); Yb (**29**)

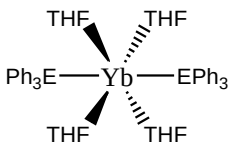

E = Si (**30**); Ge (**31**)

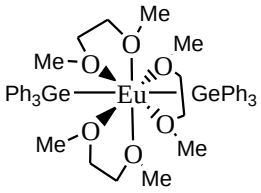

32

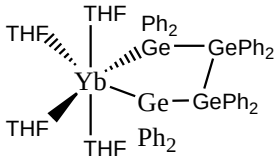

33

Figure 7. Structures of **28**-**33**.

In 1996, Lawless and co-workers prepared a complex containing a Yb-Si bond.[26] The novel half-sandwich ytterbium(II) complex, **34**, was prepared by the reaction of

[Yb(η^5-$C_5Me_5)_2(OEt_2)$] with [Li{$Si(SiMe_3)_3$}$(THF)_3$] in toluene (Figure 8). The orange needles of **34** showed a Yb-Si bond length of 3.032(3) Å.

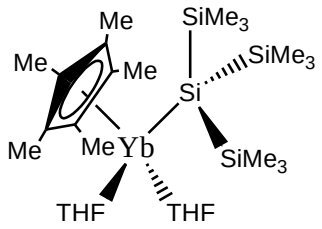

34

Figure 8. Complex **34**.

Two lanthanide-silylene complexes were reported by Lappert and co-workers, exhibiting the first examples of dative lanthanide-silicon bonds.[27] Reaction of a tris-cyclopentadienyl lanthanide complex with a silylene precursor in toluene afforded the complexes, [Ln(η^5-$C_5H_5)_3${$Si(NCH_2Bu^t)_2C_6H_4$-1,2}] (Ln=Y: **35**; Yb: **36**) (Figure 9). The Y-Si and Yb-Si bond lengths were measured at 3.038(2) Å and 2.984(2) Å and were isolated as colorless and green crystals respectively.

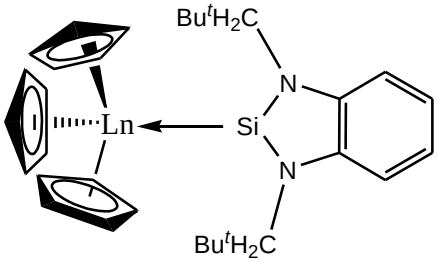

Ln = Y (**35**); Yb (**36**)

Figure 9. Complexes **35** and **36**.

In 2001, Tilley and co-workers eventually achieved the preparation of a lutetium-silicon bond containing complex.[28] Through the reaction of [Lu(η^5-$C_5Me_5)_2(\mu$-$H)_2$] and two

equivalents of H_3Si-2-$OMeC_6H_4$, colorless crystals of [Lu(η^5-C_5Me_5)$_2$(SiH_2-2-$OMeC_6H_4$)], **37**, were obtained (Figure 10). The crystals were characterized by X-ray diffraction and the Lu-Si bond was measured to be 2.823(5) Å, which is shorter than what was seen in complex **19**. The difference in distance can be attributed to the neutral and 'ate' natures of **37** and **19**, respectively.[1]

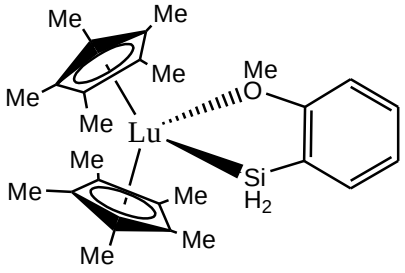

37

Figure 10. Complex **37**.

The preparation of three lanthanide-silyl complexes was attempted by Hou and co-workers.[29] The reactions of [Ln(η^5-C_5Me_5)$_2$(THF)$_2$] (Ln= Eu, Yb, Sm) with '[K(SiH_2Ph)]' led to the isolation of the complexes, [{Ln(η^5-C_5Me_5)$_2$(SiH_3)(K)(THF)}$_\infty$] (Ln= Eu: **38**; Yb: **39**) (Figure 11). Crystals from the samarium reaction were obtained, but were not of good enough quality for structural characterization. The europium complex was isolated as orange-red crystals with a Eu-Si bond distance of 3.239(3) Å, whereas the ytterbium complex was found to be dark red in color with a Yb-Si bond length of 3.091(3) Å. Both complexes were found in rather interesting forms which can be described as polymeric honeycomb 2-D sheets. The honeycomb 2-D sheets are made up of individual chains of Cp^*LnCp^*K units (Cp^*=C_5Me_5), which are cross-linked by bridging 'inter-chain' SiH_3 units.[1]

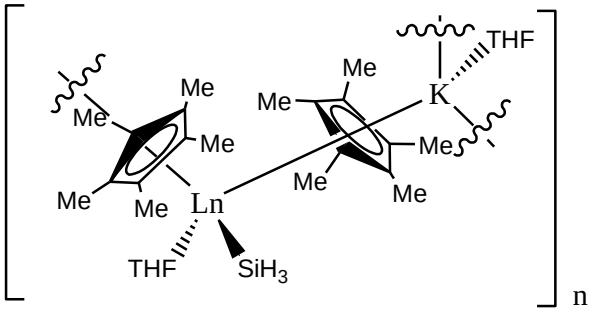

Ln = Eu (**38**); Yb (**39**)

Figure 11. Complexes **38** and **39**.

The only example of a samarium-silylene bonded complex has been reported by Evans and co-workers.[30] The isolated purple crystals of $[Sm(\eta^5\text{-}C_5Me_5)_2\{Si(NBu^tCH)_2\}]$, **40**, were measured to have a Sm-Si bond length of 3.191(1) Å (Figure 12). NMR studies on **40** were not practical due to the paramagnetic nature of the complex. The loss of the silylene ligand and coordination of one THF molecule was found to take place with complex **40** when in the presence of THF. It is interesting that the THF appears to act as a stronger donor ligand than the silylene.

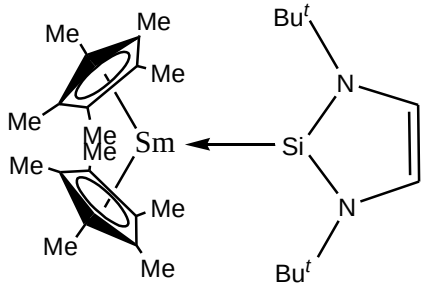

40

Figure 12. Complex **40**.

Tilley and co-workers have also prepared two scandium-silyl complexes which are very similar to the previously mentioned complexes **23** and **24**. For example, the reaction

of $[Sc(\eta^5\text{-}C_5Me_5)_2(CH_3)]$ with Ph_3SiSiH_3 afforded yellow crystals of $[Sc(\eta^5\text{-}C_5Me_5)_2(SiH_2SiPh_3)]$, **41**, (Figure 13).[31] The Sc-Si bond length was measured to be 2.797(1) Å. In addition, $[Sc(\eta^5\text{-}C_5Me_5)_2\{SiH(SiMe_3)_2\}]$, **42**, was prepared from the methane elimination reaction between $[Sc(\eta^5\text{-}C_5Me_5)_2(CH_3)]$ and $(Me_3Si)_2SiH_2$ (Figure 13).[31] Complex **42** also formed as yellow crystals, but the X-ray structure obtained was disordered therefore making the Sc-Si bond length inaccurate. In both cases an excess of silane was added to the reaction so as to combat competing σ-bond metathesis reactions.[1]

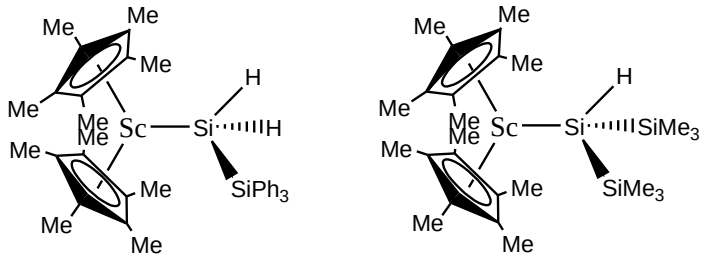

41 **42**

Figure 13. Complexes **41** and **42**.

The final example of a lanthanide-group 14 bonded complex known to date has been reported by Niemeyer. The reaction of $[K\{Si(SiMe_3)_3\}]$ with $[Yb(N'')_2]$ $[N''=N(SiMe_3)_2]$ led to the isolation of a Yb-Si bonded complex, $[\{Yb(N'')_2[Si(SiMe_3)_3]K\}_\infty]$, **43**, (Figure 14).[32] The deep orange crystals were characterized by X-ray diffraction and this showed the Yb-Si bond length to be 3.039(2) Å. The Yb-Si bond distance compares well to those previously seen in complexes **30** and **34**.

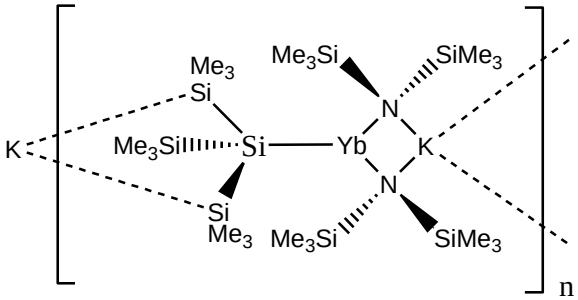

43

Figure 14. Complex **43**.

Lanthanide-Group 15 Metal Bonded Complexes

The field of f-element-metal bonded complexes is in its infancy, and this is most apparent when looking at what has been accomplished with lanthanide-group 15 metal complexes. To date, only two have been structurally authenticated. Both complexes have been reported by Evans and co-workers. The first is the red-brown samarium-bismuth complex, $[\{Sm(\eta^5\text{-}C_5Me_5)_2\}_2(\mu\text{-}\eta^2\text{:}\eta^2\text{-}Bi_2)]$, **44**, exhibiting Sm-Bi bond lengths of 3.265(1) Å, 3.283(1) Å, 3.291(1) Å, and 3.311(1) Å (Figure 15).[33] Complex **44** was prepared via the reaction between $[Sm(\eta^5\text{-}C_5Me_5)_2]$ and $[BiPh_3]$ in toluene. The reaction mixture was washed with hexane to remove $[Sm(\eta^5\text{-}C_5Me_5)_2(Ph)]$, biphenyl, and $[Sm(\eta^5\text{-}C_5Me_5)_2(CH_2Ph)]$, leaving the desired complex to crystallize from toluene. The second lanthanide-group 15 complex known to date is $[\{Sm(\eta^5\text{-}C_5Me_5)_2\}_3(\mu\text{-}\eta^2\text{: }\eta^2\text{: }\eta^1\text{-}Sb_3)(THF)]$, **45**, (Figure 15).[34] The reaction of $[Sm(\eta^5\text{-}C_5Me_5)_2]$ with $SbBu^n{}_3$ led to the isolation of **45** as dark red crystals. Complex **45** can be seen as a lanthanide adduct of a trapped Zintl trianion encompassing five Sm-Sb bonds.[1] The shortest Sm-Sb distance is 3.162(1) Å with the second being only slightly longer at 3.205(1) Å.

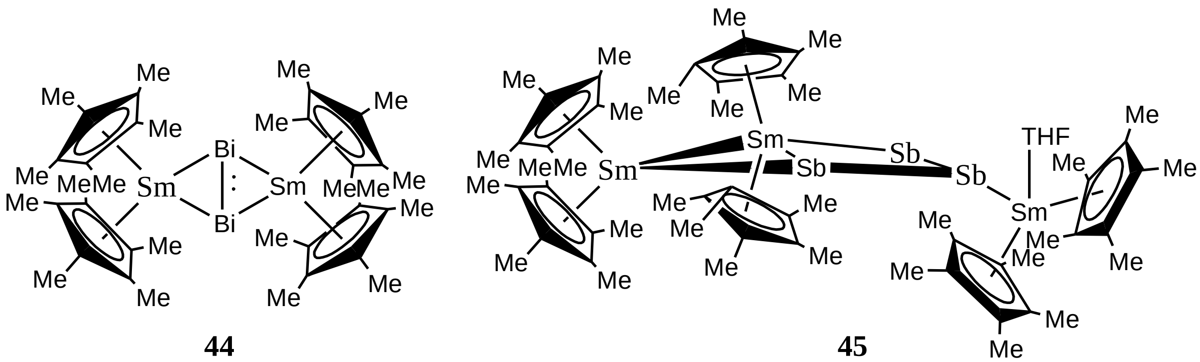

44 **45**

Figure 15. Complexes **44** and **45**.

Actinide-Transition Metal Bonded Complexes

The first structurally authenticated example of an actinide-transition metal complex was reported by Marks and co-workers. Pale yellow needles of the thorium-ruthenium complex, $[Th(\eta^5\text{-}C_5Me_5)_2(I)\{Ru(\eta^5\text{-}C_5H_5)(CO)_2\}]$, **46**, were afforded from the reaction between $[Th(\eta^5\text{-}C_5Me_5)_2(I)_2]$ and $Na[Ru(\eta^5\text{-}C_5H_5)(CO)_2]$ (Figure 16).[35] The crystals were characterized by X-ray diffraction revealing a Th-Ru bond length of 3.028(2) Å. It was also noted in the study that a bis-ruthenium derivative was not possible to synthesize due to the size and crowding at the thorium atom. Although not characterized by X-ray crystallography, the complexes, $[An(\eta^5\text{-}C_5H_4R)_3\{M(\eta^5\text{-}C_5H_5)(CO)_2\}]$ (An=Th, U; R=H, Me; M=Fe, Ru), are thought to have been prepared by the same group. This was assumed because of similarities to **46** with respect to their NMR and FTIR spectra.[36]

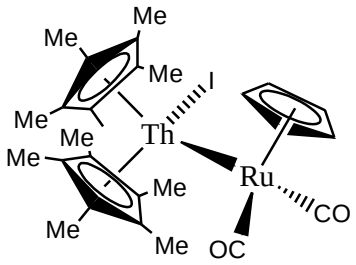

46

Figure 16. Complex **46**.

Two similar complexes exhibiting thorium-nickel and thorium-platinum bonds have been reported by Ryan and co-workers. The interesting reaction between $[Th(\eta^5\text{-}C_5Me_5)_2(PPh_2)_2]$ and $[Ni(COD)_2]$ (COD=cyclo-octadiene) under an atmosphere of carbon monoxide led to orange crystals of $[Th(\eta^5\text{-}C_5Me_5)_2(\mu\text{-}PPh_2)_2Ni(CO)_2]$, **47**, (Figure 17).[37] X-ray crystallography revealed the Th-Ni bond length to be 3.206(2) Å. Similar to **47**, a thorium-platinum bond containing complex, $[Th(\eta^5\text{-}C_5Me_5)_2(\mu\text{-}PPh_2)_2Pt(PMe_3)]$, **48**, was prepared from the reaction between $[Th(\eta^5\text{-}C_5Me_5)_2(PPh_2)_2]$ and $[Pt(COD)_2]$ in the presence of trimethylphosphine (Figure 17).[38] Complex **48** was isolated as red-brown crystals which were structurally characterized, revealing a Th-Pt bond length of 2.984(1) Å. *Ab initio* calculations conducted on a model complex led the Th-Pt bond to be regarded as a dative, donor-acceptor bond.

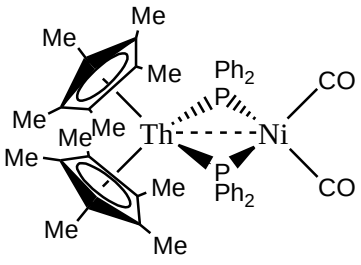

47

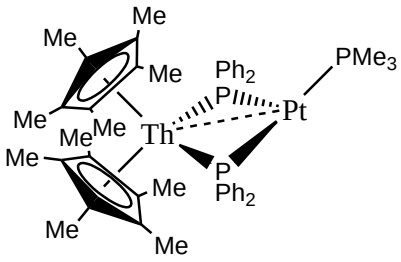

48

Figure 17. Complexes **47** and **48**.

The reaction between 1,1'-dilithioferrocene and uranium tetrachloride afforded the ferrocenophane complex, $[U(fc)_3Li_2(py)_3]$ (**49**; py=C_5H_4N) (Figure 18).[39] The isolated red crystals of **49** were characterized by X-ray diffraction, revealing three uranium-iron interactions. These bonds ranged in length from 3.122(2) to 3.165(2) Å.

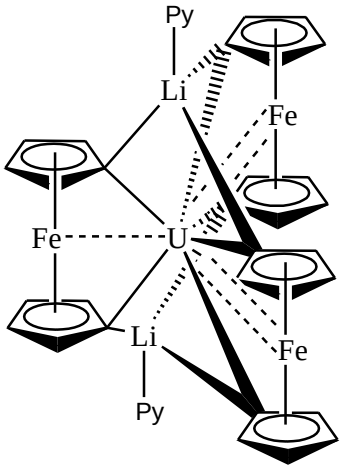

49

Figure 18. Complex **49**.

Two similar uranium-iron bond containing complexes were reported by Diaconescu and co-workers. For example, the reaction between $UI_3(THF)_4$ and $[K_2(OEt_2)_2\{fc(NSiMe_2Bu^t)_2\}_2]$ in toluene or diethyl ether, followed by oxidation with

iodine and subsequent reaction with $NaBPh_4$ afforded $[U\{fc(NSiMe_2Bu^t)_2\}_2][BPh_4]$, **50**, (Figure 19).[40] The salt elimination/disproportionation reaction yielded X-ray quality black crystals, the structural characterization of which revealed an average uranium-iron bond length of 2.962(1) Å. In addition, the same group reported that the reaction between $UI_3(THF)_4$ and $[K_2(OEt_2)_2\{fc(NSiMe_2Bu^t)_2\}_2]$ in THF affords a mixture of **50** and $[U\{fc(NSiMe_2Bu^t)_2\}(I)_2(THF)]$. The addition of hexane washed complex **50** from the mixture leaving $[U\{fc(NSiMe_2Bu^t)_2\}(I)_2(THF)]$ to undergo a salt elimination reaction with benzyl potassium, affording the di-benzyl complex, and eventually $[U\{fc(NSiMe_2Bu^t)_2\}(CH_2C_6H_5)(OEt_2)][BPh_4]$, **51**, after treatment with $[Et_3NH][BPh_4]$ (Figure 19).[40] The crystals of **51** were characterized by an X-ray diffraction experiment, which showed a U-Fe bond distance of 3.071(2) Å.

50 **51**

Figure 19. Complexes **50** and **51**.

Actinide-Group 13 Metal Bonded Complexes

Very recently, the only two known examples of actinide-group 13 metal bonded complexes have been reported. The first is the uranium-aluminum complex, $[U(\eta^5\text{-}C_5H_4SiMe_3)_3\{Al(\eta^5\text{-}C_5Me_5)\}]$, **52**, which has been prepared by Arnold and co-workers (Figure 20).[42] Dark brown crystals of **52** were isolated from the reaction between one

molar equivalent of [U(η^5-$C_5H_4SiMe_3)_3$] with a quarter molar equivalent of [{Al(η^5-C_5Me_5)}$_4$] in toluene after work-up and crystallization from pentane. X-ray crystallography revealed a U-Al distance of 3.117(3) Å. The group also conducted DFT studies on the model complex [(η^5-$C_5H_5)_3$U-Al(η^5-C_5H_5)], which showed the uranium-aluminum bond to be purely σ in character. The only other example of a complex containing an actinide-group 13 bond is [(Tren^{TMS})U{Ga(Dip-DAB)}(THF)], **53**, which was reported soon after, by Liddle and Jones (Figure 20).[43] The reaction between the five-membered anionic gallium(I) heterocycle, **1**, and the uranium precursor, [U(Tren^{TMS})(I)(THF)] [Tren^{TMS}=N($CH_2CH_2NSiMe_3)_3$], afforded orange crystals of **53**. A X-ray diffraction study on crystals of **53** revealed two almost identical molecules in the asymmetric unit. The U-Ga bond distances of the molecules were measured to be 3.221(2) Å and 3.298(2) Å. A very interesting DFT study was carried out on the model complex [{N($CH_2CH_2NSiH_3)_3$}U{Ga[N(2,6-$Me_2C_6H_3$)CH]$_2$}(OMe_2)], which revealed possible Ga→U π-bonding along with the expected Ga→U σ-bonding.[43]

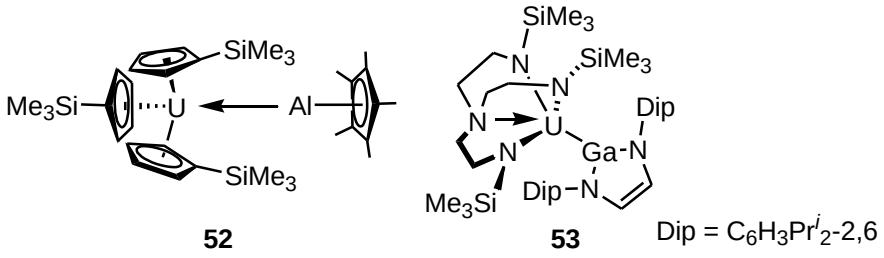

Figure 20. Complexes **52** and **53**.

Actinide-Group 14 Element Bonded Complexes

Cummins and co-workers have reported a complex containing a uranium-silicon bond.[44] The reaction between [{(3,5-$Me_2C_6H_3$)N(Bu^t)}$_3$U(I)] and [$(THF)_3$Li{Si($SiMe_3)_3$}]

in diethyl ether afforded red crystals of [{(3,5-$Me_2C_6H_3$)N(Bu^t)}$_3$U{Si($SiMe_3$)$_3$}], **54**, upon work-up (Figure 21). The crystals were characterized by X-ray diffraction, which showed the complex to have a U-Si bond length of 3.091(3) Å. A DFT study on a model of complex **54**, [$(H_2N)_3$U-SiH_3], revealed the uranium-silicon bonding orbital to be comprised of, for the most part, $3p_z$ (49%) and uranium $6d_z^2$ (15%) character.[1]

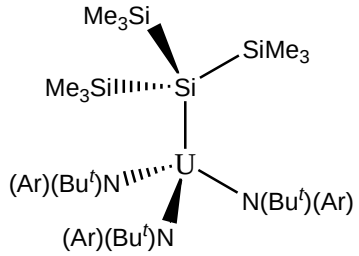

54

Figure 21. Complex **54**.

A uranium-tin bonded complex has been reported by Porchia and co-workers.[45] The complex, [(η^5-C_5H_5)$_3$U($SnPh_3$)], **55**, was characterized by X-ray diffraction, revealing a U-Sn bond length of 3.166(1) Å (Figure 22). Brown crystals of the complex were prepared from the reaction between [(η^5-C_5H_5)$_3$U(NEt_3)] and $HSnPh_3$. It is of note that although not confirmed by X-ray diffraction studies, Porchia and co-workers reported analogous uranium-silicon and a uranium-germanium complexes, [(η^5-C_5H_5)$_3$U(EPh_3)] (E = Si or Ge).[45,46]

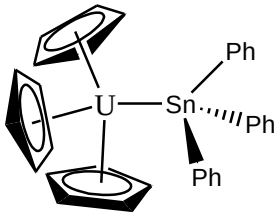

55

Figure 22. Complex **55**.

3.2 Research Proposal

Complexes containing gallium-lanthanide bonds are known. For example, as previously mentioned, Roesky and co-workers have prepared the red-purple europium complex $[(\eta^5\text{-}C_5Me_5)_2Eu\{Ga(\eta^5\text{-}C_5Me_5)\}_2]$, **16** and the red ytterbium complex $[(\eta^5\text{-}C_5Me_5)_2YbGa(\eta^5\text{-}C_5Me_5)(THF)]$, **17**.[12] In addition to these, in collaboration with Arnold and co-workers, the Jones group prepared the first known gallium-lanthanide bonded complex, **15**, using the anionic gallium(I) heterocycle, $[:Ga(Dip\text{-}DAB)]^-$ **1**. There is no known further chemistry for Ln-Ga bonded compounds. For this to advance with any pace, it seemed that the development of systems containing polar-covalent lanthanide(II)-gallium bonds would be necessary. The preparation of such compounds would allow comparisons between their redox chemistry and that of widely explored lanthanide(II) reducing agents such as SmI_2[47] and $SmCp^*_2$.[48] Given our recent success with investigations into the coordination of [K(tmeda)][**1**] towards a range of group 2 and 12 fragments, it was proposed that we apply that same methodology towards suitable lanthanide metal precursors.

3.3 Results and Discussion

3.3.1 Preparation of Gallyl-Lanthanide Complexes

The Jones group has previously, and unsuccessfully, attempted to prepare complexes of the type $[Ln\{Ga[N(Dip)C(H)]_2\}_2(THF)_n]$ (Ln = Sm, Eu or Yb) by reduction of the digallane(4), $[\{Ga^{II}[(DipNCH)_2]\}_2]$, or the paramagnetic gallium(III) iodide complex, $[GaI_2\{[N(Dip)C(H)]_2^{\cdot}\}]$, with the elemental lanthanides in THF. Salt elimination reactions of $[K(tmeda)][Ga\{N(Dip)C(H)\}_2]$ with half an equivalent of LnI_2 in THF were then investigated, but all led to intractable mixtures of products. However, when the reactions were repeated in the presence of an excess of tmeda, the bis(gallyl) lanthanide complexes, **56** (dark green), **57** (orange) and **58** (red-orange), were reproducibly obtained in low to moderate isolated yields (Scheme 9).

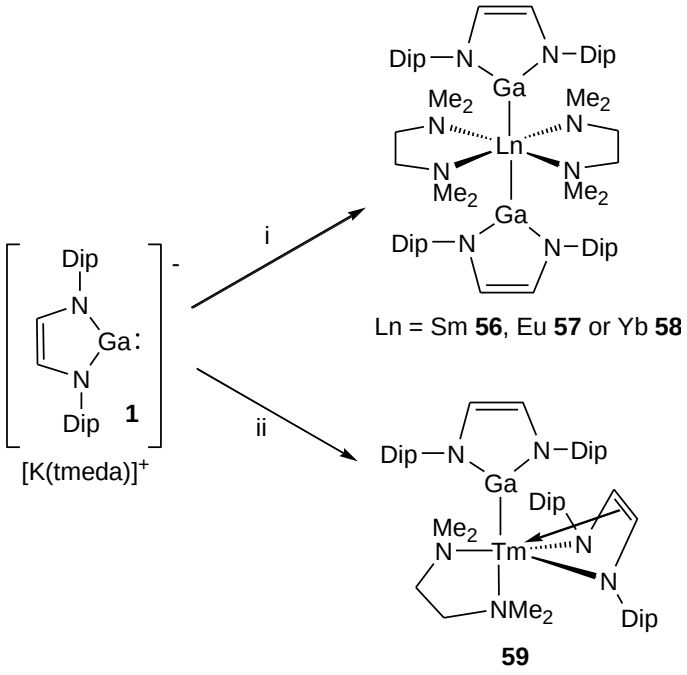

Scheme 9. *Reagents and conditions:* i, $LnI_2(THF)_n$, toluene/tmeda, -KI; ii, $TmI_2(THF)_n$, toluene/tmeda, -KI, $-Ga_{(s)}$.

After Eu^{2+}, Yb^{2+} and Sm^{2+}, Tm^{2+} is the next most stable lanthanide dication ($E°$ Tm^{3+}/Tm^{2+} = 2.22 V) and has a rapidly emerging molecular chemistry.[49] Given the thermal stability of **56 - 58**, it was thought that their thulium analogue might be a stable entity at room temperature. However, a comparable reaction between **1** and TmI_2 reproducibly led to a low isolated yield of the red thulium(III)-gallyl complex, **59**, the coordination sphere of which is completed by a molecule of tmeda and a doubly reduced diazabutadiene ligand. It seems likely that the intermediate in the reaction that gave **59** is the target thulium(II) complex, $[Tm\{Ga[N(Dip)C(H)]_2\}_2(tmeda)_2]$, which was subject to an intramolecular reduction of one gallyl ligand by the thulium centre, leading to elimination of gallium metal. A related complex, $[\{Ce^{III}[N(Dip)C(H)]_2(tmeda)(\mu\text{-}I)\}_2]$, **60**, was obtained in low yield from the reaction of $[CeI_3(THF)_4]$ with [K(tmeda)][**1**]. The complex was crystallographically characterized, but no other data was obtained due to its low yield (Figure 27).

Little useful information could be obtained from the ^1H NMR spectra of **56**, **57** and **59** due their paramagnetic nature.[50] The solution state magnetic moments (Evans method, C_6D_6, 298 K) for **56** (3.3 B.M.), **57** (7.3 B.M.) and **59** (7.0 B.M.), all lie in the expected ranges. The spectrum of **58** is, however, more informative and displays a major set of resonances that is consistent with its solid state structure. It also exhibits a more complex, minor set of resonances which we believe corresponds to the *cis*-isomer of the compound. The most compelling evidence for this proposal is that there are two chemically inequivalent sets of backbone protons for the gallyl ligands which resonate as an AB spin system. The fact that these protons are inequivalent suggests that the bulky heterocyclic ligands of the complex are "interlocked" and cannot rotate freely with respect to each other.

Very similar spectra have been observed for square planar transition metal complexes, e.g. *cis*-[Pd{Ga[N(Dip)C(H)]$_2$}$_2$(tmeda)].[51] That the two isomers of **58** exist in equilibrium in solution was confirmed by dissolving several pure samples of the *trans*-isomer of the compound in C_6D_6 which, in each case, led to spectra corresponding to identical isomeric mixtures. In addition, only *trans*-**58** could be crystallized from these solutions, suggesting this is the thermodynamically favored isomer. The low solubility of **58** in aromatic solvents at low temperature precluded a variable temperature NMR study of the equilibrium between the isomers. Furthermore, no signals were observed in the ^{171}Yb NMR spectrum of **58**, presumably because of significant peak broadening, arising from the coordination of the Yb atom of both isomers of **58** by two quradrupolar Ga centres (^{69}Ga, 60% abundant, I = 3/2; ^{71}Ga, 40% abundant, I = 3/2).

Compounds **56** - **58** were crystallographically characterized and found to be isostructural. Each compound has a distorted lanthanide octahedral geometry with the gallyl ligands *trans*- to each other. The Ln-Ga distances in the compounds follow the expected trend (Sm-Ga ~ Eu-Ga > Yb-Ga) based on the effective ionic radii for six-coordinate Ln^{2+} cations (Sm^{2+} 1.19 Å, Eu^{2+} 1.17 Å, Yb^{2+} 1.02 Å).[52] In addition, given the similarity between the ionic radii of Yb^{2+} and Ca^{2+} (1.00 Å - six-coordinate[52]), it is of note that the Ca-Ga bonds in [Ca(THF)$_4${Ga{[N(Dip)C(H)]$_2$}}$_2$] (3.1587(6) Å) are only slightly shorter than the Yb-Ga bonds of **58**. Although the Ln-Ga bonds in **56** - **58** are almost certainly very polar, they should possess some covalent character based on prior theoretical studies.[11,53] The Ln-Ga separations of the compounds in this study are, however, significantly greater than sums of the covalent radii for the atom pairs (Sm-Ga 3.20 Å, Eu-Ga 3.20 Å or Yb-Ga 3.09 Å).[54] Although there are no known Sm-Ga bonded complexes to

compare with, the Eu-Ga and Yb-Ga bonds in **57** and **58** are, not surprisingly, shorter than those in the adducts, **16** and **17**.[12]

The molecular structure of **59** is shown in Figure 26 and exhibits the first example of a structurally characterized Tm-Ga bond in a molecular compound. The doubly reduced diazabutadiene ligand is coordinated to the thulium center in what can be described as a slipped η^4-mode, as has been seen in related complexes, e.g. $[Yb\{N(Dip)C(H)\}_2(C_5Me_5)(THF)]$.[55] This gives rise to a heavily distorted trigonal bipyramidal coordination geometry with Ga(1) and N(5) in the axial positions. The Ln-Ga distance in the compound is markedly shorter than those in **15**, **56-58**, and unlike those compounds, is well within the sum of the covalent radii for the two metals (3.12 Å).[54]

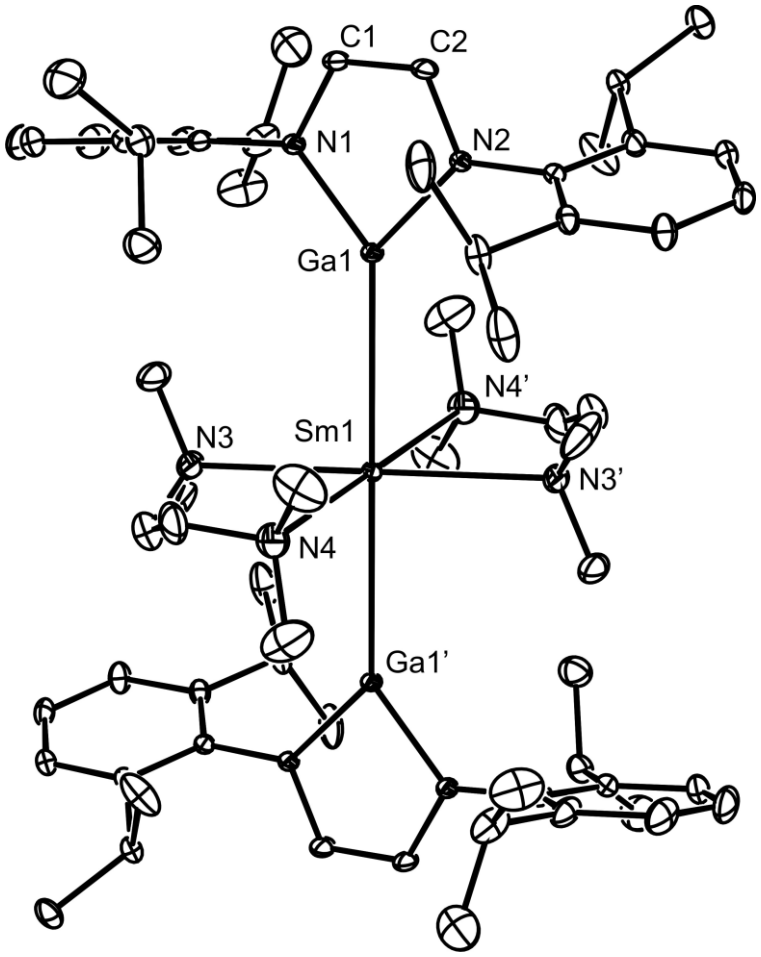

Figure 23. Thermal ellipsoid plot (20% probability surface) of the molecular structure of $[Sm\{Ga[N(Dip)C(H)]_2\}_2(tmeda)_2]$ (**56**); hydrogen atoms are omitted for clarity. Selected bond lengths (Å) and angles (^{o}): Ga-Sm 3.3124(9), Sm-N 2.724 (mean), Ga-N 1.931 (mean), N-Ga-N 83.66(8).

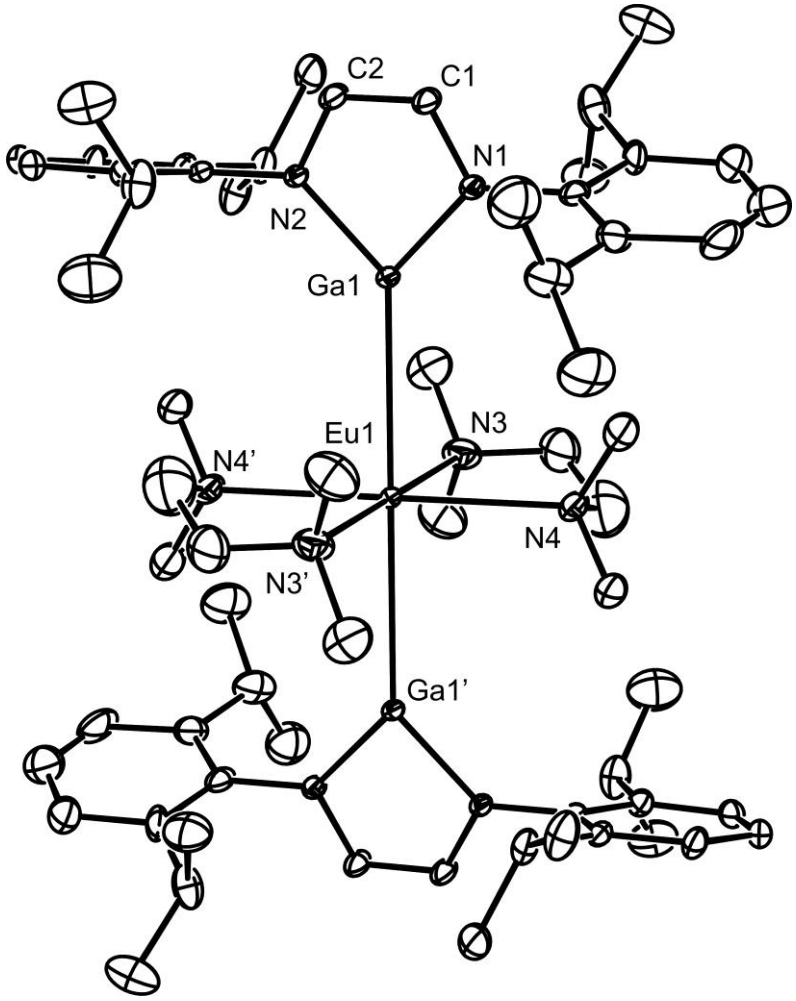

Figure 24. Thermal ellipsoid plot (20% probability surface) of the molecular structure of $[Eu\{Ga[N(Dip)C(H)]_2\}_2(tmeda)_2]$ (**57**); hydrogen atoms are omitted for clarity. Selected bond lengths (Å) and angles (°): Ga-Eu 3.3124(11), Eu-N 2.677 (mean), Ga-N 1.934 (mean), N-Ga-N 83.57(18);

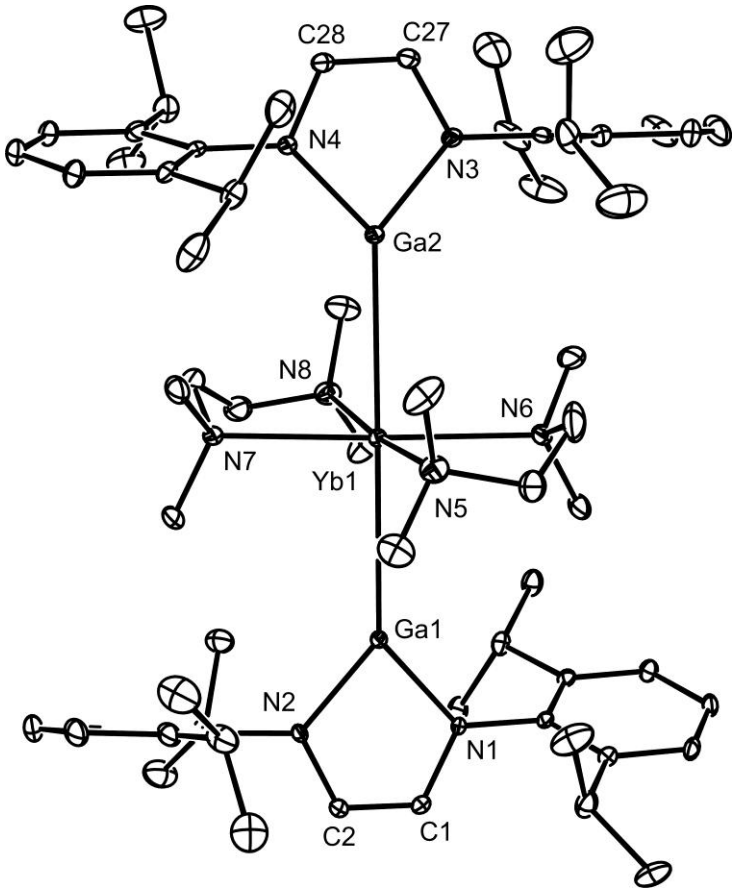

Figure 25. Thermal ellipsoid plot (20% probability surface) of the molecular structure of $[Yb\{Ga[N(Dip)C(H)]_2\}_2(tmeda)_2]$ (**58**); hydrogen atoms are omitted for clarity. Selected bond lengths (Å) and angles (^{o}): Ga-Yb 3.226 (mean), Yb-N 2.596 (mean), Ga-N 1.939 (mean), N-Ga-N 83.74 (mean).

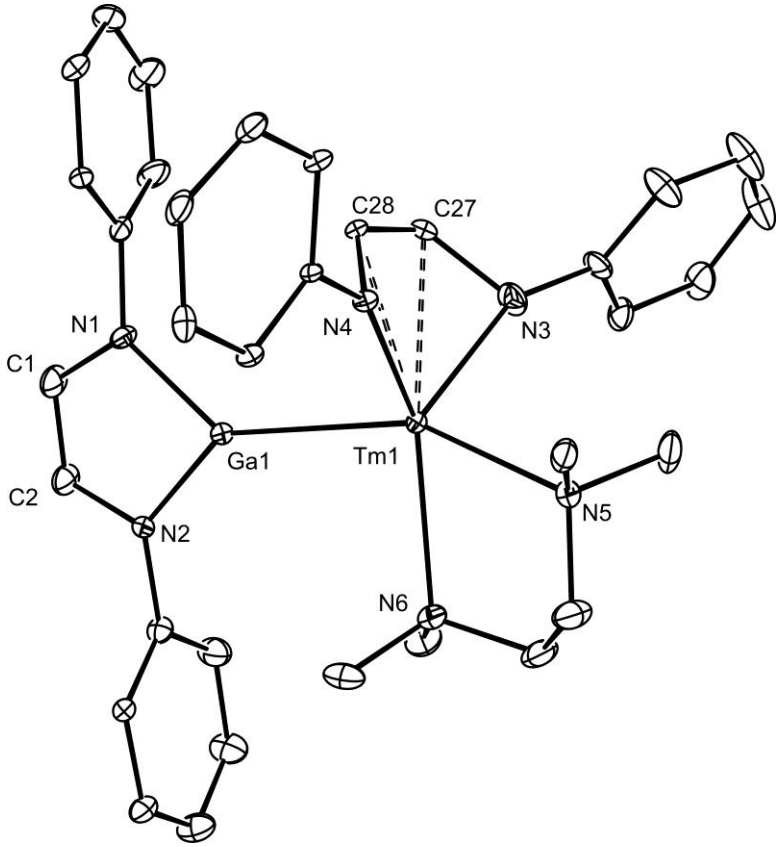

Figure 26. Thermal ellipsoid plot (20% probability surface) of the molecular structure of [Tm{Ga(Dip-DAB)}(Dip-DAB)(tmeda)] (**59**); hydrogen atoms and isopropyl groups are omitted for clarity. Selected bond lengths (Å) and angles (°): Tm(1)-Ga(1) 2.9742(16), Tm(1)-N(3) 2.163(10), Tm(1)-N(4) 2.171(8), Tm(1)-N(5) 2.481(9), Tm(1)-N(6) 2.512(10), Tm(1)-C(27) 2.547(11), Tm(1)-C(28) 2.563(10), N(3)-C(27) 1.452(15), N(4)-C(28) 1.409(14), C(27)-C(28) 1.344(16), N(3)-Tm(1)-N(4) 85.1(4), N(3)-Tm(1)-N(5) 92.2(4), N(4)-Tm(1)-N(5) 94.4(3), N(3)-Tm(1)-N(6) 128.3(4), N(4)-Tm(1)-N(6) 142.9(4), N(5)-Tm(1)-N(6) 71.4(3), N(3)-Tm(1)-Ga(1) 109.6(3), N(4)-Tm(1)-Ga(1) 97.6(2), N(5)-Tm(1)-Ga(1) 155.9(2), N(6)-Tm(1)-Ga(1) 86.7(2).

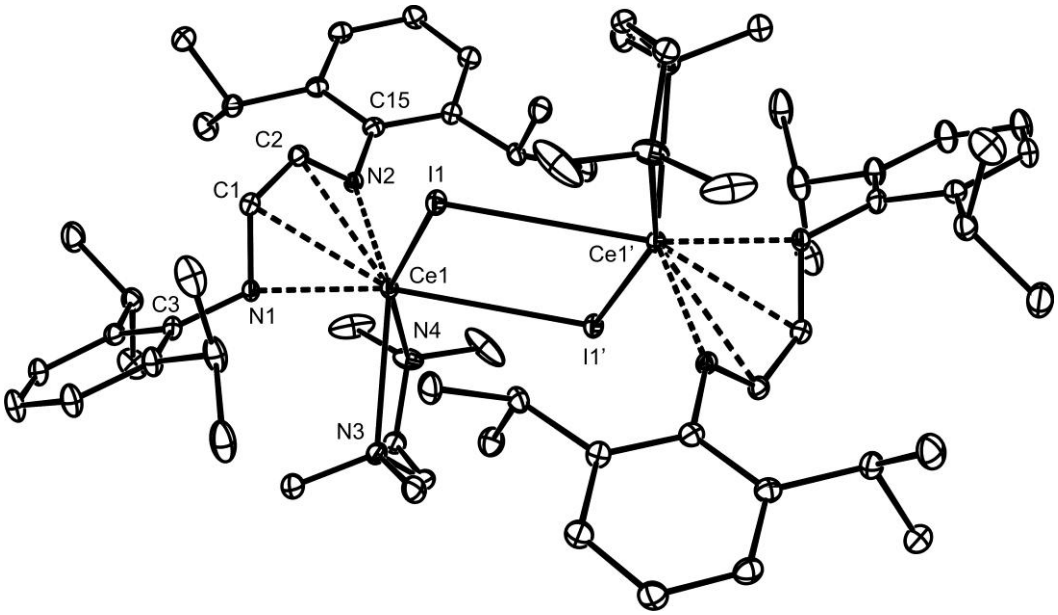

Figure 27. Molecular structure of [{Ce(Dip-DAB)(tmeda)(μ-I)}$_2$], **60**, (20% thermal ellipsoids; hydrogen atoms and isopropyl groups omitted). Selected bond lengths (Å) and angles (^{o}): Ce(1)-N(1) 2.280(3), Ce(1)-N(2) 2.333(3), Ce(1)-C(1) 2.679(4), Ce(1)-C(2) 2.691(4), Ce(1)-N(3) 2.717(4), Ce(1)-N(4) 2.808(4), Ce(1)-I(1) 3.3795(6), Ce(1)-I(1)' 3.4438(14), N(1)-C(1) 1.408(5), C(1)-C(2) 1.361(5), N(2)-C(2) 1.396(5), N(1)-Ce(1)-N(2) 80.60(11), N(3)-Ce(1)-N(4) 66.26(11), I(1)-Ce(1)-I(1)' 71.759(18), Ce(1)-I(1)-Ce(1)' 108.241(18).

3.4 Conclusion

In conclusion, a series of stable bis(gallyl) lanthanide(II) complexes have been prepared. In addition, an analogous bis(gallyl) thulium(II) complex has been implicated as an intermediate in the formation of a gallyl thulium(III) complex. Crystallographic studies on these complexes have given rise to the first structurally characterized GaTm or GaSm bonds.

3.5 Experimental

General considerations. All manipulations were carried out using standard Schlenk and glove box techniques under atmospheres of high purity argon or dinitrogen. Toluene, hexane and tmeda were distilled over molten potassium metal, while diethylether was distilled over Na/K alloy. Melting points were determined in sealed glass capillaries under argon and are uncorrected. Mass spectra were recorded at the EPSRC National Mass Spectrometric Service at Swansea University. The microanalysis on **57** was obtained from Campbell Microanalytical, Ottago. In general, however, the highly air and moisture sensitive nature of the compounds in this study led to irreproducible microanalyses. IR spectra were recorded using a Nicolet 510 FT-IR spectrometer as Nujol mulls between NaCl plates. ^{1}H and $^{13}C\{^{1}H\}$ NMR spectra were recorded on a Varian DPX 300 spectrometer. Solution state magnetic moments were determined in C_6D_6 at 298 K using the Evan's method.[56] [K(tmeda)][Ga{N(Dip)C(H)}$_2$],[2] [$TmI_2(THF)_5$][57] and THF solutions of $LnI_2(THF)_n$ (Ln = Sm, Eu or Yb)[51,58] were prepared by literature procedures. All other reagents were purchased commercially and used as received.

Synthesis of [Sm{Ga(Dip-DAB)}$_2$(tmeda)$_2$] 56. To a solution of SmI_2 (0.25 mmol) in THF (10 cm^3) at 25 ^oC was added tmeda (2.2 cm^3, 14.7 mmol) and all volatiles subsequently removed from the resultant dark green solution *in vacuo*. The residue was suspended in toluene (40 cm^3) and cooled to -80 ^oC. To this, a solution of [K(tmeda)][**1**] (0.30 g, 0.50 mmol) in toluene (20 cm^3) was added over 5 mins. The mixture was warmed to room temperature overnight and all volatiles removed *in vacuo*. The residue was extracted into diethylether (20 cm^3), the extract filtered and stored at –30 °C overnight to yield dark green crystals of **56**. Yield: 0.18g (56 %). M.p. 164-166 °C; μ_{eff} = 3.3 B.M.; IR ν/cm^{-1} (Nujol): 1651w, 1586w, 1377s, 1355s, 1319m, 1258s, 1103m, 754m; MS (EI/70eV), *m*/*z* (%): 445.2 ([Ga{(DipNCH)$_2$}]$^+$, 3), 333.3 ((DipNCH)$_2$-Pr$^{i\ +}$, 100).

Synthesis of [Eu{Ga(Dip-DAB)}$_2$(tmeda)$_2$] 57. To a solution of EuI_2 (0.25 mmol) in THF (10 cm^3) at 25 ^oC was added tmeda (2.2 cm^3, 14.7 mmol) and all volatiles subsequently removed *in vacuo*. The residue was suspended in toluene (40 cm^3) and cooled to -80 ^oC. To this, a solution of [K(tmeda)][**1**] (0.30 g, 0.50 mmol) in toluene (20 cm^3) was added over 5 mins. The mixture was warmed to room temperature overnight and all volatiles removed *in vacuo*. The residue was extracted into diethylether (20 cm^3), the extract filtered and stored at –30 °C overnight to yield orange crystals of **57**. Yield: 23 %. M.p. 185-187 °C (decomp); μ_{eff} = 7.3 B.M.; IR ν/cm^{-1} (Nujol): 1651w, 1586w, 1378s, 1356s, 1319s, 1258s, 1103s, 754s; MS (EI/70eV), *m*/*z* (%): 445.2 ([Ga{(DipNCH)$_2$}]$^+$, 5), 378 ((DipNCH)$_2$H$^+$, 72), 333.3 ((DipNCH)$_2$-Pr$^{i\ +}$, 100); $C_{64}H_{104}Ga_2N_8Eu$ requires C 60.19, H 8.22, N 8.77 %; found C 59.35, H 8.14, N 7.62 %.

Synthesis of [Yb{Ga(Dip-DAB)}$_2$(tmeda)$_2$] 58. To a solution of YbI_2 (0.25 mmol) in THF (10 cm^3) at 25 ^oC was added tmeda (2.2 cm^3, 14.7 mmol) and all volatiles

subsequently removed *in vacuo*. The residue was suspended in toluene (40 cm^3) and cooled to -80 ^oC. To this, a solution of [K(tmeda)][**1**] (0.30 g, 0.50 mmol) in toluene (20 cm^3) was added over 5 mins. The mixture was warmed to room temperature overnight and all volatiles removed *in vacuo*. The residue was extracted into diethylether (20 cm^3), the extract filtered and stored at –30 °C overnight to yield red-orange crystals of **58**. Yield: 11 %. M.p. 170-174 °C (decomp); ^1H NMR (300 MHz, C_6D_6, 298 K): major isomer δ1.26 (d, 24 H, $^3J_{HH}$ = 6.8 Hz, $CH(CH_3)_2$), 1.45 (d, 24 H, $CH(CH_3)_2$), 1.90 (br., 32 H, tmeda), 3.55 (sept., 8H, $^3J_{HH}$ = 6.8 Hz, $CH(CH_3)_2$) 6.57 (s, 4H, NC*H*), 7.02-7.34 (m, 12 H, Ar-*H*); $^{13}C\{^1H\}$ NMR (100.6 MHz, C_6D_6, 298 K): 23.8 ($CH(CH_3)_2$), 24.2 ($CH(CH_3)_2$), 28.4 ($CH(CH_3)_2$), 46.7 ($N(CH_3)_2$), 62.1 (NCH_2), 122.7 (N*C*H), 124.6, 125.2, 145.8 (Ar-*C*) *ipso*-C not observed . IR ν/cm^{-1} (Nujol): 1652w, 1584w, 1377s, 1356s, 1319s, 1257s, 1103m, 756m; MS (EI/70eV), *m*/*z* (%): 445.2 ($[Ga\{(DipNCH)_2\}]^+$, 52), 378 ($(DipNCH)_2H^+$, 40), 333.3 ($(DipNCH)_2$-Pr^{i+}, 100).

Synthesis of [Tm{Ga(Dip-DAB)}(Dip-DAB)(tmeda)] 59. Tmeda (1.5 cm^3, 10 mmol) was added neat to a solution of $[TmI_2(THF)_5]$ (0.38 mmol) in toluene (10 cm^3) at room temperature. The resultant green solution was cooled to -80 ^oC and a solution of [K(tmeda)][**1**] (0.45 g, 0.75 mmol) in 10 cm^3 added to it over 5 mins. The mixture was warmed to room temperature overnight and all volatiles removed *in vacuo*. The residue was washed with hexane (10 cm^3) and extracted into diethylether (25 cm^3) and filtered. The filtrate was concentrated to *ca.* 10 cm^3 and stored at –30 °C to give dark red crystals of **59**. Yield: 0.04g (10 %). M.p. 208-210 ^oC; μ_{eff} = 7.0 B.M.; IR ν/cm^{-1} (Nujol): 1624w, 1587w, 1378s, 1356s, 1260s, 1100s, 1022s, 799s, 759m; MS (EI/70eV), *m*/*z* (%): 445.2 ($[Ga\{(DipNCH)_2\}]^+$, 15), 378 ($(DipNCH)_2H^+$, 42), 333.3 ($(DipNCH)_2$-Pr^{i+}, 100).

3.6 References

1. Liddle, S.T.; Mills, D.P. *Dalton Transactions*., **2009**, *29*, 5592.
2. Baker, R.J.; Farley, R.D.; Jones, C.; Kloth, M.; Murphy, D.M. *Dalton Trans.*, **2002**, 3844.
3. Deng, H.; Shore, S.G. *J. Am. Chem. Soc.*, **1991**, *113*, 8538.
4. Deng, H.; Chun, S.-H.; Florian, P.; Grandinetti P.J.; Shore, S.G.; *Inorg. Chem.*, **1996**, *35*, 3891.
5. Beletskaya, P.; Voskoboynikov, A.Z.; Chuklanova, E.B.; Kirillova, N.I.; Shestakova, A.K.; Parshina, I.N.; Gusev, A.I.; Magomedov, G.K.-I. *J. Am. Chem. Soc.*, **1993**, *115*, 3156.
6. Spannenberg, A.; Oberthür, M.; Noss, H.; Tillack, A.; Arndt, A.; Kempe, R. *Angew. Chem., Int. Ed.*, **1998**, *37*, 2079.
7. Butovskii, M.V.; Tok, O.L.; Wagner, F.R.; Kempe, R. *Angew. Chem., Int. Ed.*, **2008**, *47*, 6469.
8. Carver, C.T.; Monreal, M.J.; Diaconescu, P.L. *Organometallics*, **2008**, *27*, 363.
9. Arnold, P.L.; McMaster, J.; Liddle, S.T. *Chem. Commun.*, **2009**, 818.
10. Gamer, M.T.; Roesky, P.W.; Konchenko, S.N.; Nava, P.; Ahlrichs, R. *Angew. Chem., Int. Ed.*, **2006**, *45*, 4447.

11. Arnold, P.L.; Liddle, S.T.; McMaster, J.; Jones, C.; Mills, D.P. *J. Am. Chem. Soc.*, **2007**, *129*, 5360.

12. Wiecko, M.; Roesky, P.W. *Organometallics*, **2007**, *26*, 4846.

13. Schumann, H.; Nickel, S.; Hahn, E.; Heeg, M.J. *Organometallics*, **1985**, *4*, 800.

14. Schumann, H.; Meese-Marktscheffel, J.A.; Hahn, F.E. *J. Organomet. Chem.*, **1990**, *390*, 301

15. Cloke, F.G.N.; Dalby, C.I.; Hitchcock, P.B.; Karamallakis, H.; Lawless, G.A. *J. Chem. Soc., Chem. Commun.*, **1991**, 779

16. Bochkarev, M.N.; Khramenkov, V.V.; Rad'kov, Yu.F.; Zakharov, L.N.; Struchkov, Yu,T. *J. Organomet. Chem.*, **1991**, *408*, 329

17. Bochkarev, M.N.; Khramenkov, V.V.; Rad'kov, Yu.F.; Zakharov, L.N.; Struchkov, Yu,T. *J. Organomet. Chem.*, **1991**, *421*, 29

18. Radu, N.S.; Tilley, T.D. *J. Am. Chem. Soc.*, **1992**, *114*, 8293

19. Radu, N.S.; Tilley, T.D.; Rheingold, A.L. *J. Organomet. Chem.*, **1996**, *516*, 41

20. Campion, B.K.; Heyn, R.H.; Tilley, T.D. *Organometallics*, **1993**, *12*, 2584.

21. Radu, N.S.; Hollander, F.J.; Tilley, T.D.; Rheingold, A.L. *Chem. Commun.*, **1996**, 2459.

22. Bochkarev, M.N.; Grachev, O.V.; Molosnova, N.E.; Zhiltsov, S.F.; Zakharov, L.N.; Fukin, G.K.; Yanovsky, A.I.; Struchkov, Y.T. *J. Organomet. Chem.*, **1993**, *443*, C26

23. Bochkarev, M.N.; Makarov, V.M.; Zakharov, L.N.; Fukin, G.K.; Yanovsky, A.I.; Struchkov, Y.T. *J. Organomet. Chem.*, **1994**, *467*, C3.

24. Fedorova, E.E.; Trifonov, A.A.; Bochkarev, M.N.; Girgsdies, F.; Schumann, H. *Z. Anorg. Allg. Chem.*, **1999**, *625*, 1818.

25. Bochkarev, M.N.; Makarov, V.M.; Zakharov, L.N.; Fukin, G.K.; Yanovsky, G.I.; Struchkov, Y.I. *J. Organomet. Chem.*, **1995**, *490*, C29.

26. Corradi, M.M.; Frankland, A.D.; Hitchcock, P.B.; Lappert, M.F.; Lawless, G.A. *Chem. Commun.*, **1996**, 2323.

27. Cai, X.; Gehrhus, B.; Hitchcock, P.B.; Lappert, M.F. *Can. J. Chem.*, **2000**, *78*, 1484.

28. Castillo, I.; Tilley, T.D. *Organometallics*, **2001**, *20*, 5598.

29. Hou, Z.; Zhang, Y.; Nishiura, M.; Wakatsuki, Y. *Organometallics*, **2003**, *22*, 129.

30. Evans, W.J.; Perotti, J.M.; Ziller, J.W.; Moser, D.F.; West, R. *Organometallics*, **2003**, *22*, 1160.

31. Sadow, A.D.; Tilley, D.T. *J. Am. Chem. Soc.*, **2005**, *127*, 643.

32. Niemeyer, M. *Inorg. Chem.*, **2006**, *45*, 9085

33. Evans, W.J.; Gonzales, S.L.; Ziller, J.W. *J. Am. Chem. Soc.*, **1991**, *113*, 9880.

34. Evans, W.J.; Gonzales, S.L.; Ziller, J.W. *J. Chem. Soc., Chem. Commun.*, **1992**, 1138.

35. Sternal, R.S.; Brock, C.P.; Marks, T.J. *J. Am. Chem. Soc.*, **1985**, *107*, 8270.

36. Sternal, R.S.; Marks, T.J. *Organometallics*, **1987**, *6*, 2621.

37. Ritchey, J.M.; Zozulin, A.J.; Wrobleski, D.A.; Ryan, R.R.; Wasserman, H.J.; Moody, D.C.; Paine, R.T. *J. Am. Chem. Soc.*, **1985**, *107*, 501

38. Hay, P.J.; Ryan, R.R.; Salazar, K.V.; Wrobleski, D.A.; Sattelberger, A.P. *J. Am. Chem. Soc.*, **1986**, *108*, 313.

39. Bucaille, A.; Borgne, T.Le.; Ephritikhine, M. *Organometallics*, **2000**, *19*, 4912.

40. Monreal, M.J.; Carver, C.T.; Diaconescu, P.L. *Inorg. Chem.*, **2007**, *46*, 7226.

41. Monreal, M.J.; Diaconescu, P.L. *Organometallics*, **2008**, *27*, 1702.

42. Minasian, S.G.; Krinsky, J.L.; Williams, V.A.; Arnold, J. *J. Am. Chem. Soc.*, **2008**, *130*, 10086.

43. Liddle, S.T.; McMaster, J.; Mills, D.P.; Blake, A.J.; Jones, C.; Woodul, W.D. *Angew. Chem., Int. Ed.*, **2009**, *48*, 1077

44. Diaconescu, P.L.; Odum, A.L.; Agapie, T.; Cummins, C.C. *Organometallics*, **2001**, *20*, 4993.

45. Porchia, M.; Casellato, U.; Ossola, F.; Rossetto, G.; Zanella, P.; Graziani, R. *J. Chem. Soc., Chem. Commun.*, **1986**, 1034.

46. Porchia, M.; Brianese, N.; Casellato, U.; Ossola, F.; Rossetto, G.; Zanella, P. *J. Chem. Soc., Dalton Trans.*, **1989**, 677.

47. Molander, G.A.; Harris, C.R. *Chem. Rev.*, **1996**, *96*, 307.

48. See for example, Evans, W.J.; Keyer, R.A.; Ziller, J.W. *J. Organomet. Chem.*, **1990**, *394*, 87.

49. Bochkarev, M.N. *Coord. Chem. Revs.*, **2004**, *248*, 835.

50. Evans, W.J.; Hozbor, M.A. *J. Organomet. Chem.* **1987**, *326*, 299.

51. Jones, C.; Mills, D.P.; Rose, R.P.; Stasch, A. *Dalton Trans.*, **2008**, 4395.

52. Shannon, R.D. *Acta Cryst.*, **1976**, *A32*, 751. N.B. The value for Sm^{2+} was obtained by extrapolation.

53. Jones, C.; Mills, D.P.; Platts, J.A.; Rose, R.P. *Inorg. Chem.*, **2006**, *45*, 3146.

54. Cordero, B.; Gomez, V.; Platero-Prats, A.E.; Reves, M.; Echeverria, J.; Cremades, E.; Barragan, F.; Alvarez, S. *Dalton Trans.*, **2008**, 2832.

55. Trifonov, A.A.; Borovkov, I.A.; Fedorova, E.A.; Fukin, G.K.; Larionova, J.; Druzhkov, N.O.; Cherkasov, V.K. *Chem. Eur. J.*, **2007**, *13*, 4981.

56. Cotton, F.A.; Murillo, C.A.; Walton, R.A. *Multiple Bonds Between Metal Atoms*, 3rd ed., Springer, New York, **2005**.

57. See for example (a) Green, S.P.; Jones, C.; Lippert, K.-A.; Mills, D.P.; Stasch, A. *Inorg. Chem.*, **2006**, *45*, 7242; (b) Baker, R.J.; Jones, C.; Mills, D.P.; Murphy, D.M.; Hey-Hawkins, E.; Wolf, R. *Dalton Trans.*, **2006**, 64; (c) Baker, R.J.; Jones, C.; Kloth, M. *Dalton Trans.*, **2005**, 2106; (d) Baker, R.J.; Jones, C.; Kloth, M.; Platts, J.A. *Angew. Chem. Int. Ed. Engl.*, **2003**, *43*, 2660.

58. See for example (a) Jones, C.; Rose, R.P.; Stasch, A. *Dalton Trans.*, **2007**, 2997; (b) Green, S.P.; Jones, C.; Mills, D.P.; Stasch, A. *Organometallics*, **2007**, *26*, 3424; (c) Baker, R.J.; Jones, C.; Platts, J.A. *J. Am. Chem. Soc.*, **2003**, *125*, 10534.

Chapter 4

Synthesis of the First Monomeric Germanium(I) Radical

4.1 Introduction

4.1.1 Main Group Radicals

The chemistry of radicals involving heavier main group elements is a relatively new and exciting area. This field has been thoroughly reviewed by Power.[1] This section will serve as a general introduction and overview to main group radical species and will concentrate on the group 14 elements.

Prior to the 1970's, many examples of main group radical species were known, but these were generally limited to the first-row elements carbon, nitrogen, and oxygen. The most recognizable and simple examples of unpaired electron containing species are O_2, NO, and NO_2.[1] A few examples of more complex species are Fremy's salt $K_2\{ON(SO_3)_2\}$,[2] Wurster salts (singly oxidized salts of *p*-phenylenediamines),[3] the metal ketyls $MOCR_2$,[4] and the Gomberg radical $\cdot CPh_3$.[5] It is thought that these species can exist due to a variety of reasons, including the relatively high electronegativity of the main-group atom, partial spin delocalization onto substituents, and/or steric effects.[6] There is also a wide range of examples that have been characterized in which unpaired electron density is delocalized in part onto sulfur as part of an aromatic ring[7,8], or a sulfur-nitrogen ring.[1, 9,10]

It was not until the mid 1970's that the first examples of main-group element radical complexes not involving carbon, nitrogen, oxygen, or sulfur with moderate to long half-lives were prepared. Lappert and co-workers reported a range of radical complexes of the

heavier group 14 and group 15 elements which were subsequently reviewed.[11] It was thought that these species' stability and long half-lives could be attributed primarily to steric effects. With this knowledge, investigations into preparing radical species of the heavier main-group elements has continued and work carried out on groups 13, 14, 15 and 16 systems has been summarized.[1]

Although boron is not a heavier main-group element, a brief introduction will be given here on its radical chemistry. Work on preparing boron radical complexes has been ongoing since 1926 due to boron's electronic configuration, differing from that of carbon by just one electron. Krause and co-workers prepared the anion $[BPh_3]^{\cdot -}$ from reduction of triphenylboron with alkali metals in 1,2-dimethoxyethane (DME).[12] EPR studies of $[BPh_3]^{\cdot -}$ showed that the unpaired electron was located primarily at boron with $a(^{11}B)$ = 7.84 G. This relatively low value of the boron hyperfine coupling was attributed to the unpaired electron residing in the boron 2p-orbital and the boron geometry being planar rather than pyramidal. Interestingly, an increase of the steric bulk of the anion to $[B(Mes)_3]^{\cdot -}$, led to a slightly higher boron hyperfine coupling, $a(^{11}B)$ = 9.87 G, but it was noted that these values were still fully consistent with planar boron coordination.[12,13] Also of interest is the halogenated species $[B(C_6F_5)_3]^{\cdot -}$, which has been shown to be much less stable than the sterically crowded triarylboryl anions.[14]

Stable radicals of the heavier group 13 elements, aluminum, gallium and indium, with the unpaired electron residing primarily on the group 13 element, were not reported until 1993.[15] The first two structurally characterized examples were $[Li(TMEDA)_2]^+[R_2AlAlR_2]^{\cdot -}$ [R = $-CH(SiMe_3)_2$][15a] and $[Li(12\text{-crown-}4)_2]^+$ $[R'_2AlAlR_2]^{\cdot -}$ (R' = C_6H_2-2,4,6-Pr^i_3)[15b]. A large array of radical clusters of aluminum, gallium and

indium have also been reported and reviewed.[16,17] Two of the most notable are $[Li_4I_2(Et_2O)_{10}][Al_{77}\{N(SiMe_3)_2\}_{20}]$[18] and $[Li(Et_2O)_3]$-$[Al_{12}\{N(SiMe_3)_2\}_8]$.[19] While the presence of an unpaired electron in both species was detected, the EPR signals were too broad to observe the hyperfine features. By the reaction of excess $NaSiBu^t_3$ with MCl_3, the simplest stable neutral radical compounds of aluminum or gallium, R*M$^{\cdot}$MR$_2$* (M = Al or Ga; R* = -SiBu$^t_3$), were prepared.[20,21,22]

Examples of group 15 element radicals are mostly derived from phosphorus. It has been known for quite some time that phosphorus-centered radicals play an important role in many reactions.[23,24] In 1966 the phosphinyl radical :P$^{\cdot}$Ph$_2$ and the arsenic analogue :As$^{\cdot}$Ph$_2$, were detected at low temperatures.[25] Several classes of phosphorus radicals are known, including tetravalent phosphoranyl radicals[26], phosphinyl ($\cdot$PR$_2$),[27] phosphonyl (:OP$^{\cdot}$R$_2$), and phosphoniumyl radical cations [$\cdot$PR$_3$]$^+$,[26] radical anions [:P$^{\cdot}$R$_3$]$^-$,[26] and radicals with more than one phosphorus center which have been reviewed.[28] While phosphorus dominates the heavier group 15 element radical species, the less extensively studied radicals of arsenic, antimony, and bismuth have been reviewed.[29] Interestingly, the first structural characterization of phosphorus- or arsenic- centered radicals were monomers of the type :E$^{\cdot}${CH(SiMe$_3$)$_2$}$_2$ (E = P or As).[30,31]

Radicals of the heavier group 16 elements, selenium and tellurium, have not been studied as thoroughly as those of oxygen or sulfur. Recently, this has been changing due to the role that selenoenzymes have been shown to play in the protection against free radical injury,[32,33,34] and organoselenium comopounds being used in radical reactions as precursors.[35] Like sulfur, selenium and tellurium radical species are most often found as parts of a carbon[36] or an element-nitrogen, EN (E = Se or Te), ring systems.[37] Cyclic

examples are the benzo-1,2,3-triselenolium trifluorosulfonate salt[38] and the nitrogen containing system $[SeNSeNSe]^{\cdot+}$ which is formed after dissociating from $(SeNSeNSe^{\cdot-})_2(AsF_6)_2$ in solution.[37,39] The most notable example of an acyclic selenium or tellurium radical species is the stable radical cation $[Te\{N(SiMe_3)_2\}_2]^{\cdot+}$.[40] It was shown by EPR spectroscopy to be a rare example of a structurally characterized heavier group 15 radical species having the unpaired electron localized in a p-orbital on the group 15 element. This was made apparent by the negligible spin density on the nitrogen center.

Radicals of the heavier group 14 elements are more relevent to this work and will be discussed in more depth. According to Sekiguchi and Lee, radicals of the heavier group 14 elements may be characterized into one of three classes: neutral cyclic radicals, neutral acyclic radicals, and charged anion radicals.[41] The first example of a heavier group 14 neutral cyclic radical, **1**, was prepared by Power and co-workers via the reduction of $:Ge(Cl)(2,6\text{-}Mes_2\text{-}C_6H_3)$ with potassium graphite in THF (Scheme 1).[42] Interestingly, the planarity of the solution structure of **1** was confirmed through the EPR spectrum [g = 2.0069, hfcc $a(^{73}Ge)$ = 1.6mT]. It was said that such a small $a(^{73}Ge)$ value is a telling sign of mostly p character of the SOMO, which in turn implies sp^2 hybridization of the Ge radical centers and their planarity.

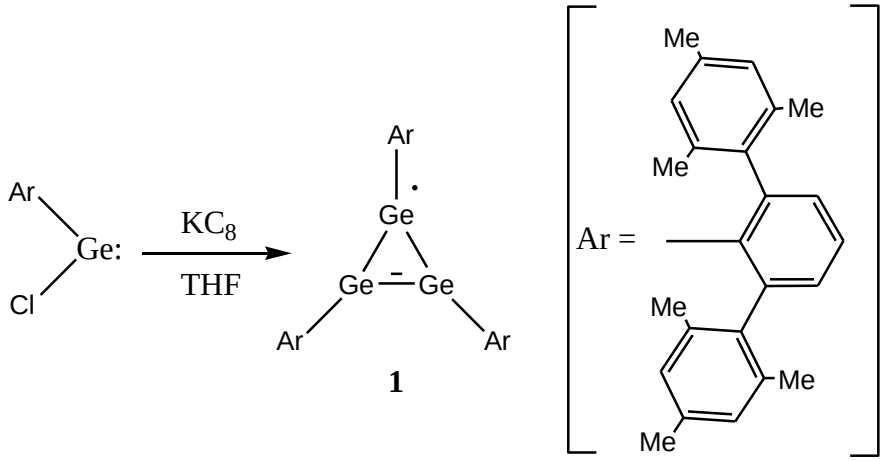

Scheme 1. Synthesis of **1**.

Sekiguchi and co-workers prepared complex **2** via the one-electron reduction of a cationic precursor with Bu^t_3SiNa or KC_8 in diethyl ether (Scheme 2).[43] Through X-ray crystallography and an examination of the bond lengths between the silicon atoms, complex **2** was found to be a planar, four membered ring with the unpaired electron delocalized over three Si atoms. An EPR study, [g = 2.0058, hfcc values $a(^{29}Si)$ = 1.55, 3.74, and 4.07 mT], showed **2** to exhibit the characteristics that are consistent with the radical being planar in solution, with overwhelming evidence coming from the small values of $a(^{29}Si)$.[43]

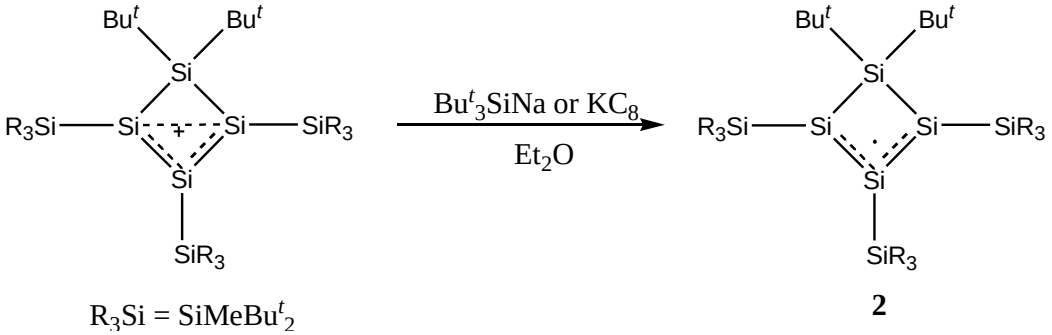

R_3Si = $SiMeBu^t_2$

Scheme 2. Synthesis of **2**.

A final example of a heavier group 14 neutral cyclic radical is the bicyclic Ge-centered radical, 1,6,7-trigermabicyclo[4.1.0]hept-3-en-7-yl, **3** (Scheme 3).[44] Sekiguchi and co-workers prepared **3** via the one-electron oxidation of the bicyclic anion with $B(C_6F_5)_3$ in THF. Unlike complexes **1** and **2**, complex **3** was found to exhibit the unpaired electron on the Ge atom featuring trigonal-planar geometry.

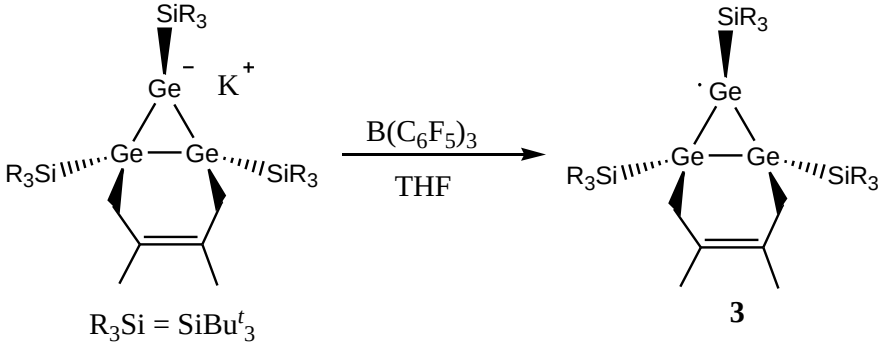

Scheme 3. Synthesis of **3**.

Recently, Sekiguchi and co-workers have prepared a series of heavier group 14 neutral acyclic radicals.[45] The series of complexes $(Bu^t_2MeSi)_3E\cdot$ [E = Si (**4**); Ge (**5**); Sn (**6**)], were prepared via the oxidation of the intermediary anionic derivatives $(Bu^t_2MeSi)_3ENa$ (E = Si, Ge, or Sn) with $GeCl_2$·dioxane or $SnCl_2$·dioxane in diethyl ether (Scheme 4).[45] X-ray crystallography showed all three complexes to have trigonal planar geometries, implying that the central element (Si, Ge, or Sn) was sp^2 hybridized and the SOMO was comprised largely of p character. The solution structures of radical complexes **4**, **5**, and **6** were studied by EPR spectroscopy revealing very small hfcc values for all (Figure 1). It was said that the small hfcc values gave evidence to the SOMO of the radicals being comprised of mostly p character as well as their planarity in solution putting them into the class of π-radicals.[45]

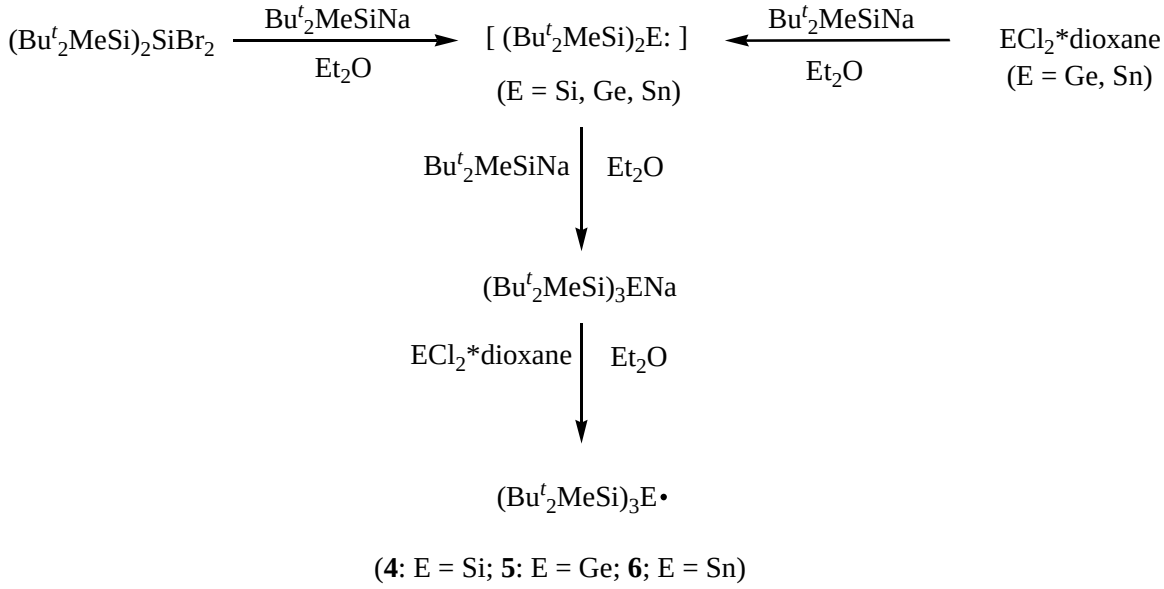

Scheme 4. Synthesis of **4**, **5**, and **6**.

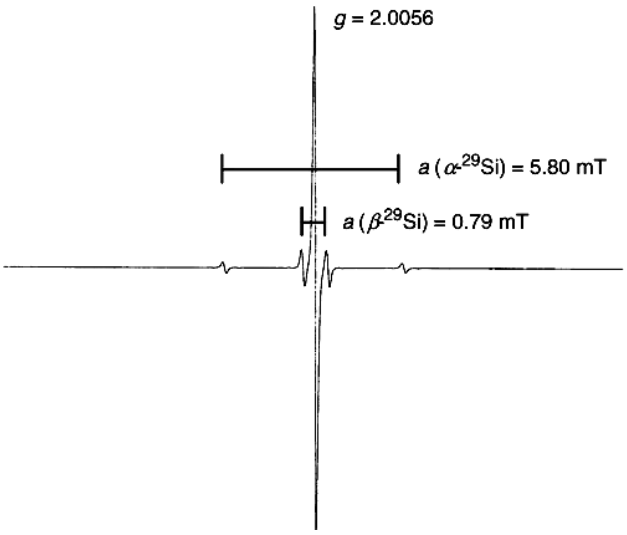

Figure 1. EPR spectrum of **4**.

There are a handful of known heavier group 14 element charged anion radicals. For example, the disilene precursor (Bu$^t_2$MeSi)$_2$Si=Si(SiMeBu$^t_2$)$_2$, was reduced with Bu^{t}Li by Sekiguchi and co-workers affording complex **7** (Scheme 5).[46] This was the first example of a stable disilene anion radical derivative. The study found the structure of the complex

to have one silicon center exhibiting planar geometry, denoting the radical center, and another silicon center featuring pyramidal geometry where the anion is centered.

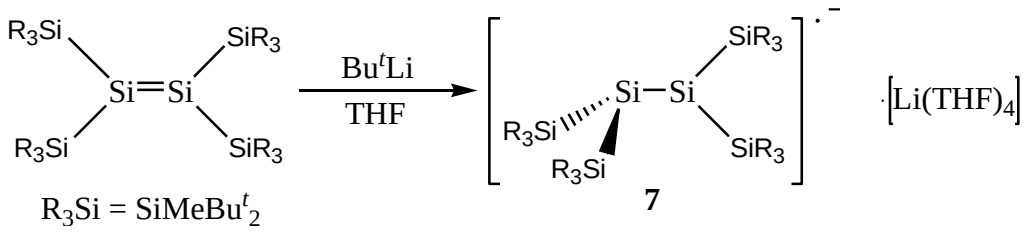

Scheme 5. The synthesis of complex **7**.

4.1.2 Heavier Group 14 Cyclopentedienide Compounds

Cyclopentadienides (Cp^-) are aromatic 6π-electron ligands that have been utilized in the preparation of complexes with nearly every metal in the periodic table. The diverse array of applications that such complexes have found in the past 50 years (e.g. in catalysis, materials science, asymmetric synthesis etc.), has led to their unquestionable importance to chemistry.[47] Considerable efforts have been made to prepare analogues of Cp^- which incorporate the heavier group 14 elements, and which could potentially be used as ligands in the formation of transition metal complexes. Considerable progress has been made in this direction with the preparation of structurally characterized examples of alkali metal salts of silole and germole anions and dianions.[48] Both experimental and theoretical evidence has shown the dianionc forms of these heterocycles, e.g. $[EC_4Ph_4]^{2-}$ (E = Si[49] or Ge[50]), to have considerable aromatic character. In contrast, the monoanions, e.g. $[\{R_3Si\}EC_4Me_4]^-$, only display aromatic delocalization when η^5-coordinated to transition metal fragments.[51] It was not until 2005 that considerable aromaticity in a crystallographically authenticated dianionic stannole complex, *viz.* $[(\mu\text{-}\eta^5\text{-}SnC_4Ph_4)\{Li(OEt_2)\}_2]$, was demonstrated.[52,53] Impressively, in 2010, a dianionic plumbole

analogue of this system, $[Li(DME)_3][(DME)Li(\eta^5\text{-}PbC_4Ph_4)]$, was reported to contain the first example of an aromatic lead heterocycle.[54] Although the intra-cyclic bonding in the above mentioned aromatic dianionic heterocycles can be represented by significant contributions from resonance forms with tetrelene character,[48] they are best described as having tetravalent group 14 centers. To date, the only known low valent heavier group 14 element Cp^- analogue is found in the N-heterocyclic germylidenide complex, **8** (Figure 2). This was reported by Driess and co-workers to result from the potassium reduction of the β-diketiminato germanium(II) chloride compound, [(^{Dip}Nacnac)GeCl] (^{Dip}Nacnac = $[\{N(Dip)C(Me)\}_2CH]^-$, Dip = $C_6H_3Pr^i_2$-2,6). The mechanism of its formation was suggested to involve several reductive processes including a ring contraction of the germanium heterocycle. Experimental spectroscopic and structural data for **8** implied it to be aromatic, a situation which was verified by the calculated negative nuclear independent chemical shift (NICS) values obtained for the heterocycle (NICS(1) = -7.4 ppm, NICS(2) = -7.7 ppm).[55] In contrast, the KC_8 reduction of [(^{Dip}Nacnac)SnCl] has been reported to generate tin metal and small amounts of the homoleptic complex, [Sn(^{Dip}Nacnac)$_2$], presumably *via* a disproportionation process.[56]

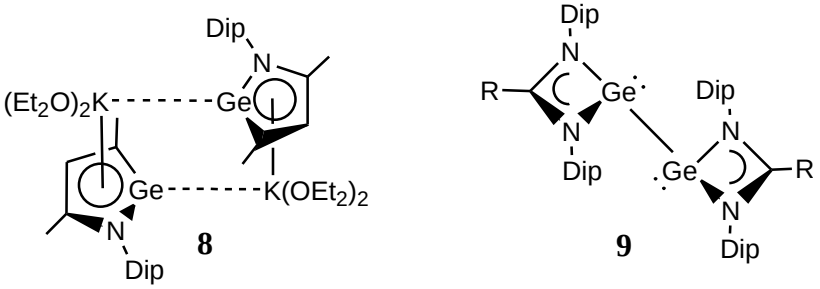

Dip = $C_6H_3Pr^i_2$-2,6 R = Bu^t or NPr^i_2

Figure 2. Complexes **8** and **9**.

The reductions of [(^{Dip}Nacnac)ECl] (E = Ge or Sn) can be compared to the potassium reductions of the closely related bulky guanidinato and amidinato germanium(II) chloride complexes, [LGeCl] (L = [{N(Dip)}$_2$CR]$^-$, R = NPr$^i_2$ (Priso), Bu^t (Piso)). Dissimilar to the ring contraction reaction that gave **8**, these afforded the germanium(I) dimers, **9**, *via* reductive coupling processes.[57,58] Compounds **9** can be considered as intra-molecularly base stabilized examples of digermynes, RGeGeR, the remarkable further chemistry of which is rapidly developing.[59]

4.2 Research Proposal

The aim of this project was to prepare the first example of a monomeric germanium(I) radical. Prior attempts at preparing low oxidation state, cyclic β-diketiminato germanium species were carried out by Driess and co-workers but these, unfortunately, led to ring contraction reactions.[60] It is proposed that novel germanium(I) species and/or germanium(II) heterocycles could be prepared by circumventing such ring contraction and/or disproportionation reactions from occurring during the reduction of suitable very bulky germanium(II) precursors. The use of a recently reported magnesium(I)[61,62a] complex as a mild reducing agent in these reactions is proposed to aid the preparation of the target complexes. Should the method be successful, it was thought that it could be applied to a range of other heavier group 14 elements.

4.3 Results and Discussion

4.3.1 Preparation of N-Heterocyclic Germylidenide and Stannylidenide Anions: Group 14 Metal(II) Cyclopentadienide Analogues

The β-diketiminate ligand that was chosen for this study was ^{But}Nacnac ([{N(Dip)C(Bu^t)}$_2$CH]$^-$), which has previously been shown to be substantially more sterically imposing towards N,N'-chelated metal centers than ^{Dip}Nacnac.[62] The monomeric germanium(II) precursor complex, [(^{But}Nacnac)GeCl] **10**, was prepared in good yield by the reaction of *in situ* generated [Li(^{But}Nacnac)] with $GeCl_2$·dioxane in diethyl ether. A small amount of [(^{But}Nacnac)Li(OEt_2)], **11**, crystallized from one reaction and was crystallographically characterized (see Figure 5). A variation of the literature procedure[63] was used to synthesize the tin(II) analogue of **10**, [(^{But}Nacnac)SnCl] **12**. Attempts to prepare the lead counterpart of **10** and **12** by reaction of [Li(^{But}Nacnac)] with $PbCl_2$ were not successful and afforded no identifiable products. It is of note that the related reaction between [Li(^{Dip}Nacnac)] and $PbCl_2$ is known to give [(^{Dip}Nacnac)PbCl].[64] Similarly, the reaction of [Li(^{But}Nacnac)] with one equivalent of $SiBr_4$ in the presence of tmeda did not give the intended product, [(^{But}Nacnac)$SiBr_3$], but instead yielded a complex mixture of products, from which a few crystals of the unusual lithium β-diketiminate adduct complex, [(^{But}Nacnac)Li{BrLi(tmeda)}$_2$], **13** resulted (see Figure 6). The related reaction between [Li(^{Dip}Nacnac)] and $SiBr_4$ in the presence of tmeda is known to give [Br_2Si{N(Dip)C(Me)C(H)C(=CH_2)N(Dip)}] *via* dehydrobromination of the β-diketiminate ligand.[65]

The spectroscopic data for **10** are comparable with those for the known tin complex, **12**.[63] Both complexes were crystallographically characterized and the molecular structures of **10** and **12** can be found in Figures 3 and 4. The compounds are isostructural with each other and have similar geometries to the previously reported systems, [(^{Dip}Nacnac)ECl] (E = Ge or Sn).[56] However, the bond lengths within the NC_3N backbones of **10** and **12** suggest a significantly reduced level of electronic delocalization than in [(^{Dip}Nacnac)ECl]. This undoubtedly results from a considerably greater distortion of the ligand backbones from planarity in the more hindered compounds. An indication of the increased steric protection afforded the metal centers in the bulkier systems, **10** and **12**, can be gauged by comparing the NCN angles in those compounds (**10**: 124.3° mean, **12**: 124.9° mean) with the same angles in [(^{Dip}Nacnac)GeCl] (120.5° mean) and [(^{Dip}Nacnac)SnCl] (121.8° mean).[56]

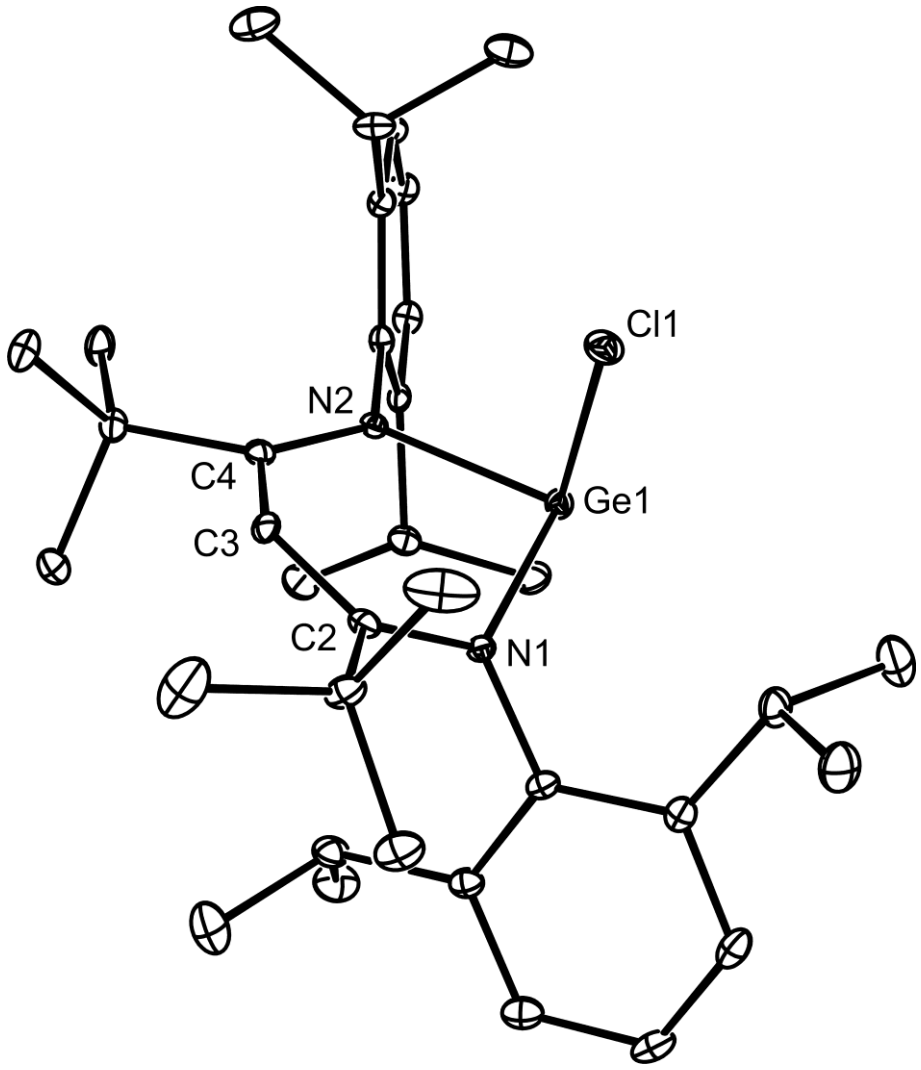

Figure 3. Thermal ellipsoid plot (25% probability surface) of the molecular structure of [(^{But}Nacnac)GeCl] (**10**); hydrogen atoms are omitted for clarity. Selected bond lengths (Å) and angles (°): Ge(1)-N(1) 1.9394(19), Ge(1)-N(2) 2.036(2), Ge(1)-Cl(1) 2.2942(8), N(1)-C(2) 1.374(3), N(2)-C(4) 1.328(3), C(2)-C(3) 1.368(4), C(3)-C(4) 1.432(3), N(1)-Ge(1)-N(2) 91.99(8), N(1)-Ge(1)-Cl(1) 95.39(6), N(2)-Ge(1)-Cl(1) 93.70(6).

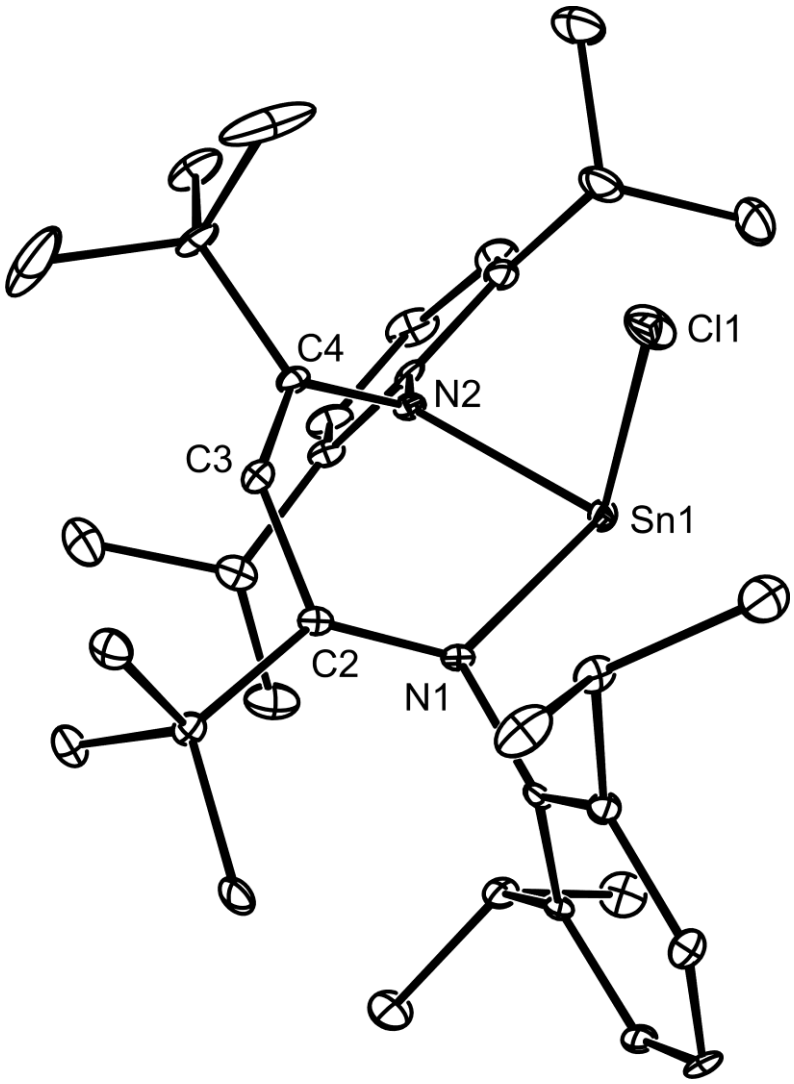

Figure 4. Thermal ellipsoid plot (25% probability surface) of the molecular structure of [($^{Bu^t}$Nacnac)SnCl] (**12**); hydrogen atoms are omitted for clarity. Selected bond lengths (Å) and angles (°): Sn(1)-N(2) 2.136(3), Sn(1)-N(1) 2.223(3), Sn(1)-Cl(1) 2.4466(13), N(1)-C(2) 1.322(5), N(2)-C(4) 1.361(5), C(2)-C(3) 1.419(5), C(3)-C(4) 1.389(5), N(2)-Sn(1)-N(1) 87.60(12), N(2)-Sn(1)-Cl(1) 91.82(10), N(1)-Sn(1)-Cl(1) 92.55(9).

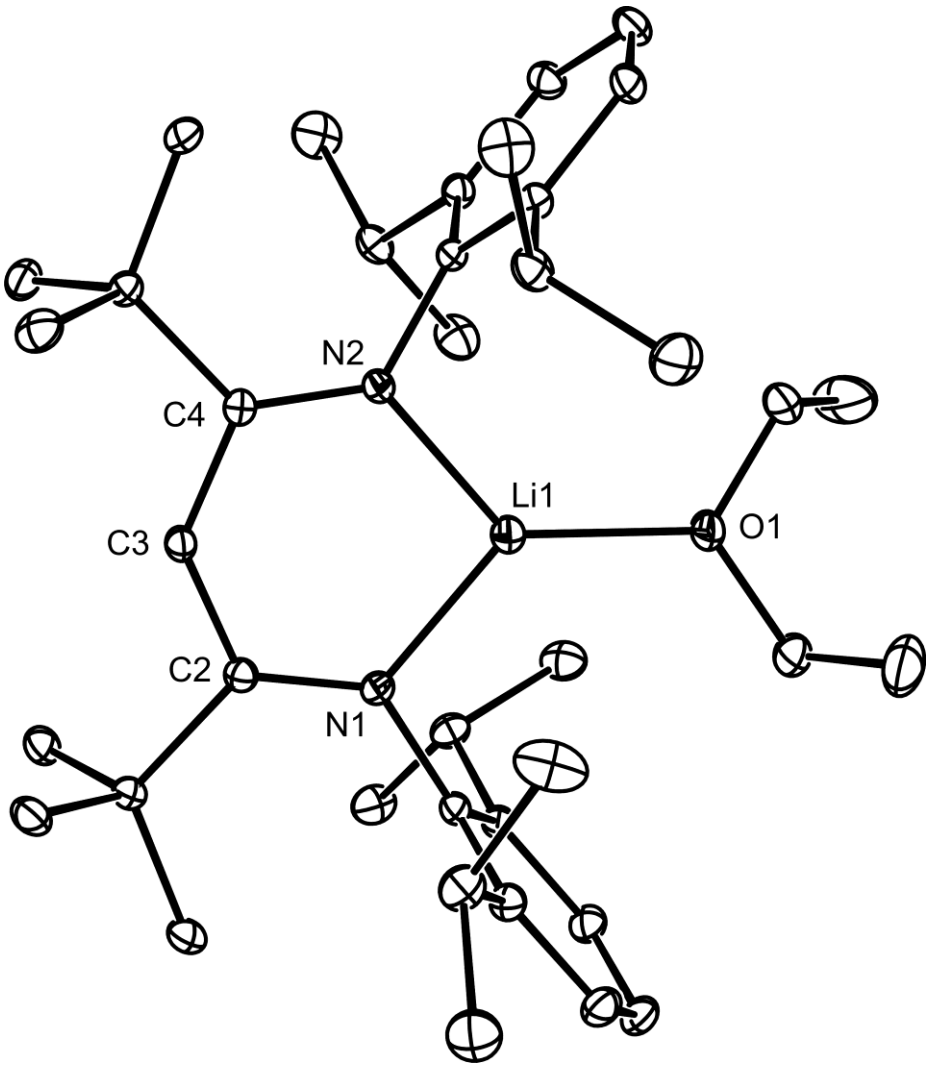

Figure 5. Thermal ellipsoid plot (25% probability surface) of the molecular structure of [(^{But}Nacnac)Li(OEt$_2$)] (**11**); hydrogen atoms are omitted for clarity. Selected bond lengths (Å) and angles (°): O(1)-Li(1) 1.949(3), N(1)-Li(1) 1.932(3), Li(1)-N(2) 1.925(3), N(1)-C(2) 1.3248(19), N(2)-C(4) 1.3276(18), C(2)-C(3) 1.414(2), C(3)-C(4) 1.412(2), N(2)-Li(1)-N(1) 98.97(12), N(2)-Li(1)-O(1) 130.94(15), N(1)-Li(1)-O(1) 130.09(15).

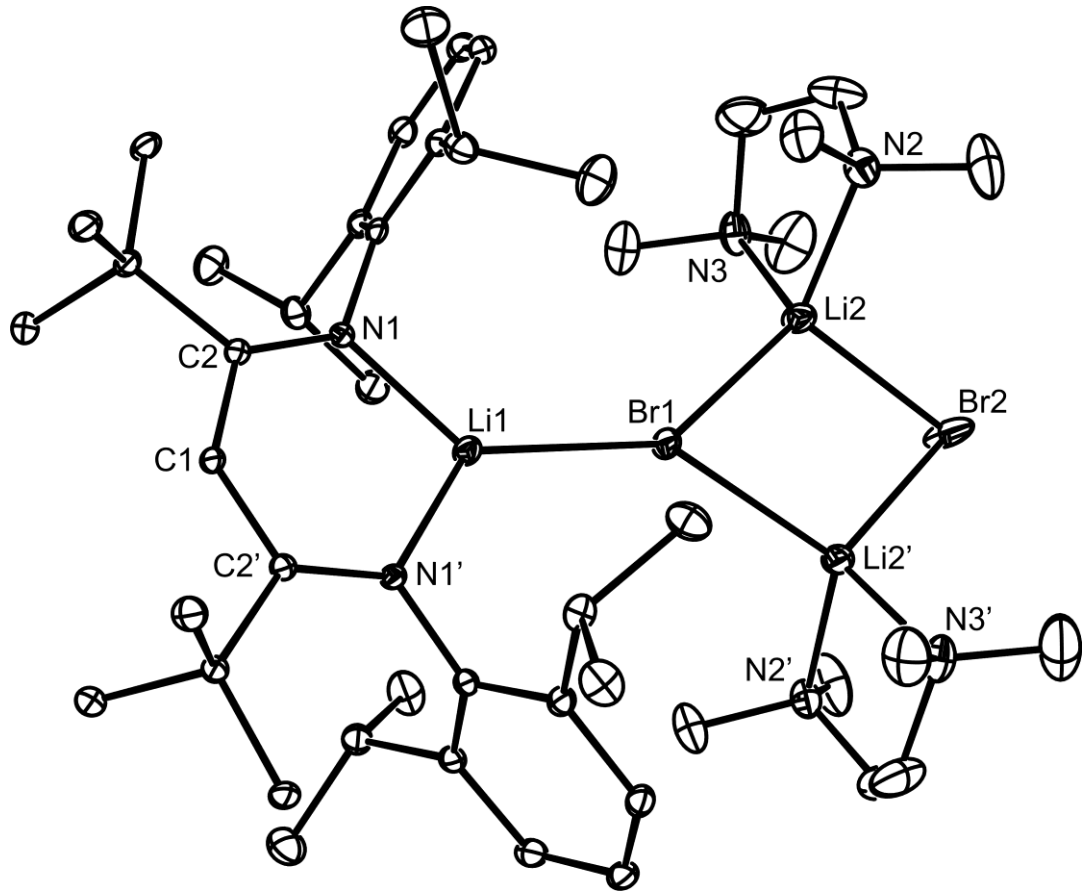

Figure 6. Thermal ellipsoid plot (25% probability surface) of the molecular structure of [(^{But}Nacnac)Li{BrLi(tmeda)}$_2$] (**13**); hydrogen atoms are omitted for clarity. Selected bond lengths (Å) and angles (°): Br(1)-Li(2) 2.607(7), Br(1)-Li(1) 2.654(8), N(1)-C(2) 1.330(4), N(1)-Li(1) 1.939(6), Br(2)-Li(2) 2.433(7), C(1)-C(2) 1.412(4), Br(2)-Li(2) 2.433(7), N(1)'1-Li(1)-N(1), 97.8(4), N(1)-Li(1)-Br(1) 131.1(2), Br(2)-Li(2)-Br(1) 107.3(2), Li(2)'-Br(1)-Li(2) 69.8(3), Li(2)-Br(2)-Li(2)' 75.7(3).

Early attempts to reduce **10** and **12** with elemental potassium or KC_8 were not encouraging as they yielded intractable product mixtures. As a result, attention turned to the milder reductant, lithium, which was reacted with the two precursors in THF to give moderate to high yields of yellow **14** and deep green **15** (Scheme 6). A moderate yield of the orange germanium(II) amide complex, **16**, was also isolated from the reaction that afforded **14**. The analogous tin amide, **17**, could not be crystallized from the mixture that gave **15**, though an ^{1}H NMR spectroscopic analysis of that mixture was consistent with its presence. It is notable that the previously reported reduction of [(^{Dip}Nacnac)GeCl] generated significant quantities of a complex analogous to **16**, *viz.* [(^{Dip}Nacnac)Ge{N(H)(Dip)}].[55] Therefore, it is apparent that the mechanisms of formation of **14**, and by implication **15**, are similar to that for **8**. These involve transient lithium germylidenide or stannylidenide salts, **18**, which undergo ring contraction reactions to give the amide complexes, **19**. These then undergo salt elimination reactions with either **10** or **12** to give **20**, which are further reduced, yielding the isolated complexes, **14** and **15**, and the transient lithium amide complexes, **21** (Scheme 6). The latter could participate in solvent hydrogen abstraction reactions, yielding **16** and **17**. It is noteworthy that several closely related reductive ring contraction reactions have been documented as arising from the alkali metal reduction of, for example, [(^{But}Nacnac)$TiCl_2$][66] or [(^{But}Nacnac)$ZrCl_3$].[67] Although **14** is stable in solution and the solid state for long periods under an inert atmosphere, its tin counterpart decomposes over several hours in solution at ambient temperature, depositing tin metal. This process generates, amongst other products, significant amounts of the enamine, (Dip)N=C(Bu^t)C(H)=C(H)(Bu^t).[68] In addition, **15** also

slowly decomposes in the solid state at 20 °C, and should, therefore, be stored in the freezer.

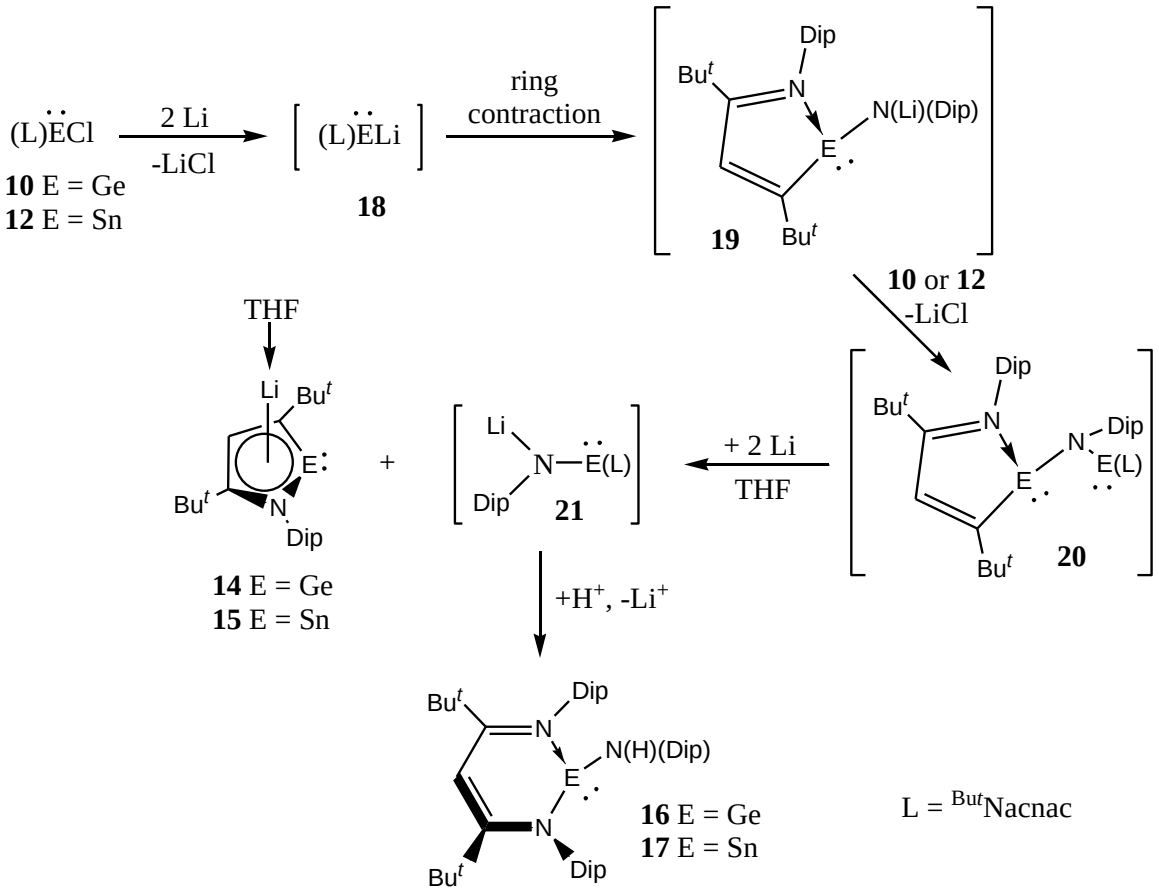

Scheme 6. Proposed mechanism of formation of **14**-**17**.

Both compounds **14** and **15** were crystallographically characterized and found to be isostructural monomers (*cf.* dimeric **8**) (Figures 7 and 8). In both **14** and **15**, the Li(THF) fragment is coordinated to an essentially planar heterocycle in an η^5-fashion with Li-Ge and Li-Sn distances that are slightly shorter than in the aromatic dianionic tetrelole complexes $[(\mu\text{-}\eta^5\text{-}GeC_4Ph_4)\{Li(dioxane)_2\}_2]$ (2.70 Å mean)[50b] and $[(\mu\text{-}\eta^5\text{-}SnC_4Ph_4)\{Li(OEt_2)\}_2]$ (2.76 Å mean)[52] respectively. Likewise, the Li-C distances in **14** and **15** are of the same order as

those in the dianionic complexes (2.28-2.43 Å and 2.19-2.41 Å respectively). The intra-cyclic bond lengths for **14** are close to those reported for **8** (Ge-N 1.944(2) Å, Ge-C 1.887(2) Å, N-C 1.382(3) Å, C-C 1.371(3) Å and 1.411(3)Å)[55] and thus, are strongly suggestive of appreciable π-resonance stabilization within the heterocycle. Although there are no stannylidenide anions to compare with that in **15**, the magnitude of the bond lengths within the NC_3 fragment of the stannacycle imply a similar level of delocalization to that in **8** and **14**. Consistent with this is the Sn-C distance of the compound, which is considerably shorter than those in the aromatic stannole dianion $[(\mu\text{-}\eta^5\text{-}SnC_4Ph_4)\{Li(OEt_2)\}_2]$ (2.16 Å mean)[52] and the tetravalent precursor to this complex, $[Ph_2SnC_4Ph_4]$ (2.13 Å mean).[69] Slightly at odds with the proposed delocalization over the stannacycle is its Sn-N separation which is comparable with those in **12**, but longer than such bonds in neutral N-heterocyclic stannylenes (known range: 2.051-2.189 Å).[70] That said, the tin centers in those heterocycles have a lower coordination number than that in **15**. Moreover, the Sn-N distance in **15** is considerably shorter than those between localized imine fragments and divalent Sn atoms, e.g. 2.278 Å in $[\{(SiMe_3)_2N\}Sn\{\kappa^2\text{-}N,N'\text{-}N(Bu^t)=C(H)C(H)N(Bu^t)\}]$.[71]

The molecular structure of **16** is portrayed in Figure 9, and shows it to be essentially isostructural to $[(^{Dip}Nacnac)Ge\{N(H)(Dip)\}]$,[55] with a puckered heterocycle that is reminiscent of the heterocycle in **10**. As was the case for $[(^{Dip}Nacnac)Ge\{N(H)(Dip)\}]$, the exocyclic Ge-N distance in **16** is significantly shorter than both of its endocyclic interactions. The acuteness of the angles about the germanium(II) center (93.4° mean) of the complex indicate a high degree of s-character to its lone pair.

The solution state ^1H and ^{13}C NMR spectra of **16** signify that it retains its solid state structure in solution. Contrastingly, the NMR data for **14** and **15** correspond to the

compounds possessing C_s symmetry in solution. It seems plausible that this is a result of an intermolecular exchange and/or intra-molecular migration of their Li(THF) fragments, which is rapid on the NMR timescale. Cooling d_8-toluene solutions of each compound to -30 °C (i.e. close to their solubility limits) did not result in resolution of their spectra. Consistent with the proposed π-delocalization within the heterocycles are the signals for their backbone protons which appear at δ 7.08 ppm (**14**) and δ 7.78 ppm (**15**), i.e. considerably downfield from the corresponding signals in the precursor molecules, **10** (δ 6.41 ppm) and **12** (δ 6.14 ppm).[63] Furthermore, the downfield chemical shifts of the *α*-carbon centers of the anions (**14**: δ 194.7 ppm, **15**: δ 226.9 ppm) are not dissimilar to those normally observed for germole and stannole dianions.[48,50,52,53] Perhaps, more illuminating are the high field resonances observed in the ^{7}Li NMR spectra of **14** (δ -5.31 ppm) and **15** (δ -4.66 ppm). These are at comparable chemical shifts to those reported for germole and stannole dianionic complexes (e.g. δ -4.36 ppm for $[(\mu\text{-}\eta^5\text{-}SnC_4Ph_4)\{Li(OEt_2)\}_2]$).[52] The high field positions of the signals for such complexes are thought to arise from strong shielding of their lithium centers by diatropic ring currents above and below the aromatic 6π-electron heterocycles.[72] Delocalization of the π-system within the stannacycle of **15** is also indicated by the remarkable downfield chemical shift of the signal in its ^{119}Sn NMR spectrum (δ 524.2 ppm). This lies more than 770 ppm to lower field than the signal for the precursor complex, **12** (δ -252.0 ppm),[63] and is markedly downfield of resonances reported for isoelectronic stannole dianions (e.g. $[(\mu\text{-}\eta^5\text{-}SnC_4Ph_4)\{Li(OEt_2)\}_2]$, δ 163.3 ppm)[52] and neutral N-heterocyclic stannylenes (e.g. $[:Sn\{N(Mes)C(H)\}_2]$ (Mes = mesityl), δ 259 ppm).[73] That said, such comparisons should be treated with some caution as ^{119}Sn NMR chemical shifts for tin(II) compounds are very sensitive to the coordination number of the

metal and the nature of the atoms bonded to it. Indeed, they can range over more than 2000 ppm.[74] What is clear, however, is that there is a significant delocalization of the negative charge on the heterocycle in **15** away from the tin atom.

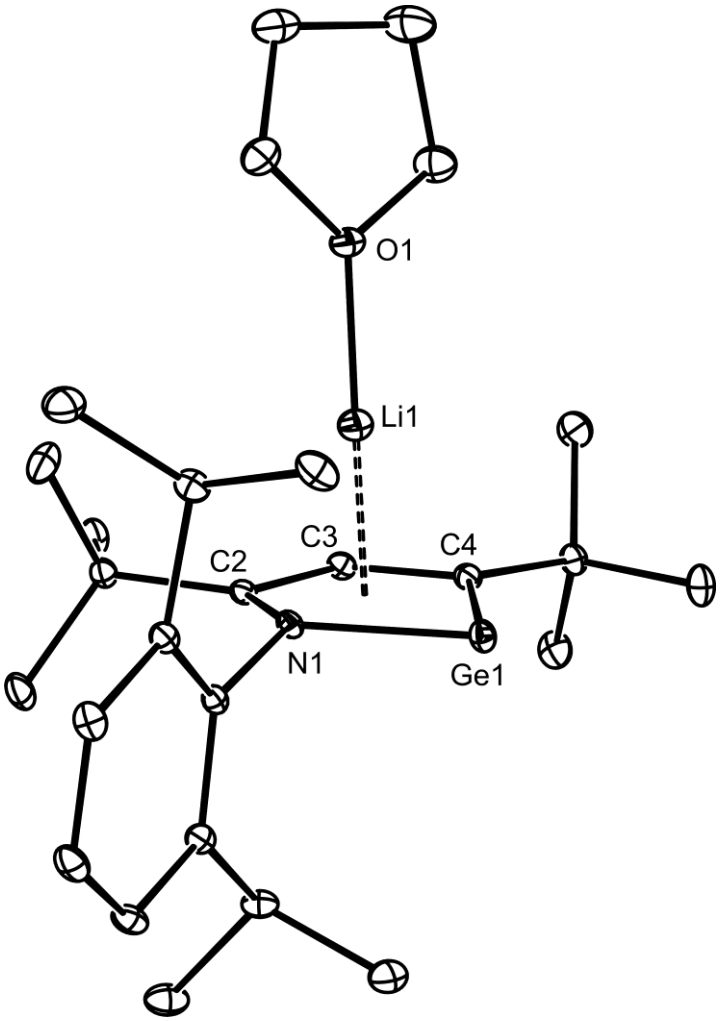

Figure 7. Thermal ellipsoid plot (25% probability surface) of the molecular structure of [(THF)Li{η^5-GeC(Bu^t)C(H)C(Bu^t)N(Dip)}] (**14**); hydrogen atoms are omitted for clarity. Selected bond lengths (Å) and angles (°): Ge(1)-C(4) 1.896(2), Ge(1)-N(1) 1.9660(16), N(1)-C(2) 1.404(2), C(2)-C(3) 1.387(3), C(3)-C(4) 1.421(3), Ge(1)-Li(1) 2.596(4), N(1)-Li(1) 2.215(4), C(2)-Li(1) 2.225(4), C(3)-Li(1) 2.204(4), C(4)-Li(1) 2.303(4), C(4)-Ge(1)-N(1) 83.13(8).

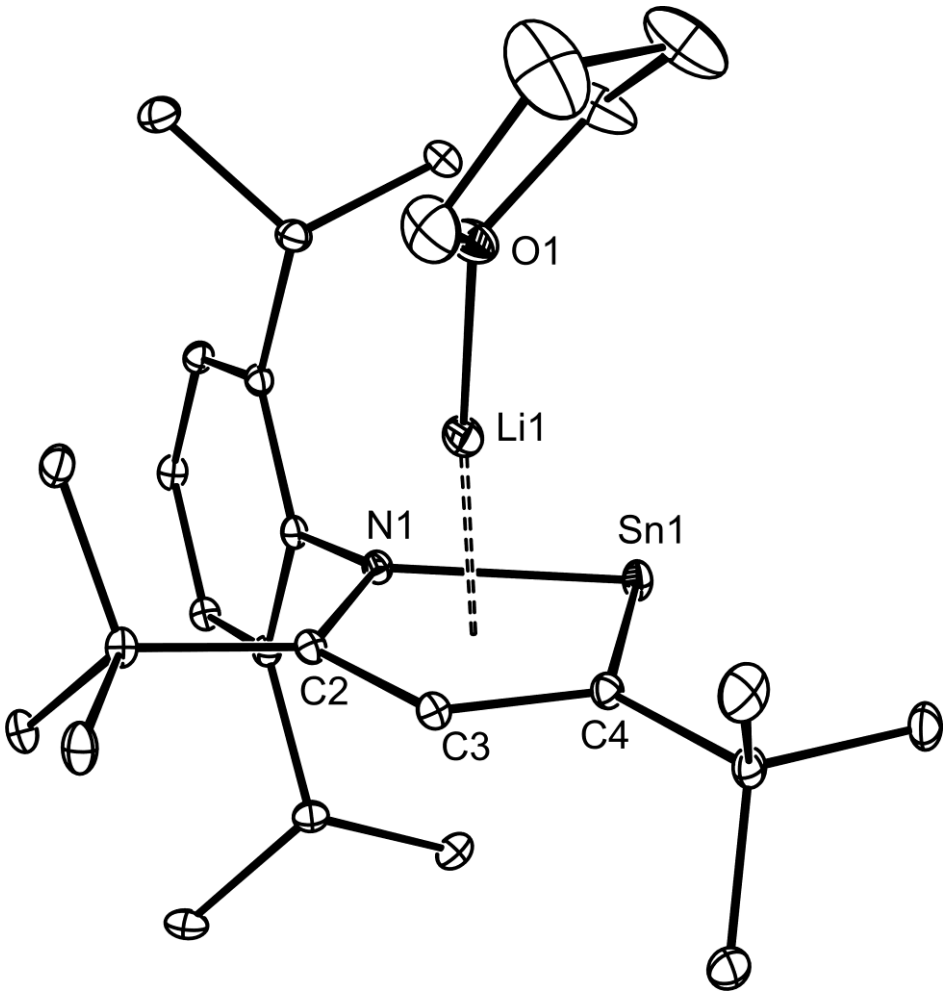

Figure 8. Thermal ellipsoid plot (25% probability surface) of the molecular structure of [(THF)Li{η^5-SnC(Bu^t)C(H)C(Bu^t)N(Dip)}] (**15**); hydrogen atoms are omitted for clarity. Selected bond lengths (Å) and angles (°): Sn(1)-C(4) 2.0981(19), Sn(1)-N(1) 2.1907(16), N(1)-C(2) 1.400(2), C(2)-C(3) 1.394(3), C(3)-C(4) 1.415(3), Sn(1)-Li(1) 2.759(4), N(1)-Li(1) 2.208(4), C(2)-Li(1) 2.184(4), C(3)-Li(1) 2.175(4), C(4)-Li(1) 2.316(4), O(1)-Li(1) 1.866(4), C(4)-Sn(1)-N(1) 77.12(7).

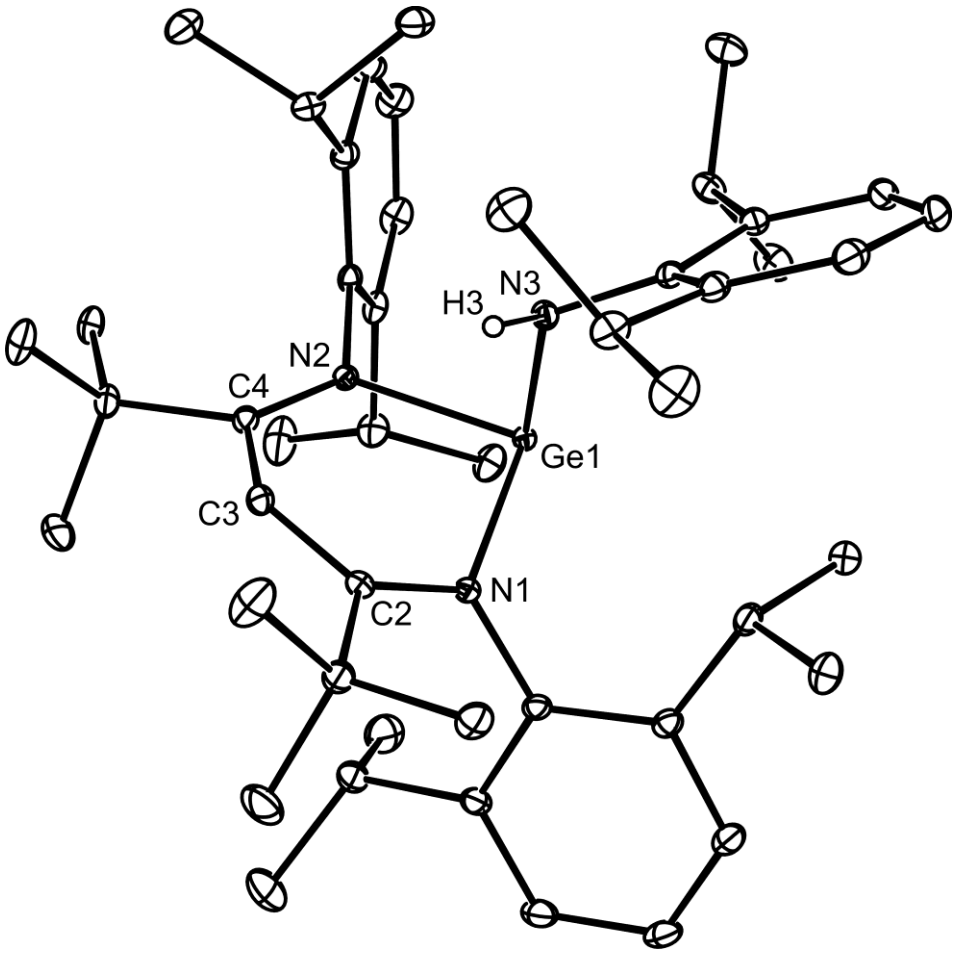

Figure 9. Thermal ellipsoid plot (25% probability surface) of the molecular structure of [(^{But}Nacnac)Ge{N(H)(Dip)}] (**16**); hydrogen atoms (except H(3)) are omitted for clarity. Selected bond lengths (Å) and angles (°): Ge(1)-N(3) 1.9097(12), Ge(1)-N(1) 1.9963(11), Ge(1)-N(2) 2.0377(11), N(1)-C(2) 1.3603(17), N(2)-C(4) 1.3173(17), C(2)-C(3) 1.3755(19), C(3)-C(4) 1.4300(19), N(3)-Ge(1)-N(1) 99.31(5), N(3)-Ge(1)-N(2) 88.60(5), N(1)-Ge(1)-N(2) 92.18(4).

4.3.2 Preparation of a monomeric Ge(I) radical

In an attempt at preparing novel six-membered germanium(I) species and/or germanium(II) heterocycles, complex **10** was reacted with half an equivalent of

[(^{Mes}Nacnac)Mg]$_2$[62a] in toluene. Work up of the reaction below 0°C in n-hexane afforded the novel monomeric germanium(I) radical species, **22**, in moderate yield (Scheme 7). It is of note that reaction of **10** with stoichiometric amounts of sodium naphthalide afforded **22** in a similar yield.

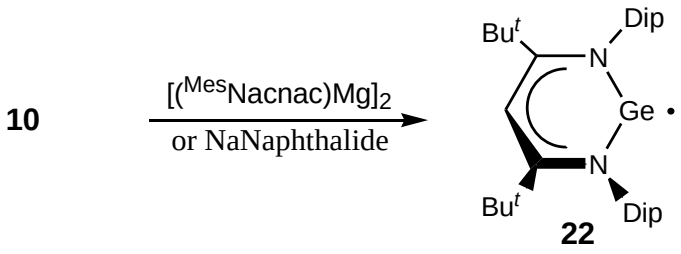

Scheme 7. Synthesis of complex **22**.

In an attempt to confirm the presence of a π-based, germanium centered radical in complex **22**, an CW-EPR investigation was carried out in collaboration with Dr. Damien Murphy of Cardiff University. For a π-based radical, one expects a rhombic g tensor (at X-band frequencies the signal may appear axial, particularly if the line widths are broad). Two components of g (g_x and g_y) were found to be associated with in-plane directions and one component of g (g_z) is associated with the out-of-plane direction (Figure 10). The out-of-plane g value is usually of little diagnostic value since the spin-orbit coupling is essentially zero. One component of g should therefore have a value close to 2.0023, another with a small negative g shift (for a one electron π-based system) and finally one component should produce a relatively large negative g shift. The experimental g values for **22** reported in Table 1 (g_1=1.968, g_2= 1.997, g_3=2.001; g_{iso} = 1.988) are therefore consistent with that expected of a one electron π-based radical. (One may assign these g values labels g_x=1.968, g_y= 1.997, g_z=2.001 by analogy with other π-radicals).

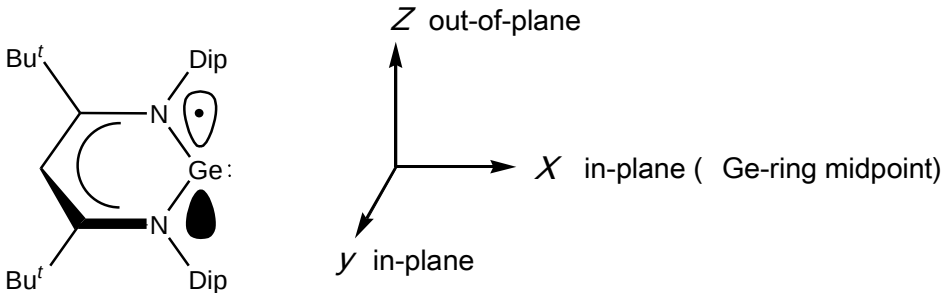

Figure 10. Complex **22**.

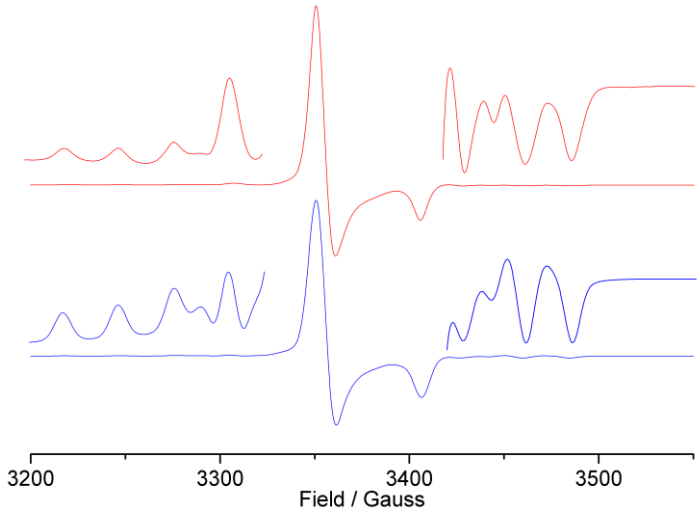

Figure 11: cw X-band EPR spectra (140K) of **22**. Top = experimental, Bottom = simulation. Simulated EPR parameters: g_1=1.968, g_2= 1.997, g_3=2.001, A_1 = ±42 MHz, A_2 = ±37.5 MHz, A_3 = ±82.5 MHz (A_1/A_2 values ± 0.5 MHz).

The hyperfine coupling is also a very diagnostic tool for the characterization of π-based radicals. The largest hyperfine component (A_z) is usually directed out-of-plane along g_z. The other two components A_x and A_y are expected to be much smaller in magnitude (for example as seen in nitroxides). In the current radical, the ^{73}Ge isotope (I = 9/2) is only 7.76% abundant. The hyperfine couplings in **22** are therefore only weakly observed in the spectral wings (shown magnified in Figure 11). The largest observed hyperfine coupling

(labelled A_3) of 82.5 MHz is centred on g_3=2.001. This observation is essentially consistent with a π-based radical. The remaining two hyperfine components are expected to be very small for a pure π-based radical. In the current system however the couplings are appreciable (A_1 = ±42 MHz, A_2 = ±37.5 MHz) perhaps resulting from some spin delocalization onto the NC_3N ring.

Further supporting evidence for spin delocalization comes from the observed ^{14}N and ^{1}H couplings detected in the pulsed ENDOR spectra of **22**. The Mims ENDOR spectra (Figure 12) show characteristic couplings from the ^{14}N and ^{1}H nuclei of the ligand. A series of high frequency peaks is also visible in the spectra (from *ca.* 25-50 MHz) which were tentatively assigned to ^{73}Ge hyperfine and quadrupole couplings (spectra not optimized for ^{73}Ge, therefore features due to blind spots are apparent).

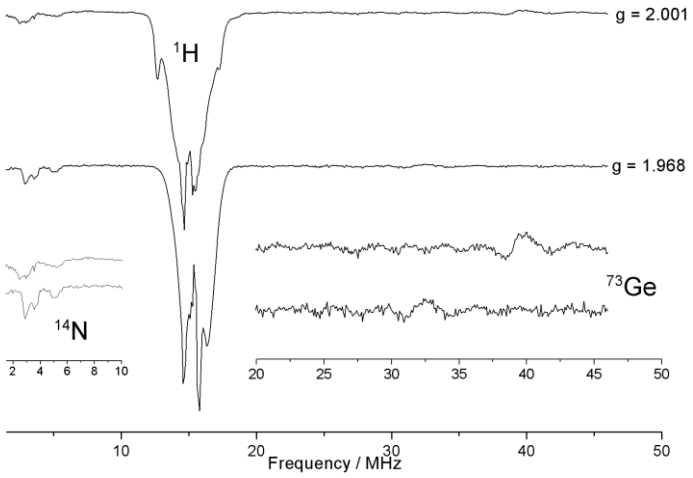

Figure 12: Mims ENDOR spectra (10K) of **22** recorded at the field positions corresponding to g = 2.001 and g = 1.968. Hyperfine couplings corresponding to ^{1}H, ^{14}N and ^{73}Ge are clearly visible in the spectra.

The ENDOR spectra have not been simulated. Nevertheless some general comments can be made by analysis of the experimental data. Firstly, the largest component of the ^{1}H coupling is about 6.3 MHz, with other clearly visible 4.65 and 2.35 MHz couplings. No larger ^{1}H couplings were visible. Secondly the largest component of the ^{14}N coupling is about 6.5 MHz, while the other two components are close to this. A coupling of *ca*. 5.5 MHz can in fact be observed superimposed on the ^{73}Ge hyperfine lines in the CW-EPR spectrum, consistent with the ENDOR data.

	g_1	g_2	g_3	g_{iso}	$^{1}A_1$	$^{1}A_2$	$^{1}A_3$	a_{iso}
	EPR Data							
^{73}Ge	1.968	1.997	2.001	1.988	±42	±37.5	±82.5	
	^{2}ENDOR Data							
^{14}N	-	-	-	-	*-5.9*	*-5.3*	*-6.3*	*-6*
^{1}H	-	-	-	-	*-6.3*	*-4.6*	*-2.3*	*-4.5*

[1]Sign of the coupling not known from the frozen solution spectrum. [2]Accurate values of N and H couplings to be determined from the simulations.

Table 1. EPR and ENDOR data for complex **22**.

The crystal structure of **22** revealed it to exhibit a very symmetric heterocycle with planar geometry (Figure 13). The germanium-nitrogen bond lengths were measured to be 1.9988(11) Å. The N-^{But}C bond distance is 1.3251(18) Å and the backbone C-C bond length is 1.4074(16) Å. These NC_3N values are much more uniform compared to the precursor **10**, which has a more localized ^{But}Nacnac ligand. The ^{1}H NMR spectrum of complex **22** was of little diagnostic use due to the paramagnetic nature of the complex. However, upon standing, the NMR sample revealed a pattern consistent with a small

amount of a decomposition product emerging from the expected broad paramagnetic spectrum of **22**. It was determined from the ^{1}H NMR spectrum that the observed signals were due to the enamine decomposition product that also arose from the decomposition of complex **14**. It is of note that, while not a definite test for the presence of a Ge^{I} radical species, it was seen by ^{1}H NMR spectroscopy that the addition of the mild chlorinating agent C_2Cl_6 to complex **22** immediately and quantitatively led to the formation of complex **10**.

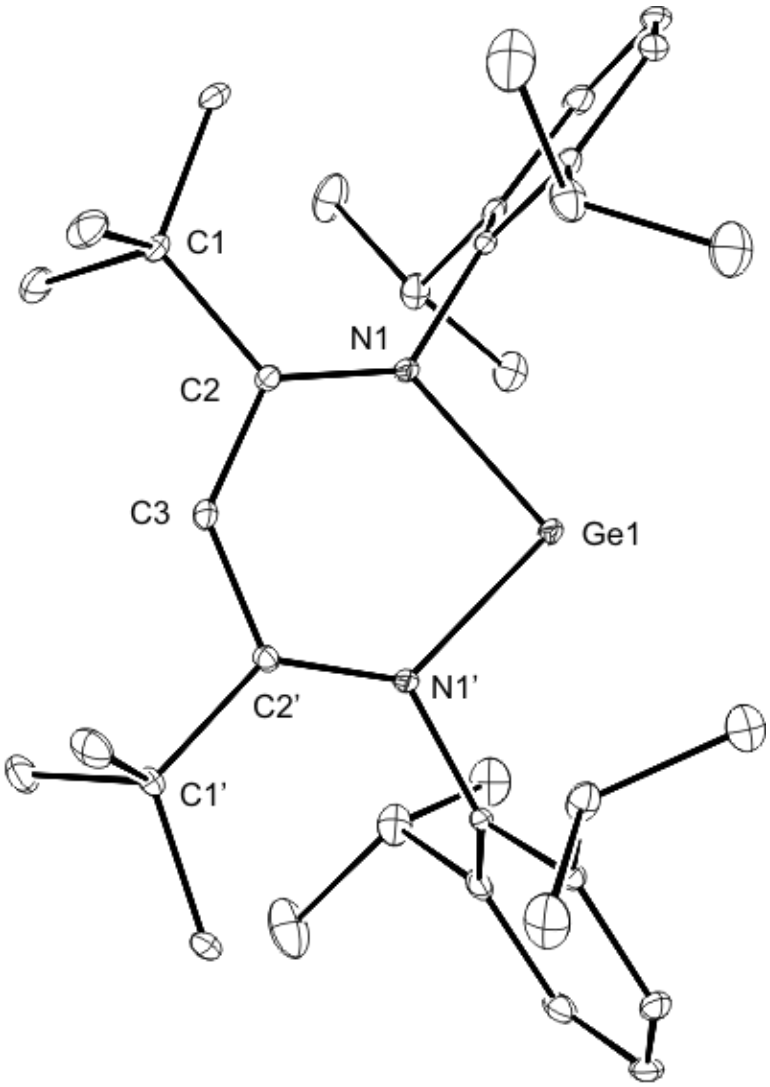

Figure 13. Thermal ellipsoid plot (25% probability surface) of the molecular structure of [(^{But}Nacnac)·Ge:] (**22**); hydrogen atoms are omitted for clarity. Selected bond lengths (Å) and angles (°): Ge(1)-N(1) 1.9988(11), N(1)-C(2) 1.3251(18), C(1)-C(2) 1.5553(19), C(2)-C(3) 1.4074(16), N(1)-Ge(1)-N(1') 91.97(7), N(1)-C(2)-C(3) 120.77(13).

In order to rule out the possibility of **22** being a germanium hydride complex, it was decided to intentionally prepare the hydride analogue of **10** and compare the complex to **22** and similar species of lesser steric bulk. It has been shown previously that [(^{Dip}Nacnac)GeCl] reacts with AlH_3·NMe_3 or KEt_3BH in 1:1 ratios to give the hydride

species [(^{Dip}Nacnac)GeH].[75] Interestingly, the much bulkier complex **10** did not form a hydride species upon reaction with KEt_3BH, but instead the yellow crystaline novel germylene, **23** was formed in low yield (Scheme 8). In the solid state (Figure 13), complex **23** exhibits a non-planar heterocycle, significantly more distorted from planarity than that in **10** or **22**. This distortion arises from the protonation of the imino backbone carbon of **23** and was confirmed by examination of the backbone C-C bond lengths of the complex. The C-C bond lengths of the ligand backbone in the precursor complex **10** are closer in distance, 1.368(4) and 1.432(3) Å, whereas the same bonds of **23** are found to be 1.357(6) and 1.500(6) Å. This suggests no ligand backbone delocalization in **23**.

The formation of complex **23**, instead of the expected complex [(^{But}Nacnac)GeH], (*cf.* [(^{Dip}Nacnac)GeH])[75] was of great interest to us. It is proposed that the mechanism for the formation of **23** is one similar to that described by Piers and co-workers for reduction of a related scandium complex (Scheme 8).[68] The germanium precursor, **10**, reacts with KEt_3BH forming the hydride species [(^{But}Nacnac)GeH] as an intermediate. It is thought that the ligand backbone then undergoes a nucleophilic attack from the hydride, affording the germylene species **23**. Like complex **10**, [(^{But}Nacnac)GeH] most likely has a much more distorted planar heterocycle geometry than its [(^{Mes}Nacnac)GeH] (see later) and [(^{Dip}Nacnac)GeH][56] counterparts due to its greater ligand steric bulk. This increase in planar distortion causes a decrease in the degree of delocalization over the ^{But}Nacnac ligand backbone, which in turn allows the NC_3N ring to be more susceptible to nucleophilic attack. Complex **23** is stable in the solid state under an inert atmosphere. However, it decomposes in solution to give the known enamine, (Dip)N=C(Bu^t)C(H)=C(H)(Bu^t).[68] The ^{1}H NMR spectrum of a crystallographically characterized sample of **23** is consistent with

the germylene structure, but after approximately twenty minutes, the characteristic quartet resonance of the enamine at δ 5.80 ppm can clearly be seen and continues to grow over time until no trace of **23** remains after 24 hours. This AB quartet corresponds to the *trans*-coupled olefinic protons of the enamine.[68] It became very evident after structural and spectroscopic comparisons between [(^{Dip}Nacnac)GeH],[75] and complex **22**, that the latter is indeed not a germanium hydride species. Specifically, the Ge-H singlet and a Ge-H stretching mode are clearly observed in the ^{1}H NMR and IR spectra of [(^{Dip}Nacnac)GeH] at δ 8.25 ppm and 1525 ν/cm^{-1} respectively. Similar features are absent from the spectra of **22**.

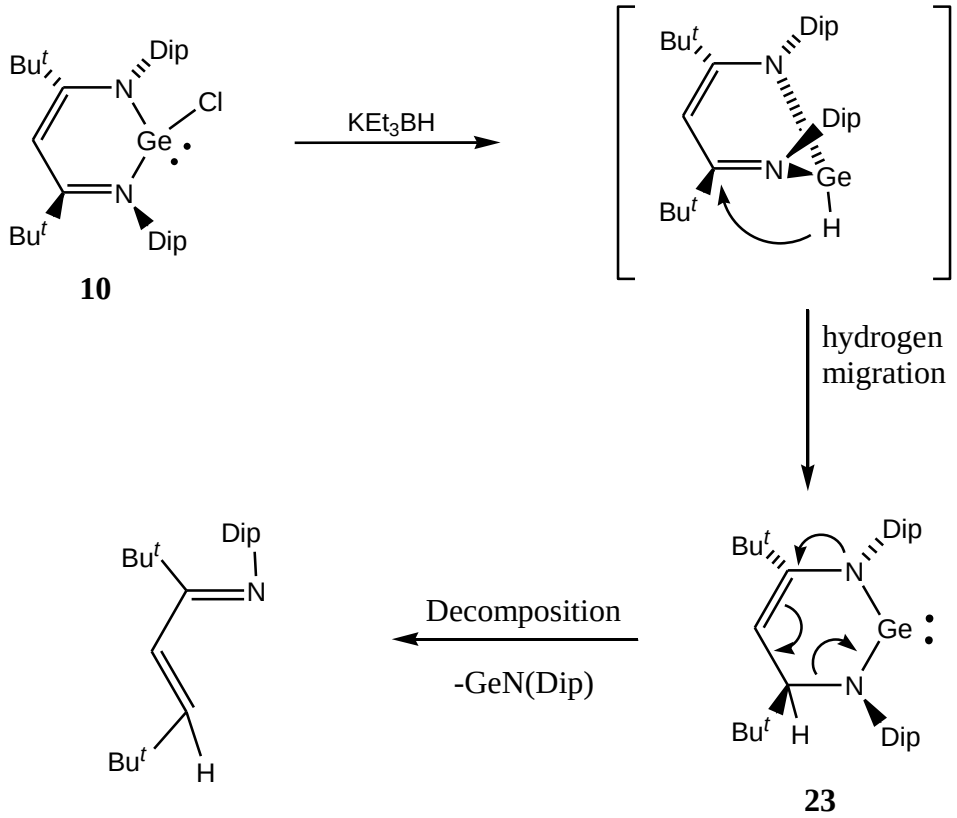

Scheme 8. Proposed mechanism of formation of complex **23**.

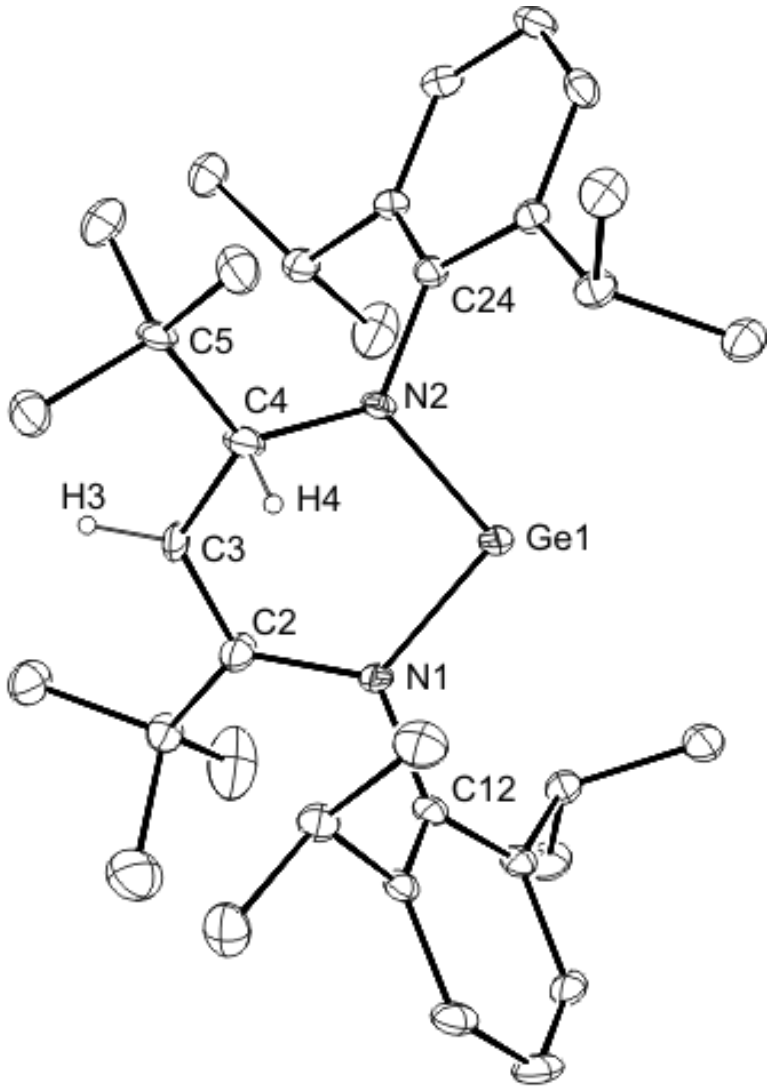

Figure 14. Thermal ellipsoid plot (25% probability surface) of the molecular structure of [(^{But}HNacnac)Ge] (**23**); hydrogen atoms are omitted for clarity (except for the backbone protons). Selected bond lengths (Å) and angles (°): Ge(1)-N(1) 1.841(4), Ge(1)-N(2) 1.829(4), N(1)-C(2) 1.439(6), N(2)-C(4) 1.488(5), C(2)-C(3) 1.357(6), C(3)-C(4) 1.500(6), C(4)-C(5) 1.536(6), N(1)-C(12) 1.448(6), N(2)-C(24) 1.449(6), N(1)-Ge(1)-N(2) 98.58(17), Ge(1)-N(1)-C(2) 120.9(3), Ge(1)-N(2)-C(4) 118.0(4), C(2)-C(3)-C(4) 121.9(8).

It was then thought to intentionally prepare a cationic germanium species in order to compare to complex **10** and **22**, and its potential in forming complex **22** upon reduction. Complex **10** was reacted with $Ag[Al\{OC(CF_3)_3\}_4]$ affording the cationic germanium species, $[(^{But}Nacnac)Ge]^+$ $[Al\{OC(CF_3)_3\}_4]^-$ **24**, in very low yield. Spectroscopic data were difficult to obtain due to the very low solubility of the complex; however, the complex was characterized by X-ray crystallography (Figure 15). The germanium-nitrogen bond lengths were measured at 1.898(9) Å and 1.902(10) Å. The N-^{But}C bond distances are 1.337(14) Å and 1.370(15) Å while the backbone C-C bond lengths are 1.443(17) Å and 1.385(17) Å. Apart from the germanium-nitrogen bonds, the NC_3N ring bond lengths are quiet similar to that of complex **10**. A small scale reaction of **24** with $[(^{Mes}Nacnac)Mg]_2$ did not afford **22**, but instead gave, as determined by ^1H NMR spectroscopy, the decomposed enamine product previously seen by Piers and co-workers.

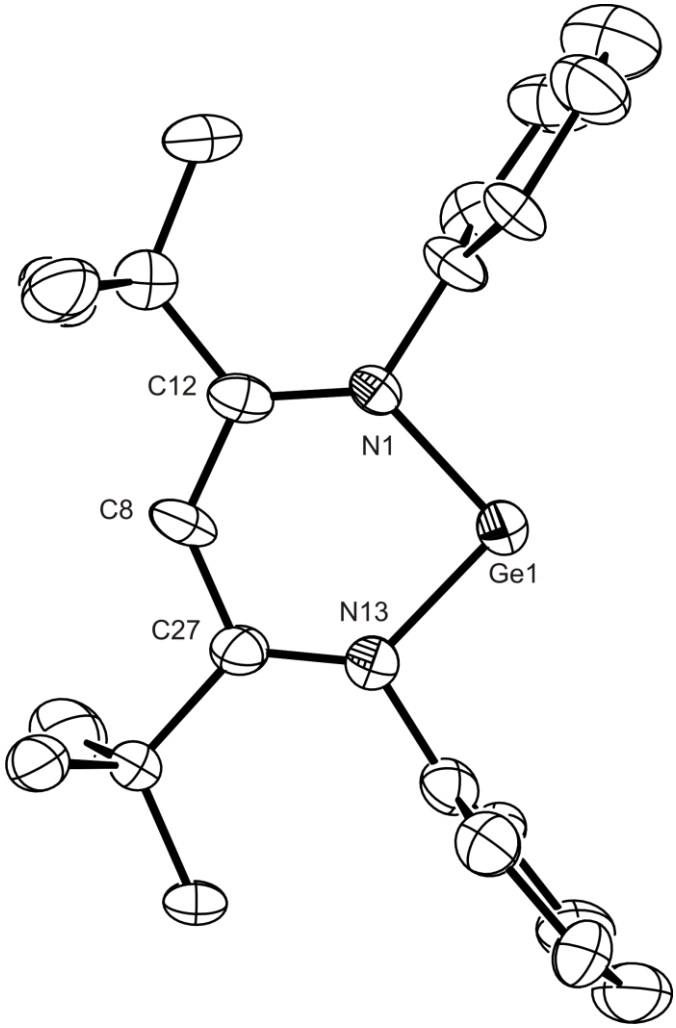

Figure 15. Thermal ellipsoid plot (25% probability surface) of the molecular structure of [(^{But}Nacnac)Ge]$^{+}$ **24** (anion not shown); hydrogen atoms and isopropyl groups are omitted for clarity. Selected bond lengths (Å) and angles (°): Ge(1)-N(1) 1.898(9), Ge(1)-N(13) 1.902(10), N(1)-C(12) 1.337(14), N(13)-C(27) 1.370(15), C(8)-C(27) 1.385(17), C(8)-C(12) 1.443(17), N(1)-Ge(1)-N(13) 93.3(4), C(12)-N(1)-Ge(1) 130.8(8), C(27)-N(13)-Ge(1) 127.1(8), C(12)-C(8)-C(27) 129.4(11), C(8)-C(27)-N(13) 121.4(10), C(8)-C(12)-N(1) 117.9(10).

It was decided to compare the reactivity of complex **10** with that of the less bulky precursor complex, [(^{Mes}Nacnac)GeCl].[76] In an attempt to prepare a germanium hydride species, [(^{Mes}Nacnac)GeCl] was reacted with KEt_3BH in a 1:1 ratio, cleanly affording the thermally stable orange germanium hydride species [(^{Mes}Nacnac)GeH] **25** in moderate yield (Scheme 9). In addition, in an effort to prepare a complex similar to **22**, reduction of the less hindered chlorogermylene, [(^{Mes}Nacnac)GeCl], with [(^{Mes}Nacnac)Mg]$_2$ led to a mixture of β-diketiminate products including a very small amount of crystallographically characterized **26** (Scheme 9) which is closely related to intermediate **19** in the preparation of **14**-**17** (Scheme 6).

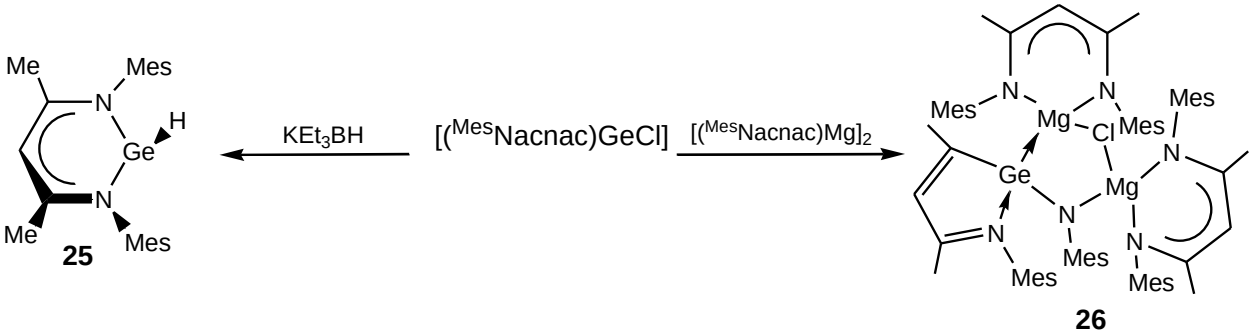

Scheme 9. Synthesis of complexes **25** and **26**.

It is very evident from the spectroscopic data that complex **25** is indeed a germanium hydride species. It exhibits a Ge-H singlet resonance in its ^{1}H NMR spectrum and a Ge-H stretching band in its IR spectrum at δ 8.25 ppm and 1525 *ν*/cm-1 respectively. Complex **25** was also characterized by X-ray crystallography. It was determined that its germanium-nitrogen bond lengths are 1.991(2) Å and 1.977(2) Å. The NC_3N ring bond lengths are very uniform in nature. The N-^{Me}C bond distances are 1.336(3) Å and 1.329(3) Å while the backbone C-C bond lengths are 1.394(4) Å. Complex **26** was also

characterized by X-ray crystallography. The structure of **26** can be thought of as arising from a ring contraction, which is similar to what has been seen by Driess and co-workers.[60] It is thought that the less bulky ligands, ^{Dip}Nacnac and ^{Mes}Nacnac, do not provide enough steric protection for a radical species similar to complex **22** to be stable.

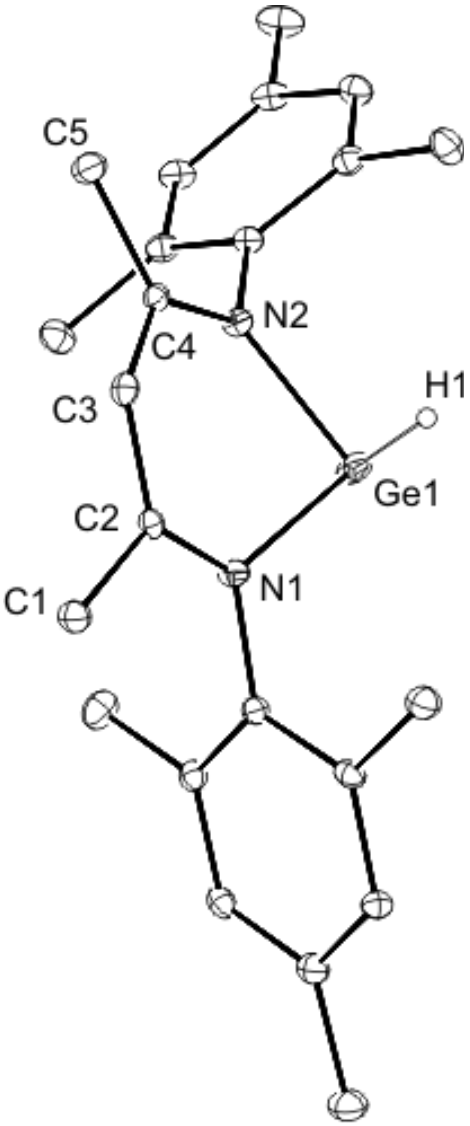

Figure 16. Thermal ellipsoid plot (25% probability surface) of the molecular structure of [(^{Mes}Nacnac)GeH] (**25**); hydrogen atoms are omitted for clarity except for Ge-H. Selected bond lengths (Å) and angles (°): Ge(1)-H(1) 1.569(10), Ge(1)-N(1) 1.991(2), Ge(1)-N(2) 1.977(2), N(1)-C(2) 1.329(3), N(2)-C(4) 1.336(3), C(2)-C(3) 1.394(4), C(3)-C(4) 1.394(4), N(1)-Ge(1)-N(2) 90.70(9), N(1)-Ge(1)-H(1) 91.6(12), N(2)-Ge(1)-H(1) 90.5(13), N(1)-C(2)-C(3) 122.6(2), C(2)-C(3)-C(4) 127.3(3), N(2)-C(4)-C(3) 122.9(2).

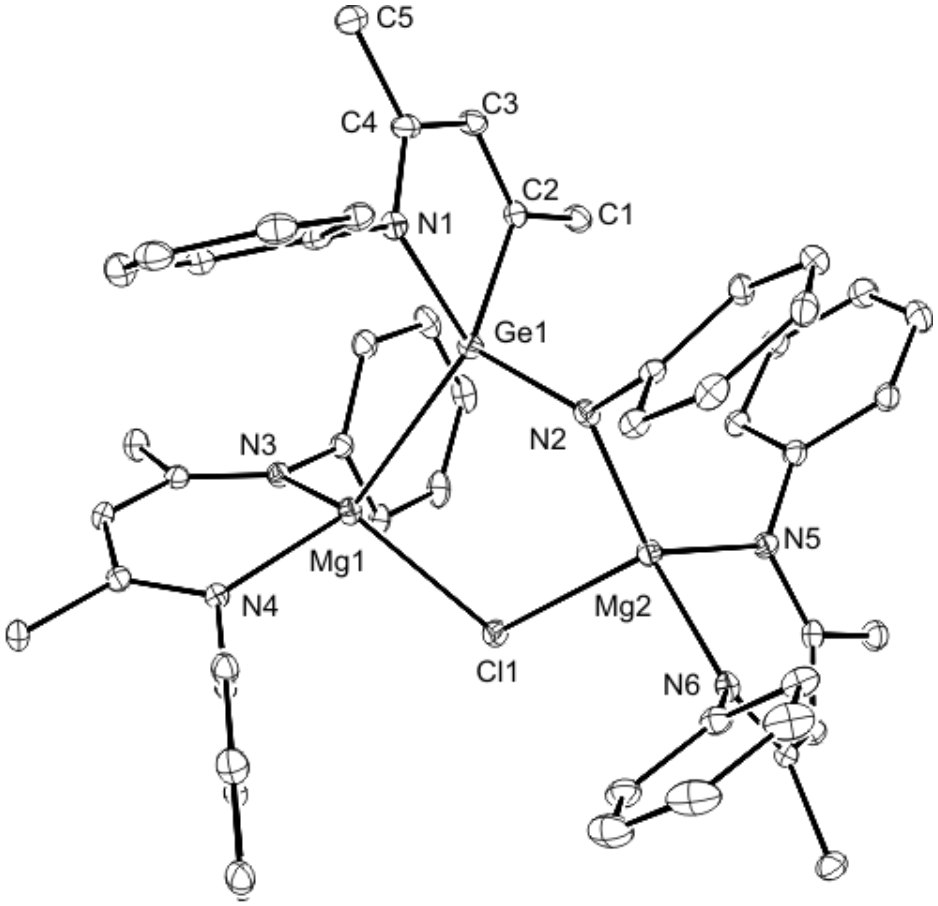

Figure 17. Thermal ellipsoid plot (25% probability surface) of the molecular structure of **26**; hydrogen atoms are omitted for clarity. Selected bond lengths (Å) and angles (°): Ge(1)-N(2) 1.826(3), Ge(1)-C(2) 2.000(4), Ge(1)-N(1) 2.084(3), Ge(1)-Mg(1) 2.7472(14), Cl(1)-Mg(1) 2.3681(15), Cl(1)-Mg(2) 2.4542(15), Mg(1)-N(4) 2.043(3), Mg(1)-N(3) 2.046(3), N(1)-C(4) 1.304(5), N(1)-C(6) 1.448(4), C(1)-C(2) 1.487(5), Mg(2)-N(2) 2.008(3), Mg(2)-N(5) 2.071(3), Mg(2)-N(6) 2.078(3), C(3)-C(4) 1.453(5), C(4)-C(5) 1.495(5), N(2)-Ge(1)-C(2) 112.66(13), N(2)-Ge(1)-N(1) 110.49(12), C(2)-Ge(1)-N(1) 81.54(15), N(2)-Ge(1)-Mg(1) 105.61(10), N(1)-Ge(1)-Mg(1) 119.63(8), Mg(1)-Cl(1)-Mg(2) 107.80(6), N(4)-Mg(1)-N(3) 92.33(12), N(5)-Mg(2)-N(6) 93.11(13), N(2)-Mg(2)-Cl(1) 104.04(9).

In an attempt at preparing the Sn analogue of **22**, complex **12** was reacted with $[(^{Mes}Nacnac)Mg]_2$ in toluene, but this led to the deposition of Sn metal. The same result occured when **12** was reacted with KEt_3BH. Complex **12** was then reacted with AgOTF [OTF = $(CF_3SO_3)^-$] in THF affording $[(^{But}Nacnac)Sn(OTF)]$ **27**, in good yield (Scheme 8). The analogous lead complex, $[(^{But}Nacnac)Pb(OTF)]$ **28**, was thought to be formed from the reaction between $[(^{But}Nacnac)K]$ and $Pb(OTF)_2$, but the complex could not be crystallographically characterized due to the low yield of its formation (< 5%) and the poor quality of its crystals (Scheme 10).

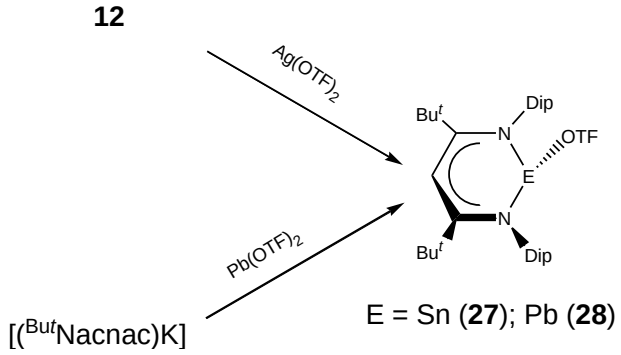

Scheme 10. Synthesis of complexes **27** and **28**.

Complex **27** was crystallographically characterized and found to have a close to planar heterocycle. The tin-nitrogen bond legnths are 2.153(3) Å and 2.138(2) Å, compared to the tin-nitrogen bond lengths of complex **12** which are 2.136(3) Å and 2.223(3) Å. In addition, the N-^{But}C bond distances are 1.344(4) Å and 1.349(4) Å while the backbone C-C bond lengths are 1.406(4) Å and 1.395(4) Å which are all more similar in distances compared to the corresponding bond lengths of complex **12**. Interestingly, the ^{119}Sn NMR spectrum of **27** revealed a resonance at δ -343.5 ppm, whereas the spectrum for **12** showed the Sn resonance at δ -252.0 ppm. Complex **27** was reacted with

[(^{Mes}Nacnac)Mg]$_2$ and KEt$_3$BH, and in both cases the deposition of Sn metal was observed, as was the formation of the enamine decomposition product (Dip)N=C(Bu^t)C(H)=C(H)(Bu^t).

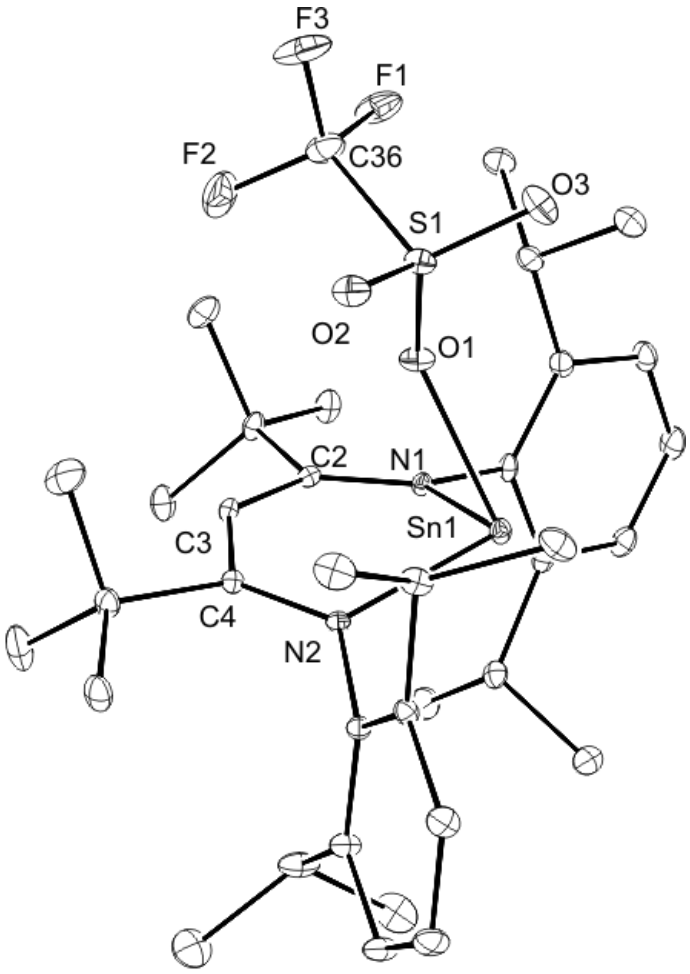

Figure 18. Thermal ellipsoid plot (25% probability surface) of the molecular structure of [(^{But}Nacnac)Sn(OTF)] **27**; hydrogen atoms are omitted for clarity. Selected bond lengths (Å) and angles (°): Sn(1)-N(1) 2.153(3), Sn(1)-N(2) 2.138(2), Sn(1)-O(1) 2.248(2), S(1)-O(1) 1.474(2), S(1)-O(2) 1.421(2), S(1)-O(3) 1.425(2), S(1)-C(36) 1.809(4), N(1)-C(2) 1.344(4), N(2)-C(4) 1.349(4), C(2)-C(3) 1.406(4), C(3)-C(4) 1.395(4), N(1)-Sn(1)-N(2) 89.64(9), N(1)-Sn(1)-O(1) 85.21(9), N(2)-Sn(1)-O(1) 87.61(9), S(1)-O(1)-Sn(1) 144.48(14), N(1)-C(2)-C(3) 121.0(3), C(2)-C(3)-C(4) 134.7(3), N(2)-C(4)-C(3) 121.7(3).

4.4 Conclusion

In summary, germanium(II) and tin(II) heterocyclic complexes incorporating a very bulky β-diketiminate ligand have been prepared and structurally characterized. Reduction of the germanium species with $[(^{Mes}Nacnac)Mg]_2$ or sodium napthalenide has resulted in the first example of a monomeric germanium(I) radical. The X-ray crystallographic, spectroscopic, and EPR data for this, reveal it to be a planar heterocycle with a π-based radical centered on the germanium atom. Attempts at preparing a germanium hydride species from the aforementioned germanium precursor were futile, but they did lead to the isolation of a novel germylene compound. Similar reactions, but involving the less bulky ^{Mes}Nacnac ligand, led to the preparation of a germanium hydride species. In addition, reduction of the germanium(II) and tin(II) heterocyclic complexes with elemental lithium has afforded anionic N-heterocyclic germylidenide and stannylidenide complexes, the latter of which has no precedent in the literature. The X-ray crystallographic and spectroscopic data for these compounds indicate significant aromatic π-delocalization over their heterocycles. Accordingly, the systems can be viewed as group 14 metal(II) cyclopentadienide analogues.

4.5 Experimental

General methods. All manipulations were carried out using standard Schlenk and glove box techniques under an atmosphere of high purity dinitrogen or argon. THF and hexane were distilled over potassium whilst diethyl ether was distilled over Na/K alloy. ^{1}H and $^{13}C\{^{1}H\}$ NMR spectra were recorded on either Bruker DXP300 or DPX400 spectrometers and were referenced to the resonances of the solvent used. $^{7}Li\{^{1}H\}$ and $^{119}Sn\{^{1}H\}$ NMR

spectra were recorded on a Bruker Avance 400 spectrometer and were referenced to external 1M aqueous LiCl and $SnMe_4$ respectively. Mass spectra were obtained from the EPSRC National Mass Spectrometric Service at Swansea University. IR spectra were recorded using a Nicolet 510 FT-IR spectrometer as Nujol mulls between NaCl plates. Microanalyses were carried out by Campbell Microanalytical, Ottago. Melting points were determined in sealed glass capillaries under dinitrogen and are uncorrected. The compounds ^{But}NacnacH[77] and [(^{But}Nacnac)SnCl][63] were prepared by variations of literature procedures. All other reagents were used as received.

Preparation of [(^{But}Nacnac)GeCl] (10): A solution of 1.6M Bu^nLi in hexane (0.63 cm^3, 1.0 mmol) was added to a solution of ^{But}NacnacH (0.50 g, 1.0 mmol) in diethyl ether (15 cm^3) at -80 °C over 5 mins. The solution was warmed to ambient temperature and stirred for 2 hr, after which time it was cooled to -80 °C and a suspension of $GeCl_2$·dioxane (0.23 g, 1.0 mmol) in diethyl ether (15 cm^3) at -80°C was added to it. The reaction mixture was warmed to room temperature and stirred for 2 hr, whereupon volatiles were removed *in vacuo*. The residue was extracted into hexane (40 cm^3), the extract filtered and stored at -30 °C overnight to yield yellow crystals of **10** (0.37g, 61%). M.p. 231-233 °C; ^{1}H NMR (300 MHz, C_6D_6, 298 K): δ 1.05 (d, $^3J_{HH}$ = 6.9 Hz, 6 H, CH(CH_3)$_2$), 1.11 (s, 18 H, C(CH_3)$_3$), 1.17 (d, $^3J_{HH}$ = 6.9 Hz, 6 H, CH(CH_3)$_2$), 1.30 (d, $^3J_{HH}$ = 6.9 Hz, 6 H, CH(CH_3)$_2$), 1.52 (d, $^3J_{HH}$ = 6.9 Hz, 6 H, CH(CH_3)$_2$), 2.97 (sept, $^3J_{HH}$ = 6.9 Hz, 2 H, CH(CH$_3$)$_2$), 4.05 (sept, $^3J_{HH}$ = 6.9 Hz, 2 H, CH(CH$_3$)$_2$), 6.41 (s, 1 H, NCCHCN); ^{13}C NMR (75 MHz, C_6D_6, 298 K): δ 24.3, 24.5, 26.3, 28.3 (CH(*C*H$_3$)$_2$), 28.4, 28.5 (*C*H(CH$_3$)$_2$), 31.9 (C(*C*H$_3$)$_3$), 41.9 (C(*C*H$_3$)$_3$), 105.6 (NC*C*CN), 123.9, 125.1, 127.3, 141.6, 144.5, 146.3 (Ar-*C*), 173.2 (*C*Bu^t); IR ν/cm^{-1} (Nujol): 1548w, 1378s, 1359m, 1312m, 1260m, 1130m, 1098m, 798m, 785m;

MS (EI 70eV), *m*/*z* (%): 610.3 (M^+, 25), 575.3 (M^+-Cl, 15), 244.1 (DipNCCBu^{t}H$^+$, 100); anal. calc. for $C_{35}H_{53}ClGeN_2$: C 68.93 %, H 8.76 %, N 4.59 %; found: C 68.94 %, H 8.63 %, N 4.61 %.

Preparation of [(THF)Li{η^5-GeC(Bu^t)C(H)C(Bu^t)N(Dip)}] (14) and [(Bu^{t}Nacnac)Ge{N(H)(Dip)}] (16): To a slurry of lithium powder (40 mg, 5.7 mmol) in THF (40 cm^3) at -80 °C was added a solution of **10** (0.15 g, 0.25 mmol) in THF (40 cm^3) over 5 min. The mixture was warmed to 20 °C and stirred overnight. All volatiles were subsequently removed *in vacuo* and the residue extracted into hexane (15 cm^3). The extract was filtered and stored at -30 °C overnight to yield yellow crystals of **14** (0.05 g, 83%). The mother liquor was concentrated to *ca.* 7 cm^3 and stored at -30 °C overnight to yield orange crystals of **16** (0.035 g, 37%). Data for **14**: M.p. 137-139 °C; ^{1}H NMR (300 MHz, C_6D_6, 298 K): δ 1.20 (d, $^3J_{HH}$ = 6.9 Hz, 6 H, CH(C*H*$_3$)$_2$), 1.23 (br. m, 4 H, THF-C*H*$_2$), 1.26 (s, 9 H, NCC(C*H*$_3$)$_3$), 1.48 (d, $^3J_{HH}$ = 6.9 Hz, 6 H, CH(C*H*$_3$)$_2$), 1.65 (s, 9 H, GeCC(C*H*$_3$)$_3$), 2.64 (sept., $^3J_{HH}$ = 6.9 Hz, 2 H, C*H*(CH$_3$)$_2$), 3.37 (br. m, 4 H, THF-OC*H*$_2$), 7.08 (s, 1 H, NCC*H*), 7.12-7.34 (m, 3 H, Ar-*H*); ^{13}C{^{1}H} NMR (75 MHz, C_6D_6, 300K): δ 22.6 (CH(*C*H$_3$)$_2$), 23.0 (CH(*C*H$_3$)$_2$), 25.3 (THF-*C*H$_2$), 28.5 (*C*H(CH$_3$)$_2$), 33.2 (NCC(*C*H$_3$)$_3$), 35.1 (GeCC(*C*H$_3$)$_3$), 37.4 (NC*C*(CH$_3$)$_3$), 37.8 (GeC*C*(CH$_3$)$_3$), 68.7 (THF-O*C*H$_2$), 112.5 (NC*C*H), 123.1, 125.8, 132.0, 146.4 (Ar-*C*), 147.5 (N*C*C), 194.7 (Ge*C*C); ^{7}Li{^{1}H} NMR (155.4 MHz, C_6D_6, 300K): δ -5.31; IR *ν*/cm^{-1} (Nujol): 1664w, 1546w, 1466m, 1245s, 1190m, 1135m, 985m, 801m, 758m, 719w; MS (EI 70eV), *m*/*z* (%): 328.3 (DipNC(Bu^t)C(H)C(Bu^t)H$^+$, 10), 270.2 (DipNC(Bu^t)C(H)CH$^+$, 100); anal. calc. for $C_{27}H_{44}GeLiNO$: C 67.82 %, H 9.27 %, N 2.93 %; found: C 67.61 %, H 9.01 %, N 2.86 %. Data for **16**: M.p. 155-160 °C (decomp.); ^{1}H NMR (300 MHz, C_6D_6, 298 K): δ 1.01, 1.13,

1.20, 1.22, 1.23, 1.33 (6 x d, $^{3}J_{HH}$ = 6.9 Hz, 36 H, CH(CH_3)$_2$), 1.13 (s, 18 H, C(CH_3)$_3$), 2.83 (sept, $^{3}J_{HH}$ = 6.9 Hz, 1 H, CH(CH$_3$)$_2$), 3.18 (sept, $^{3}J_{HH}$ = 6.9 Hz, 2 H, CH(CH$_3$)$_2$), 3.24 (sept, $^{3}J_{HH}$ = 6.9 Hz, 2 H, CH(CH$_3$)$_2$), 3.24 (sept, $^{3}J_{HH}$ = 6.9 Hz, 1 H, CH(CH$_3$)$_2$), 4.85 (s, 1 H, NH), 6.15 (s, 1 H, NCCHCN), 6.86-7.13 (m, 9 H, Ar-H); ^{13}C{^{1}H} NMR (75 MHz, C_6D_6, 300K): δ 23.1, 23.9, 25.2, 26.6, 26.8, 27.4 (6 x CH(CH_3)$_2$), 28.6, 28.7, 28.8, 29.1 (4 x CH(CH$_3$)$_2$), 32.3 (C(CH_3)$_3$), 42.5 (C(CH$_3$)$_3$), 101.3 (NCCCN), 117.8, 121.8, 124.1, 124.7, 125.6, 126.8, 135.2, 137.5, 143.4, 144.1, 145.7, 146.0 (Ar-C), 174.1 (C Bu^{t}); IR ν/cm^{-1} (Nujol): 1547m, 1489m, 1388m, 1362m, 1260s, 1155m, 1129m, 800m, 782m, 750m; MS (EI 70eV), m/z (%): 751.5 (M^{+}, 3), 575.3 (M^{+}-DipNH, 100); anal. calc. for $C_{47}H_{71}GeN_3$: C 75.20 %, H 9.53 %, N 5.60 %; found: C 74.89 %, H 9.32 %, N 5.41 %.

N.B. The quoted yields of **14** and **16** assume the mechanism proposed for their formation (see Scheme 6) is in operation.

Preparation of [(THF)Li{η^5-SnC(Bu^t)C(H)C(Bu^t)N(Dip)}] (15): To a slurry of lithium powder (40 mg, 5.7 mmol) in THF (30 cm^3) at -80 °C was added a solution of **12** (0.15 g, 0.23 mmol) in THF (30 cm^3) over 5 min. The mixture was warmed to 0 °C and stirred for 6 hrs yielding a deep red solution. All volatiles were subsequently removed *in vacuo* and the deep green residue extracted into hexane (15 cm^3). The extract was filtered and stored at -30 °C overnight to yield deep green crystals of **15** (0.04 g, 52%). M.p. 137-139 °C; ^{1}H NMR (300 MHz, C_6D_6, 298 K): δ1.25 (d, $^{3}J_{HH}$ = 6.9 Hz, 6 H, CH(CH_3)$_2$), 1.23 (br. m, 4 H, THF-CH_2), 1.27 (s, 9 H, NCC(CH_3)$_3$), 1.46 (d, $^{3}J_{HH}$ = 6.9 Hz, 6 H, CH(CH_3)$_2$), 1.58 (s, 9 H, SnCC(CH_3)$_3$), 2.77 (sept., $^{3}J_{HH}$ = 6.9 Hz, 2 H, CH(CH$_3$)$_2$), 3.40 (br. m, 4 H, THF-OCH_2), 7.16-7.33 (m, 3 H, Ar-H), 7.78 (s, 1 H, NCCH),; ^{13}C{^{1}H} NMR (75 MHz, C_6D_6, 300K): δ 23.0 (CH(CH_3)$_2$), 23.4 (CH(CH_3)$_2$), 25.2 (THF-CH_2), 28.6 (CH(CH$_3$)$_2$), 33.4 (NCC(CH_3)$_3$),

35.1 (SnCC(CH_3)$_3$), 39.6 (NCC(CH_3)$_3$), 40.2 (SnCC(CH_3)$_3$), 67.9 (THF-OCH_2), 116.6 (NCCH), 122.7, 124.7, 131.6, 147.7 (Ar-C), 156.6 (NCC), 226.9 (SnCC); ^{7}Li{^{1}H} NMR (155.4 MHz, C_6D_6, 300K): δ -4.66; ^{119}Sn{^{1}H} NMR (149.1 MHz, C_6D_6, 300K): δ 524.2 (p.w. at 1/2 height = 44 Hz); IR ν/cm^{-1} (Nujol): 1663w, 1546w, 1464m, 1245s, 1191m, 1136m, 985m, 804m, 757m; MS (EI 70eV), *m*/*z* (%): 328.3 (DipNC(Bu^{t})C(H)C(Bu^{t})H^{+}, 20), 178.1 (DipNH$_2^{+}$, 100).

N.B. The quoted yield of **15** assumes the mechanism proposed for its formation (see Scheme 6) is in operation.

Synthesis of [(^But^Nacnac)Ge·] (22): Method A: To a solution of [(^But^Nacnac)GeCl] (0.15g, 0.25mmol) in toluene (25 cm^3) at -80°C was added [(^Mes^Nacnac)Mg]$_2$ (0.09g, 0.12mmol) in toluene (25 cm^3). The mixture was stirred and slowly warmed to room temperature overnight. All volatiles were subsequently removed *in vacuo*. The residue was extracted into n-hexane (25 cm^3), the extract filtered and stored at -30°C overnight to yield red/purple crystals. Yield: (0.05g, 38%). M.p. 178-180°C; IR *v*/cm–1 (Nujol): 1619 w, 1547w, 1377s, 1261m, 1097m, 1020m, 799m; UV-vis (toluene): λ_{max}, (ε, L mol^{-1} cm^{-1}): 500nm (480, sh); MS (EI 70eV), *m*/*z* (%): 162.3 (Dip^{+}, 10), 270.4 (DipNC(Bu^{t})C(H)CH^{+}, 100), 517 (M^{+}-Pr^{i}-Me, 6) 575.3 (M^{+} ^{70}Ge, 22); anal. calc. for $C_{35}H_{53}GeN_2$: C 73.18%, H 9.30%, N 4.88%; found: C 72.47%, H 9.23%, N 4.69%.

Method B: To a solution of [(^But^Nacnac)GeCl] (0.15g, 0.25 mmol) in THF (25 cm^3) at -80°C was added sodium napthalenide (0.032g, 0.25 mmol) in THF (25 cm^3). The mixture was stirred and slowly warmed to 0°C over 8 hours. All volatiles were subsequently

removed *in vacuo*. The residue was extracted into n-hexane (25 cm^3), the extract filtered and stored at -30°C overnight to yield red/purple crystals. Yield: (0.05g, 36%).

Synthesis of [H(^But^Nacnac)Ge:] (23): To a solution of [(^But^Nacnac)GeCl] (0.15g, 0.25 mmol) in toluene (20 cm^3) at -80 °C was added a solution of 1.0M KEt_3BH (0.25 cm^3, 0.25mmol). The mixture was stirred and slowly warmed to room temperature overnight. All volatiles were subsequently removed *in vacuo*. The residue was extracted into hexane (25 cm^3), the extract filtered and stored at -30 °C overnight to yield yellow crystals. Yield: 0.02g (22 %). M.p. 122-124°C; ^{1}H NMR (300 MHz, C_6D_6, 298 K): δ 1.05 (s, 9H, C(CH_3)$_3$), 1.09 (s, 9H, C(CH_3)$_3$), 1.11 (d, $^3J_{HH}$ = 6.9 Hz, 3H, CH(CH_3)$_2$), 1.20 (d, $^3J_{HH}$ = 6.9 Hz, 3H, CH(CH_3)$_2$), 1.22 (d, $^3J_{HH}$ = 6.9 Hz, 3H, CH(CH_3)$_2$), 1.24 (d, $^3J_{HH}$ = 6.9 Hz, 3H, CH(CH_3)$_2$), 1.29 (d, $^3J_{HH}$ = 6.9 Hz, 3H, CH(CH_3)$_2$), 1.33 (d, $^3J_{HH}$ = 6.9 Hz, 3H, CH(CH_3)$_2$), 1.36 (d, $^3J_{HH}$ = 6.9 Hz, 3H, CH(CH_3)$_2$), 1.44 (d, $^3J_{HH}$ = 6.9 Hz, 3H, CH(CH_3)$_2$), 3.43 (sept., $^3J_{HH}$ = 6.9 Hz, 1H, CH(CH$_3$)$_2$), 3.71 (sept., $^3J_{HH}$ = 6.9 Hz, 1H, CH(CH$_3$)$_2$), 3.93 (sept., $^3J_{HH}$ = 6.9 Hz, 1H, CH(CH$_3$)$_2$), 3.96 (sept., $^3J_{HH}$ = 6.9 Hz, 1H, CH(CH$_3$)$_2$), 3.99 (d, $^3J_{HH}$ = 6.9 Hz, 1H), 4.90 (d, $^3J_{HH}$ = 6.9 Hz, 1H), 6.80-7.22 (mult., 6H, ArH); δ ^{13}C NMR (300MHz, C_6D_6, 300K), 20.1 C(CH$_3$)$_3$, 20.8 C(CH$_3$)$_3$, 21.0 CH(CH$_3$)$_2$, 21.4 CH(CH$_3$)$_2$, 21.8 CH(CH$_3$)$_2$, 22.0 CH(CH$_3$)$_2$, 22.3 CH(CH$_3$)$_2$, 22.8 CH(CH$_3$)$_2$, 23.1 CH(CH$_3$)$_2$, 23.7 CH(CH$_3$)$_2$, 24.1 CH(CH$_3$)$_2$, 25.8 CH(CH$_3$)$_2$, 27.0 CH(CH$_3$)$_2$, 27.1 CH(CH$_3$)$_2$, 39.0 (NCCMe$_3$), 39.6 (NCCMe$_3$), 74.8 (NCHCHCN), 101.9 (NCCHCN), 123.5 (Ar-C), 124.2 (Ar-C), 124.4 (Ar-C), 124.9 (Ar-C), 125.7 (Ar-C), 127.2 (Ar-C), 143.0 (Ar-C), 144.6 (Ar-C), 146.8 (Ar-C), 147.3 (Ar-C), 149.1 (Ar-C), 149.8 (Ar-C),; IR ν/cm–1 (Nujol): 1601w, 1388s, 1365s, 1260w, 1230s, 950w, 923w, 795w, 755m, 698s; MS (EI 70eV), m/z (%): 270.4 (DipNC(Bu^t)C(H)CH$^+$, 100), 519.3 (M$^+$-Pr^i-Me, 60), 575.3 (M$^+$, 1).

Synthesis of [(^{But}Nacnac)Ge]$^+$ [Al{OC(CF$_3$)$_3$}$_4$]$^-$ (24): To a solution of [(^{But}Nacnac)GeCl] (0.10g, 0.16mmol) in THF (15 cm^3) at -80 °C was added Ag[Al{OC(CF$_3$)$_3$}$_4$] (0.17, 0.16mmol) in THF (15 cm^3). The mixture was stirred and slowly warmed to room temperature overnight. All volatiles were subsequently removed *in vacuo*. The residue was extracted into diflurobenzene (5 cm^3), the extract filtered, concentrated to < 1 cm^3 and layered with hexane. After 4 days light yellow crystals of **24** deposited. Yield: 0.08g (32%); M.p. decomp. 168-170°C; ^{1}H NMR (400 MHz, C$_6$D$_6$, 298 K): δ 0.67 (d, 6 H, CH(C*H*$_3$)$_2$), 0.73 (s, 18 H, C(C*H*$_3$)$_3$), 0.98 (d, 6 H, CH(C*H*$_3$)$_2$), 1.14 (d, 6 H, CH(C*H*$_3$)$_2$), 2.27 (sept, 2 H, C*H*(CH$_3$)$_2$); ^{19}F NMR (376 MHz, C$_6$D$_6$, 298 K): δ -74.8; IR ν/cm^{-1} (Nujol): 1601m, 1365s, 1229s, 1056w, 974s, 830m, 786m, 756s, 728s, 699s; MS (EI 70eV), *m*/*z* (%): 244.1 (DipNCCBu^{t}H$^+$, 100), 575.4 (M$^+$ ^{70}Ge, 50). Due to the low solubility of the complex, complete NMR data could not be obtained.

Synthesis of [(^{Mes}Nacnac)GeH] (25): To a solution of [(^{Mes}Nacnac)GeCl] (0.20g, 0.45 mmol) in toluene (20 cm^3) at -80 °C was added a solution of 1M KEt$_3$BH (0.45 cm^3, 0.45 mmol). The mixture was stirred and slowly warmed to room temperature overnight. All volatiles were subsequently removed *in vacuo*. The residue was extracted into hexane (30 cm^3), the extract filtered and stored at -30 °C overnight to yield orange crystals. Yield: 0.12g (65%); M.p. decomp 160-162°C; ^{1}H NMR (300 MHz, C$_6$D$_6$, 298 K): 1.52 (s, 6H, NCC*H*$_3$), 2.09 (s, 6H, *o*-C*H*$_3$), 2.29 (s, 6H, *p*-C*H*$_3$), 2.31 (s, 6H, *o*-C*H*$_3$), 4.92 (s, 1H, NCC*H*CN), 6.80-7.12 (mult., 6H, Ar*H*), 8.25 (s, 1H, Ge*H*); ^{13}C NMR (300 MHz, C$_6$D$_6$, 300K), 18.3 (*o*-CH3), 18.6 (*o*-CH$_3$), 20.7 (*p*-CH$_3$), 22.0 (NC*C*H$_3$), 97.5 (NC*C*HCN), 129.3 (Ar-*C*), 129.7 (Ar-*C*), 132.7 (Ar-*C*), 134.9 (Ar-*C*), 135.2 (Ar-*C*), 142.0 (Ar-*C*), 166.3

(N*C*CH); IR *v*/cm–1 (Nujol): 1722m, 1525s, 1376s, 1261w, 1229w, 1198w,1147m, 1015m, 859m, 706m, 567m; MS (EI 70eV), *m*/*z* (%): 407.2 (M-H^+, 100)

Synthesis of [(^{But}Nacnac)Sn(CF_3SO_3)] (27): To a solution of [(^{But}Nacnac)SnCl] (0.39g, 0.60mmol) in (15 cm^3) at -80 °C was added [Ag(CF_3SO_3)] (0.24, 0.60mmol) in (15 cm^3). The mixture was stirred and slowly warmed to room temperature overnight. All volatiles were subsequently removed *in vacuo*. The residue was extracted into hexane (30 cm^3), the extract filtered and stored at -30 °C overnight to yield yellow crystals. Yield: 0.21g (46%); M.p. 188-190°C; ^{1}H NMR (400 MHz, C_6D_6, 298 K): δ 1.11 (s, 18H, C(C*H*$_3$)$_3$), 1.28 (d, $^3J_{HH}$ = 6.9 Hz, 12 H, CH(C*H*$_3$)$_2$), 1.38 (d, $^3J_{HH}$ = 6.9 Hz, 12 H, CH(C*H*$_3$)$_2$), 3.91 (b, 2H, C*H*(CH$_3$)$_2$), 6.10 (s, 1H, NCC*H*CN), 6.80-7.12 (mult., 6H, Ar*H*); ^{119}Sn{^{1}H} NMR (149.1 MHz, C_6D_6, 300K): δ -343.5; IR *v*/cm–1 (Nujol): 1537w, 1376m, 1261s, 1097s, 802s, 689w, 632m; MS (EI 70eV), *m*/*z* (%): 244.1 (DipNCCBu^{t}H$^+$, 100).

Synthesis of [(^{But}Nacnac)Pb(CF_3SO_3)] (28): To a solution of Pb(CF_3SO_3)$_2$ (0.19g, 0.37mmol) in THF (15 cm^3) at -80 °C was added [(^{But}Nacnac)K] (0.20, 0.37mmol) in THF (15 cm^3). The mixture was stirred and slowly warmed to room temperature overnight. All volatiles were subsequently removed *in vacuo*. The residue was extracted into pentane (30 cm^3), the extract filtered and stored at -30 °C overnight to yield light yellow crystals. Yield: 0.014g (4.4%); M.p. decomp 220-222°C; ^{1}H NMR (400 MHz, C_6D_6, 298 K): δ 1.12 (s, 18H, C(C*H*$_3$)$_3$), 1.22 (d, $^3J_{HH}$ = 6.9 Hz, 12 H, CH(C*H*$_3$)$_2$), 1.31 (d, $^3J_{HH}$ = 6.9 Hz, 12 H, CH(C*H*$_3$)$_2$), 3.34 (mult, 4 H, C*H*(CH$_3$)$_2$), 5.64 (s, 1 H, NCC*H*CN), 6.80-7.12 (mult., 6H, Ar*H*); ^{13}C NMR (75 MHz, C_6D_6, 298 K): δ 22.7, 26.3, (CH(*C*H$_3$)$_2$), 27.6 (*C*H(CH$_3$)$_2$), 31.1 (C(*C*H$_3$)$_3$), 44.1 (C(*C*H$_3$)$_3$), 94.0 (NC*C*CN), 110.1, 121.7, 123.4, 125.7, 140.7, 142.3 (Ar-*C*), 172.5 (*C*Bu^t); ^{19}F NMR (376 MHz, C_6D_6, 298 K): δ -76.9; IR *ν*/cm^{-1} (Nujol): 1626m,

1377m, 1261m, 1108m, 1022m, 802m, 762w; MS (EI 70eV), *m*/*z* (%): 244.1 (DipNCCBu^{t}H^{+}, 100).

4.6 References

1. Power, P.P. *Chem. Rev*., **2003**, *103*, 789.

2. Fremy, E. *Ann. Chim. Phys.*, **1845**, *15*, 459.

3. (a) Würster, C.; Sendtner, R. *Ber. Dtsch. Chem. Ges.*, **1879**, *12*, 1803. (b) Würster, C.; Scholig, E. *Ber. Dtsch. Chem. Ges.*, **1879**, *12*, 1807.

4. Beckmann, E.; Paul, T. *Ann. Chem.*, **1891**, *266*, 1.

5. Gomberg, M. *J. Am. Chem. Soc.*, **1900**, *22*, 757; *Ber. Dtsch. Chem. Ges.*, **1900**, *33*, 3150.

6. Ruchardt, C. *Top Curr. Chem.*, **1980**, *88*, 1.

7. *S-centered Radicals*; Alfassi, Z.B., Ed.; Wiley: New York, **1999**.

8. Glass, R.S. *Top. Curr. Chem.*, **1999**, *205*, 1.

9. Preston, K.F.; Sutcliffe, L.H. *Magn. Reson. Chem.*, **1990**, *28*, 189.

10. Cordes, A.W.; Haddon, R.C.; Oakley, R.T. In *Chemistry of Inorganic Ring Systems*; Steudel, R., Ed.; Elsevier: Amsterdam, **1992**.

11. Lappert, M.F.; Lednor, P.W. *Adv. Organomet. Chem.*, **1976**, *14*, 345.

12. Leffler, J.E.; Watts, G.B.; Tanigaki, T.; Dolan, E.; Miller, D.S. *J. Am. Chem. Soc.*, **1970**, *92*, 6825.

13. Griffin, R.G.; van Willigen, H. *J. Chem. Phys.*, **1972**, *57*, 86.

14. Kwan, R.J.; Harlan, J.; Norton, J.R. *Organometallics*, **2001**, *20*, 3818.

15. (a) Pluta, C.; Porschke, K.-R.; Kruger, C.; Hildebrand, K. *Angew. Chem. Int. Ed. Engl.*, **1993**, *32*, 388. (b) He, X.; Bartlett, R.A.; Olmstead, M.M.; Ruhlandt-Senge, K.; Sturgeon, B.E.; Power, P.P. *Angew. Chem., Int. Ed. Engl.*, **1993**, *32*, 717. (c) Uhl, W.; Vester, A.; Kaim, W.; Poppe, J. *J. Organomet. Chem.*, **1993**, *454*, 9.

16. (a) Schnöckel, H.; Schnepf, A. *Adv. Organomet. Chem.*, **2001**, *47*, 235. (b) Schnöckel, H.; Schnepf, A. *Angew. Chem., Int. Ed.*, **2002**, *41*, 3532.

17. Schnöckel, H.; Köhnlein, H. *Polyhedron*, **2002**, *21*, 489.

18. Ecker, A.; Weckert, E.; Schnöckel, H. *Nature*, **1997**, *387*, 379.

19. Purath, A.; Köppe, R.; Schnöckel, H. *Chem. Commun.*, **1999**, 1933.

20. Wiberg, N.; Amelunxen, K.; Nöth, H.; Kaim, W.; Klein, A.; Scheiring, T. *Angew. Chem., Int. Ed. Engl.*, **1997**, *36*, 1213.

21. Wiberg, N.; Blank, T.; Kaim, W.; Schwerderski, B.; Linti, G. *Eur. J. Chem.*, **2000**, 1475.

22. Wiberg, N.; Blank, T.; Amelunxen, K.; Nöth, H.; Knizek, J.; Habereden, T.; Kaim, W.; Wanner, M. *Eur. J. Inorg. Chem.*, **2001**, 1719.

23. *Free Radicals*; Kochi, J. K., Ed.; Wiley: New York, **1973**.

24. Walling, C.; Pearson, M.S. *Top. Phosphorus Chem.*, **1966**, *3*, 1.

25. Schmidt, U.; Kabitzke, K.; Markau, K.; Müller, A. *Chem. Ber.*, **1966**, *99*, 1497.

26. Roberts, B.P. *Adv. Free Radical Chem.*, **1980**, *6*, 225.

27. Tordo, P. In *The Chemistry of Organophosphorus Compounds*; Hartley, F.R., Ed.; Wiley: Chichester, **1990**; Vol. 1, Chapter 6.

28. Geoffroy, M. *Recent Res. Dev. Phys. Chem.*, **1998**, *2*, 311.

29. Geoffroy, M.; Berclaz, T. In *The Chemistry of Organic Arsenic Antimony and Bismuth Compounds*; Patai, S., Ed.; Wiley: Chichester, **1994**; Chapter 12.

30. Hinchley, S.L.; Morrison, C.A.; Rankin, D.W.H.; Macdonald, C.L.; Wiacek, R.J.; Cowley, A.H.; Lappert, M.F.; Gundersen, G.; Clyburne, J.A.C.; Power, P.P. *Chem. Commun.*, **2000**, 2045.

31. Hinchley, S.L.; Morrison, C.A.; Rankin, D.W.H.; Macdonald, C.L.B.; Wiacek, R.J.; Voigt, A.H.; Cowley, A.H.; Lappert, M.F.; Gundersen, G.; Clyburne, J.A.C.; Power, P.P. *J. Am. Chem. Soc.*, **2001**, *123*, 9045.

32. Richard, M.J.; Koukay, N.; Faver, A. *Med. Nutr.*, **1987**, *23*, 291.

33. Jackson, M.J.; Edwards, R.H.T. *Curr. Top. Nutr. Dis.*, **1988**, *18*, 431.

34. Burk, R.F. *Pharmacol. Ther.*, **1990**, *45*, 383.

35. Renaud, D. *Top. Curr. Chem.*, **2000**, *208*, 81.

36. see for example: Chiu, M. F.; Gilbert, B. C. *J. Chem. Soc., Perkin Trans.*, **1973**, *2*, 258.

37. see for example: Awere, E. G.; Passmore, J.; White, P. S.; Klapötke, T. *Chem. Commun.*, **1989**, 1415.

38. Wolmershäuser, G.; Heckmann, G. *Angew. Chem., Int. Ed. Engl.*, **1992**, *31*, 779.

39. Awere, E.G.; Passmore, J.; White, P.S. *Dalton Trans.*, **1993**, 299.

40. Björgvinsson, M.; Heinze, T.; Roesky, H.W.; Pauer, F.; Stalke, D.; Sheldrick, G.M. *Angew. Chem., Int. Ed. Engl.*, **1991**, *30*, 1677.

41. Lee, V.Ya.; Sekiguchi, A. *Acc. Chem. Res.*, **2007**, *40*, 410.

42. Olmstead, M.M.; Pu, L.; Simons, R.S.; Power, P.P. *Chem. Commun.*, **1997**, 1595.

43. Sekiguchi, A.; Matsuno, T.; Ichinohe, M. *J. Am. Chem. Soc.*, **2001**, *123*, 12436.

44. Ishida, Y.; Sekiguchi, A.; Kobayashi, K.; Nagase, S. *Organometallics*, **2004**, *23*, 4891.

45. Sekiguchi, A.; Fukawa, T.; Nakamoto, M.; Lee, V. Ya.; Ichinohe, M. *J. Am. Chem. Soc.*, **2002**, *124*, 9865.

46. Sekiguchi, A.; Inoue, S.; Ichinohe, M. ; Arai, Y. *J. Am. Chem. Soc.*, **2004**, *126*, 9626.

47. *Metallocenes. Synthesis, Reactivity, Applications*; Togni, A., Halterman, R., Eds.; VCH; Weinheim, Germany **1998**; Vols. 1 and 2.

48. For reviews see (a) Lee, V.Y.; Sekiguchi, A. *Angew. Chem. Int. Ed.*, **2007**, *46*, 6596. (b) Saito, M.; Yoshioka, M. *Coord. Chem. Rev.*, **2005**, *249*, 765. (c) Dubac, J.; Guérin, C.; Meunier, P. in *The Chemistry of Organosilicon Compounds*;

Rappoport, Z., Apeloig, Y., Eds.; Wiley-Interscience: Chichester **1998**; Vol. 2, Part 3, p 1961.

49. (a) Hong, J.-H.; Boudjouk, P.; Castelino, S. *Organometallics*, **1994**, *13*, 3387. (b) West, R.; Sohn, U.; Bankwitz, J.; Calabrase, J.; Apeloig, Y.; Mueller, T. *J. Am. Chem. Soc.* **1995**, *117*, 11608.

50. (a) Hong, J.-H.; Boudjouk, P. *Bull. Soc. Chim. Fr.*, **1995**, *132*, 495. (b) West, R.; Sohn, U.; Powell, D.R.; Mueller, T.; Apeloig, Y. *Angew. Chem. Int. Ed. Engl.*, **1996**, *35*, 1002.

51. (a) Freeman, W.P.; Dysard, J.M.; Tilley, T.D.; Rheingold, A.L. *Organometallics*, **2002**, *21*, 1734. (b) Dysard, J.M.; Tilley, T.D. *J. Am. Chem. Soc.*, **2000**, *122*, 3097. (c) Dysard, J.M.; Tilley, T.D. *J. Am. Chem. Soc.*, **1998**, *120*, 8245. (d) Freeman, W.P.; Tilley, T.D.; Rheingold, A.L. *J. Am. Chem. Soc.*, **1994**, *116*, 8428. (e) Freeman, W.P.; Tilley, T.D.; Rheingold, A.L.; Ostrander, R.L. *Angew. Chem. Int. Ed.*, **1993**, *32*, 1744.

52. Saito, M.; Haga, R.; Yoshioka, M.; Ishimura, K.; Nagase, S. *Angew. Chem. Int. Ed.*, **2005**, *44*, 6533.

53. The solution spectroscopic characterization and reactivity of several aromatic stannole dianions has also been reported. See for example (a) Saito, M.; Haga, R.;

Yoshioka, M. *Chem. Commun.*, **2002**, 1002. (b) Saito, M.; Haga, R.; Yoshioka, M. *Chem. Lett.*, **2003**, *32*, 912. (c) Haga, R.; Saito, M.; Yoshioka, M. *J. Am. Chem. Soc.*, **2006**, *128*, 4934. (d) Saito, M.; Shomosawa, M.; Yoshioka, M.; Ishimura, K.; Nagase, S. *Organometallics*, **2006**, *25*, 2967. (e) Saito, M.; Shomosawa, M.; Yoshioka, M.; Ishimura, K.; Nagase, S. *Chem. Lett.*, **2006**, *35*, 940.

54. Saito, M.; Sakaguchi, M.; Tajima, T.; Ishimura, K.; Nagase, S.; Hada, M. *Science*, **2010**, *328*, 339.

55. Wang, W.; Yao, S.; von Wüllen, C.; Driess, M. *J. Am. Chem. Soc.*, **2008**, *130*, 9640. N.B. Two related hetero-aromatic six-membered germanium(II) heterocycles derived from [(^{Dip}Nacnac)GeCl] have also been reported. (a) Stender, M.; Phillips, A.D.; Power, P.P. *Inorg. Chem*., **2001**, *40*, 5314. (b) Yao, S.; Zhang, X.; Xiong, Y.; Schwarz, H.; Driess, M. *Organometallics*, **2010**, *29*, 5353.

56. Ding, Y.; Roesky, H.W.; Noltemeyer, M.; Schmidt, H.-G.; Power, P.P. *Organometallics*, **2001**, *20*, 1190.

57. Green, S.P.; Jones, C.; Junk, P.C.; Lippert, K.-A.; Stasch, A. *Chem. Commun.*, **2006**, 3978.

58. Several related 1,2-digermylene compounds bearing unsupported Ge-Ge bonds have since been reported. (a) Wang, W.; Inoue, S.; Yao, S.; Driess, M. *Chem.*

Commun., **2009**, 2661. (b) Nagendran, S.; Sen, S.S.; Roesky, H.W.; Koley, D.; Grubmuller, H.; Pal, A.; Herbst-Irmer R. *Organometallics,* **2008**, *27*, 5459. (c) Leung, W.-P.; Chiu, W.-K.; Chong, K.-H.; Mak, C.W. *Chem. Commun.,* **2009**, 6822.

59. Power, P.P. *Organometallics*, **2007**, *26*, 4362.

60. Driess, M.; Yao, S.; Brym, M.; vanWuellen, C. *Angew. Chem. Int. Ed.*, **2006**, *45*, 4349.

61. Green, S.P.; Jones, C.; Stasch, A. *Science*, **2007**, *318*, 1754.

62. (a) Bonyhady, S.J.; Jones, C.; Nembenna, S.; Stasch, A.; Edwards, A.J.; McIntyre, G.J. *Chem. Eur. J.,* **2010**, *16,* 938. (b) Holland, P.L. *Acc. Chem. Res.,* **2008**, *41*, 905.

63. Dove, A.P.; Gibson, V.C.; Marshall, E.L.; Rzepa, H.S.; White, A.J.P.; Williams, D.J. *J. Am. Chem. Soc.,* **2006**, *128,* 9834.

64. Chen, M.; Fulton, J.R.; Hitchcock, P.B.; Johnstone, N.C.; Lappert, M.F.; Protchenko A.V. *Dalton Trans.,* **2007**, 2770.

65. Driess, M.; Yao, S.; Brym, M.; von Wüllen, C.; Lentz, D. *J. Am. Chem. Soc.,* **2006**, *128*, 9628.

66. Basuli, F.; Huffman, J.C.; Mindiola, D.J. *Inorg. Chim. Acta*, **2007**, *360*, 246.

67. Basuli, F.; Kilgore, U.J.; Brown, D.; Huffman, J.C.; Mindiola D.J. *Organometallics*, **2004**, *23*, 6166.

68. Conroy, K.D.; Piers, W.E.; Parvez, M. *Organometallics,* **2009**, *28*, 6228.

69. Ferman, J.; Kakareka, J.P.; Klooster, W.T.; Mullin, J.L.; Quattrucci, J.; Ricci, J.S.; Tracy, H.J.; Vining, W.J.; Wallace S. *Inorg. Chem.,* **1999**, *38*, 2464.

70. As determined from a survey of the Cambridge Crystallographic Database, June, 2010.

71. Guzei, I.A.; Timokhin, V.I.; West, R. *Acta Cryst., Sect. C* **2006**, *62*, m90.

72. (a) Sekiguchi, A.; Sugai, Y.; Ebata, K.; Kabuto, C.; Sakurai, H. *J. Am. Chem. Soc.*, **1993**, *115*, 1144. (b) Paquette, L.A.; Bauer, W.; Sivik, M.R.; Bühl, M.; Feigel, M.; Schleyer, P.v.R. *J. Am. Chem. Soc.*, **1990**, *112*, 8776.

73. Gans-Eichler, T.; Gudat, D.; Nieger, M. *Angew. Chem. Int. Ed.*, **2002**, *41*, 1888.

74. (a) Lappert, M.F.; Power, P.P.; Protchenko, A.V.; Seeber, A.L. *Metal Amide Chemistry*; Wiley-VCH: Weinheim, **2009**; Chap. 9. (b) Wrackmeyer, B. in *Tin Chemistry: Fundamentals, Frontiers and Applications*; Davies, A.G., Gielen, M., Pannell, K., Tiekink, E., Eds.; Wiley: Chichester, **2008**.

75. Pineda, L.W.; Jancik, V.; Starke, K.; Oswald, R.B.; Roesky, H.W. *Angew. Chem. Int. Ed.*, **2006**, *45*, 2602.

76. Ayers, A.E., Klapoetke, T.M.; Dias, H.V.R. *Inorg. Chem.*, **2001**, *40*, 1000.

77. Budzelaar, P.H.M.; van Oort, A.B.; Orpen, A.G. *Eur. J. Inorg. Chem.*, **1998**, 1485.

Chapter 5

Miscellaneous *p*-Block Element Guanidinate Chemistry

5.1 Introduction

The core area of research being undertaken in the Jones group is the synthesis of novel complexes, containing main group elements in low oxidation states. Throughout the last two decades, it has been shown that ligand electronics and sterics play vital roles in the stabilization of such complexes. This chapter will describe several miscellaneous results largely derived from attempts to prepare bulky guanidinate complexes of *p*-block elements in low oxidation states.

There are a wide range of ligands that have been shown to successfully stabilize metals in low oxidation states (Figure 1).[1] Most of these have been summarized in great detail in Chapter 1. This introduction will only cover examples pertinent to the work reported in this chapter.

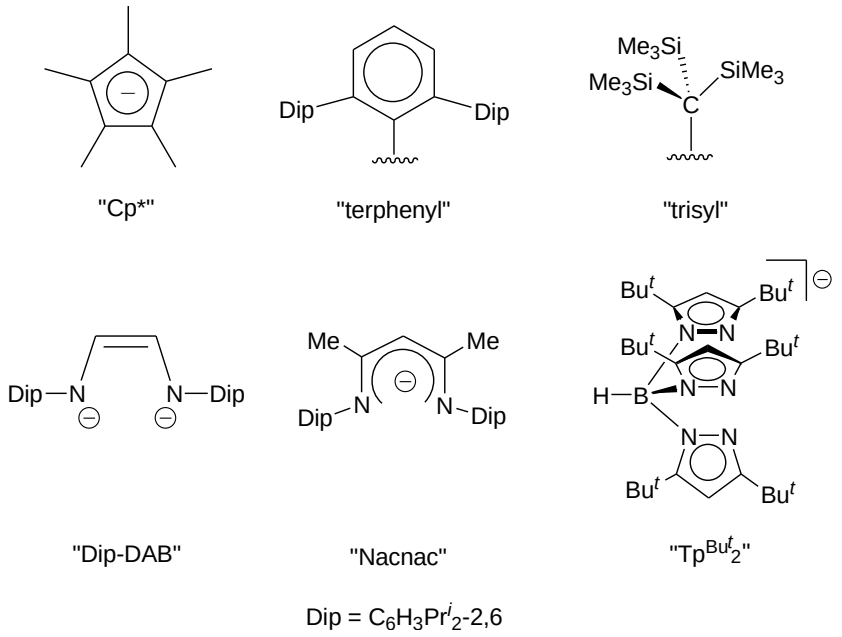

Figure 1. Structures and colloquial names of some commonly used bulky ligands.

Bulky guanidinate anions, which have the general formula $[(RN)_2CNR'_2]^-$ (R, R' = alkyl, aryl, silyl etc.), are often used in the preparation of novel low oxidation state complexes. They are used because the sterics of the ligand are easily tuned and because they are able to exhibit several coordination modes (Figure 2).[1] The steric bulk of the ligand also provides kinetic protection to the coordinated metal fragment from disproportionation and other decomposition processes. A review article on this subject has recently appeared.[1]

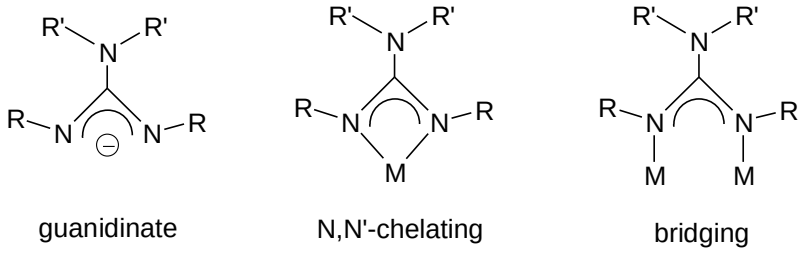

Figure 2. General formula of guanidinate anions and two of their common bonding modes.

One of the most commonly used guanidinate ligands in the Jones group is Priso$^-$ ([DipNC(NPr$^i_2$)NDip]$^-$).[2] Most of the compounds described within this Chapter incorporate Priso$^-$, therefore, prior work involving this ligand will be briefly discussed. As with most other guanidinate ligands, Priso$^-$ is easily prepared via the insertion of a carbodiimide into the metal-nitrogen bond of a metal amide (Scheme 1).[3,4] Throughout this introduction, other guanidinate and amidinate complexes will be included for comparison.

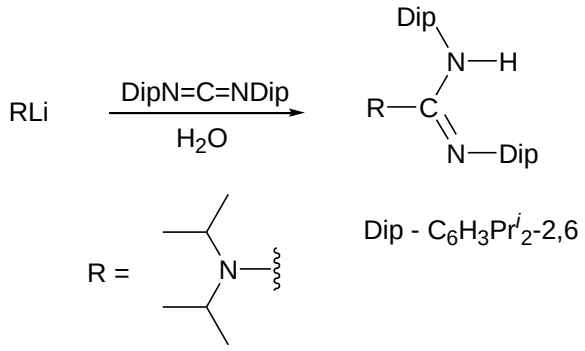

Scheme 1. Synthesis of PrisoH.

In 2006, Jones et al. prepared the novel germanium(I) heterocycles, **1** and **2**, via the reductions of the guanidinate and amidinate precursors, [(Priso)GeCl], and [(Piso)GeCl] (Piso$^-$ = [DipNC(Bu^t)NDip]$^-$) respectively, with excess potassium in toluene (Scheme 2).[5] The dichroic compounds were obtained as green-red or lime-green crystals in low yield. Interestingly, X-ray crystallographic studies carried out on the species revealed Ge-Ge distances of 2.6721(13) Å for complex **1** and 2.6380(8) Å for complex **2**. These distances are consistent with single bond interactions.

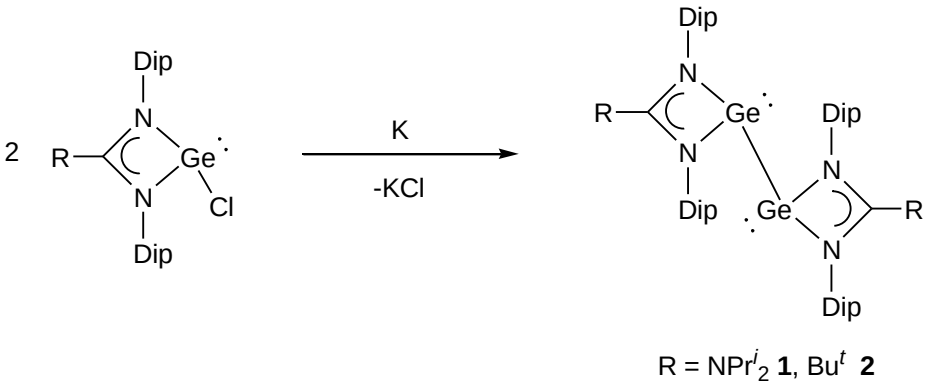

Scheme 2. Synthesis of complexes **1** and **2**.

In 2007, a range of guanidinato and amidinato arsenic and antimony +3 oxidation state precursors were successfully synthesized, **3**-**8** (Scheme 3).[6] All attempts at preparing Sb(I) species via the reduction of Sb(III) precursors led to the deposition of Sb metal. This, however, was not the case for the arsenic analogues. Reduction of complexes **3**-**5** with KC_8 led to the first examples of base stabilized amidodiarsenes, **9**-**11**, in low to moderate yields (Scheme 3).[6] Interestingly, through X-ray crystallography, it was determined that upon reduction, the coordination mode switched from N,N'-chelating in the precursor complex to bridging in the reduced product. The As-As bond length in complex **9** was found to be 2.2560(5) Å which lies within the normal range for As=As double bonds.

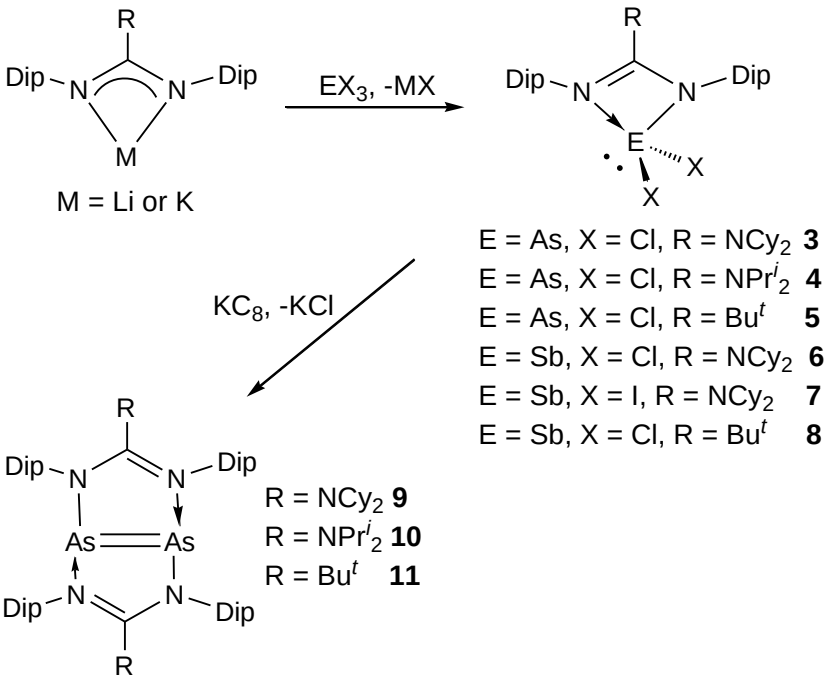

Scheme 3. Synthesis of complexes **3-11**.

A range of guanidinato lead and tin chloride complexes **12-18** have also been reported (Scheme 4).[5,7,8,9] X-ray crystallographic studies determined that the tin complexes crystallize in the monomeric state, whereas the lead(II) species are associated into dimeric units through weak chloride bridges in the solid state. Reductions of complexes **12-18** with potassium metal have all been unsuccessful to date.[1] Interestingly, however, it was seen that complex **13** underwent a ligand modification reaction with atmospheric oxygen to give a low yield of the lead alkoxide species, **19**.[9]

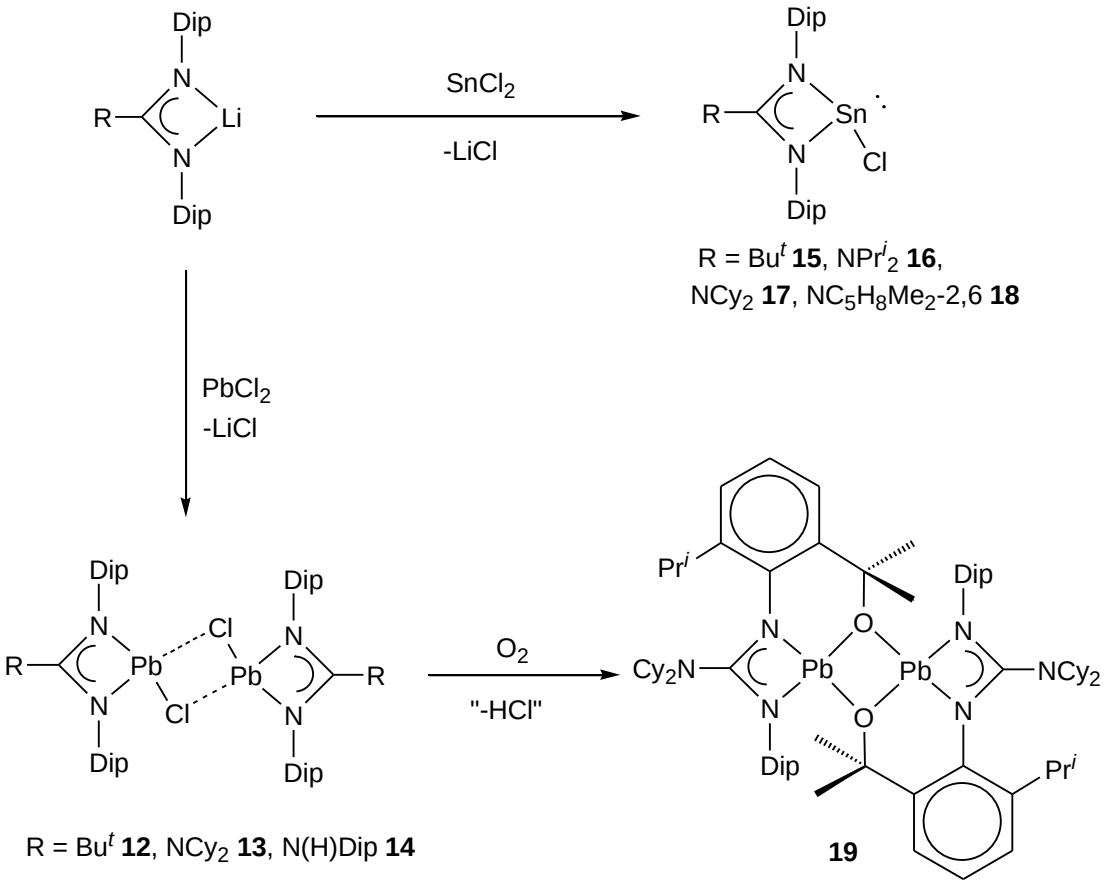

Scheme 4. Synthesis of complexes **12- 19**.

Extensive work with an anionic five-membered gallium(I) heterocycle, [:Ga{[N(Dip)C(H)]$_2$}]$^-$ **20** has been discussed in chapters two and three.[10] In 2006, the boron analogue of **20** was reported by Segawa and co-workers. The reduction of [BrB{N(Dip)C(H)}$_2$] with lithium metal in DME, in the presence of a catalytic amount of naphthalene, afforded the dimeric lithium boryl complex, **21** (Scheme 5).[11] This is of much interest as **21** can be viewed as a lithium salt of the first crystallographically characterized boryl anion. This result is related to one reaction described in this chapter.

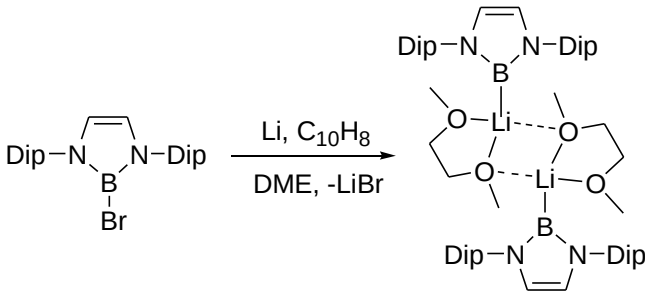

21

Scheme 5. Synthesis of complex **21**.

5.2 Research Proposal

As this chapter summarizes miscellaneous results obtained during this candidature, there was not a specific research proposal. There was however a common goal of synthesizing novel metal-metal bonded complexes, as well as novel low-oxidation state complexes, stabilized by the bulky guanidinate ligand, Priso.

5.3 Results and Discussion

The reported synthesis of a Ge(I) dimer, complex **1**, involved the reduction of [(Priso)GeCl] with an excess of potassium metal in toluene.[5] Complex **1** was the desired product of this reaction, but the yield was very low. It was thought that the low yield was due to the use of an excess of potassium, leading to over reduced products. In an attempt to increase the yield of **1**, it was thought that a reducing agent that could be used in stoichiometric amounts would be required. To this end, the addition of the novel Mg(I) reducing agent, $[(^{Mes}\text{Nacnac})\text{Mg}]_2$[12] ($\{[\{\text{N(Mes)C(Me)}\}_2\text{CH}]\text{Mg}\}_2$), to a toluene solution of

[(Priso)GeCl] in a 0.5:1 ratio, afforded complex **1** in moderate yield, 55% (Scheme 6). This was a welcome result, as not only was the yield for complex **1** optimized, but the reaction could be carried out in a more controlled fashion.

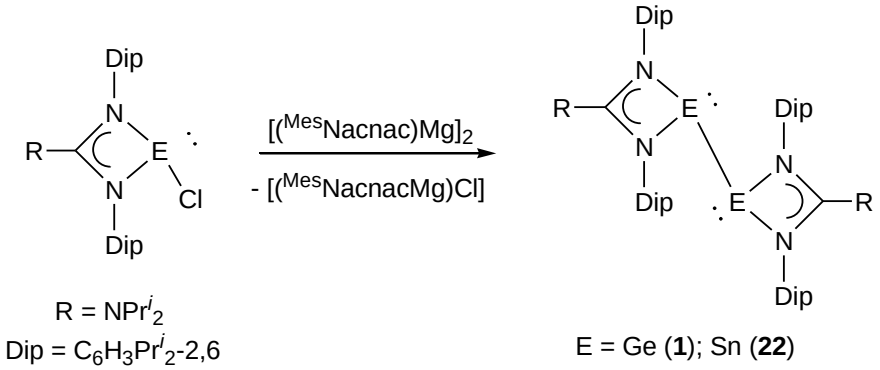

Scheme 6. Synthesis of complexes **1** and **22**.

In an attempt to prepare the tin analogue of complex **1**, [(^{Mes}Nacnac)Mg]$_2$ was added in a 0.5:1 ratio to a toluene solution of [(Priso)SnCl]. Upon workup and crystallization from hexane, small green crystals of complex **22** were obtained. The crystals of complex **22** were, however, not of sufficient quality for X-ray crystallographic studies. It was determined through a comparison of the ^{1}H NMR spectra of complexes **1** and **22**, that the intended diamagnetic Sn(I) complex was indeed synthesized.

Similar to complexes **1** and **22** is the arsenic(I) species **10**. It was formed from the reduction of **4** with KC_8. In contrast, attempts to reduce the previously known guanidinate and amidinate antimony complexes **6**-**8** all led to the deposition of antimony metal. As the analogous complex [(Priso)$SbCl_2$] had not been prepared, it was thought that the bulky Priso$^-$ ligand could possibly provide the steric protection needed to access the analogue of complex **10**. The addition of an *in situ* prepared solution of [(Priso)Li] to $SbCl_3$ afforded colorless crystals of complex **23** in low yield (Scheme 7). An X-ray crystallographic study

on complex **23** found it to be the desired complex [(Priso)$SbCl_2$]. Complex **23** is monomeric and isostrucutral to complex **4**. They each exhibit a distorted "saw-horse" geometry. The four-coordinate group 15 elements have stereochemcially active lone pairs and the geometry of the chelating guanidinate ligand implies they have predominantly localized ligand backbones. The metal-nitrogen bond lengths in complex **23** are 2.119(3) Å and 2.222(3) Å (Figure 3), while the antimony-chloride distances were measured at 2.4882(10) Å and 2.3848(10) Å. The backbone N-C bond lengths were measured at 1.368(4) Å and 1.337(4) Å. The ^{1}H NMR spectrum of complex **23** is very similar to that of complex **4**. Unfortunately, due to the low yield, attempts to reduce **23** were not possible.

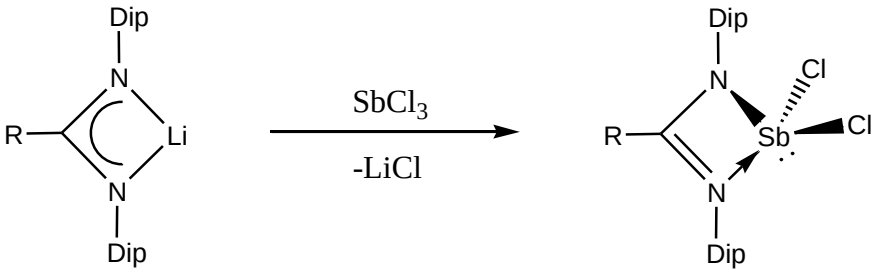

Dip = $C_6H_3Pr^i_2$-2,6

R = NPr^i_2

23

Scheme 7. Synthesis of complex **23**.

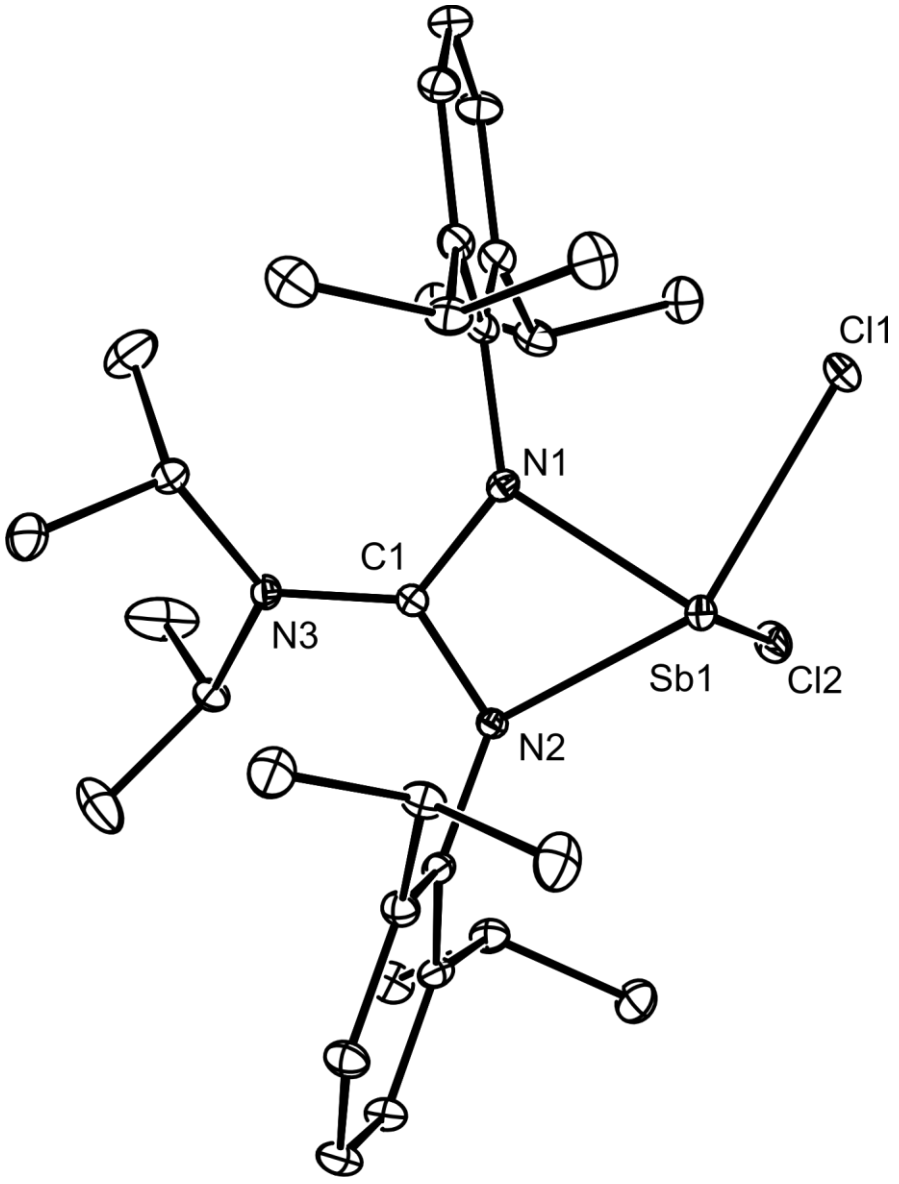

Figure 3. Thermal ellipsoid plot (20% probability surface) of the molecular structure of [(Priso)$SbCl_2$] (**23**); hydrogen atoms and isopropyl groups are omitted for clarity. Selected bond lengths (Å) and angles (^{o}): Sb(1)-Cl(1) 2.4882(10), Sb(1)-Cl(2) 2.3848(10), Sb(1)-N(1) 2.119(3), Sb(1)-N(2) 2.222(3), N(1)-C(1) 1.368(4), N(2)-C(1) 1.337(4), Cl(1)-Sb(1)-Cl(2) 89.95(4), Cl(1)-Sb(1)-N(1) 87.75(7), Cl(2)-Sb(1)-N(1) 104.00(8), Cl(2)-Sb(1)-N(2) 86.55(7), N(1)-C(1)-N(2) 108.8(3).

To date, all attempts to reduce complexes **12**, **13**, and **14** have led to the deposition of lead metal. The analogous complex [(Priso)PbCl] has yet to be reported, and it was thought that upon its successful synthesis, it may act as a bulky precursor to a stable Pb(I) species. The addition of an *in situ* prepared solution of [(Priso)Li] to $PbCl_2$ in toluene afforded colorless crystals of the dimeric complex [(Priso)PbCl] **24** (Scheme 8). The more sterically hindered lead β-diketiminate complexes, $[(Nacnac)Pb^{II}X]$[13], are monomeric, but interestingly, an X-ray crystallographic study found complex **24** to be associated into dimeric units through weak chloride bridges, in a similar fashion to complexes **12**, **13**, and **14**. The Pb-N bond lengths in complex **24** were found to be 2.297(3) Å and 2.414(3) Å (Figure 4), while the Pb-Cl distances are 2.6411(11) Å and 2.8989(11) Å respectively, which are similar to the previously reported distances in complexes **12**-**14**. Complex **24** exhibits a sterochemically active lone pair. Unfortunately, no spectroscopic data were obtained, and no reductions were attempted, due to the very low yield for complex **24** (<1%).

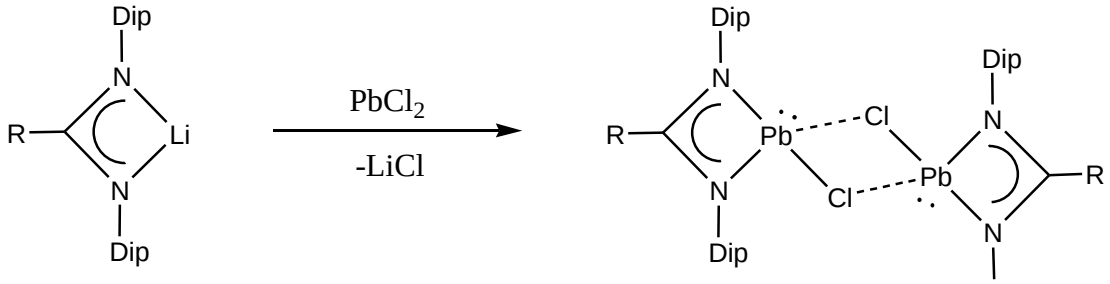

Dip = $C_6H_3Pr^i_2$-2,6

R = NPr^i_2

Scheme 8. Synthesis of complex **24**.

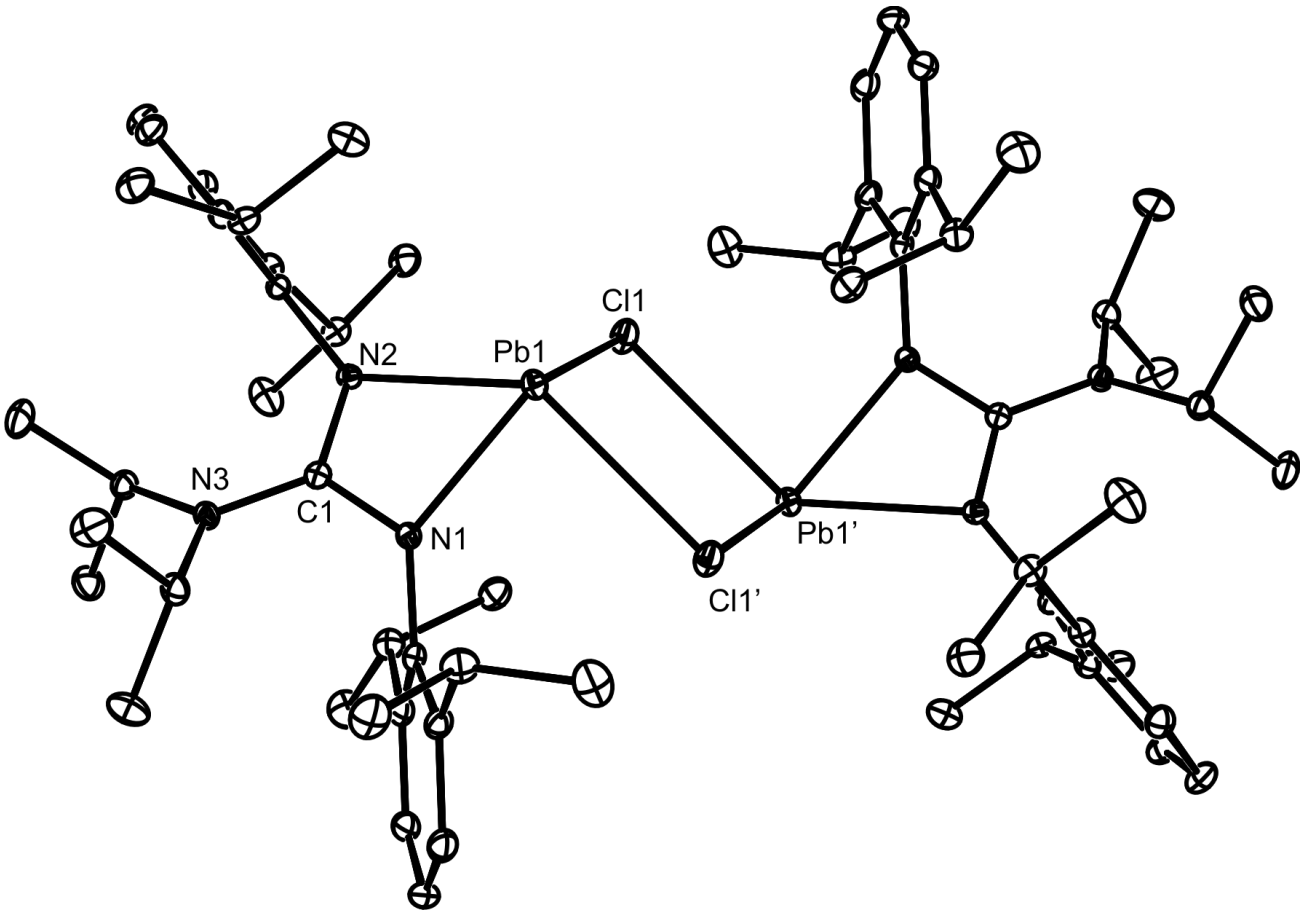

Figure 4. Thermal ellipsoid plot (20% probability surface) of the molecular structure of [(Priso)PbCl] (**24**); hydrogen atoms and isopropyl groups are omitted for clarity. Selected bond lengths (Å) and angles (^{o}): Pb(1)-N(1) 2.297(3), Pb(1)-N(2) 2.414(3), Pb(1)-Cl(1) 2.6411(11), Pb(1)-Cl(1') 2.8989(11), N(1)-C(1) 1.358(4), N(2)-C(1) 1.323(4), N(1)-Pb(1)-N(2) 56.12(10), Cl(1)-Pb(1)-N(1) 115.82(7), Cl(1)-Pb(1)-N(2) 91.10(7), Pb(1)-Cl(1)-Pb(1') 100.99(4), N(1)-C(1)-N(2) 111.7(3).

Jones et al. had recently prepared the guanidinato aluminum complex, [(Priso)AlI_2], and it was proposed that preparing an aluminum complex analogous to the previously reported germanium or tin-gallyl complexes[14] (see Chp. 2.1) would be interesting. Accordingly, the 1:1 reaction of [K(tmeda)][**20**] with [(Priso)AlI_2] was carried out and afforded orange crystals of the novel aluminum-gallyl complex **25** in moderate yield (Scheme 9). X-ray crystallographic studies revealed a Ga-Al bond length of 2.458(2) Å (Figure 5). The ^{1}H NMR and ^{13}C NMR spectra of the complex are consistent with its solid state structure.

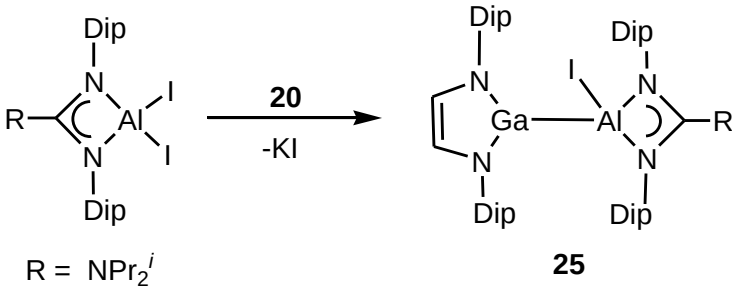

Scheme 9. Synthesis of complex **25**.

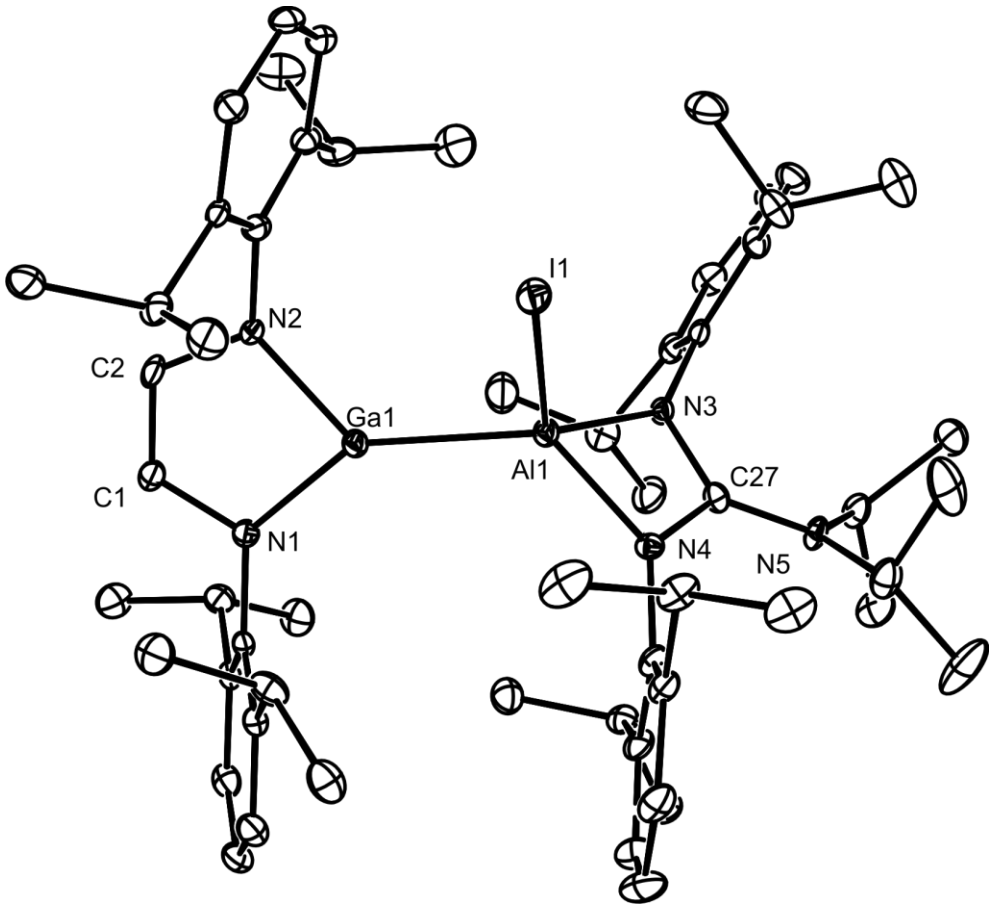

Figure 5. Thermal ellipsoid plot (20% probability surface) of the molecular structure of [(Priso)AlI{Ga(Dip-DAB)}] (**25**); hydrogen atoms and isopropyl groups are omitted for clarity. Selected bond lengths (Å) and angles (^{o}): Ga(1)-Al(1) 2.458(2), Ga(1)-N(1) 1.871(5), Ga(1)-N(2) 1.879(5), Al(1)-I(1) 2.5305(19), Al(1)-N(3) 1.898(5), Al(1)-N(4) 1.886(5), N(3)-C(27) 1.361(7), N(4)-C(27) 1.381(7), Ga(1)-Al(1)-I(1) 100.53(7), N(1)-Ga(1)-N(2) 87.9(2), N(3)-Al(1)-N(4) 71.0(2), I(1)-Al(1)-N(3) 116.26(17), I(1)-Al(1)-N(4) 113.21(16), N(3)-C(27)-N(4) 106.4(5), Ga(1)-Al(1)-N(3) 125.66(17), Ga(1)-Al(1)-N(4) 129.63(17).

In an attempt at preparing a novel gallium-boron bonded complex, [(Dip-DAB)B-Ga(Dip-DAB)], [K(tmeda)][**20**] was reacted with [BrB(Dip-DAB)] in a mixture of diethyl ether and toluene at 25 °C (Scheme 10). Upon workup and placement overnight at -30 °C, deep red crystals of complex **26** were isolated in low yield. Interestingly, instead of the predicted gallium-boron bonded complex, **26** was found to be an anionic benzyl-digallane species. It is thought that the mechanism of reaction likely involves oxidation of the gallium(I) starting material by [BrB(Dip-DAB)] to give the known gallium(II) dimer, [{Ga(Dip-DAB)}$_2$] (see Chapter 2). The toluene solvent could then be deprotonated by an excess of the base, [K(tmeda)][**20**], yielding K[CH_2Ph] which reacts with [{Ga(Dip-DAB)}$_2$] to give compound **26**. The compound displays negligible solubility in normal deuterated solvents. As a result meaningful NMR spectroscopic data for the compound could not be obtained. An X-ray crystallographic study revealed a Ga-Ga bond length of 2.5007(8) Å, which is significantly shorter than the Ga-Ga interaction (2.88 Å) in the starting material [K(tmeda)][**20**] (Figure 6). It is however in the range of several known digallanes (2.332–2.584 A˚) (see Chapter 2).

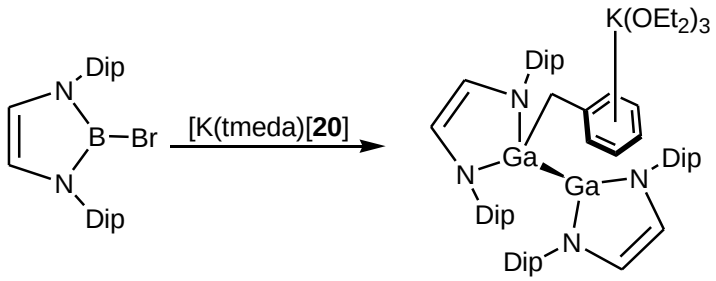

26

Scheme 10. Synthesis of **26**.

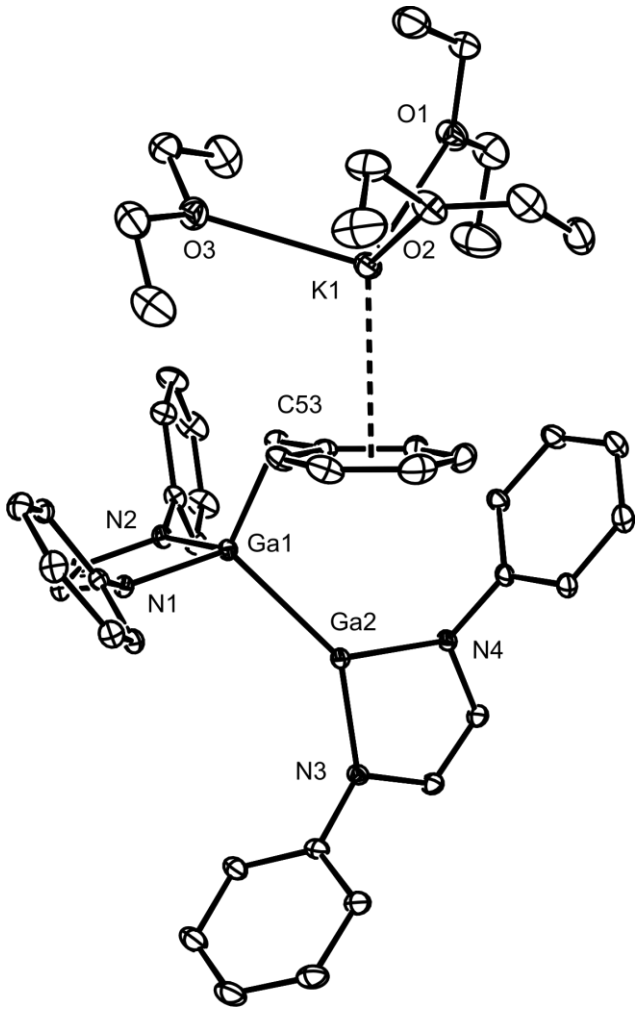

Figure 6. Thermal ellipsoid plot (20% probability surface) of the molecular structure of $[K(OEt_2)_3][(Dip\text{-}DAB)Ga^{II}(CH_2Ph)Ga^{II}(Dip\text{-}DAB)]$ (**26**); hydrogen atoms and isopropyl groups are omitted for clarity. Selected bond lengths (Å) and angles (^{o}): Ga(1)-Ga(2) 2.5007(8), Ga(1)-N(1) 1.9275(18), Ga(1)-N(2) 1.9364(19), Ga(2)-N(3) 1.9052(18), Ga(2)-N(4) 1.9020(18), Ga(1)-C(53) 2.027(2), K(1)-O(1) 2.742(2), K(1)-O(2) 2.686(2), K(1)-O(3) 2.709(2), N(1)-Ga(1)-N(2) 86.89(8), N(3)-Ga(2)-N(4) 86.86(8), N(1)-Ga(1)-C(53) 113.33(9), N(2)-Ga(1)-C(53) 115.86(9), N(1)-Ga(1)-Ga(2) 116.41(6), N(2)-Ga(1)-Ga(2) 112.24(6), C(53)-Ga(1)-Ga(2) 110.49(7), N(3)-Ga(2)-Ga(1) 143.04(6), N(4)-Ga(2)-Ga(1) 126.57(6).

5.4 Conclusion

In conclusion, a novel guanidinato Sn(I) dimeric species has been prepared, as have been several guanidinato antimony(III) and lead(II) chloride complexes. In addition, a novel aluminum-gallyl species is reported, along with an interesting anionic benzyl-digallane complex.

5.5 Experimental

General considerations. All manipulations were carried out using standard Schlenk and glove box techniques under atmospheres of high purity argon or dinitrogen. Toluene, hexane and tmeda were distilled over molten potassium metal, while diethyl ether was distilled over Na/K alloy. Melting points were determined in sealed glass capillaries under argon and are uncorrected. Mass spectra were recorded at the EPSRC National Mass Spectrometric Service at Swansea University. In general, the highly air and moisture sensitive nature of the compounds in this study led to irreproducible microanalyses. IR spectra were recorded using a Nicolet 510 FT-IR spectrometer as Nujol mulls between NaCl plates. ^{1}H and $^{13}C\{^{1}H\}$ NMR spectra were recorded on a Varian DPX 300 spectrometer.

Preparation of [{(Priso)Sn}$_2$] (22). To a solution of [(Priso)SnCl] (0.16g, 0.26 mmols) in toluene (20 cm^3) at -80 ^{o}C was added a solution of [(^{Mes}NacnacMg)$_2$] (0.09g, 0.13 mmols) in toluene (20 cm^3). The mixture was warmed to room temperature over a period of 5 hours and subsequently all volatiles removed *in vacuo*. The residue was extracted into hexane (40 cm^3), the extract filtered and stored at –30 °C overnight to yield green crystals

of **22**. Yield: < 1%. M.p. 185-187°C (decomp); ^{1}H NMR (300 MHz, C_6D_6, 298 K): δ 0.58 (d, $^{3}J_{HH}$=6.8Hz, 12H, CH(CH_3)$_2$), 0.81 (d, $^{3}J_{HH}$=6.8Hz, 12H, CH(CH_3)$_2$), 1.17 (d, $^{3}J_{HH}$=6.8Hz, 12H, CH(CH_3)$_2$), 1.21 (d, $^{3}J_{HH}$=6.8Hz, 12H, CH(CH_3)$_2$), 1.38 (d, $^{3}J_{HH}$=6.8Hz, 12H, CH(CH_3)$_2$), 1.57 (d, $^{3}J_{HH}$=6.8Hz, 12H, CH(CH_3)$_2$), 3.41 (sept., $^{3}J_{HH}$=6.8Hz, 4H, C*H*(CH$_3$)$_2$), 3.92 (sept., $^{3}J_{HH}$=6.8Hz, 4H, C*H*(CH$_3$)$_2$), 4.16 (m, 2H, NC*H*(CH$_3$)$_2$), 7.18-7.27 (m, 12H, Ar*H*); ^{13}C NMR (75 MHz, C_6D_6, 298 K): δ 20.5 (CH(*C*H$_3$)$_2$), 20.7 (CH(*C*H$_3$)$_2$), 21.4 (CH(*C*H$_3$)$_2$), 23.1 (CH(*C*H$_3$)$_2$), 26.7 (CH(*C*H$_3$)$_2$), 27.0 (*C*H(CH$_3$)$_2$), 27.9 (*C*H(CH$_3$)$_2$), 46.6 (N*C*H(CH$_3$)$_2$), 121.4, 122.5, 126.0, 138.6, 144.5, 147.4 (Ar-*C*), 155.1 (backbone *C*N$_2$); IR ν/cm^{-1} (Nujol): 1610m, 1582w, 1377s, 1262w, 1155w, 1109w, 932w, 868w, 799w, 756w; MS (EI 70eV), *m*/*z* (%): 582.3 (M/2^{+}, 5).

Preparation of [(Priso)SbCl$_2$] (23). To a solution of $SbCl_3$ (0.15g, 0.65 mmols) in THF (20 cm^3) at -80 ^{o}C was added an *in situ* prepared solution of [(Priso)Li] (0.30g, 0.65 mmols) in THF (20 cm^3). The reaction mixture was stirred and warmed to room temperature overnight, whereupon volatiles were removed *in vacuo*. The residue was extracted into diethyl ether (40 mL), the extract filtered and stored at -30 °C overnight to yield light yellow crystals of **23**. Yield: < 5%; M.p. 168-170 ^{o}C (decomp.); ^{1}H NMR (300 MHz, C_6D_6, 298 K): δ 0.64 (d, $^{3}J_{HH}$=6.8Hz, 12H, CH(CH_3)$_2$), 1.19 (d, $^{3}J_{HH}$=6.8Hz, 12H, CH(CH_3)$_2$), 1.21 (d, $^{3}J_{HH}$=6.8Hz, 12H, CH(CH_3)$_2$), 3.41 (sept., $^{3}J_{HH}$=6.8Hz, 4H, C*H*(CH$_3$)$_2$), 3.92 (m, 2H, NC*H*(CH$_3$)$_2$), 7.18-7.27 (m, 6H, Ar*H*); ^{13}C NMR (75 MHz, C_6D_6, 298 K): δ 21.9 (CH(*C*H$_3$)$_2$), 23.4 (CH(*C*H$_3$)$_2$), 23.7 (CH(*C*H$_3$)$_2$), 27.6 (CH(*C*H$_3$)$_2$), 28.3 (CH(*C*H$_3$)$_2$), 28.5 (*C*H(CH$_3$)$_2$), 29.1 (*C*H(CH$_3$)$_2$), 47.8 (N*C*H(CH$_3$)$_2$), 122.7, 123.8, 124.3, 137.1, 145.7, 146.5 (Ar-*C*), 148.6 (backbone *C*N$_2$); IR ν/cm^{-1} (Nujol): 1611m, 1580m, 1538w, 1376s, 1260m, 1107m, 934w, 877m, 804s, 762m, 725w, 658w.

Preparation of [(Priso)PbCl] (24). To a solution of $PbCl_2$ (0.34g, 1.22 mmols) in THF (20 cm^3) at -80 ^oC was added an *in situ* prepared solution of [(Priso)Li] (0.50g, 1.10 mmols) in THF (20 cm^3). The reaction mixture was stirred and warmed to room temperature overnight, whereupon volatiles were removed *in vacuo*. The residue was extracted into hexane (40 mL), the extract filtered and stored at -30 °C overnight to yield light yellow crystals of **24**. Yield: <1%.

Preparation of [(Dip-DAB)Ga-Al(Priso)I] (25). To a solution of [(Priso)AlI_2] (0.47 mmols) in toluene (30 cm^3) at -80^{o}C was added [K(tmeda)][**20**] (0.50 mmols) in toluene (30 cm^3). The reaction mixture was stirred and warmed to room temperature overnight, whereupon volatiles were removed *in vacuo*. The residue was extracted in hexane (30 cm^3), the extract filtered and stored at -30 ^{o}C overnight to yield orange crystals of **25**. Yield: 0.12g (24 %); M.p. 135-137°C (decomp); ^{1}H NMR (300 MHz , C_6D_6, 300K) δ 0.75 (d, 12H, CH(C*H*$_3$)$_2$), 1.10-1.60 , (m, 48H, CH(C*H*$_3$)$_2$), 3.54 (sept., 2H, Pr$^i_2$C*H*), 3.68 (sept., 4H, Pr$^i_2$C*H*), 3.95 (sept., 4H, Pr$^i_2$C*H*), 6.45 (s, 2H, C*H*(DAB)), 7.03-7.31 (m, 12H, Ar*H*); ^{13}C NMR (300MHz, C6D6, 300K), 23.1(CH(*C*H$_3$)$_2$), 24.3(CH(*C*H$_3$)$_2$), 25.7(CH(*C*H$_3$)$_2$), 26.9(CH(*C*H$_3$)$_2$), 28.3(CH(*C*H$_3$)$_2$), 29.8 *C*H(CH$_3$)$_2$, 30.1 *C*H(CH$_3$)$_2$, 50.3 *C*H(CH$_3$)$_2$, 123.1 (*C*N), 123.2, 123.7, 125.2, 125.3, 144.7, 144.9, 145.7, 147.3 (Ar*C*), 168.7 (*C*N); IR *v*/cm–1 (Nujol): 1788w, 1664w, 1614m, 1584m, 1377s, 1306w, 1154w, 1097w, 1020w, 974w, 798m, 752m, 723m; MS (EI/70eV), m/z (%): 1061.5 , (M^+ , 4).

Preparation of [K(OEt$_2$)$_3$][(Dip-DAB)Ga^{II}(CH$_2$Ph)Ga^{II}(Dip-DAB)] (26). To a solution of [(Dip-DAB)BBr] (0.22g, 0.47 mmols) in toluene (15 cm^3) at -80 ^{o}C was added a solution of [K(tmeda)][**20**] (0.30g, 0.50 mmols) in toluene (15 cm^3). The solution was stirred and allowed to warm to room temperature overnight, whereupon volatiles were removed *in*

vacuo. The residue was extracted into diethyl ether (20 cm^3), the extract filtered and stored at -30 ^oC overnight to yield deep red crystals of **26**. Yield: (6%); M.p. 205–209 °C (decomp.); MS (EI), m/z (%): 889 ({Ga(Dip-DAB)}$_2H^+$, 23), 445 (Ga(Dip-DAB)H^+, 100), 377 (Dip-DABH^+, 42); IR v/cm^{-1} (Nujol): 1666w, 1587s, 1351s, 1316m, 1259m, 1098s, 800 s, 758 m; anal. calc. for $C_{71}H_{109}N_4Ga_2KO_3$: C 68.48%, H 8.82%, N 4.50%; found: C 68.12%, H 8.71%, N 4.48%.

5.6 References

1. Jones, C. *Coord. Chem. Rev.*, **2010**, *254*, 1273.

2. Jin, G.; Jones, C.; Junk, P.C.; Lippert, K.-A.; Rose, R.P.; Stasch, A. *New J. Chem.*, **2009**, *33*, 64.

3. Edelmann, F.T. *Adv. Organomet. Chem.*, **2008**, *57*, 183.

4. Bailey, P.J.; Pace, S. *Coord. Chem. Rev.*, **2001**, *214*, 91.

5. Green, S.P.; Jones, C.; Junk, P.C.; Lippert, K.-A.; Stasch, A. *Chem. Commun.*, **2006**, 3978.

6. See for example, Power, P.P. *Dalton Trans*., **1998**, 2939.

7. Jones, C.; Rose, R.P.; Stasch, A. *Dalton Trans*., **2008**, 2871.

8. Brym, M.; Francis, M.D.; Jin, G.; Jones, C.; Mills, D.P.; Stasch, A. *Organometallics*, **2006**, *25*, 4799.

9. Stasch, A.; Forsyth, C.M.; Jones, C.; Junk, P.C. *New J. Chem*., **2008**, *32*, 829.

10. Baker, R.J.; Farley, R.D.; Jones, C.; Kloth, M.; Murphy, D.M. *Dalton Trans*., **2002**, 3844.

11. Segawa, Y.; Yamashita, M.; Nozaki, K. *Science* **2006**, *314*, 113.

12. Bonyhady, S.J.; Jones, C.; Nembenna, S.; Stasch, A.; Edwards, A.J.; McIntyre, G.J. *Chem. Eur. J.* **2010**, *16*, 938.

13. Chen, M.; Fulton, J.R.; Hitchcock, P.B.; Johnstone, N.C.; Lappert, M.F.; Protchenko, A.V. *Dalton Trans*., **2007**, 2770.

14. Green, S.P.; Lippert, K.-A.; Jones, C.; Mills, D.P.; Stasch, A. *Inorg. Chem.*, **2006**, *45*, 7242.

Appendix

Publications in Support of this thesis

- 'N-Heterocyclic Germylidenide and Stannylidenide Anions: Group 14 Metal(II) Cyclopentadienide Analogues.' W. D. Woodul, A. F. Richards, A. Stasch, M. Driess, C. Jones, *Organometallics*, 2010, **29**, 3655-3660.
- 'Synthesis and Crystal Structures of Anionic Gallium(II) and Gallium(III) Heterocyclic Compounds Derived from a Gallium(I) *N*-Heterocyclic Carbene.' C. Jones, D. P. Mills, E. Rivard, A. Stasch, W. D. Woodul, *J. Chem. Cryst.*, 2010, **40**, 965-969.
- 'Synthesis and Further Reactivity Studies of Some Transition Metal Gallyl Complexes.' C. Jones, D. P. Mills, R. P. Rose, A. Stasch, W. D. Woodul, *J. Organomet. Chem.*, 2010, **695**, 2410-2417.
- 'Synthesis and Characterization of Neutral and Cationic Boron Guanidinate Complexes.' C. Jones, D. P. Mills, A. Stasch, W. D. Woodul, *Main Group Chem.*, 2010, **9**, 23-30.
- 'Group 2 and 12 Metal Gallyl Complexes Containing Unsupported Ga-M Covalent Bonds (M = Mg, Ca, Sr, Ba, Zn, Cd).' O. Bonello, C. Jones, A. Stasch, W. D. Woodul, *Organometallics*, 2010, **29**, 4914.
- 'Amidinato- and Guanidinato-Cobalt(I) Complexes: Characterization of Exceptionally Short Co-Co Interactions' C. Jones, C. Schulten, R. P. Rose, A. Stasch, S. Aldridge, W. D. Woodul, K. S. Murray, B. Moubaraki, B. Brynda, G. La Macchia, L. Gagliardi, *Angew. Chem. Int. Ed.*, 2009, **48**, 7406-7410.

- ‘Gallyl Lanthanide Complexes Containing Unsupported Ln-Ga (Ln = Sm, Eu, Yb, or Tm) Bonds’ C. Jones, A. Stasch, W. D. Woodul, *Chem. Commun.*, 2009, 113-115.
- ‘Complexes of Four-Membered Group 13 Metal(I) N-Heterocyclic Carbene Analogues with Platinum(II) Fragments’ G. J. Moxey, C. Jones, A. Stasch, P. C. Junk, G. B. Deacon, W. D. Woodul, P. R. Drago, *Dalton Trans.* 2009, 2630-2636.
- ‘A Heterobimetallic Gallyl Complex Containing an Unsupported Ga-Y Bond’ S. T. Liddle, D. P. Mills, B. M. Gardner, J. McMaster, C. Jones, W. D. Woodul, *Inorg. Chem.*, 2009, **48**, 3520-3522.
- ‘Sigma and Pi Donation in an Unsupported Uranium-Gallium Bond’ S. T. Liddle, J. McMaster, D. P. Mills, A. J. Blake, C. Jones, W. D. Woodul, *Angew. Chem. Int. Ed.*, 2009, **48**, 1077-1080.

‘Group 13 Metal(I) and (II) Guanidinate Complexes: Effect of Ligand Backbone on Metal Oxidation State and Coordination Sphere’ G. Jin, C. Jones, P. C. Junk, A. Stasch, W. D. Woodul, *New J. Chem.y*, 2008, **32**, 835-842.